NEUROGENETICS IN NEUROLOGY: FROM MOLECULAR NEUROSCIENCE TO PRECISION MEDICINE

EDITED BY: Matthew James Farrer and Guy Rouleau
PUBLISHED IN: Frontiers in Neurology and Frontiers in Pediatrics

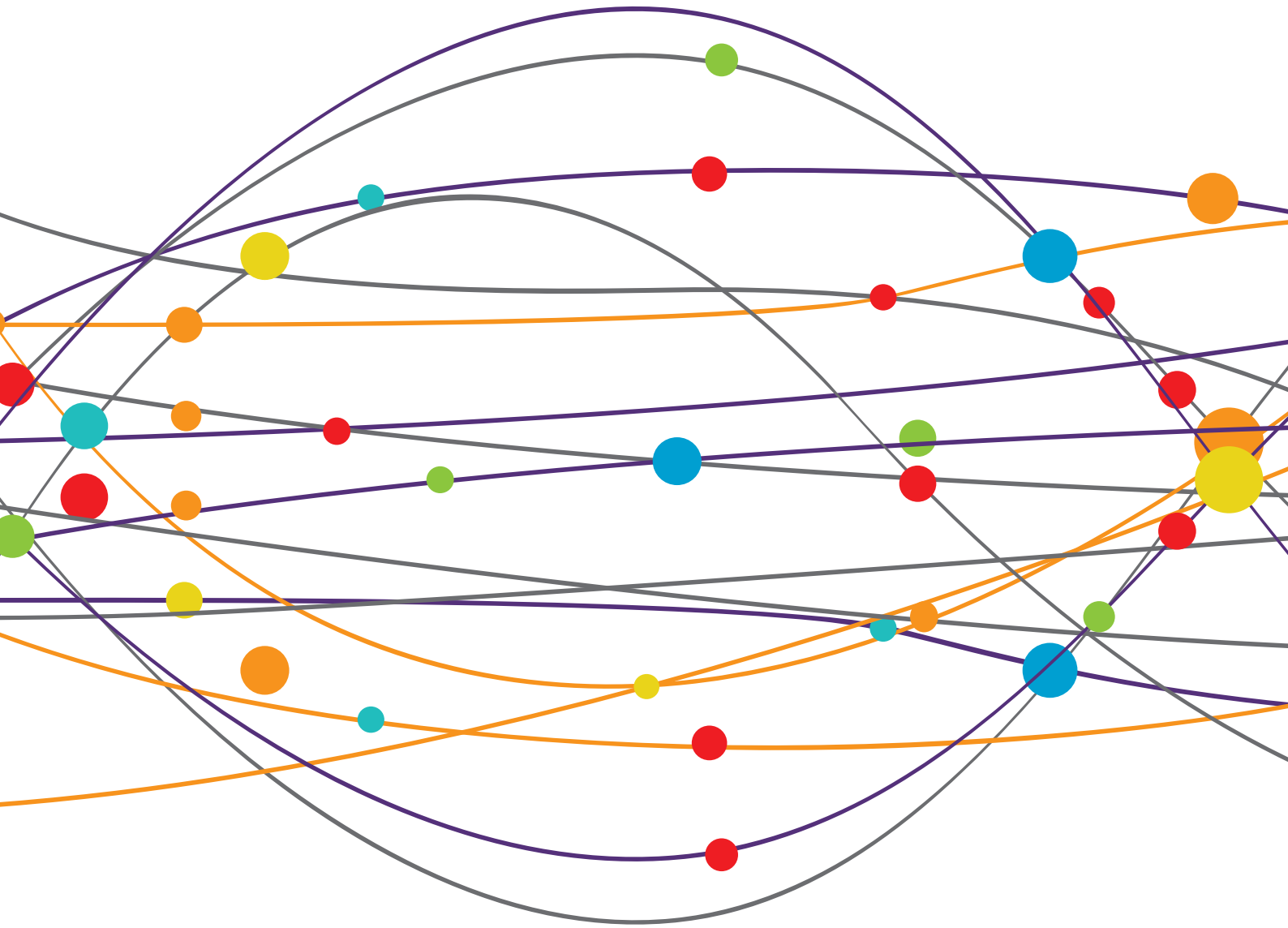

frontiers Research Topics

frontiers

ISSN 1664-8714
ISBN 978-2-88966-251-7
DOI 10.3389/978-2-88966-251-7

About Frontiers

Frontiers is more than just an open-access publisher of scholarly articles: it is a pioneering approach to the world of academia, radically improving the way scholarly research is managed. The grand vision of Frontiers is a world where all people have an equal opportunity to seek, share and generate knowledge. Frontiers provides immediate and permanent online open access to all its publications, but this alone is not enough to realize our grand goals.

Frontiers Journal Series

The Frontiers Journal Series is a multi-tier and interdisciplinary set of open-access, online journals, promising a paradigm shift from the current review, selection and dissemination processes in academic publishing. All Frontiers journals are driven by researchers for researchers; therefore, they constitute a service to the scholarly community. At the same time, the Frontiers Journal Series operates on a revolutionary invention, the tiered publishing system, initially addressing specific communities of scholars, and gradually climbing up to broader public understanding, thus serving the interests of the lay society, too.

Dedication to Quality

Each Frontiers article is a landmark of the highest quality, thanks to genuinely collaborative interactions between authors and review editors, who include some of the world's best academicians. Research must be certified by peers before entering a stream of knowledge that may eventually reach the public - and shape society; therefore, Frontiers only applies the most rigorous and unbiased reviews.
Frontiers revolutionizes research publishing by freely delivering the most outstanding research, evaluated with no bias from both the academic and social point of view. By applying the most advanced information technologies, Frontiers is catapulting scholarly publishing into a new generation.

What are Frontiers Research Topics?

Frontiers Research Topics are very popular trademarks of the Frontiers Journals Series: they are collections of at least ten articles, all centered on a particular subject. With their unique mix of varied contributions from Original Research to Review Articles, Frontiers Research Topics unify the most influential researchers, the latest key findings and historical advances in a hot research area! Find out more on how to host your own Frontiers Research Topic or contribute to one as an author by contacting the Frontiers Editorial Office: researchtopics@frontiersin.org

NEUROGENETICS IN NEUROLOGY: FROM MOLECULAR NEUROSCIENCE TO PRECISION MEDICINE

Topic Editors:
Matthew James Farrer, University of Florida, United States
Guy Rouleau, McGill University, Canada

Citation: Farrer, M. J., Rouleau, G., eds. (2020). Neurogenetics in Neurology: From Molecular Neuroscience to Precision Medicine. Lausanne: Frontiers Media SA.
doi: 10.3389/978-2-88966-251-7

Table of Contents

frontiers in Neurology

CASE REPORT
published: 24 April 2019
doi: 10.3389/fneur.2019.00413

A Novel Variant in Non-coding Region of *GJB1* Is Associated With X-Linked Charcot-Marie-Tooth Disease Type 1 and Transient CNS Symptoms

*Si Luo, Hui Jin, Jiajun Chen and Lei Zhang**

Department of Neurology, China-Japan Union Hospital of Jilin University, Changchun, China

X-linked Charcot-Marie-Tooth disease type 1 (CMTX1) is a dominantly inherited peripheral neuropathy and is caused by mutations in gap junction beta 1 gene (*GJB1*). Here, a novel variant of c.-170T>G in *GJB1* was identified in a large Chinese CMTX1 pedigree. The proband presented transient "stroke-like" episodes in addition to the peripheral neuropathy. At the time of episode, he had transient hyperthyroidism. To our knowledge, this is the first variant found in non-coding region associated with transient central nervous system (CNS) symptoms and in this case, thyroid dysfunction might contribute to the episode. The mechanism of CMTX1 as well as the transient CNS symptoms waits to be elucidated.

Keywords: Charcot-Marie-Tooth disease, *GJB1*, central nervous system manifestations, variant, pedigree

OPEN ACCESS

Edited by:
Matthew James Farrer, University of British Columbia, Canada

Reviewed by:
Arianna Tucci, Genomics England, United Kingdom
Mario Reynaldo Cornejo-Olivas, Instituto Nacional de Ciencias Neurológicas, Peru

****Correspondence:***
Lei Zhang
zhang_lei@jlu.edu.cn

Specialty section:
This article was submitted to Neurogenetics, a section of the journal Frontiers in Neurology

Received: *26 December 2018*
Accepted: *04 April 2019*
Published: *24 April 2019*

Citation:
Luo S, Jin H, Chen J and Zhang L (2019) A Novel Variant in Non-coding Region of GJB1 Is Associated With X-Linked Charcot-Marie-Tooth Disease Type 1 and Transient CNS Symptoms. Front. Neurol. 10:413. doi: 10.3389/fneur.2019.00413

INTRODUCTION

X-linked Charcot-Marie-Tooth disease (CMTX) is an inherited axonal or mixed axonal-demyelinating disease of the peripheral nervous system, characterized by slowly progressive distal muscle weakness and atrophy, decreased or absent deep tendon reflexes, sensory abnormalities, and foot deformities (pes cavus and hammer toes). CMTX type 1 (CMTX1), occupying 90% of CMTX (1), is caused by mutations in gap junction beta 1 gene (*GJB1*) on chromosome Xq13.1. Apart from the neuromuscular manifestations, a small number of CMTX1 patients have transient central nervous system (CNS) symptoms and reversible cerebral white matter lesions (1) whose mechanisms are not completely understood (2). In this report, the clinical features of a big Chinese CMTX1 pedigree were described, in which the proband presented with transient CNS symptoms and transient hyperthyroidism. A novel NM_000166.5 c.-170T>G (chrX:70443032 GRCh37) variant in *GJB1* was found in this pedigree. To current reports, this is the first variant identified in non-coding region associated with transient CNS symptoms (3, 4) and thyroid dysfunction might be a contributor of this episode in this case.

CASE PRESENTATION

The proband (IV-1 in **Figure 1**), a 28-year-old man, was admitted into our department for recurrent dysphonia and asymmetric weakness of four limbs with the right side more severely affected. He had experienced the similar episodes twice when he was 14 and 20 years old. The symptoms lasted 4–6 h and resolved without treatment. He denied any infection, exercises, or other possible inducer before the onsets. This time the symptoms completely disappeared after 5 h. During this episode, physical examination revealed bilateral facial palsy, dysarthria, and bilateral positive Babinski sign,

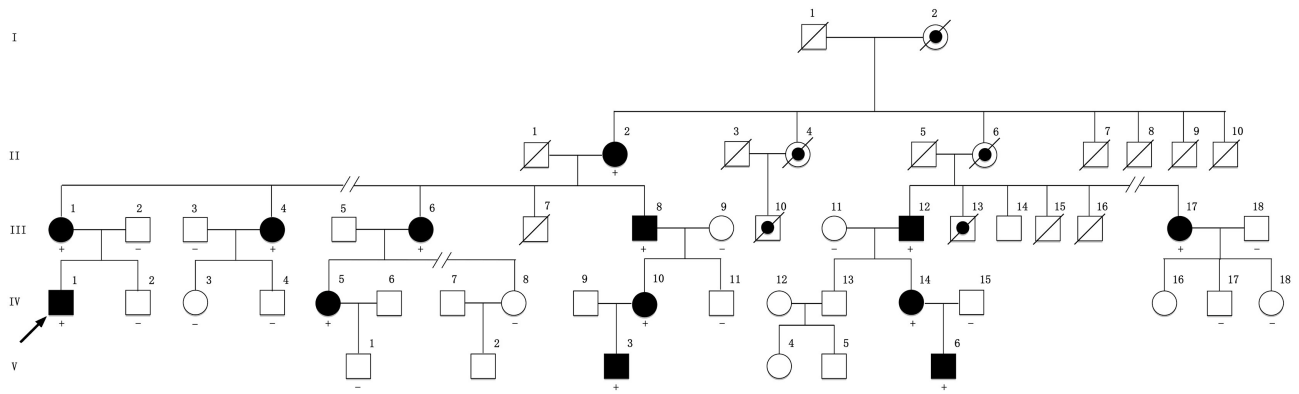

FIGURE 1 | Pedigree of the family compiled with X-linked dominant inheritance. Square represents male and circle represents female. Filled symbol indicates affected. Dot symbol indicates deduced affected individual with medical history. A slash through a symbol indicates deceased individual. Arrow indicates the proband. The symbol "+" indicates a carrier of the variant. The symbol "–" indicates wild genotype. No symbol means the individual's genetic test is not available. The pedigree has been edited to maintain the confidentiality of family members.

with muscle strength grade 3 in the left limbs and grade 2 in the right limbs. After the episode, the neurologic examination showed normal muscle strength, slight intention tremor and unsteadiness when walking on a straight line as well as in the Romberg test. He also had high-arched feet and areflexia in all extremities.

Comprehensive infectious, metabolic, paraneoplastic, and inflammatory panels of the proband were negative. Serum potassium was normal. However, his free T_3 (FT_3) and free T_4 (FT_4) value were increased to 9.56 pmol/L (3.10–6.80 pmol/L) and 39.2 pmol/L (12.0–22.0 pmol/L), respectively. Meanwhile, the value of thyrotropin (TSH) was 0.006 mIU/L, much lower than the limit (0.372–4.94 mIU/L). Further, radioactive iodine uptake scan showed his iodine uptake rates were lower than normal and thyroid-specific autoantibody assays were all negative. Twenty days later, his FT_3 and FT_4 returned to normal. Five months after the episode, all thyroxine test results, including TSH, were all within the reference range and remained for the following 1 year.

During the episode, his brain MRI (**Figures 2A–D**) showed bilaterally symmetric abnormal T2 FLAIR hyperintensity in the deep white matter and the splenium of the corpus callosum (**Figure 2C**) and reduced diffusion (**Figure 2D**). The diffusion reduction disappeared mostly 8 days later (**Figure 2E**). Five months after the episode, the MRI of his brain were almost normal (**Figures 2F–I**). Electroneuromyography (EMG) showed reduced motor and sensory nerve conduction velocities, prolonged distal latency as well as reduced sensory and motor nerve amplitudes, indicating both demyelination and axon loss (**S-Table 1**). Specifically, his right/left median motor nerve conduction velocity is 33.6/37.7 m/s, comforming to the intermediate CMT (5). Brainstem auditory evoked potentials were normal.

This family is Chinese Muslim living in Jilin province. Pedigree analysis indicates an X-linked dominant inheritance (**Figure 1**). The proband is the only individual in the family who experienced "stroke-like" episodes. EMG was carried out to determine the affected in the pedigree. The common findings among affected males included difficulty running, distal weakness, pescavus, absent tendon reflexes, and atrophy of distal muscles with older affected more severely. III-8 presented typically with all the features above (**Figure 3**). Manifestations in female carriers were less severe and varied greatly. Some exhibited weakness and atrophy of hand muscles while some had lower limbs involved. However, a number of female carriers didn't show any symptom at all. The mother of the proband (III-1) was asymptomatic. However, examination displayed that she had high-arched feet and unsteadiness when walking on a straight line. EMG showed that she has demyelinating neuropathy with prominent axonal degeneration (**S-Table 1**).

All exons of *GJB1* of the proband were sequenced by Sanger sequencing. A novel hemizygous variant c.-170T>G was found (**Figure 4A**). It is located in the nerve-specific promoter P2 region of *GJB1*, neighboring c.-171G>C (designated as c.-146-25 G>C in the earlier edition of HGMD, **Figure 4G**), which has been shown reducing the expression of Cx32 (6). c.-170T>G cosegragated with the disease in this pedigree (**Figure 1**, **Figures 4B–F**) and was not present in 100 control DNA samples.

DISCUSSION

The clinical phenotype of CMTX1 is characterized by progressive muscle atrophy and weakness, areflexia, and variable sensory abnormalities. Electrophysiological and pathological studies of peripheral nerves showed the evidence of demyelinating neuropathy with prominent axonal degeneration. However, several patients also have manifestations of the CNS involvement or acute "stroke-like" symptoms (3, 7). These transient "stroke-like" symptoms usually have a childhood or adolescence onset and can present multiple neurological dysfunctions such as hemiparesis, paraparesis, monoparesis, ataxia, and dysarthria (7–10). In addition, respiratory distress (11), dysphagia (10),

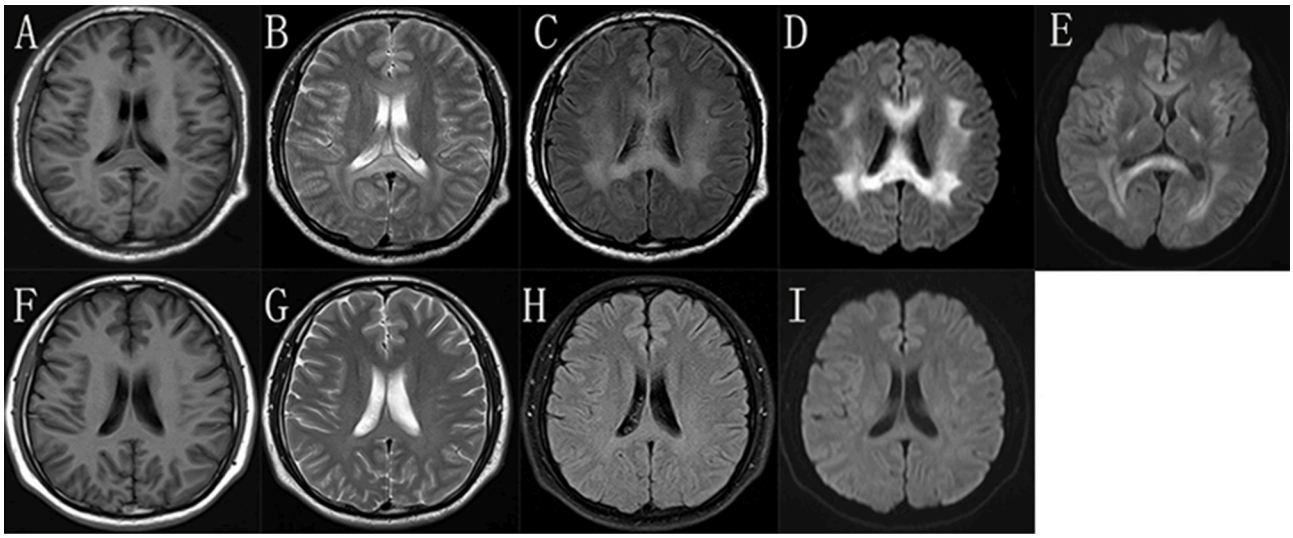

FIGURE 2 | The brain MRI images of the proband. In the "stroke-like" episode, brain MRI showed slightly hypointensity in T1-weighted imaging **(A)** and slightly hyperintensity in T2-weighted imaging **(B)** in the bilateral deep white matter and the splenium of the corpus callosum. But there was obviously bilaterally symmetric hyperintensity in T2 FLAIR images and reduced diffusion in the same region **(C,D)**. MRI after 8 days showed improvement of the abnormal diffusion signal in white matter **(E)**. After 5 months, the images of T1-weighted **(F)**, T2-weighted **(G)**, T2 FLAIR **(H)**, and DWI **(I)** of his brain were almost normal.

FIGURE 3 | The pictures of III-8's limbs. He had atrophy of distal muscles below the knee and in the hands with cavus deformity.

and disorientation (12) have also been reported. The episodes typically last for a few minutes to hours to days. Brain MRI during the acute phase typically presents increased signals in diffusion-weighted and T2-weighted sequences without the enhancement of gadolinium, involving the subcortical white matter and splenium of the corpus callosum. It usually takes months for these MRI changes to return to the baseline (7, 9, 10, 13–15). People have found these CNS manifestations do not correlate with the stage and severity of peripheral neuropathy. The patients in this pedigree compiled with the typical neuromuscular manifestations and the proband presented recurrent episodes of transient CNS symptoms, consistent with the features of CMTX1.

The protein of Cx32, encoded by *GJB1*, is a gap junction protein apportioned in the peripheral nervous system and CNS (16). Myelinating Schwann cells express Cx32, which provides a shorter pathway for the diffusion of small molecules and ions athwart the myelin sheath directly (17). Oligodendrocytes also express Cx32, which participates in the gap junction coupling with astrocytes (18). Mutations in non-coding DNA are considered a major cause of CMTX1 (4), but none has been related with transient CNS symptoms. The variant c.-170T>G, identified in this pedigree, is located in nerve-specific promoter P2 region of *GJB1*, where up to now, 4 mutations have been reported (**Figure 4G**) without benign variant found. Across a variety of species, the promoter P2 region is highly conserved. This variant we found is absent in 1,000 Genomes and dbSNP database and is not present in 100 control DNA samples. The phenotype of the patients is consistent with CMTX1 and this variant cosegregates with the disease in this big pedigree. So according to American College of Medical Genetics and Genomics standards and guidelines, this variant is classified as "likely pathogenic." As to the pathogenic mechanism, since the neighboring c.-171G>C has been shown to impair SOX10-mediated transcription of *GJB1*, leading to a significant reduction in Cx32 expression (6), we speculated that c.-170T>G might cause the disease in the same way, but it waits verifying. On the other hand, the proband is the only patient with these CNS symptoms

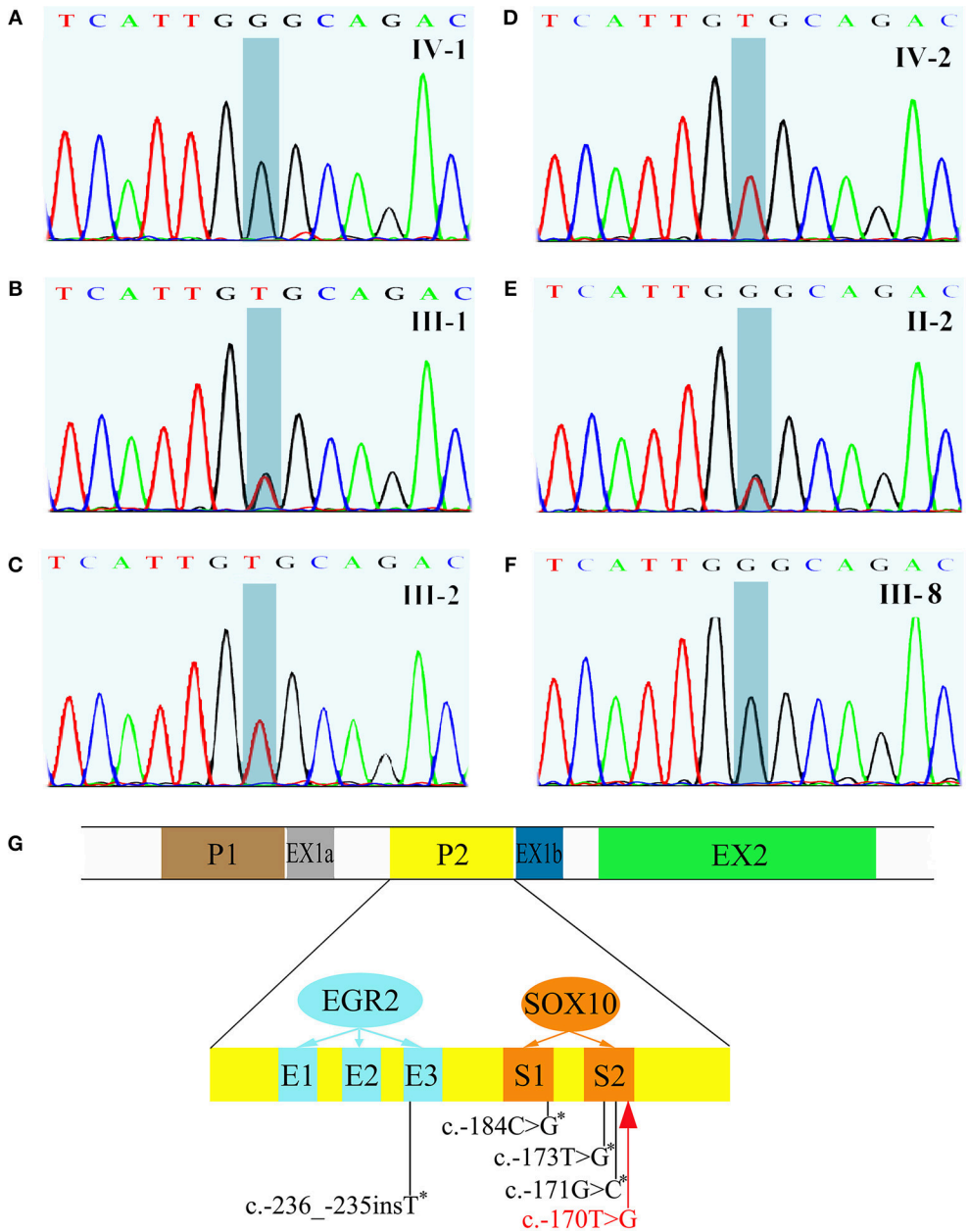

FIGURE 4 | Sequencing results of *GJB1* and its schematic representation of the proximal Cx32 promoter region. **(A)** The proband had a hemizygous c.-170T>G variant. **(B)** III-1, the mother of the proband, had a heterozygous c.-170T>G. **(C,D)** III-1, the father of the proband and IV-2, the brother of the proband, were both wild genotype. **(E)** II-2, a 93-year old woman and the grandma of the proband without any clinical manifestation, carried a heterozygous c.-170T>G. **(F)** III-8, an affected male with typical neuromuscular manifestations had hemizygous c.-170T>G. **(G)** Schematic representation of the proximal Cx32 promoter region which indicates the positions of SOX10 (S1 and S2) and EGR2 (E1, E2, and E3) binding sites. *GJB1* has 2 tissue-specific promoters (P1 and P2) which are alternatively spliced. In neural tissue, *GJB1* transcription is driven via the nerve-specific promoter 2 (P2) upstream of non-coding exon 1b. Up to now, four mutations in the P2 region have been reported (indicated with asterisk). The c.-170T>G variant identified in this pedigree (red) neighbors c.-171G>C which has been proved impairing SOX10-mediated transcription of *GJB1*. This figure was modified from Neurology 2017;88:1445–1453. with permission.

in the pedigree, although every patient in the family carries the variant. The reason might be the coexistence of another modifying pathogenic gene mutation. Expression studies of this variant in cultured cells and animal models are necessary to clarify the mechanism.

Transient CNS symptoms in CMTX1 patients have often been associated with metabolic stresses such as hyperventilation, febrile illnesses, infections, exercises, or high altitude (9, 10, 15, 19). In this case, a transient hyperthyroidism coexisted with this transient "stroke-like" episode of the proband. The CNS

symptoms disappeared within several hours; the abnormality of brain MRI vanished mostly within several days; and hyperthyroidism gained remission in several months. It is possible that thyroid malfunction contributed to the incidence of CNS symptoms in this case and it needs more observation and reports from other doctors and researchers.

The mechanism by which *GJB1* mutations cause the transient CNS dysfunction in CMTX1 is still not clear. Paulson et al. argue that these CNS symptoms does not likely involve demyelination because they demonstrated increased magnetization transfer ratio, nor axonal degeneration because they were reversible over a short interval (9). But a detailed MRI examination using diffusion tensor imaging and magnetic resonance spectroscopy in a man with CMTX1 and transient CNS symptoms showed reversible reductions in fractional anisotropy and N-acetyl-aspartate levels, indicating reversible axonal damage associated with deficient oligodendrocyte gap junctions (20). The mutation in *GJB1* might disrupt the gap junction communication between oligodendrocytes and astrocytes, which leads to inability of these cells to regulate fluid exchange and finally cell edema. This can be proved by restricted diffusion in MRI (3, 7, 9). Some CMTX1 mutants associated with transient CNS events were expressed *in vitro* and their ability to form functional gap junctions was found reduced, thereby reducing the coupling between oligodendrocytes and astrocytes (2). At the same time, physiologic triggers, including metabolic stress, pro-inflammatory factors, and lower pH of the cerebrospinal fluid in the setting of altitudinal changes, may exacerbate this tenuous gap junction coupling and lead to the episodes of CNS symptoms (21–23). *In vivo*, neuroinflammation induced by lipopolysaccharide disrupted the main astrocyte-oligodendrocyte gap junctions, contributing to the increased sensitivity of Cx32 KO mice to lipopolysaccharide. The mutant of *GJB1* T55I, which was associated with transient CNS phenotypes, induced ER stress under inflammatory conditions, further exacerbating oligodendrocyte dysfunction and pathological changes in CNS (24). Elucidating the consequences of *GJB1* mutations both in peripheral nervous system and CNS is very important for the development of effective CMTX1 treatments, and waits more work.

CONCLUSION

A novel *GJB1* variant of c.-170T>G in non-coding region was found in this big Chinese CMTX1 pedigree. This is the first report of variant in non-coding DNA sequence associated with transient CNS symptoms. Thyroid malfunction may contribute to the CNS symptoms in this case.

ETHICS STATEMENT

This study has been reviewed and approved by the Ethics Committee of the China-Japan Union Hospital of Jilin University. Each member of the family provided written informed consent to the participation in the study, the genetic test, and authorized to publish the study including the photos in accordance with the Declaration of Helsinki.

AUTHOR CONTRIBUTIONS

SL and HJ were responsible for acquisition of data, drafting the manuscript. JC was responsible for revising the manuscript. LZ was responsible for study concept or design, drafting/revising the manuscript, and the final approval.

FUNDING

This work was supported by Norman Bethune Program of Jilin University (2015216) and Jilin Provincial Science and Technology Department, China (20180414049GH) to LZ.

SUPPLEMENTARY MATERIAL

The Supplementary Material for this article can be found online at: https://www.frontiersin.org/articles/10.3389/fneur.2019.00413/full#supplementary-material

REFERENCES

1. Ouvrier R, Geevasingha N, Ryan MM. Autosomal-recessive and X-linked forms of hereditary motor and sensory neuropathy in childhood. *Muscle Nerve.* (2007) 36:131–43. doi: 10.1002/mus.20776
2. Abrams CK, Scherer SS. Gap junctions in inherited human disorders of the central nervous system. *Biochim Biophys Acta.* (2012) 1818:2030–47. doi: 10.1016/j.bbamem.2011.08.015
3. Wang Y, Yin F. A review of X-linked charcot-marie-tooth disease. *J Child Neurol.* (2016) 31:761–72. doi: 10.1177/0883073815604227
4. Tomaselli PJ, Rossor AM, Horga A, Jaunmuktane Z, Carr A, Saveri P, et al. Mutations in non-coding regions of GJB1 are a major cause of X-linked CMT. *Neurology.* (2017) 88:1445–53. doi: 10.1212/wnl.0000000000003819
5. Wen Q, Cao L, Yang C, Xie Y. The electrophysiological features in X-linked charcot-marie-tooth disease with transient central nervous system deficits. *Front Neurol.* (2018) 9:461. doi: 10.3389/fneur.2018.00461
6. Houlden H, Girard M, Cockerell C, Ingram D, Wood NW, Goossens M, et al. Connexin 32 promoter P2 mutations: a mechanism of peripheral nerve dysfunction. *Ann Neurol.* (2004) 56:730–4. doi: 10.1002/ana.20267
7. Taylor RA, Simon EM, Marks HG, Scherer SS. The CNS phenotype of X-linked charcot-marie-tooth disease-more than a peripheral problem. *Neurology.* (2003) 61:1475–8. doi: 10.1212/01.wnl.0000095960.48964.25
8. Panas M, Kalfakis N, Karadimas C, Vassilopoulos D. Episodes of generalized weakness in two sibs with the C164T mutation of the connexin 32 gene. *Neurology.* (2001) 57:1906–8. doi: 10.1212/wnl.57.10.1906
9. Paulson HL, Garbern JY, Hoban TF, Krajewski KM, Lewis RA, Fischbeck KH, et al. Transient central nervous system white matter abnormality in X-linked charcot-marie-tooth disease. *Ann Neurol.* (2002) 52:429–34. doi: 10.1002/ana.10305
10. Hanemann CO, Bergmann C, Senderek J, Zerres K, Sperfeld AD. Transient, recurrent, white matter lesions in X-linked charcot-marie-tooth disease with novel connexin 32 mutation. *Arch Neurol.* (2003) 60:605–9. doi: 10.1001/archneur.60.4.605
11. Schelhaas HJ, van Engelen BGM, Gabreels-Festen A, Hageman G, Vliegen JHR, van der Knaap MS, et al. Transient cerebral white matter lesions in a patient with connexin 32 missense mutation. *Neurology.* (2002) 59:2007–8. doi: 10.1212/01.wnl.0000038390.29853.46

12. Fusco C, Frattini D, Pisani F, Spaggiari F, Ferlini A, Della Giustina E. Coexistent central and peripheral nervous system involvement in a charcot-marie-tooth syndrome X-linked patient. *J Child Neurol.* (2010) 25:759–63. doi: 10.1177/0883073809344119
13. Anand G, Maheshwari N, Roberts D, Padeniya A, Hamilton-Ayers M, Van Der Knaap M, et al. X-linked hereditary motor sensory neuropathy (type 1) presenting with a stroke-like episode. *Dev Med Child Neurol.* (2010) 52:677–9. doi: 10.1111/j.1469-8749.2010.03674.x
14. Kim GH, Kim KM, Suh Si, Ki CS, Eun BL. Charcot-marie-tooth disease masquerading as acute demyelinating encephalomyelitis-like illness. *Pediatrics.* (2014) 134:E270–3. doi: 10.1542/peds.2012-3243
15. Srinivasan J, Leventer RJ, Kornberg AJ, Dahl HH, Ryan MM. Central nervous system signs in X-linked charcot-marie-tooth disease after hyperventilation. *Pediatr Neurol.* (2008) 38:293–5. doi: 10.1016/j.pediatrneurol.2007.12.003
16. Kumar NM, Gilula NB. Cloning and characterization of human and rat liver cDNAs coding for a gap junction protein. *J Cell Biol.* (1986) 103:767–76. doi: 10.1083/jcb.103.3.767
17. Balice-Gordon RJ, Bone LJ, Scherer SS. Functional gap junctions in the schwann cell myelin sheath. *J Cell Biol.* (1998) 142:1095–104. doi: 10.1083/jcb.142.4.1095
18. Rash JE, Yasumura T, Dudek FE, Nagy JI. Cell-specific expression of connexins and evidence of restricted gap junctional coupling between glial cells and between neurons. *J Neurosci.* (2001) 21:1983–2000. doi: 10.1523/jneurosci.21-06-01983.2001
19. McKinney JL, De Los Reyes EC, Lo WD, Flanigan KM. Recurrent central nervous system white matter changes in charcot-marie-tooth type X disease. *Muscle Nerve.* (2014) 49:451–4. doi: 10.1002/mus.24108
20. Sato K, Kubo S, Fujii H, Okamoto M, Takahashi K, Takamatsu K, et al. Diffusion tensor imaging and magnetic resonance spectroscopy of transient cerebral white matter lesions in X-linked charcot-marie-tooth disease. *J Neurol Sci.* (2012) 316:178–80. doi: 10.1016/j.jns.2012.01.017
21. Chandross KJ, Spray DC, Cohen RI, Kumar NM, Kremer M, Dermietzel R, et al. TNF alpha inhibits schwann cell proliferation, connexin46 expression, and gap junctional communication. *Mol Cell Neurosci.* (1996) 7:479–500. doi: 10.1006/mcne.1996.0035
22. Abrams CK, Goman M, Wong S, Scherer SS, Kleopa KA, Peinado A, et al. Loss of coupling distinguishes GJB1 mutations associated with CNS manifestations of CMT1X from those without CNS manifestations. *Sci Rep.* (2017) 7:40166. doi: 10.1038/srep40166
23. Harris AL. Emerging issues of connexin channels: biophysics fills the gap (vol 34, pg 325, 2001). *Q Rev Biophys.* (2001) 34:325–472. doi: 10.1017/s0033583502009101
24. Olympiou M, Sargiannidou I, Markoullis K, Karaiskos C, Kagiava A, Kyriakoudi S, et al. Systemic inflammation disrupts oligodendrocyte gap junctions and induces ER stress in a model of CNS manifestations of X-linked charcot-marie-tooth disease. *Acta Neuropathol Commun.* (2016) 4:95. doi: 10.1186/s40478-016-0369-5

Conflict of Interest Statement: The authors declare that the research was conducted in the absence of any commercial or financial relationships that could be construed as a potential conflict of interest.

frontiers in Neurology

ORIGINAL RESEARCH
published: 21 May 2019
doi: 10.3389/fneur.2019.00434

Diagnostic Yield and Treatment Impact of Targeted Exome Sequencing in Early-Onset Epilepsy

Michelle Demos[1†], Ilaria Guella[2†], Conrado DeGuzman[1], Marna B. McKenzie[2], Sarah E. Buerki[1,3], Daniel M. Evans[2], Eric B. Toyota[1], Cyrus Boelman[1], Linda L. Huh[1], Anita Datta[1], Aspasia Michoulas[1], Kathryn Selby[1], Bruce H. Bjornson[1], Gabriella Horvath[4], Elena Lopez-Rangel[5], Clara D. M. van Karnebeek[6,7], Ramona Salvarinova[4], Erin Slade[1], Patrice Eydoux[8,9], Shelin Adam[10], Margot I. Van Allen[10], Tanya N. Nelson[8,9], Corneliu Bolbocean[11,12], Mary B. Connolly[1] and Matthew J. Farrer[2]*

[1] Division of Neurology, Department of Pediatrics, University of British Columbia and BC Children's Hospital, Vancouver, BC, Canada, [2] Department of Medical Genetics, Centre for Applied Neurogenetics (CAN), University of British Columbia, Vancouver, BC, Canada, [3] Division of Neuropediatrics, University Children's Hospital Zurich, Zurich, Switzerland, [4] Division of Biochemical Diseases, Department of Pediatrics, BC Children's Hospital, University of British Columbia, Vancouver, BC, Canada, [5] Division of Developmental Pediatrics, Department of Pediatrics, BC Children's Hospital, University of British Columbia, Vancouver, BC, Canada, [6] Department of Pediatrics, Centre for Molecular Medicine and Therapeutics, BCCHRI, University of British Columbia, Vancouver, BC, Canada, [7] Department of Pediatrics, Academic Medical Centre, Amsterdam, Netherlands, [8] Division of Genome Diagnostics, Department of Pathology and Laboratory Medicine, BC Children's Hospital, Vancouver, BC, Canada, [9] Department of Pathology and Laboratory Medicine, University of British Columbia, Vancouver, BC, Canada, [10] Department of Medical Genetics, BC Children's and BC's Women's Hospitals, University of British Columbia, Vancouver, BC, Canada, [11] University of Tennessee Health Science Center, Memphis, TN, United States, [12] Centre for Addiction and Mental Health, Toronto, ON, Canada

OPEN ACCESS

Edited by:
Giovanni Stevanin,
INSERM U1127 Institut du Cerveau et de la Moelle épinière, France

Reviewed by:
Gaetan Lesca,
Université Claude Bernard Lyon 1, France
Albena Jordanova,
University of Antwerp, Belgium
Caroline Nava,
Institut National de la Santé et de la Recherche Médicale (INSERM), France

***Correspondence:**
Michelle Demos
mdemos@cw.bc.ca

[†]These authors have contributed equally to this work

Specialty section:
This article was submitted to Neurogenetics, a section of the journal Frontiers in Neurology

Received: 17 November 2018
Accepted: 09 April 2019
Published: 21 May 2019

Citation:
Demos M, Guella I, DeGuzman C, McKenzie MB, Buerki SE, Evans DM, Toyota EB, Boelman C, Huh LL, Datta A, Michoulas A, Selby K, Bjornson BH, Horvath G, Lopez-Rangel E, van Karnebeek CDM, Salvarinova R, Slade E, Eydoux P, Adam S, Van Allen MI, Nelson TN, Bolbocean C, Connolly MB and Farrer MJ (2019) Diagnostic Yield and Treatment Impact of Targeted Exome Sequencing in Early-Onset Epilepsy. Front. Neurol. 10:434. doi: 10.3389/fneur.2019.00434

Targeted whole-exome sequencing (WES) is a powerful diagnostic tool for a broad spectrum of heterogeneous neurological disorders. Here, we aim to examine the impact on diagnosis, treatment and cost with early use of targeted WES in early-onset epilepsy. WES was performed on 180 patients with early-onset epilepsy (≤5 years) of unknown cause. Patients were classified as Retrospective (epilepsy diagnosis >6 months) or Prospective (epilepsy diagnosis <6 months). WES was performed on an Ion Proton™ and variant reporting was restricted to the sequences of 620 known epilepsy genes. Diagnostic yield and time to diagnosis were calculated. An analysis of cost and impact on treatment was also performed. A molecular diagnoses (pathogenic/likely pathogenic variants) was achieved in 59/180 patients (33%). Clinical management changed following WES findings in 23 of 59 diagnosed patients (39%) or 13% of all patients. A possible diagnosis was identified in 21 additional patients (12%) for whom supporting evidence is pending. Time from epilepsy onset to a genetic diagnosis was faster when WES was performed early in the diagnostic process (mean: 145 days Prospective vs. 2,882 days Retrospective). Costs of prior negative tests averaged $8,344 per patient in the Retrospective group, suggesting savings of $5,110 per patient using WES. These results highlight the diagnostic yield, clinical utility and potential

cost-effectiveness of using targeted WES early in the diagnostic workup of patients with unexplained early-onset epilepsy. The costs and clinical benefits are likely to continue to improve. Advances in precision medicine and further studies regarding impact on long-term clinical outcome will be important.

Keywords: targeted WES, early-onset epilepsy, diagnostic yield, cost estimation, Canada

INTRODUCTION

Epilepsy is a common pediatric neurological disorder associated with an increased risk of developmental delay, autism and psychiatric illness; and for which treatment is ineffective in 30–40% of patients. High-throughput sequencing (HTS) has become a widespread diagnostic tool in various genetic conditions, including epilepsy (1), vastly improving molecular diagnosis. Its clinical utility has been proven in epileptic encephalopathies and in mixed epilepsy cohorts (2–11); and in neurodevelopmental disorders (12–14) in which epilepsy is a comorbid feature. The diagnostic yield ranges between 10 and 60%, settling around 25% in large studies with broader inclusion criteria, and with comparable diagnostic rates between gene panels and WES (1). A genetic diagnosis of epilepsy may enable more accurate counseling regarding prognosis and recurrence risk, avoids unnecessary medical investigations and may change care. It also allows families to connect with the same genetic condition and/or join support groups. Recent studies have demonstrated the potential cost savings of WES in the diagnostic work-up of children with suspected monogenic disorders (15–22). However, in Canada, access to such technology in clinical care is variable. In this British Columbia study, we assess the effectiveness of using WES by comparing diagnostic yield, time to diagnosis, and cost to current clinical practices. The potential treatment impact of a genetic diagnosis is also described.

METHODS

Patients

One-hundred and eighty patients with epilepsy (23) were enrolled between December 2014 and September 2018. All had seizure onset at ≤5 years of undefined cause after clinical evaluation, EEG, brain MRI and chromosome microarray investigations. Seizure types and electroclinical syndromes were classified according to the International League Against Epilepsy (ILAE) (24). Patients with self-limiting benign electroclinical syndromes, such as Childhood Absence Epilepsy (onset >4 years), were excluded as they most likely have multifactorial inheritance. Patients were classified as **Retrospective** ($n = 127$), defined as an epilepsy diagnosis >6 months before study enrollment with a standard clinical approach to genetic testing (variable genetic tests which include gene-by-gene approach using Sanger sequencing, small epilepsy gene panels using high-throughput sequencing, and/or mitochondrial DNA sequencing; or **Prospective** ($n = 53$), which included an epilepsy diagnosis <6 months before study enrollment date and having limited to no genetic testing. Varying degrees of screening tests for inborn errors of metabolism; such as plasma amino acids, lactate and ammonia, were also performed in both groups. Clinical data was recorded using a secure Research Electronic Data Capture (REDCap) (25) information system hosted at the Child and Family Research Institute.

This study was approved by the BC Children's Hospital and University of British Columbia Ethics Board (protocol number H14-01531). Informed consent and/or assent were obtained before study inclusion in accordance with the Declaration of Helsinki.

Whole-Exome Sequencing

Genomic DNA was extracted from peripheral blood lymphocytes following standard protocols. Exonic regions were captured using the Ion AmpliSeq Exome Kit (57.7 Mb) and WES was performed on an Ion Proton™ according to manufacturers' recommendations (Life Technologies Inc., CA) within 2 weeks of receiving samples. Reads were aligned against the human reference genome hg19. Variant annotation was performed with ANNOVAR (26) integrating data from PHAST PhyloP (27), SIFT (28), Polyphen2 (29), LRT (30), and MutationTaster (31) algorithms, Combined Annotation Dependent Depletion (CADD) scores (32), dbSNP (www.ncbi.nlm.nih.gov/SNP/), the Genome Aggregation Database (gnomAD; gnomad.broadinstitute.org) and ClinVar (33) (www.ncbi.nlm.nih.gov/clinvar). Additionally, variants were compared to an in-house database containing more than 900 exomes to exclude platform artifacts and common variants not present in public databases.

Analysis was restricted to 620 genes previously implicated in epilepsy (**Supplementary Table 1**), using a gene-reporting pipeline developed in-house. The gene list was compiled through the combination of a comprehensive literature search (Pubmed, OMIM) and clinically available epilepsy panels. Annotation was limited to exonic non-synonymous and splicing (±5 bp) substitutions. Homozygous variants, potential compound heterozygous variants (defined as genes with >1 variant locus per individual) with a minor allele frequency (MAF) <1% and heterozygous variants with MAF <0.01% were reported. All samples were required to meet minimum quality standards, with a WES average coverage >80X.

Sanger sequencing, performed as previously described (34), was used on a case-specific basis in a few individuals with very specific clinical phenotypes to complete regions of poor coverage in genes related to the patient's phenotype when no candidate variants were identified, or when a heterozygous and potentially pathogenic variant was identified in gene previously

implicated in autosomal recessive disease. No additional variants were identified though post-WES Sanger sequencing.

Variant Prioritization and Validation

Cases were reviewed at a bi-weekly meeting by a multi-disciplinary genomic team. Variant prioritization was performed based on: (1) frequency in public databases; (2) predicted protein impact; (3) disease inheritance, and; (4) correlation of patient phenotype and candidate gene literature. Up to 3 putative causative variants were validated by Sanger sequencing in patient and parental samples. Clinical Sanger sequencing confirmation and interpretation in accordance with ACMG guidelines (35) allowed disclosure to families and management adjustments when indicated. Two time intervals were measured for the first 50 patients: (1) from a clinical diagnosis of epilepsy to Sanger validation of a putative pathogenic variant; and (2) from enrollment with genetic counseling to Sanger validation of the same.

Additional Analysis

Exome data was periodically reanalyzed in patients, if no genetic diagnosis was identified in the initial analysis. Moreover, trio WES was performed in 27 patients (22 Retrospective and 5 Prospective) with no diagnosis.

Genetic Counseling and Treatment Implications

Pre- and post-test genetic counseling was performed for each patient/family. As only a limited set of 620 genes related to seizure disorders were annotated, and only in affected probands, reporting related to incidental (secondary) findings was uncommon (36). Genetic disorders with specific therapeutic implications (47 genes) were defined as conditions in which current literature supports a preferred antiepileptic medication and/or approach (37–39).

Cost Estimation

For the first 50 patients, resource use data were retrospectively acquired from electronic health records and medical charts. Cost estimates in Canadian dollars were based on micro-cost information from the British Columbia Provincial Medical Service Plan Index (2015), Canadian Interprovincial Reciprocal Billing Rates (2014/2015), Children's and Women's Health Center of British Columbia Internal Fee Schedule (2015) and the internal accounting system. Diagnostic costs included: biochemical tests, imaging tests, genetic tests, neurophysiological tests, and biopsies (a complete list of tests is provided in **Appendix 1**). Academic and/or hospital pricing is used throughout. Inpatient hospitalization costs, outpatient visits such as clinic visits, and indirect costs such as parental time off work for medical visits related to their child's epilepsy were not included. All categorical and quantitative variables were analyzed using STATA (Release 13, College Station, TX).

TABLE 1 | Results: Demographics and diagnostic yield.

	All Patients ($N = 180$)	Prospective ($N = 53$)	Retrospective ($N = 127$)
Age at Epilepsy Onset (months) average (range)	18 (0.03–60)	16 (0.1–60)	18 (0.03–60)
Males; Females	77;103	27;26	50;77
DIAGNOSIS			
Definite/likely	59 (33%)	21 (40%)	38 (30%)
Treatment Implications	**27 (46%)**	**15 (71%)**	**12 (32%)**
Possible	21 (12%)	4 (8%)	17 (13%)

Patients highlighted in bold are those for whom a genetic diagnosis had treatment implications.

RESULTS

Targeted WES was performed on 180 subjects and clinical features are summarized (**Supplementary Table 2**-first 50 patients are indicated in bold). Detailed clinical information has previously been reported for subjects 002, 013, 044, 073, and 144 (40–43). The average age of epilepsy onset was 18 months (range 0.03–60 months), 16 months for Prospective cases ($n = 53$) and 18 months for Retrospective cases ($n = 127$) (**Tables 1**, **2**). Of the 620 genes, 87% had at least 80% of their consensus-coding region sequenced with >20X coverage (**Supplementary Table 1**).

Diagnostic Yield

A molecular diagnosis was established in 59/180 patients (33%) (**Table 1**). Pathogenic/likely pathogenic variants were identified in 41 genes. The majority of the diagnosed patients (41/59) had an autosomal-dominant disorder; of these 33 had a *de-novo* variant and remaining inherited from an affected parent and/or inheritance status unknown for one or more parent. Five patients had an autosomal-recessive disorder and the remaining 13 patients had an X-linked disorder (10 patients with X-linked dominant variants and 3 male patients with maternally inherited X-linked recessive disorders). In addition, a variant of uncertain significance (VUS) possibly explaining the clinical symptoms of the index patient was identified in 21 cases (12%) (**Supplementary Table 3**).

The diagnostic yield was higher in the Prospective (40%) than Retrospective group (30%). Patients in whom a diagnosis was made had earlier onset epilepsy (mean 13.2 vs. 21.9 months), and an epileptic encephalopathy was more common (**Table 3**). Of 82 patients with epileptic encephalopathy a definite or likely pathogenic variant was identified in 36 (44%) (**Supplementary Table 4**).

Treatment Implications

A genetic disorder with specific therapeutic implications was diagnosed in 27 patients and management was influenced and/or altered in 23 (12 Prospective and 11 Retrospective). Clinical information, treatment changes, and impact are summarized (**Table 2**).

TABLE 2 | Patients with definite/likely diagnosis and treatment impact.

ID Sex	AAO	Epilepsy type	Gene (IP)	GRCh37/hg19	Variant	Zyg	Origin	Treatment Impact
PROSPECTIVE PATIENTS								
001 M	3 m	Dravet	*SCN1A (AD)*	chr2:166848491	NM_001165963:c.5294T>C;p.F1765S	het	*De novo*	Change from levetiracetam to clobazam, valproic acid, and topiramate
010 F	18.3 m	Unclassified	*SMC1A (XLD)*	chrX:53409269	NM_006306:c.3321C>G;p.Y1107X	het	*De novo*	
018 F	6 m	Ohtahara, West	*STXBP1 (AD)*	chr9:130434396	NM_003165:IVS12+1GT>AA;NA[c]	het	*De novo*	
033 F	9.2 m	EE	*POLG (AR)*	chr15:89871929	NM_002693:c.1157G>C;p.R386P	comp het	♀carrier	Stopped valproic acid; early palliative care; prenatal testing for next pregnancy
				chr15:89866657	NM_002693:c.2243G>C;p.W748S		♂carrier	
059 M	24 m	Unclassified	*GABRA1 (AD)*	chr5:161322788	NM_000806:c.973T>C;p.F325L	het	*De novo*	
069 M	51.5 m	Unclassified	*MED23 (AR)*	chr6:131944505	NM_015979:c.382G>A;p.G128R	comp het	♀carrier	
				chr6:131941826	NM_015979:c.539C>A;p.A180D		♂carrier	
098 M	1.5 m	Unclassified	*KCNT1 (AD)*	chr9:138660693	NM_020822:c.1420C>G;p.R474G	het	*De novo*	No change in management
104 M	0.9 m	SLFNE	*KCNQ2 (AD)*	chr20:62059782	NM_172107:c.154delT;p.I385TfsTer4	het	♀carrier	Stopped phenobarbital at 2 m; avoided MRI with anesthetic; seizure free and normal development at 6 m
120 F	1.8 m	West syndrome	*ADSL (AR)*	chr22:40754948	NM_000026:c.563G>A;p.R188H	comp het	♀carrier	S-Adenosyl-l-methionine trial proposed but patient died just prior to implementation
				chr22:40760969	NM_000026:c.1277G>A;p.R426H		♂carrier	
144 F	3 days	Unclassified	*FGF12*[a] *(AD)*	chr3:192053223	NM_021032:c.341G>A;p.R114H	het	*De novo*	Remains seizure free with normal development on carbamazepine
165 M	21.6 m	Dravet	*SCN1A (AD)*	chr2:166915162	NM_001165963:c.301C>T;p.R101W	het	*De novo*	Avoiding sodium channel blockers and started Valproic acid early
167 F	7.7 m	Unclassified	*SCN8A (AD)*	chr12:52200900	NM_014191:c.5630A>G;p.N1877S	het	♂carrier	Kept on Sodium channel blockers. Seizure free and normal development
193 M	1.5 m	West syndrome	*ARX (XLR)*	chrX:25022869	NM_139058:c.1607G>C;p.R536T	hemi	♀carrier	
197 M	4.4 m	Dravet	*SCN1A (AD)*	chr2:166866246	NM_001165963:c.3985C>T;p.R1329X	het	*De novo*	Avoiding sodium channel blockers and started Valproic acid early
200 F	8.9 m	Dravet	*SCN1A (AD)*	chr2:166859067	NM_001165963:c.4198delA;p.I1400X	het	Unknown	Avoiding sodium channel blockers and started Valproic acid early
201 M	4.6 m	Dravet	*SCN1A (AD)*	chr2:166848872	NM_001165963:c.4913T>A;p.I1638N	het	*De novo*	Avoiding sodium channel blockers and started Valproic acid early
205 M	3 days	EE	*SCN1A (AD)*	chr2:166848429	NM_001165963:c.5356C>G;p.L1786V	het	*De novo*	Influenced medication choice: topiramate
206 M	4.6 m	Unclassified	*PRRT2 (AD)*	chr16:29824973	NM_145239:c.604_607delTCAC; p.S202HfsTer26	het	♂carrier	No change in management
222 F	52.1 m	EE	*MECP2 (XLD)*	chrX:153296878	NM_004992:c.401C>G;p.S134C	het	*De novo*	

(Continued)

TABLE 2 | Continued

ID Sex	AAO	Epilepsy type	Gene (IP)	GRCh37/hg19	Variant	Zyg	Origin	Treatment Impact
234 M	0.8 w	Unclassified	*ALDH7A1 (AR)*	chr5:125882034	NM_001182:c.1547A>G;p.Y516C	het	♀carrier	Treated with B6, lysine restricted diet
				chr5:125887751	NM_001182:c.1279G>C;p.E427Q	het	♂carrier	
237 F	1 m	SLFIE	*SCN2A (AD)*	chr2:166231307	NM_021007:c.4085A>T;p.K1362M	het	♀carrier	Discontinue medication early because of predicted benign course
RETROSPECTIVE PATIENTS								
002 M	3.2 m	Dravet-like	*ATP1A2 (AR)*	chr1:160100072	NM_000702:c.1642C>T;p.R548C	comp het	♀carrier	Stopped stiripentol; started flunarizine. No further episodes on flunarizin
				chr1:160109762	NM_000702:c.3022C>T;p.R1008W		♂carrier	
005 F	7 m	West syndrome	*ALG13 (XLD)*	chrX:110928268	NM_001099922:c.320A>G;p.N107S	het	*De novo*	
006 M	10.4 m	LGS	*GABRB3 (AD)*	chr15:27017551	NM_000814:c.238A>G;p.M80V	het	Not ♀, ♂ NA	
013 F	5 m	EE	*KCNQ5*[a] *(AD)*	chr6:73821107	NM_001160133:c.1106C>G;p.P369R	het	*De novo*	
014 M	0.5 w	EE	*PNPT1*[b] *(AR)*	chr2:55910954	NM_033109:c.419C>T;p.P140L	hom	♀ & ♂ carrier	
023 M	11.2 m	EE	*PIGA (XLR)*	chrX:15344061	NM_002641:c.823C>T;p.R275T	hemi	♀carrier	
039 M	1 day	EE	*KCNQ2 (AD)*	chr20:62070997	NM_172107:c.881C>T;p.A294V	het	*De novo*	Topiramate changed to carbamazepine: no improvement in seizure frequency 6 months later
040 F	3 days	EE	*KCNQ2 (AD)*	chr20:62071034	NM_172107:c.844G>T;p.D282Y	het	*De novo*	Phenytoin changed to carbamazepine: seizures less frequent and shorter 9 months later
043 F	3 m	West syndrome	*PAFAH1B1 (AD)*	chr17:2577530	NM_000430:c.849_853delCTGGG; p.W292SfsTer10	het	*De novo*	
044 M	2.1 m	EE	*SLC1A2*[b] *(AD)*	chr11:35336636	NM_004171:c.244G>A;p.G82R	het	*De novo*	
050 M	13.7 m	Unclassified	*TUBB2B (AD)*	chr6:3226887	NM_178012:c.74G>A;p.S25N	het	*De novo*	
063 M	18.5 m	Unclassified	*RORA*[b] *(AD)*	chr15:60803740	NM_134261:c.505C>T;p.Q169X	het	*De novo*	
065 F	3.5 m	West syndrome	*SLC35A2 (AD)*	chr20:62070997	NM_001282651:c.550_552delTCC; p.S184del	het	*De novo*	Galactose trial: 6 months later more alert and interactive; no change in seizure frequency
071 F	46.5 m	Unclassified	*HNRNPH2*[b] *(XLD)*	chrX:100667593	NM_01959:c.617G>A;p.R206Q	het	Not ♀, ♂ NA	
072 M	29.2 m	Unclassified	*TCF20*[b] *(AD)*	chr22:42611134	NM_181492:c.178C>T;p.R60X	het	*De novo*	
073 F	12 m	EE	*YWHAG*[b] *(AD)*	chr7:75959244	NM_012479:c.394C>T;p.R132C	het	*De novo*	
077 F	2.1 m	West, LGS	*CDKL5 (XLD)*	chrX:18622288	NM_003159:c.1245_1246delAG; p.E416VfsTer2	het	*De novo*	
093 F	21.4 m	EE	*SMARCA2*[a] *(AD)*	chr9:2081857	NM_139045:c.2210C>A;p.S737Y	het	*De novo*	
094 F	7 m	Dravet	*SCN1A (AD)*	chr2:166915157	NM_001165963:c.305delT; p.F102SfsTer10	het	*De novo*	Changed medications: added clobazam and stiripentol

(Continued)

TABLE 2 | Continued

ID Sex	AAO	Epilepsy type	Gene (IP)	GRCh37/hg19	Variant	Zyg	Origin	Treatment Impact
100 F	10.1 m	Unclassified	*ATP1A3 (AD)*	chr19:42471896	NM_152296:c.2839G>A;p.G947R	het	*De novo*	No change in management. Already on Flunarizine
106 F	3.7 m	EE	*STXBP1 (AD)*	chr9:130413885	NM_003165:c.41T>G;p.I14S	het	*De novo*	
113 F	7.5 m	West syndrome	*DYNC1H1 (AD)*	chr14:102469031	NM_001376:c.4700G>A;p.R1567Q	het	*De novo*	
123 F	11.8 m	EE	*GABRA1 (AD)*	chr5:161309644	NM_000806:c.604C>T;p.R214C	het	*De novo*	Based on functional studies, will be started on new medication (pending publication)
126 F	60 m	Unclassified	*RORA*[b] *(AD)*	chr15:60803459	NM_134261:c.785dupG; p.E263RfsTer20	Het	*De novo*	
130 F	1.1 m	West syndrome	*DEPDC5 (AD)*	chr22:32239187	NM_001242896:c.2623delT; p.Y875Tfs46	het	*De novo*	
132 M	28.1 m	CSWS	*CNKSR2 (XLR)*	chrX:21609267	NM_014927:c.1785G>A; p.W595X	hemi	♀carrier	
137 F	24 m	Unclassified	*DYRK1A (AD)*	chr21:38865409	NM_001396:c.1042G>A;p.G348R	het	Not ♂, ♀ NA	
138 F	18 m	EE	*DCX (XLD)*	chrX:110653428	NM_178151:c.199G>A;p.G67R	het	*De novo*	
148 F	12 m	Unclassified	*DYRK1A (AD)*	chr21:38865409	NM_001396:c.763C>T;p.R255X	het	*De novo*	
152 F	7 m	EE	*NEXMIF*[b] *(XLD)*	chrX:73962510	NM_001008537:c.1882C>T;p.R628X	het	unknown	
158 F	26.4 m	MAE/Febrile seizures plus	*SCN1A (AD)*	chr2:166848429	NM_001165963:c.298T>G.F100V	het	*De novo*	No change in management
160 F	27.5 m	EE	*MECP2 (XLD)*	chrX:153296777	NM_004992:c.502C>T;p.R168X	het	*De novo*	
168 F	41.5 m	EE	*MECP2 (XLD)*	chrX:153296857	NM_004992:c.422A>C;p.Y141S	het	*De novo*	
171 F	10 m	EE	*HNRNPU (AD)*	chr1:245025823	NM_031844:c.817C>T;p.Q273X	het	*De novo*	
208 F	10.8 m	Unclassified	*PCDH19 (XLD)*	chrX:99662976	NM_001184880:c.619_620delCGinsA; p.R207KfsTer5	het	*De novo*	Trial of steroids, but no response
213 M	1 day	Unclassified	*ATP1A3 (AD)*	chr19:42471896	NM_152296:c.2443G>A;p.E815K	het	*De novo*	Started Flunarizine with reduced hemiplegic episodes
230 F	3.5 m	West, LGS	*SCN8A (AD)*	chr12:52099304	NM_014191:c.1238C>A;p.A413D	het	*De novo*	Sodium channel blocker tried, not continued
248 F	37 m	Unclassified	*SCN1A (AD)*	chr2:166909410	NM_001165963:c.646A>T;p.R216X	het	*De novo*	Influenced choice of future treatment (stiripentol, CBD oil)

[a]*Variants identified by trio WES.*

[b]*Variants identified by WES reanalysis.*

AAO, Age At Onset; AD, autosomal dominant; AR, autosomal recessive; CSWS, Epileptic Encephalopathy with continuous spike-and-wave during sleep; D, days; EE, unspecified Epileptic Encephalopathy; FS, Febrile seizure; IP, inheritance pattern; LGS, Lennox-Gastaut syndrome; MAE, Epilepsy with myoclonic-atonic seizures; M, months; NA, not available; SE, status epilepticus; SLFNE, Self-limited familial neonatal/infantile epilepsy; XL, X-linked; Zyg, zygosity; het; heterozygous; hom, homozygous; hemi, hemizygous.

[C]*c.1029+1_1029+2delGTinsAA disrupts the canonical splice donor site of exon 12 and is predicted to abolish normal splicing.*

Patients highlighted in bold are those for whom a genetic diagnosis had treatment implications.

TABLE 3 | Clinical features in patients with and without a genetic diagnosis.

Genetic Diagnosis[a]	Mean AAO (range)	Males (%)	EE (%)	Treatment Resistant[b] (%)	GDD/ID (%)	Autism (%)	MRI Abnormal (%)
Definite or Likely ($n = 59$)	13.2 months (0.03–60)	39	61	80	85	25	37
No Diagnosis ($n = 100$)	21.9 months (0.03–60)	43	46	81	76	20	30

[a] *Individuals with variants of unknown significance or a possible genetic diagnosis are excluded (8).*
[b] *Treatment resistant refers to failure to respond to 2 or more appropriate anti-seizure medications.*
AAO, Age at onset; EE, Epileptic Encephalopathy; GDD/ID, Global Developmental Delay/Intellectual Disability.

Comparative Time to Diagnosis in First 50 Patients

The mean time to genetic diagnosis from study enrolment with genetic counseling to research validation of the variant was 38 days (20–70) for the Prospective group, 54 days (22–105) for the Retrospective group, and 47 days (20–105) overall. The mean time from epilepsy diagnosis to research validation of genetic diagnosis was 145 days (42–242) for the Prospective group and 2,882 days (429–7,686) or ∼8 years for the Retrospective group.

Cost Analysis in First 50 Patients

Point estimates and 95% confidence intervals based on bootstrapped standard errors (1,000 times with replacement) for each category of diagnostic test by cohorts were calculated (**Table 4**). All cost estimates use rates effective for the 2014–2015 fiscal year. The mean total cost related to the diagnosis of epilepsy was $4,524 (range $1,223–$7,852) for the Prospective cohort and $8,344 (range $3,319–$17,579) for the Retrospective cohort. Diagnostic imaging and electrophysiological tests comprise >60% of total epilepsy-related diagnostic costs. The mean for diagnostic imaging testing constituted $1,391 and $3,276, for Prospective and Retrospective cohorts, respectively. The mean for electrophysiological testing constituted $1,353 and $2,731, for Prospective and Retrospective cohorts, respectively. Our alternative scenario for diagnostic testing is MRI, EEG, chromosome microarray (CMA) and WES testing with Sanger sequencing validation, which amounts to $3,234 per patient (**Supplementary Table 5**). The difference in mean total cost related to the diagnosis of epilepsy for Prospective ($4,524) and Retrospective ($8,344) groups, exceeds the cost of our diagnostic alternative ($3,234). The potential average savings of targeted WES in the diagnostic workup constitute $1,290 per Prospective patient and $5,110 per Retrospective patient.

DISCUSSION

High-throughput sequencing has been proven to be a great diagnostic tool in clinical practice in a variety of genetic conditions, and if used early in the diagnostic workup can lead to a reduction of costs associated with obtaining a molecular diagnosis (22). Gene panel sequencing is often favored over WES based on diagnostic yield, higher coverage and cost-savings (1). However, direct comparisons of diagnostic yield and/or costs of gene panel testing are limited. A comparative coverage analysis restricted to disease-causing variants identified through panels demonstrated that targeted WES detects ≥98.5% of those mutations (44), and targeted WES has been recently shown to have a higher diagnostic yield compared to gene panels (45). A major advantage of WES over panels is the ability to sequence the entire coding genome. Such comprehensive assessment can facilitate re-analysis for novel genes as they are implicated. In the course of this study several new epilepsy genes were identified by other research groups and published in the medical literature. We were able to go back to the original WES data and examine those genes in patients without a diagnosis. Re-analysis of WES data identified new diagnoses in eight patients (014, 044, 063, 071, 072, 073, 126, 152) and three additional diagnosis (013, 093, 144) were identified by trio WES, overall increasing the diagnostic rate from 27 to 33%. Given its static nature, panel sequencing is unable to include such contemporary targets. Newly discovered genes cannot be added to the test without re-design and validation, ultimately reducing the cost-effectiveness of gene panel testing.

The clinical utility of targeted WES with Sanger validation (limited ≤3 variants/exome) is supported by the identification of a definite or likely diagnosis in 59/180 (33%) patients and a possible diagnosis in an additional 21/180 (12%) (**Table 1**). A higher yield was found in the Prospective group with new-onset epilepsy and supports earlier testing, though the number of patients is small. However, this may also reflect increased severity of the disease, survival and potentially some bias in case referral. The Retrospective group had already undergone extensive clinical testing that was non-diagnostic. Nevertheless, our ability to still identify a genetic diagnosis supports the technology's superior resolution, while related data on phenotypes, management and outcomes may yet inform clinical practice.

The diagnostic yield in our study is comparable to previous findings (2–11). Most variants were *de-novo* and the genetic causes identified were heterogeneous. However, multiple variants were identified in several genes with the most common being *SCN1A*, followed by *KCNQ2* and *MECP2* (**Table 2**). In a comparable cohort, positive results were identified by WES in 112/293 (38.2%) epilepsy patients (3). We concur that the diagnostic yield is likely affected by the characteristics of the group studied, sample size, platform used (gene panel or WES) and the timing of the study, given ongoing gene discoveries in epilepsy. In our study, patients with a genetic diagnosis were younger and more likely to have an epileptic encephalopathy

TABLE 4 | Average diagnostic investigation cost per patient.

	Mean	Bootstrap Std. Err.	95% CI		Range Min	Range Max
COMBINED DIAGNOSTIC COST						
Retrospective	$8,344.27	$556.97	$7,252.61	$9,435.90	$3,318.50	$17,578.8
Prospective	$4,524.07	$497.57	$3,548.85	$5,499.29	$1,223.18	$7,852
LAB TESTS						
Retrospective	$1,333.5	$83.71	$1,169.42	$1,497.56	$123.30	$3,129.91
Prospective	$1,151.32	$135.14	$886.43	$1,416.19	$209.75	$1,959.19
GENETIC TESTS						
Retrospective	$1,179.55	$98.80	$985.90	$1,373.20	0	$2,279.34
Prospective	$633.187	$144.27	$350.41	$915.96	0	$1,720
DIAGNOSTIC IMAGING						
Retrospective	$3,276.10	$214.10	$2,856.47	$3,695.74	$1,460	$6,836
Prospective	$1,391.38	$150.26	$1,096.86	$1,686	$630	$2,290
ELECTROPHYSIOLOGICAL						
Retrospective	$2,731.22	$376.26	$1,993.75	$3,468.70	0	$8,460.45
Prospective	$1,353.12	$315.64	$734.4	$1,971.78	$188.01	$3,572.19

when compared to patients in which no genetic cause was found. Similar to a prior study (3), patients with an epileptic encephalopathies had a high rate of positive findings (44%).

Our results support the feasibility of targeted WES to rapidly provide clinically-confirmed genetic diagnoses in early-onset epilepsy. Time to Sanger sequencing validation from enrollment averaged 7 weeks which is similar to the 6–8 week turn-around-time quoted by most commercial testing labs. However, this estimate did not include the additional time required to obtain provincial government approval, on a case-by-case basis, to fund WES.

A timely genetic diagnosis is important when considering the potential for treatment impact and optimization of patient outcomes. Twenty-seven of the fifty nine patients with a genetic diagnosis (46%) had a disorder with specific treatment implications; for 23 patients an immediate change in medical management was made (**Table 2**). The number of genetic disorders identified to have specific treatments implications is likely to grow with ongoing advances in precision medicine.

In British Columbia, the average savings are estimated to be between $1,290 and $5,110 per patient, depending on whether they are new Prospective referrals or Retrospective. Of note, price estimates reflect academic and/or hospital costs rather than commercial costs which are 1–5X higher. The Canadian sequencing costs cited are comparable to previous reports but will decrease as even higher throughput sequencing technologies become accessible (15–18). Current healthcare cost estimates are also conservative as patients without a genetic diagnosis will undoubtedly require additional clinic visits and inpatient hospital stays, including epilepsy monitoring unit admissions related to finding the cause of their condition. Of note, a targeted WES approach did not lead to a substantial increase in referrals for incidental findings. Overall, our findings show targeted WES may provide an effective end to an otherwise invasive, time consuming and costly diagnostic odyssey, with societal and economic benefits. Our results also support WES implementation beyond early-onset epileptic encephalopathies as we have examined a larger and more diverse group of children (18).

Limitations and Strengths

Our study has several limitations including small sample size although our diagnostic yield is comparable to previous studies. Incomplete coverage of the 620 genes analyzed was partially addressed as outlined in the methods. Proband-parent trio-based WES analyses were not used primarily for financial reasons. Analysis was restricted to 620 epilepsy genes, rather than the entire exome, to identify a genetic diagnosis as quickly as possible and to minimize secondary findings. Assessing relevance of secondary findings and proving pathogenicity of variants in novel candidate epilepsy genes is costly; thus, this approach was taken to maximize patient care and minimize cost. WES data from patients with initial negative results continues to be periodically reviewed for variants in newly described epilepsy genes. In subsequent WES trio analysis, a subset of families has helped identify novel genetic etiologies (41). All rare variants were considered however the Ion Proton™ sequencing platform tends to make mis-leading variant calling errors with small in/dels and homo-polymer stretches, with an excess of between 58 and 76% false positive calls (46). We have also identified instances of negative calls. Illumina sequencing platforms have better performance but assessing exon dosage from exome data is challenging at this sequencing depth. Panel sequencing, designed for more uniform coverage and greater depth, would be advantageous if the candidate gene was included or whole genome sequencing given the ability to detect all variants albeit for greater cost at lower coverage. Limited demographic information was provided for on the majority of patients and may be helpful in assessing variant frequencies in specific ethnic groups. Unfortunately, the ability to infer ancestry information

from exome data is rather limited, in contrast to high-density SNP arrays, and not entirely reliable.

Although a significant number of genetic diagnoses had potential treatment implications, the long-term impact on clinical outcome following genetically-informed therapeutic interventions is unknown. Early diagnosis and early intervention are important, but advances in precision medicine are also required.

The methods employed for cost analysis cannot replace a prospective randomized controlled trial (RCT) and may not have accurately assessed or included all healthcare costs related to an epilepsy diagnosis. However, an RCT assessing the effect of WES testing on healthcare costs is not yet a practical consideration. Our estimates are not a perfect or a complete description of the current diagnostic work-up, as test records are scattered across different electronic health records systems and paper charts. Data collation within an accessible unified health electronic record would help identify where additional savings are possible. In this study, indirect costs, and the psychosocial impact on the child and family were not measured.

CONCLUSION/SUMMARY

Targeted WES with limited Sanger sequencing validation is a rapid and minimally invasive test with potential to save costs within the Canadian healthcare system. An early genetic diagnosis may improve a patient's clinical outcome and quality of life. Further research on larger cohorts is warranted to inform diagnosis, clinical outcome and precision medicine. Acknowledging the limitations of our study, targeted WES with Sanger sequencing validation substantially improves current practice and is recommended as the dominant diagnostic strategy in early onset epilepsy. Minimally, as high-throughput sequencing costs continue to fall, trio-based whole exome sequencing reporting (and potentially re-reporting if negative), averting the need for Sanger validation for *de novo* variants, should be implemented as a first-line test strategy in British Columbia.

ETHICS STATEMENT

This study was carried out in accordance with the recommendations of BC Children's Hospital and University of British Columbia Ethics Board with written informed consent from all subjects. All subjects gave written informed consent in accordance with the Declaration of Helsinki. The protocol was approved by the BC Children's Hospital and University of British Columbia Ethics Board (protocol number H14-01531).

AUTHOR CONTRIBUTIONS

MD contributed to study conception and design, data analysis and interpretation, review of patients clinically, obtaining funding, drafting the manuscript. IG contributed to genetic data acquisition, analysis and interpretation, revised the manuscript. CD contributed to data acquisition, analysis and interpretation, and revised the manuscript. MM contributed to genetic data acquisition and to data analysis. CyB contributed to clinical assessments, data acquisition and interpretation, revised the manuscript. DE performed bioinformatics analysis. SB designed REDCap database, contributed to data acquisition, analysis and interpretation, revised the manuscript. ET contributed to data acquisition and organization. LH, AD, AM, KS, EL-R, and BB contributed to clinical assessments and data acquisition/interpretation. GH and RS performed biochemical clinical assessments, contributed to data interpretation. CvK contributed to study design and variant interpretation. ES assisted preparation of execution of study. PE performed cytogenetic assessment. SA performed genetic counseling, contributed to data acquisition and literature review. MV contributed to genetic counseling, review of results and literature, and revising manuscript. TN contributed to data analysis and interpretation, performed clinical variant interpretation, revised the manuscript, negotiated funding for variant clinical validation. CoB performed economics data acquisition, analysis and interpretation; drafted economics section of manuscript. MC performed electroclinical phenotyping, revised the manuscript, obtained funding. MF contributed to study conception and design, data analysis and interpretation, obtained funding, and revised the manuscript.

ACKNOWLEDGMENTS

The Djavad Mowafaghian Foundation generously enabled this molecular research to take place at the Djavad Mowafaghian Centre for Brain Health. The work was also supported by Canada Excellence Research Chair and Leading Edge Endowment funds, the Rare Disease Foundation, Grocholski Foundation and the Alva Foundation. We thank the children and families that took part in this study. We gratefully acknowledge Dr. Suzanne Vercauteren MD, PhD (Director), Dr. William Gibson MD, PhD (Chair and Biospecimen Advisory Committee member), Tamsin Tarling (Biobank Administrative Manager), and the technical expertise of Katelin Townsend of the BC Children's Hospital BioBank, which is supported by Mining for Miracles through the BC Children's Hospital Foundation. We also thank the BC Children's Hospital Department of Pathology and Laboratory Medicine and the BC Children's Hospital EEG (Electroencephalogram) Department. We are also grateful to Dr. Vesna Popovska MD, Katie Pezarro, and Giselle Hunt BSc, from the Neurology Research Team at BC Children's Hospital; and Dr. Hilary Vallance MD and Dr. Graham Sinclair PhD, from the Department of Pathology, Biochemical Genetics Laboratory at BC Children's Hospital, for their assistance on this project.

SUPPLEMENTARY MATERIAL

The Supplementary Material for this article can be found online at: https://www.frontiersin.org/articles/10.3389/fneur.2019.00434/full#supplementary-material

REFERENCES

1. Dunn P, Albury CL, Maksemous N, Benton MC, Sutherland HG, Smith RA, et al. Next generation sequencing methods for diagnosis of epilepsy syndromes. *Front Genet.* (2018) 9:20. doi: 10.3389/fgene.2018.00020
2. Lemke JR, Riesch E, Scheurenbrand T, Schubach M, Wilhelm C, Steiner I, et al. Targeted next generation sequencing as a diagnostic tool in epileptic disorders. *Epilepsia.* (2012) 53:1387–98. doi: 10.1111/j.1528-1167.2012.03516.x
3. Helbig KL, Farwell Hagman KD, Shinde DN, Mroske C, Powis Z, Li S, et al. Diagnostic exome sequencing provides a molecular diagnosis for a significant proportion of patients with epilepsy. *Genet Med.* (2016) 18:898–905. doi: 10.1038/gim.2015.186
4. Allen NM, Conroy J, Shahwan A, Lynch B, Correa RG, Pena SDJ, et al. Unexplained early onset epileptic encephalopathy: exome screening and phenotype expansion. *Epilepsia.* (2016) 57:e12–17. doi: 10.1111/epi.13250
5. Della Mina E, Ciccone R, Brustia F, Bayindir B, Limongelli I, Vetro A, et al. Improving molecular diagnosis in epilepsy by a dedicated high-throughput sequencing platform. *Eur J Hum Genet.* (2015) 23:354–62. doi: 10.1038/ejhg.2014.92
6. Mercimek-Mahmutoglu S, Patel J, Cordeiro D, Hewson S, Callen D, Donner EJ, et al. Diagnostic yield of genetic testing in epileptic encephalopathy in childhood. *Epilepsia.* (2015) 56:707–16. doi: 10.1111/epi.12954
7. de Kovel CGF, Brilstra EH, van Kempen MJA, van't Slot R, Nijman IJ, Afawi Z, et al. Targeted sequencing of 351 candidate genes for epileptic encephalopathy in a large cohort of patients. *Mol Genet Genomic Med.* (2016) 4:568–80. doi: 10.1002/mgg3.235
8. Perucca P, Scheffer IE, Harvey AS, James PA, Lunke S, Thorne N, et al. Real-world utility of whole exome sequencing with targeted gene analysis for focal epilepsy. *Epilepsy Res.* (2017) 131:1–8. doi: 10.1016/j.eplepsyres.2017.02.001
9. Peng J, Pang N, Wang Y, Wang X-L, Chen J, Xiong J, et al. Next-generation sequencing improves treatment efficacy and reduces hospitalization in children with drug-resistant epilepsy. *CNS Neurosci Ther.* (2018) 25:14–20. doi: 10.1111/cns.12869
10. Yang L, Kong Y, Dong X, Hu L, Lin Y, Chen X, et al. Clinical and genetic spectrum of a large cohort of children with epilepsy in China. *Genet Med.* (2018) 21:564–71. doi: 10.1038/s41436-018-0091-8
11. Parrini E, Marini C, Mei D, Galuppi A, Cellini E, Pucatti D, et al. Diagnostic targeted resequencing in 349 patients with drug-resistant pediatric epilepsies identifies causative mutations in 30 different genes. *Hum Mutat.* (2017) 38:216–25. doi: 10.1002/humu.23149
12. Evers C, Staufner C, Granzow M, Paramasivam N, Hinderhofer K, Kaufmann L, et al. Impact of clinical exomes in neurodevelopmental and neurometabolic disorders. *Mol Genet Metab.* (2017) 121:297–307. doi: 10.1016/J.YMGME.2017.06.014
13. Chérot E, Keren B, Dubourg C, Carré W, Fradin M, Lavillaureix A, et al. Using medical exome sequencing to identify the causes of neurodevelopmental disorders: experience of 2 clinical units and 216 patients. *Clin Genet.* (2018) 93:567–76. doi: 10.1111/cge.13102
14. Thevenon J, Duffourd Y, Masurel-Paulet A, Lefebvre M, Feillet F, El Chehadeh-Djebbar S, et al. Diagnostic odyssey in severe neurodevelopmental disorders: toward clinical whole-exome sequencing as a first-line diagnostic test. *Clin Genet.* (2016) 89:700–7. doi: 10.1111/cge.12732
15. Soden SE, Saunders CJ, Willig LK, Farrow EG, Smith LD, Petrikin JE, et al. Effectiveness of exome and genome sequencing guided by acuity of illness for diagnosis of neurodevelopmental disorders. *Sci Transl Med.* (2014) 6:265ra168. doi: 10.1126/scitranslmed.3010076
16. Valencia CA, Husami A, Holle J, Johnson JA, Qian Y, Mathur A, et al. Clinical impact and cost-effectiveness of whole exome sequencing as a diagnostic tool: a pediatric center's experience. *Front Pediatr.* (2015) 3:67. doi: 10.3389/fped.2015.00067
17. Stark Z, Schofield D, Alam K, Wilson W, Mupfeki N, Macciocca I, et al. Prospective comparison of the cost-effectiveness of clinical whole-exome sequencing with that of usual care overwhelmingly supports early use and reimbursement. *Genet Med.* (2017) 19:867–74. doi: 10.1038/gim.2016.221
18. Joshi C, Kolbe DL, Mansilla MA, Mason SO, Smith RJH, Campbell CA. Reducing the cost of the diagnostic odyssey in early onset epileptic encephalopathies. *Biomed Res Int.* (2016) 2016:1–8. doi: 10.1155/2016/6421039
19. Payne K, Gavan SP, Wright SJ, Thompson AJ. Cost-effectiveness analyses of genetic and genomic diagnostic tests. *Nat Rev Genet.* (2018) 19:235–46. doi: 10.1038/nrg.2017.108
20. Vrijenhoek T, Middelburg EM, Monroe GR, van Gassen KLI, Geenen JW, Hövels AM, et al. Whole-exome sequencing in intellectual disability; cost before and after a diagnosis. *Eur J Hum Genet.* (2018) 26:1566–71. doi: 10.1038/s41431-018-0203-6
21. Dragojlovic N, Elliott AM, Adam S, van Karnebeek C, Lehman A, Mwenifumbo JC, et al. The cost and diagnostic yield of exome sequencing for children with suspected genetic disorders: a benchmarking study. *Genet Med.* (2018) 20:1013–21. doi: 10.1038/gim.2017.226
22. Howell KB, Eggers S, Dalziel K, Riseley J, Mandelstam S, Myers CT, et al. A population-based cost-effectiveness study of early genetic testing in severe epilepsies of infancy. *Epilepsia.* (2018) 59:1177–87. doi: 10.1111/epi.14087
23. Scheffer IE, Berkovic S, Capovilla G, Connolly MB, French J, Guilhoto L, et al. ILAE classification of the epilepsies: position paper of the ILAE Commission for Classification and Terminology. *Epilepsia.* (2017) 58:512–21. doi: 10.1111/epi.13709
24. Fisher RS, Cross JH, French JA, Higurashi N, Hirsch E, Jansen FE, et al. Operational classification of seizure types by the International League Against Epilepsy: position paper of the ILAE Commission for Classification and Terminology. *Epilepsia.* (2017) 58:522–30. doi: 10.1111/epi.13670
25. Harris PA, Taylor R, Thielke R, Payne J, Gonzalez N, Conde JG. Research electronic data capture (REDCap)-A metadata-driven methodology and workflow process for providing translational research informatics support. *J Biomed Inform.* (2009) 42:377–81. doi: 10.1016/j.jbi.2008.08.010
26. Wang K, Li M, Hakonarson H. ANNOVAR: functional annotation of genetic variants from high-throughput sequencing data. *Nucleic Acids Res.* (2010) 38:e164. doi: 10.1093/nar/gkq603
27. Pollard KS, Hubisz MJ, Rosenbloom KR, Siepel A. Detection of nonneutral substitution rates on mammalian phylogenies. *Genome Res.* (2010) 20:110–21. doi: 10.1101/gr.097857.109
28. Kumar P, Henikoff S, Ng PC. Predicting the effects of coding non-synonymous variants on protein function using the SIFT algorithm. *Nat Protoc.* (2009) 4:1073–81. doi: 10.1038/nprot.2009.86
29. Adzhubei IA, Schmidt S, Peshkin L, Ramensky VE, Gerasimova A, Bork P, et al. A method and server for predicting damaging missense mutations. *Nat Methods.* (2010) 7:248–9. doi: 10.1038/nmeth0410-248
30. Chun S, Fay JC. Identification of deleterious mutations within three human genomes. *Genome Res.* (2009) 19:1553–61. doi: 10.1101/gr.092619.109
31. Schwarz JM, Rödelsperger C, Schuelke M, Seelow D. MutationTaster evaluates disease-causing potential of sequence alterations. *Nat Methods.* (2010) 7:575–6. doi: 10.1038/nmeth0810-575
32. Kircher M, Witten DM, Jain P, O'Roak BJ, Cooper GM, Shendure J. A general framework for estimating the relative pathogenicity of human genetic variants. *Nat Genet.* (2014) 46:310–15. doi: 10.1038/ng.2892
33. Landrum MJ, Lee JM, Benson M, Brown G, Chao C, Chitipiralla S, et al. ClinVar: public archive of interpretations of clinically relevant variants. *Nucleic Acids Res.* (2016) 44:D862–8. doi: 10.1093/nar/gkv1222
34. Steele JC, Guella I, Szu-Tu C, Lin MK, Thompson C, Evans DM, et al. Defining neurodegeneration on Guam by targeted genomic sequencing. *Ann Neurol.* (2015) 77:458–68. doi: 10.1002/ana.24346
35. Richards S, Aziz N, Bale S, Bick D, Das S, Gastier-Foster J, et al. Standards and guidelines for the interpretation of sequence variants: a joint consensus recommendation of the American College of Medical Genetics and Genomics and the Association for Molecular Pathology. *Genet Med.* (2015) 17:405–23. doi: 10.1038/gim.2015.30
36. Kalia SS, Adelman K, Bale SJ, Chung WK, Eng C, Evans JP, et al. Recommendations for reporting of secondary findings in clinical exome and genome sequencing, 2016 update (ACMG SF v2.0): a policy statement of the American College of Medical Genetics and Genomics. *Genet Med.* (2017) 19:249–55. doi: 10.1038/gim.2016.190
37. Quilichini PP, Chiron C, Ben-Ari Y, Gozlan H. Stiripentol, a putative antiepileptic drug, enhances the duration of opening of GABAA-receptor channels. *Epilepsia.* (2006) 47:704–16. doi: 10.1111/j.1528-1167.2006.00497.x
38. Stewart JD, Horvath R, Baruffini E, Ferrero I, Bulst S, Watkins PB, et al. Polymerase γ gene POLG determines the risk of sodium valproate-induced liver toxicity. *Hepatology.* (2010) 52:1791–6. doi: 10.1002/hep.23891

39. Klepper J, Scheffer H, Leiendecker B, Gertsen E, Binder S, Leferink M, et al. Seizure control and acceptance of the ketogenic diet in GLUT1 deficiency syndrome: a 2- to 5-year follow-up of 15 children enrolled prospectively. *Neuropediatrics.* (2005) 36:302–8. doi: 10.1055/s-2005-872843
40. Wilbur C, Buerki SE, Guella I, Toyota EB, Evans DM, McKenzie MB, et al. An infant with epilepsy and recurrent hemiplegia due to compound heterozygous variants in ATP1A2. *Pediatr Neurol.* (2017) 75:87–90. doi: 10.1016/j.pediatrneurol.2017.06.003
41. Lehman A, Thouta S, Mancini GMS, Naidu S, van Slegtenhorst M, McWalter K, et al. Loss-of-function and gain-of-function mutations in KCNQ5 cause intellectual disability or epileptic encephalopathy. *Am J Hum Genet.* (2017) 101:65–74. doi: 10.1016/j.ajhg.2017.05.016
42. Guella I, McKenzie MB, Evans DM, Buerki SE, Toyota EB, Van Allen MI, et al. *De novo* mutations in YWHAG cause early-onset epilepsy. *Am J Hum Genet.* (2017) 101:300–10. doi: 10.1016/j.ajhg.2017.07.004
43. Guella I, Huh L, McKenzie MB, Toyota EB, Bebin EM, Thompson ML, et al. *De novo FGF12* mutation in 2 patients with neonatal-onset epilepsy. *Neurol Genet.* (2016) 2:e120. doi: 10.1212/NXG.0000000000000120
44. LaDuca H, Farwell KD, Vuong H, Lu H-M, Mu W, Shahmirzadi L, et al. Exome sequencing covers >98% of mutations identified on targeted next generation sequencing panels. *PLoS ONE.* (2017) 12:e0170843. doi: 10.1371/journal.pone.0170843
45. Dillon OJ, Lunke S, Stark Z, Yeung A, Thorne N, Gaff C, et al. Exome sequencing has higher diagnostic yield compared to simulated disease-specific panels in children with suspected monogenic disorders. *Eur J Hum Genet.* (2018) 26:644–51. doi: 10.1038/s41431-018-0099-1
46. Seo H, Park Y, Min BJ, Seo ME, Kim JH. Evaluation of exome variants using the Ion Proton Platform to sequence error-prone regions. *PloS ONE.* (2017) 12:e0181304. doi: 10.1371/journal.pone.0181304

Conflict of Interest Statement: MD has received research support from the Rare Disease Foundation and the Alva Foundation. TN has received research support from the BCCH Foundation and Genome BC. MC has received research grants and/or speakers honoraria from UCB, Novartis, Biocodex, Eisai, and Sage Therapeutics. All honoraria are donated to the Epilepsy Research and Development Fund. She has also received research grants from CIHR (Canadian Institute for Health Research) and The Alva Foundation. She is Co-Chair of the Canadian Pediatric Epilepsy Network. MF was a founding partner Neurocode Labs Inc., that currently provides commercial exome sequencing, but has since relinquished any ownership stake in that company.

The remaining authors declare that the research was conducted in the absence of any commercial or financial relationships that could be construed as a potential conflict of interest.

APPENDIX

List of Relevant Tests:

Laboratory Services/Tests:

- Bloodspot acylcarnitines
- Plasma amino acids
- Plasma total homocysteine
- Serum ceruloplasmin
- Serum copper
- Ammonia Serum
- Lactate Serum/plasma
- Lactate whole blood
- Acylcarnitine Serum
- Homocysteine total from Plasma
- Plasma amino-acids
- Serum copper
- Serum coeruloplasmin
- Plasma very long chain fatty acids
- Plasma cholesterol
- Urine creatine metabolites
- Urine glycosaminoglycans
- Urine oligosaccharides
- Urine organic acids
- Urine purines and pyrimidines
- Amino acids-urine
- Urine creatine metabolites
- Urine mucopolysaccharides
- CSF Protein
- CSF Protein
- CSF Glucose
- CSF Cell
- CSF Lactate
- CSF Amino-Acids
- CSF Neurotransmitters
- Plasma Vit B12

Genetic Tests:

- Chromosome microarray
- Fluorescence *in situ* Hybridization
- Single Gene testing
- Gene Panel/HTS testing
- Mitochondrial DNA analysis

Diagnostic Imaging Tests:

- MRI
- CT
- PET
- PET/CT
- Ultrasound **Electrophysiological Tests:**
- EEG
- EMG

Biopsies:

- Skin biopsy
- Muscle biopsy

frontiers in Neurology

ORIGINAL RESEARCH
published: 21 May 2019
doi: 10.3389/fneur.2019.00531

Hierarchical Data-Driven Analysis of Clinical Symptoms Among Patients With Parkinson's Disease

*Tal Kozlovski[1], Alexis Mitelpunkt[1,2,3], Avner Thaler[2,4,5], Tanya Gurevich[2,4,5], Avi Orr-Urtreger[2,6], Mali Gana-Weisz[6], Netta Shachar[1], Tal Galili[1], Mira Marcus-Kalish[1], Susan Bressman[7], Karen Marder[8], Nir Giladi[2,4,5], Yoav Benjamini[1,5,9] and Anat Mirelman[2,4,5,10]**

[1] Department of Statistics and Operations Research, Tel Aviv University, Tel Aviv, Israel, [2] Sackler School of Medicine, Tel Aviv University, Tel Aviv, Israel, [3] Pediatric Neurology Unit, Dana Children Hospital, Tel Aviv Medical Center, Tel Aviv, Israel, [4] Movement Disorders Unit, Tel Aviv Medical Center, Neurological Institute, Tel Aviv, Israel, [5] Sagol School of Neuroscience, Tel Aviv University, Tel Aviv, Israel, [6] Genetic Institute, Tel Aviv Medical Center, Tel Aviv, Israel, [7] Department of Neurology, Icahn School of Medicine at Mount Sinai, Mount Sinai Beth Israel Medical Center, New York, NY, United States, [8] Department of Neurology, Taub Institute for Alzheimer's Disease and the Aging Brain, College of Physicians and Surgeons, Columbia University, New York, NY, United States, [9] Edmond J. Safra Center for Bioinformatics, Tel Aviv University, Tel Aviv, Israel, [10] Laboratory of Early Markers of Neurodegeneration, Tel Aviv Medical Center, Neurological Institute, Tel Aviv, Israel

OPEN ACCESS

Edited by:
Matthew James Farrer, University of British Columbia, Canada

Reviewed by:
Emilia Mabel Gatto, Sanatorio de la Trinidad Miter, Argentina
Joanne Trinh, Universität zu Lübeck, Germany

***Correspondence:**
Anat Mirelman
anatmi@tlvmc.gov.il

Specialty section:
This article was submitted to Movement Disorders, a section of the journal Frontiers in Neurology

Received: *17 March 2019*
Accepted: *03 May 2019*
Published: *21 May 2019*

Citation:
Kozlovski T, Mitelpunkt A, Thaler A, Gurevich T, Orr-Urtreger A, Gana-Weisz M, Shachar N, Galili T, Marcus-Kalish M, Bressman S, Marder K, Giladi N, Benjamini Y and Mirelman A (2019) Hierarchical Data-Driven Analysis of Clinical Symptoms Among Patients With Parkinson's Disease. Front. Neurol. 10:531. doi: 10.3389/fneur.2019.00531

Mutations in the LRRK2 and GBA genes are the most common inherited causes of Parkinson's disease (PD). Studies exploring phenotypic differences based on genetic status used hypothesis-driven data-gathering and statistical-analyses focusing on specific symptoms, which may influence the validity of the results. We aimed to explore phenotypic expression in idiopathic PD (iPD) patients, G2019S-LRRK2-PD, and GBA-PD using a data-driven approach, allowing screening of large numbers of features while controlling selection bias. Data was collected from 1525 Ashkenazi Jews diagnosed with PD from the Tel-Aviv Medical center; 161 G2019S-LRRK2-PD, 222 GBA-PD, and 1142 iPD (no G2019S-LRRK2 or any of the 7 AJ GBA mutations tested). Data included 771 measures: demographics, cognitive, physical and neurological functions, performance-based measures, and non-motor symptoms. The association of the genotypes with each of the measures was tested while accounting for age at motor symptoms onset, gender, and disease duration; *p*-values were reported and corrected in a hierarchical approach for an average over the selected measures false discovery rate control, resulting in 32 measures. GBA-PD presented with more severe symptoms expression while LRRK2-PD had more benign symptoms compared to iPD. GBA-PD presented greater cognitive and autonomic involvement, more frequent hyposmia and REM sleep behavior symptoms while these were less frequent among LRRK2-PD compared to iPD. Using a data-driven analytical approach strengthens earlier studies and extends them to portray a possible unique disease phenotype based on genotype among AJ PD. Such findings could help direct a more personalized therapeutic approach.

Keywords: Parkinson's disease, G2019S-LRRK2, GBA, hierarchical testing, selective inference

INTRODUCTION

Mutations in the LRRK2 and GBA genes are the most common known genetic risk factors of Parkinson's disease (PD) (1, 2). The phenotype of genetic-associated PD has been described mainly compared to idiopathic PD (iPD). Some reported similarities in disease symptoms between LRRK2-PD and iPD (3), while others found a higher frequency of the postural instability gait difficulty subtype (4, 5), with less non-motor symptoms (4, 6–10) in LRRK2-PD. GBA-PD phenotype points to a younger age of motor symptoms onset, earlier and higher rate of cognitive decline and faster rate of progression compared with iPD (11–14).

Establishing differences between genetic-associated PD and iPD may help to understand the molecular pathogenesis of the disease and ultimately lead to new therapeutic strategies. However, studies comparing phenotype in the three groups using identical methods are lacking. In addition, previous explorations were based on a hypothesis driven approach, comparing specific features or data summaries between groups, and adjusting (in best case scenarios) for a limited number of multiple comparisons. The magnitude of variables measured and the breadth of domains are often large. Such abundance of data requires accounting for multiple comparisons and selective inference in order to maintain results replicability (15, 16), and avoid loss of information because of summation into means and total scores. Data-driven analysis enables the inclusion of large numbers of measures while controlling for False Discovery Rate (FDR), both for dimensions reduction and for hypotheses testing. The aim of this study was to explore phenotypic expression in iPD, LRRK2-PD and GBA-PD using a well-guarded data-driven approach.

METHODS

Participants and Procedures

The study was conducted in the Movement Disorder Unit at the Tel-Aviv Medical Center between 2005 and 2015. Patients were included in the study if they were of Ashkenazi Jewish (AJ) descent, and fulfilled the UK PD Brain bank criteria (including patients with family history) (17). All AJ PD patients who approached any of the neurologists in the MDU (tertiary center in Tel-Aviv) were offered to participate in this observational study. The study was approved by the ethical committee of the Tel Aviv Medical Center. All patients signed an informed written consent prior to participation.

Upon inclusion, 1525 patients were screened for the seven most common AJ GBA mutations (N370S, L444P, c.84insG, IVS2+1G->A, V394L, R496H, and 370Rec) and the G2019S mutation in the LRRK2 gene. Patients underwent a wide battery of medical exams and questionnaires assessing motor and non-motor symptoms (**Table 1**). Information on disease symptoms and management were collected from structured interviews and medical charts as well as using standardized questionnaires before the genetic status of each patient was ascertained (2, 4, 10, 18). Disease severity was assessed using the Unified Parkinson Disease Rating Scale (UPDRS part III) (19) and the H&Y staging (20). Cognitive function was evaluated using the Montreal Cognitive Assessment test (MoCA) (21), Stroop test (22), verbal fluency (23), and Trail Making Test (TMT color version) (24). Depression was assessed using the Beck Depression Inventory (BDI) (25) and the Geriatric Depression Scale (GDS) (26), anxiety was measured using the Spielberger State and Trait Anxiety Inventory (27). The Non-Motor Symptom Questionnaire (NMS) (28) and the Scale for Autonomic Function (SCOPA-AUT) (29) were used to assess autonomic function. Olfaction was assessed using the University of Pennsylvania Smell Identification Test (UPSIT) (21), hyposmia was defined based on age and gender cut-offs and the REM sleep Behavior Questionnaire (RBDQ) (30) was administered to evaluate RBD. Patients were assessed during morning office hours and were requested not to alter their medication schedule, thus tested during "ON" medication condition.

Standard Protocol Approvals, Registrations, and Patient Consents

The study was approved by the local ethical committee at Tel Aviv Medical Center and was performed according to the principles of the Declaration of Helsinki. Eligible participants provided informed written consent.

STATISTICAL ANALYSIS

Overall, 771 potential measures were available about the patients in various databases (resulting flatly in ∼2300 genotype associations to be screened). They included both fine and gross level measures, for example, both the individual questions in a questionnaire and their overall scores. Each of the 1,525 participants contributed a different subset of those measures (due to time limits, availability of questionnaires, etc.) during their visits to the research center. In the data cleansing stage, dozens of variables were removed due to redundancy of information or if more than 99% of records were missing. The remaining 509 measures were tested for their association with the genotypes in the following hierarchical way (see **Figure 1**).

Each measure was fitted a generalized linear model with the genotype as a categorical explanatory variable, where iPD patients were considered as the reference level. The model further included 3 covariates: age at onset, disease duration and gender, in order to adjust for their potential influence. The generalized model used was either linear, logistic, ordered logistic or multinomial, according to the measure's type. Furthermore, if the contingency table of genotype and the categorical measure had at least one cell with <2 observations we used a logistic regression with bias reduction (31, 32).

From each regression model we obtained p-values for the two genotypes effects, and for the categorical variables we obtained a pair for each one of the categories of the dependent measure. Associations related to the same measure were grouped into a family of hypotheses, and their intersection is the hypothesis of no association of the measure with any

TABLE 1 | Characteristics of study participants.

Variable	*GBA*	*LRRK2*	Non carriers	Total observations
Number	222	161	1,142	1,525
Age at onset, years (*SD*) [range in years]	58.3 (11.08) [24-85]	58.1 (10.97) [28-91]	60.9 (11.39) [20-94]	1,525
Age at enrollment, years (*SD*) [range in years]	65.5 (10.5) [33-89]	66.5 (10.11) [36-93]	67.6 (10.52) [29-96]	1,525
GENDER				
Male *n* (%)	129 (58.11)	82 (50.93)	734 (64.27)	1,525
Male/Female ratio	1.39	1.04	1.8	
FAMILY HISTORY OF PD				
1st degree relative with PD *n* (%)	44 (19.82%)	51 (31.67%)	192 (16.81%)	1,489
Total with any family history of PD *n* (%)	81 (36.48%)	80 (49.69%)	306 (26.79%)	1,496
BMI				
mean (*SD*)	26.6 (5.23)	26.1 (3.77)	26.6 (5.38)	462

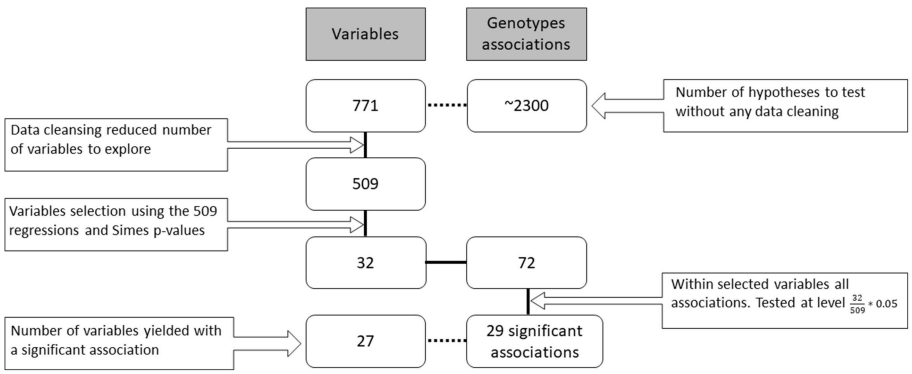

FIGURE 1 | Research workflow. Data gathering, cleansing, screening, hypotheses testing and number of findings. The boxes on the left side of the figure indicate the number of variables (families of hypotheses) in each part of the analysis. On the right side are the total number of genotype associations considered for each of the family hypotheses (individual hypotheses). The solid black connecting line represents the actual workflow of anlaysis while the dashed connecting line describes additional information on the data. The number of final family variables in the analysis was 32 for which 72 hypotheses were examined resulting in 29 significant hypotheses.

genotype. As suggested before (16), we first tested the above intersection hypothesis across the measures. For that, a p-value for each intersection hypothesis was calculated using Simes test (33). Then, the adaptive step-up Benjamini-Hochberg (BH) procedure (34) was used to select the measures that have some significant association with any of the genotypes (35), while guaranteeing FDR control on the selected measures. Finally, after the measures screening stage, the family of associations related to each selected measure were tested again using the FDR control procedure. The level of the test at the second stage was set according to Benjamini and Bogomolov (16) to control the average FDR over the selected groups (see **Figure 2**).

After adjusting the *p*-values with the BH procedure within each group, the threshold for significance within the selected groups was reduced from α by the proportion of the number of selected measures (R) out of total tested (m) $q = \left(\frac{R}{m}\right) * \alpha$ (in this case: $\left(\frac{32}{509}\right) * \alpha$). All the presented p-values below were adjusted to keep the average error rate over the selected groups, are denoted as p^{adj}, and hence can be compared to the regular 0.05 and 0.1 thresholds. Analysis was preformed using R software version 3.2.4.

RESULTS

A total of 1525 AJ patients with PD participated in this study: 1142 iPDs, 161 carriers of the G2019S-LRRK2 mutation and 222 carriers of the 7 common AJ mutations in the GBA gene. The majority of the mutations in the GBA gene (65%) were considered mild GBA (N370S and R496H). Due to the small proportion of the other mutations, all carriers of the GBA gene were considered one group. In the second stage 72 associations were tested, 36 for each of the mutations. Twelve associations of LRRK2-PD and 17 associations of the GBA-PD were significantly different from the iPDs at the 0.05 level. Five more associations were found significant at a 0.1 level. Below we detail the specific differences in phenotype. The respective effect sizes are presented in **Figure 3**.

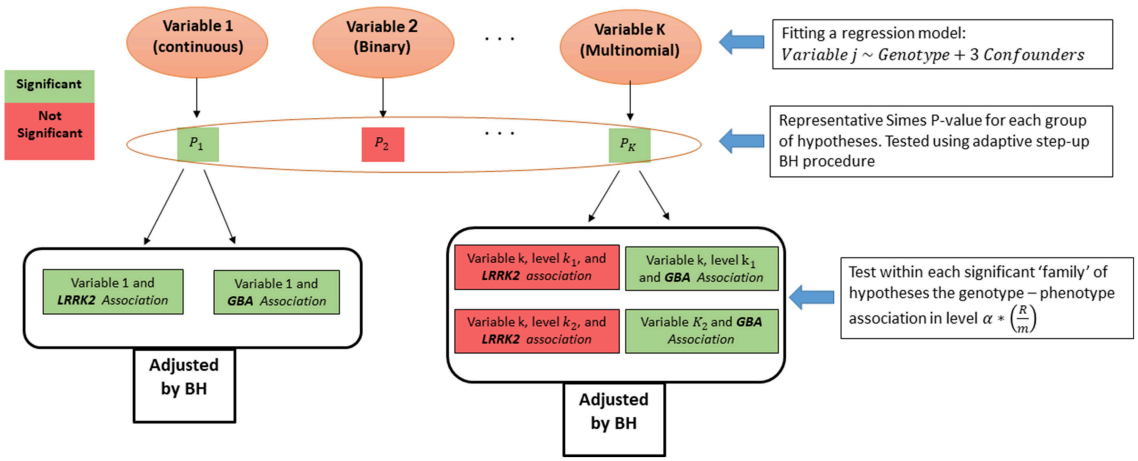

FIGURE 2 | Statistical analysis algorithm. Measure screening and hypotheses testing algorithm.

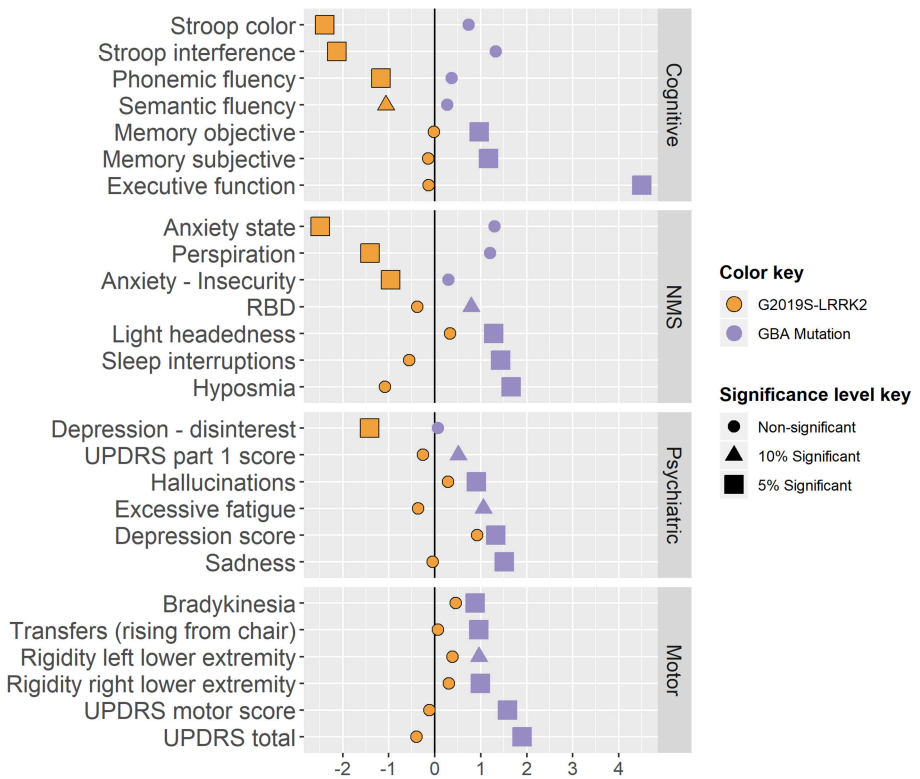

FIGURE 3 | Results standardized effect sizes. Standardized effect sizes divided by domains and phenotypes of the two genotypes coefficients. The calculation of the standardized effect sizes varies across the different linear models as follows:

- Linear regression models: $\frac{\beta_{genotype}}{SD(y)}$
- Logistic regression model (multinomial and binomial models): $\log(OR)$
- Ordered logistic regression models: $\log(Cumulative\ OR)$

The effect sizes are colored by genotype, and their shape and size present the minimal significance level they pass (0.05, 0.1 or none of them).

Cognition

LRRK2-PD performed better than iPD patients on cognitive tests such as the congruent Stroop, Stroop interference and Verbal fluency tests (p^{adj} are $<$ 0.001, 0.0047, 0.056 & 0.039 respectively). GBA–PD showed more difficulty in executive function (TMT test A-B; $p^{adj} = 0.002$) and reported more subjective memory complaints ($p^{adj} = 0.017$) and concentration difficulties ($p^{adj} = 0.016$). The MoCA

test was not sensitive enough to pass the screening stage (Simes $p^{adj} = 0.127$).

Non-motor Symptoms

GBA-PD were more hyposmic ($p^{adj} = 0.009$) and had more complains about headaches ($p^{adj} < 0.001$) compared to patients with iPD. GBA-PD had higher scores on the RBDQ ($p^{adj} = 0.057$), and more specifically reported more frequent awakenings during nighttime sleep ($p^{adj} = 0.008$). LRRK2-PD were correlated with less reports of perspiration ($p^{adj} = 0.001$).

Mood and Psychiatric Symptoms

LRRK2-PD reported less activity withdrawal (GDS question 2) and scored lower on both the State and Trait Anxiety Inventory (p^{adj} are 0.006 and 0.045 respectively), while GBA-PD reported less satisfaction from their lives ($p^{adj} = 0.012$), and more symptoms of depression (from the BDI, p^{adj} are 0.01 and 0.041).

In addition, a larger percentage of GBA-PD reported hallucinations (NMSQ question 14, $p^{adj} = 0.052$) and in total received higher total scores in the UPDRS-part I ($p^{adj} = 0.057$).

Motor Symptoms

GBA-PD presented with greater motor signs on the UPDRS-part III compared to iPD patients ($p^{adj} = 0.022$). More specifically, GBA-PD presented with more bradykinesia, difficulty in transfers and rigidity (questions 23.b and 27, p^{adj} are 0.003 and 0.023 and question 22.d and 22.e, p^{adj} are < 0.001 and 0.057 , respectively) compared to iPD and had a higher total UPDRS score ($p^{adj} = 0.019$).

Other Measures

Six additional measures that passed the screening stage (AJ origin, number of children, initiation of dopa-Y/N, work hazard-Y/N, maternal mother risk-Y/N, and a clinically duplicate score from the GDS questionnaire) were of no clinical implications and are therefore omitted from **Figure 3**. Omitting the duplicated variable made no change in the results of the analysis; when omitting all six from the analysis, the FDR at the families' level increased to 0.069 (see **Supplementary Material** for a detailed version of **Figure 3**).

DISCUSSION

This paper presents findings based on the exploration of a large set of data in order to assess phenotype-genotype associations in PD. We used a new hierarchical statistical testing approach that facilitates analysis of a large sets of data from different domains, incorporates all data points without summation of tests with the ability to explore directionality without prior hypothesis. Furthermore, the methodology allows inference on the results while controlling an appropriate error rate, thus ensuring the validity of the discoveries. Our exploration provided evidence of differences in phenotypes based on genetic mark up (**Figure 3**). The results validate through replication some previous results in the literature, as well as refuting others.

Differences between iPD, LRRK2-PD, and GBA-PD were found in multiple domains. In general, despite adjusting for disease duration, gender and age at onset, patients with GBA-PD presented with more severe symptoms and signs while LRRK2-PD had more moderate symptoms and signs as compared to iPD. Consistent with previous studies, our analysis showed greater cognitive impairment in patients with GBA-PD than iPD (2, 36–39), while LRRK2-PD demonstrated more preserved cognitive functions. Patients with GBA-PD also showed more autonomic involvement, more hyposmia and RBD symptoms, while olfaction disturbances and RBD were minimal in LRRK2-PD as compared to iPD. This is consistent with previous studies reporting on greater autonomic involvement in GBA related PD (11, 37) and less hyposmia and RBD in LRRK2-PD (9, 40–42).

Reports on depression, anxiety and psychiatric involvement in LRRK2 related PD are equivocal in the literature. Marras et al. reported higher BDI scores in patients with LRRK2 associated PD (3), while Ben-Sassi et al. reported less depressive symptoms in a cohort of Tunisians with G2019S-LRRK2 (43, 44). Our findings support the latter, with LRRK2-PD patients showing significantly lower apathy and hallucinations than iPD, and presenting with less depressive and anxiety symptoms than iPD, and less psychiatric involvement compared to GBA-PD.

Previously we and others reported that LRRK2 related PD was more frequently associated with postural instability and gait difficulty phenotype and presented with more motor involvement (4, 5). In this study, we observed greater motor involvement in the GBA-PD group than the LRRK2 related PD while the LRRK2-PD had more motor involvement than iPD (recall **Figure 3**). This finding is interesting and potentially relates to the methodology of assessment. In this study, the assessment of motor function was based on the UPDRS and did not include sensitive quantifiable gait assessment such as in our previous work (5). Such quantifiable assessment could provide additional information that is not detected in the UPDRS. This may also reflect the vigor of data-driven analysis and the strength of including multiple domains in the search, while controlling for selection stemming from the multiple hypotheses screened.

The study has several limitations. Participants were recruited into the study in an ongoing process that spanned over 10 years. All patients of AJ descent were asked to participate resulting in a wide variability of patients' stages and ages. Subjects were screened for the G2019S mutation in the LRRK2 gene and the 7 common mutations in the GBA gene, as those were the known genetic risk factors for PD. It is possible that patients may harbor additional mutations that were not screened at this time, however we expect that in this population their impact would be very low. The protocol was amended several times during this process and thus not all participants had all data points. Data was not imputed but rather all available data for each regression model was used. In our hierarchical procedure, we first selected measures that showed significant evidence, at 0.05 level of FDR control. This eliminated many families of symptoms. However, when performing the same analysis with respect to our selected measures at a higher significance level of 0.1, all selected families

yielded a significant association. This implies that an association may exist between the selected families and the genotypes, but the signal is not strong enough to be discovered at the current sample size and at our pre-determined significance level. We included all GBA mutations in the same group due to the small proportion of severe GBA mutations in this cohort and the constraints of the method in use. Based on previous reports, it is possible that the findings may have been driven by the severity of the mutations. This should be further explored in future studies with larger samples from each mutation.

Nevertheless, the uniqueness in this study is the absence of the domain experts in selecting which hypotheses to test, and thus reducing result-bias. By using testing procedures on the whole data set while controlling for the relevant error rate both in the screening stage and in the testing stage, we were able to shed light on multiple genotypes-phenotypes associations at once. The findings from this study provide a more complete portrayal of symptomatic manifestation in genetic PD and could help direct future studies into disease modifying trials and direct personalized treatment approaches.

DATA AVAILABILITY

Data sharing is unauthorized by our Helsinki committee due to the sensitivity of genetic information and privacy. Anonymized data could be shared on request, as well as the study protocol, statistical plan, and reproducible code.

AUTHOR CONTRIBUTIONS

TK, AMit, NG, AMir, and YB: conception and design of the study. TK, AMit, AT, TGu, AO-U, MG-W, NS, TGa, MM-K, KM, SB, NG, AMir, and YB: acquisition and analysis of data. TK, AMit, NG, AMir, and YB: drafting a significant portion of the manuscript or figures.

FUNDING

The study was partially funded by Tel Aviv Sourasky Medical Center internal grant, the Michal J Fox Foundation, the Israeli Science Foundation, the European Research Council grants FP7/2007-2013 ERC agreement no [294519]-PSARPS, European Union Seventh Framework Programme (FP7/2007-2013) under grant agreement no. 604102 (Human Brain Project) and funds provided by the Khan Foundation.

ACKNOWLEDGMENTS

We would like to thank the participants of this study and the researchers who participated in data collection.

SUPPLEMENTARY MATERIAL

The Supplementary Material for this article can be found online at: https://www.frontiersin.org/articles/10.3389/fneur.2019.00531/full#supplementary-material

REFERENCES

1. Marras C, Alcalay RN, Caspell-Garcia C, Coffey C, Chan P, Duda JE, et al. Motor and nonmotor heterogeneity of LRRK2-related and idiopathic Parkinson's disease. *Mov Disord.* (2016) 31:1192–202. doi: 10.1002/mds.26614
2. Thaler A, Gurevich T, Shira AB, Weisz MG, Ash E, Shiner T, et al. A "dose" effect of mutations in the GBA gene on Parkinson's disease phenotype. *Parkinsonism Relat Disord.* (2017) 36:47–51. doi: 10.1016/j.parkreldis.2016.12.014
3. Marras C, Schüle B, Munhoz RP, Rogaeva E, Langston JW, Kasten M, et al. Phenotype in parkinsonian and nonparkinsonian LRRK2 G2019S mutation carriers. *Neurology.* (2011) 77:325–333. doi: 10.1212/WNL.0b013e318227042d
4. Alcalay RN, Mirelman A, Saunders-Pullman R, Tang MX, Mejia Santana H, Raymond D, et al. Parkinson disease phenotype in Ashkenazi Jews with and without LRRK2 G2019S mutations. *Mov Disord.* (2013) 28:1966–71. doi: 10.1002/mds.25647
5. Mirelman A, Heman T, Yasinovsky K, Thaler A, Gurevich T, Marder K, et al. Fall risk and gait in Parkinson's disease: the role of the LRRK2 G2019S mutation. *Mov Disord.* (2013) 28:1683–90. doi: 10.1002/mds.25587
6. Aasly JO, Toft M, Fernandez-Mata I, Kachergus J, Hulihan M, White LR, et al. Clinical features of LRRK2-associated Parkinson's disease in central Norway. *Ann Neurol.* (2005) 57:762–5. doi: 10.1002/ana.20456
7. Gosal D, Ross OA, Wiley J, Irvine GB, Johnston JA, Toft M, et al. Clinical traits of LRRK2-associated Parkinson's disease in Ireland: a link between familial and idiopathic PD. *Parkinsonism Relat Disord.* (2005) 11:349–52. doi: 10.1016/j.parkreldis.2005.05.004
8. Healy DG, Falchi M, O'Sullivan SS, Bonifati V, Durr A, Bressman S, et al. Phenotype, genotype, and worldwide genetic penetrance of LRRK2-associated Parkinson's disease: a case-control study. *Lancet Neurol.* (2008) 7:583–90. doi: 10.1016/S1474-4422(08)70117-0
9. Johansen KK, Warø BJ, Aasly JO. Olfactory dysfunction in sporadic P arkinson's D isease and LRRK 2 carriers. *Acta Neurol Scand.* (2014) 129:300–6. doi: 10.1111/ane.12172
10. Saunders-Pullman R, Mirelman A, Alcalay RN, Wang C, Ortega RA, Raymond D, et al. Progression in the LRRK2-associated Parkinson disease population. *JAMA Neurol.* (2018) 75:312–9. doi: 10.1001/jamaneurol.2017.4019
11. Brockmann K, Srulijes K, Hauser AK, Schulte C, Csoti I, Gasser T, et al. GBA-associated PD presents with nonmotor characteristics. *Neurology.* (2011) 77:276–80. doi: 10.1212/WNL.0b013e318225ab77
12. Neumann J, Bras J, Deas E, O'sullivan SS, Parkkinen L, Lachmann RH, et al. Glucocerebrosidase mutations in clinical and pathologically proven Parkinson's disease. *Brain.* (2009) 132:1783–94. doi: 10.1093/brain/awp044
13. Sidransky E, Samaddar T, Tayebi N. Mutations in GBA are associated with familial Parkinson disease susceptibility and age at onset. *Neurology.* (2009) 73:1424–6. doi: 10.1212/WNL.0b013e3181b28601
14. Sidransky E, Nalls MA, Aasly JO, Aharon-Peretz J, Annesi G, Barbosa ER, et al. Multicenter analysis of glucocerebrosidase mutations in Parkinson's disease. *N Engl J Med.* (2009) 361:1651–61. doi: 10.1056/NEJMoa0901281
15. Benjamini Y. Simultaneous and selective inference: Current successes and future challenges. *Biometrical J.* (2010) 52:708–21. doi: 10.1002/bimj.200900299
16. Benjamini Y, Bogomolov M. Selective inference on multiple families of hypotheses. *J R Stat Soc Ser B Stat Methodol.* (2014) 76:297–318. doi: 10.1111/rssb.12028
17. Hughes AJ, Daniel SE, Kilford L, Lees AJ. Accuracy of clinical diagnosis of idiopathic Parkinson's disease: a clinico-pathological study of 100 cases. *J Neurol Neurosurg Psychiatry.* (1992) 55:181–4. doi: 10.1136/jnnp.55.3.181
18. Marder K, Wang Y, Alcalay RN, Mejia-Santana H, Tang MX, Lee A, et al. Age-specific penetrance of LRRK2 G2019S in the Michael

J. Fox Ashkenazi Jewish LRRK2 consortium. *Neurology.* (2015) 85:89–95. doi: 10.1212/WNL.0000000000001708
19. Fahn S. Unified Parkinson's disease rating scale. *Recent Dev Park Dis.* (1987) 2:153–63, 293–304.
20. Hoehn MM, Yahr MD. Parkinsonism: onset, progression, and mortality. *Neurology.* (1967) 17:427. doi: 10.1212/WNL.17.5.427
21. Doty RL, Frye RE, Agrawal U. Internal consistency reliability of the fractionated and whole University of Pennsylvania smell identification test. *Percept Psychophys.* (1989) 45:381–4. doi: 10.3758/BF03210709
22. Hsieh YH, Chen KJ, Wang CC, Lai CL. Cognitive and motor components of response speed in the Stroop test in Parkinson's disease patients. *Kaohsiung J Med Sci.* (2008) 24:197–203. doi: 10.1016/S1607-551X(08)70117-7
23. Piatt AL, Fields JA, Paolo AM, Koller WC, Tröster AI. Lexical, semantic, and action verbal fluency in Parkinson's disease with and without dementia. *J Clin Exp Neuropsychol.* (1999) 21:435–43. doi: 10.1076/jcen.21.4.435.885
24. Tombaugh TN. Trail Making Test A and B: normative data stratified by age and education. *Arch Clin Neuropsychol.* (2004) 19:203–14. doi: 10.1016/S0887-6177(03)00039-8
25. Steer RA, Rissmiller DJ, Beck AT. Use of the beck depression inventory-II with depressed geriatric inpatients. *Behav Res Ther.* (2000) 38:311–8. doi: 10.1016/S0005-7967(99)00068-6
26. Meara J, Mitchelmore E, Hobson P. Use of the GDS-15 geriatric depression scale as a screening instrument for depressive symptomatology in patients with Parkinson's disease and their carers in the community. *Age Ageing.* (1999) 28:35–8. doi: 10.1093/ageing/28.1.35
27. Speilberger CD, Vagg PR. Psychometric properties of the STAI: a reply to Ramanaiah, Franzen, and Schill. *J Pers Assess.* (1984) 48:95–7. doi: 10.1207/s15327752jpa4801_16
28. Chaudhuri KR, Martinez-Martin P, Schapira AHV, Stocchi F, Sethi K, Odin P, et al. International multicenter pilot study of the first comprehensive self-completed nonmotor symptoms questionnaire for Parkinson's disease: the NMSQuest study. *Mov Disord.* (2006) 21:916–23. doi: 10.1002/mds.20844
29. Visser M, Marinus J, Stiggelbout AM, Van Hilten JJ. Assessment of autonomic dysfunction in Parkinson's disease: the SCOPA-AUT. *Mov Disord.* (2004) 19:1306–12. doi: 10.1002/mds.20153
30. Stiasny-Kolster K, Mayer G, Schäfer S, Möller JC, Heinzel-Gutenbrunner M, Oertel WH. The REM sleep behavior disorder screening questionnaire—a new diagnostic instrument. *Mov Disord.* (2007) 22:2386–93. doi: 10.1002/mds.21740
31. Firth D. Bias reduction of maximum likelihood estimates. *Biometrika.* (1993) 80:27–38. doi: 10.1093/biomet/80.1.27
32. Kosmidis I, Firth D. Multinomial logit bias reduction via the Poisson log-linear model. *Biometrika.* (2011) 98:755–9. doi: 10.1093/biomet/asr026
33. Simes RJ. An improved bonferroni procedure for multiple tests of significance. *Biometrika.* (1986) 73:751–4. doi: 10.1093/biomet/73.3.751
34. Benjamini Y, Hochberg Y. On the adaptive control of the false discovery rate in multiple testing with independent statistics. *J Educ Behav Stat.* (2000) 25:60–83. doi: 10.3102/10769986025001060
35. Peterson CB, Bogomolov M, Benjamini Y, Sabatti C. Many phenotypes without many false discoveries: error controlling strategies for multitrait association studies. *Genet Epidemiol.* (2016) 40:45–56. doi: 10.1002/gepi.21942
36. Alcalay RN, Caccappolo E, Mejia-Santana H, Tang M-X, Rosado L, Reilly MO, et al. Cognitive performance of GBA mutation carriers with early-onset PD: the CORE-PD study. *Neurology.* (2012) 78:1434–40. doi: 10.1212/WNL.0b013e318253d54b
37. Alcalay RN, Dinur T, Quinn T, Sakanaka K, Levy O, Waters C, et al. Comparison of Parkinson risk in Ashkenazi Jewish patients with Gaucher disease and GBA heterozygotes. *JAMA Neurol.* (2014) 71:752–7. doi: 10.1001/jamaneurol.2014.313
38. Moran EE, Wang C, Katz M, Ozelius L, Schwartz A, Pavlovic J, et al. Cognitive and motor functioning in elderly glucocerebrosidase mutation carriers. *Neurobiol Aging.* (2017) 58:239-e1. doi: 10.1016/j.neurobiolaging.2017.06.010
39. Swan M, Doan N, Ortega RA, Barrett M, Nichols W, Ozelius L, et al. Neuropsychiatric characteristics of GBA-associated Parkinson disease. *J Neurol Sci.* (2016) 370:63–9. doi: 10.1016/j.jns.2016.08.059
40. Saunders-Pullman R, Mirelman A, Wang C, Alcalay RN, San Luciano M, Ortega R, et al. Olfactory identification in LRRK 2 G2019S mutation carriers: a relevant marker? *Ann Clin Transl Neurol.* (2014) 1:670–8. doi: 10.1002/acn3.95
41. Saunders-Pullman R, Alcalay RN, Mirelman A, Wang C, Luciano MS, Ortega RA, et al. REM sleep behavior disorder, as assessed by questionnaire, in G2019S LRRK2 mutation PD and carriers. *Mov Disord.* (2015) 30:1834–9. doi: 10.1002/mds.26413
42. Trinh J, Amouri R, Duda JE, Morley JF, Read M, Donald A, Vilariño-Güell C, et al. A comparative study of Parkinson's disease and leucine-rich repeat kinase 2 p. G2019S parkinsonism. *Neurobiol Aging.* (2014) 35:1125–31. doi: 10.1016/j.neurobiolaging.2013.11.015
43. Sassi SB, Nabli F, Hentati E, Nahdi H, Trabelsi M, Ayed HB, et al. Cognitive dysfunction in Tunisian LRRK2 associated Parkinson's disease. *Parkinsonism Relat Disord.* (2012) 18:243–6. doi: 10.1016/j.parkreldis.2011.10.009
44. Nabli F, Ben Sassi S, Amouri R, Duda JE, Farrer MJ, Hentati F. Motor phenotype of LRRK2-associated Parkinson's disease: a tunisian longitudinal study. *Mov Disord.* (2015) 30:253–8. doi: 10.1002/mds.26097

Conflict of Interest Statement: SB reports grants from Michael J. Fox Foundation, during the conduct of the study. KM reports grants from NIH UL1TR001873 (Riley), grants from Parkinson's Disease Foundation, and grants from Michael J. Fox, during the conduct of the study; grants from CHDI, grants from HDSA, grants from NIH, grants from TEVA, grants from Vaccinex, and personal fees from Springer LLC, outside the submitted work. NG reports grants from MJF Foundation during the conduct of the study; personal fees from Sanofi, grants and personal fees from Lysosomal Therapeutics, personal fees from Denali, grants and personal fees from Biogen, grants and non-financial support from Michael J. Fox Foundation, outside the submitted work. AM reports grants from Michael J. Fox, and grants from Israeli Science Foundation, during the conduct of the study.

The remaining authors declare that the research was conducted in the absence of any commercial or financial relationships that could be construed as a potential conflict of interest.

frontiers in Neurology

OPINION
published: 22 May 2019
doi: 10.3389/fneur.2019.00530

Cathepsin Oxidation Alters Alpha-Synuclein Processing

*Andrew W. Ferree**

Neurology Department, Boston University Medical Center, Boston, MA, United States

Keywords: Parkinson's disease, alpha synuclein, lysosome, chaperone-mediated autophagy, synuclein pores, membrane permeabilization

INTRODUCTION

The protein aggregation properties of α-synuclein (α-syn) and mitochondrial dysfunction are believed to be central to Parkinson's disease pathophysiology, however unifying mechanisms driving pathology remain uncertain. This paper proposes mitochondria-derived increased intralysosomal oxidative stress shifts cathepsin cleavage patterns to favor truncated forms of α-syn that increase its propensity to aggregate. Ultimately the shift toward intralysosomal aggregation leads to pores that destabilize lysosomal membranes and bring about cell death. The hypothesis is built on α-syn's protein structure, cathepsin cleavage profiles, aggregation properties, and processing by chaperone-mediated autophagy. This paper is not a comprehensive explanation of all α-syn biology, but rather the author's opinion on some of the most salient and important biology that's relevant to disease. In addition, this paper aims to help seed a grand unifying theory that bridges leading proposed mechanisms for Parkinson's disease (PD) pathogenesis.

OPEN ACCESS

Edited by:
Matthew James Farrer, University of British Columbia, Canada

Reviewed by:
Georgia Xiromerisiou, University of Thessaly, Greece
Manabu Funayama, Juntendo University, Japan

***Correspondence:**
Andrew W. Ferree
Andrew.Ferree@bmc.org

Specialty section:
This article was submitted to Neurogenetics, a section of the journal Frontiers in Neurology

Received: *28 November 2018*
Accepted: *03 May 2019*
Published: *22 May 2019*

Citation:
Ferree AW (2019) Cathepsin Oxidation Alters Alpha-Synuclein Processing. Front. Neurol. 10:530. doi: 10.3389/fneur.2019.00530

BACKGROUND ON α-SYN

Structure

The 140 amino acids of the α-syn protein generate 3 distinct domains (**Figure 1A**). Residues 1–60 create an amphipathic N-terminal domain with abundant lysines and a histidine collectively resulting in a relative positive charge for this region (1). Curiously all known disease-causing point mutations cluster within the N-terminal region. Central residues 61–95 form a hydrophobic domain with affinity for membranes with increased curvature and anionic phospholipids (2–4). The final residues 96–140 create an acidic C-terminal region with several truncation sites (5, 6). Removal of negative charges with C-terminal truncation increases aggregation propensity (7) and affinity for dipolar lipids (2). As will be discussed further, this dynamic would allow α-syn to aggregate and assemble pores within membranes.

Chaperone-Mediated Autophagy

Receptor-mediated lysosomal import of individual proteins containing selective targeting sequences, including α-syn, describes chaperone-mediated autophagy (CMA) (8). The function ascribed to CMA is to eliminate targeted proteins from the cytosol as a means of regulating expression levels. Additionally, CMA likely functions as a protective mechanism for cellular quality control (9).

Oxidative stress increases CMA activity by multiple mechanisms including upregulation of essential import components (10). Mitochondria are the major intracellular producers

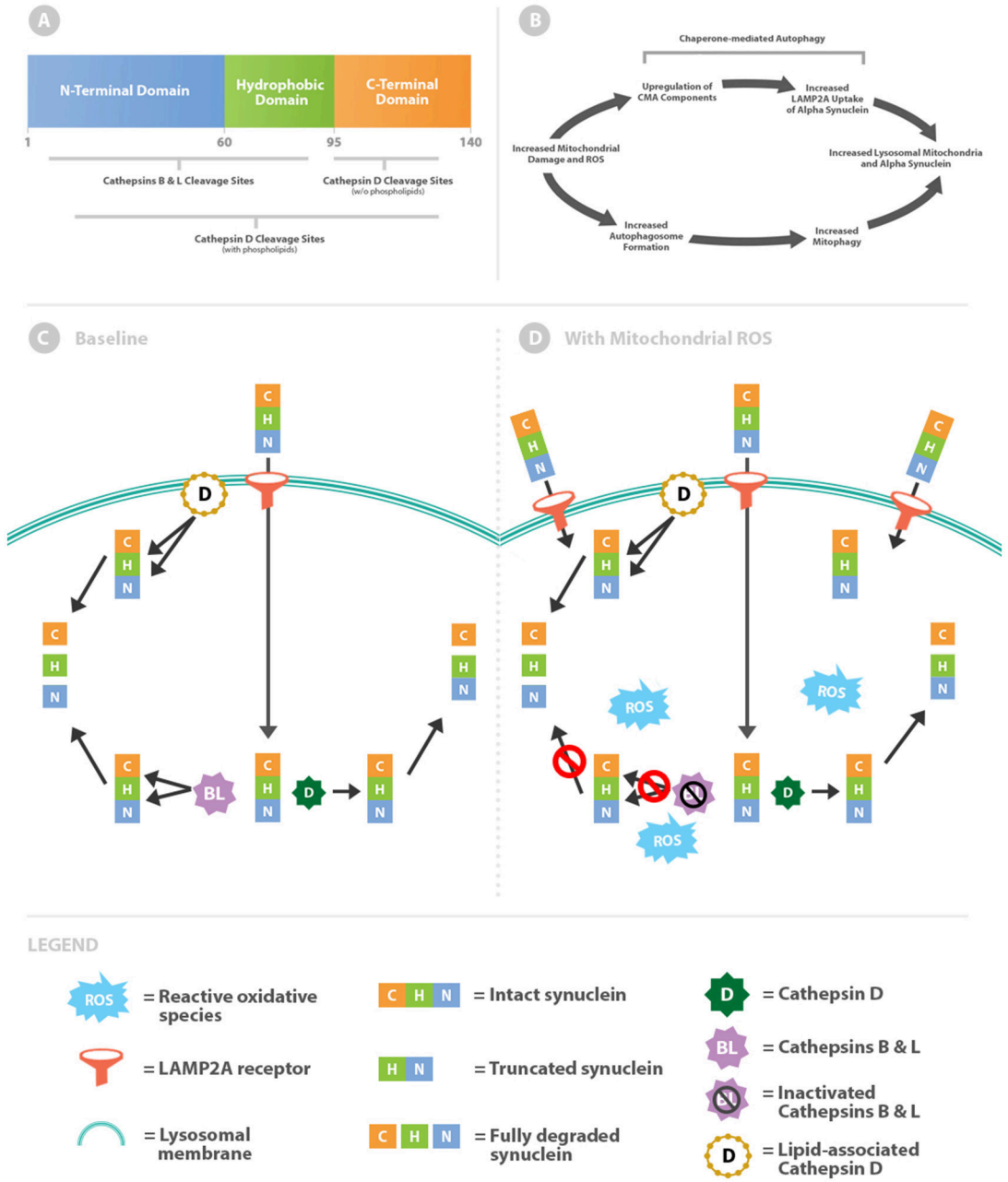

FIGURE 1 | Intralysosomal oxidative stress alters cathepsin metabolism of α-syn. **(A)** Schematic of the α-syn protein highlighting differential cathepsin cleavage sites. **(B)** Mitochondrial damage simultaneously leads to increased levels of intralysosomal mitochondria and α-syn. **(C)** α-syn is imported across the lysosomal membrane via chaperone-mediated autophagy through the LAMP2A receptor. Within the lysosome, α-syn is truncated through removal of the C-terminal by cathepsin D (free solution pathway). Alternatively α-syn is more completely degraded by lipid-associated cathepsin D or cathepsins B and L. **(D)** Oxidative stress increases lysosomal import of α-syn by upregulation of chaperone-mediated autophagy. Cathepsins B and L are inactivated by reactive oxidative species, whereas cathepsin D processing (both lipid-associated and free solution) remains unaffected.

of reactive oxidative species (ROS) and production increases when they become damaged. Therefore, elevated levels of oxidative stress from damaged mitochondria would be expected to upregulate CMA and thereby increase α-syn within the lysosomal system. Damaged mitochondria pose a major internal threat to the cell and are also cleared via lysosomes through the process of mitophagy. Ultimately elevated lysosomal concentrations of α-syn likely coincide with increased autophagic delivery of damaged mitochondria (**Figure 1B**).

Abbreviations: α-syn, alpha synuclein; ROS, Reactive oxidative species; PD, Parkinson's disease; CMA, Chaperone mediated autophagy.

INCREASED INTRALYSOSOMAL OXIDATIVE STRESS ALTERS CATHEPSIN CLEAVAGE OF α-SYN

Delivery of damaged mitochondria would be expected to increase levels of reactive oxidative species within the lysosomal lumen. A mechanism is outlined below in which intralysosomal oxidative stress alters cathepsin-mediated processing of α-syn thereby promoting aggregation and ultimately pore formation (11, 12). A protective countermeasure is additionally outlined which may serve to prevent aggregated α-syn pores from permeabilizing the lysosomal membrane.

Cathepsin Cleavage of α-Syn: Baseline Balance

McGlincy and colleagues identified differences in α-syn cleavage sites by cathepsins B, L, and D in free solution and in combination with phospholipids (**Figure 1C**) (13). In free solution, cathepsins B and L cleave throughout the length of α-syn but primarily within the N-terminus and hydrophobic regions. In contrast, cathepsin D in free solution cleaves almost exclusively in the C-terminus. By removing the negatively charged C-terminus, the truncated α-syn molecule increases oligomerization (7) and ultimately the downstream potential for pore formation.

Cathepsins B and L oppose oligomerization by virtue of cleavage sites within the N-terminal and hydrophobic regions. Targeting these regions prevents oligomerization by reducing intermolecular α-syn interactions. Moreover, cathepsin L is unique in its capacity to degrade the most stable (fibrillar) form of oligomers (13). In this baseline scenario antagonistic forces are counterbalanced, as cathepsin D promotes oligomerization and downstream pore formation whilst cathepsins B and L hinder the process (**Figure 1C**).

Intralysosomal Oxidative Stress Increases α-Syn Oligomerization

Tipping the enzymatic balance toward cathepsin D activity and away from cathepsins B and L would promote α-syn aggregation and pore formation. Cathepsins B and L, but not cathepsin D, are susceptible to inactivation by oxidation from reactive carbonyls (**Figure 1D**) (14, 15). This effect is due to oxidation of cysteine residues within cathepsin B and L catalytic sites. Thus, a lysosomal lumen high in oxidants would shift toward cathepsin D processing of α-syn and as a consequence higher likelihood of downstream aggregation.

Preventing Lysosomal Permeabilization by α-Syn Aggregates

The regional selectivity for cleavage between the cathepsins outlined thus far is contingent on being in free solution, which mimics the lysosomal lumen. However, cathepsin D activity is intriguingly altered when in association with membranes. In the presence of phospholipids the activity of cathepsin D broadens beyond the C-terminus to encompass the N-terminal and hydrophobic regions of α-syn (**Figure 1**) (13). While cathepsin D promotes oligomerization in free solution, as oligomers develop into membrane-associated pores cathepsin D can put a brake on the process. Altered activity of cathepsin D provides a critical limitation on oligomer propagation, given that baseline anti-oligomerization factors (cathepsins B and L) are inactivated by exposure to oxidized material. This regulatory mechanism is critical because pores within lysosomal membranes leads subsequent disastrous permeabilization if unchecked (16).

Advanced age is a well-known significant risk factor for PD. Moreover, all neuronal subtypes displaying α-syn pathology are unified in their abundance of lipofuscin or other oxidized lysosomal age pigments (17). It is highly probable that over time and in conditions of elevated or defective mitochondrial turnover that the capacity of lysosomal processing is exceeded and subsequent pathological cascades ensue.

CONCLUSIONS AND FUTURE DIRECTIONS

This paper proposes a simple mechanism for altered α-syn metabolism based on levels of intralysosomal oxidative stress. Mitchondria are the most significant source of ROS within cells and lysosomes are the ultimate mediators of mitochondrial degradation. The major determinant modulating the mechanistic pathway outlined here would likely be the efficiency and rate mitochondrial degradation for a given cell.

Excessive production and inability to inactivate pores could lead to disease from several pathways. Mutations or oxidative modification of target sequences could render α-syn a sub-optimal substrate for cathepsins. Impaired lysosomal capacity (18) through mutations or aging could also prevent deactivation of α-syn pores. If not inactivated, pores could promote cell death by inserting within lysosomal membranes and allowing cytoplasmic release of cathepsins. Beyond damaging individual neurons, transcellular transmission of pores is plausible as chemical blockage of lysosomal function promotes exocytosis of α-syn oligomers (19).

The two most prominent proposed mechanisms of PD pathogenesis are centered on α-syn oligomerization and mitochondrial dysfunction. Recently autophagosomal and lysosomal dysfunction have also gained traction. So far a grand unifying theory for these mechanisms has remained elusive. This paper proposes a novel mechanism connecting α-syn aggregation with mitochondrial autophagy that bridges the current theories of PD pathogensis. The multivariable mechanisms outlined here represent exciting opportunities for future discovery and drug intervention.

AUTHOR CONTRIBUTIONS

The author confirms being the sole contributor of this work and has approved it for publication.

FUNDING

The Department of Neurology at Boston University Medical Center has provided funds for the open access publication fees and figure preparation.

ACKNOWLEDGMENTS

I have been blessed with numerous mentors; these three have been instrumental in my thought development around Parkinson's disease and the autophagic-mitochondrial axis. Thank you Drs. Ole Isacson, Ben Wolozin, and Orian Shirihai.

REFERENCES

1. Croke RL, Patil SM, Quevreaux J, Kendall DA, Alexandrescu AT. NMR determination of pKa values in α-synuclein. *Protein Sci.* (2011) 20:256–69. doi: 10.1002/pro.556
2. Ramakrishnan M, Jensen PH, March D. Association of α-synuclein and mutants with lipid membranes: spin-label ESR and polarized IR. *Biochemistry*. (2006) 45:3386–95. doi: 10.1021/bi052344d
3. Eliezer D, Kutluay E, Bussell R Jr, Browne G. Conformational properties of α-synuclein in its free and lipid-associated states. *J Mol Biol*. (2001) 307:1061–73. doi: 10.1006/jmbi.2001.4538
4. Beyer K. Mechanistic aspects of Parkinson's disease: α-synuclein and the biomembrane. *Cell Biochem Biophys*. (2007) 47:285–99. doi: 10.1007/s12013-007-0014-9
5. Villar-Pique A, Lopes Da Fonseca T, Outeiro TF. Structure, function and toxicity of alpha-synuclein: the Bermuda triangle in synucleinopathies. *J Neurochem*. (2016) 139(Suppl. 1):240–55. doi: 10.1111/jnc.13249
6. Mutane G, Ferrer I, Martinez-Vincente α-synuclein phosphorylation and truncation are normal events in the adult human brain. *Neuroscience.* (2012) 200:106–19. doi: 10.1016/j.neuroscience.2011.10.042
7. Li, W, West N, Colla E, Pletnikova O, Troncoso JC, Marsh L, et al. Aggregation promoting C-terminal truncation of alpha-synuclein is a normal cellular process and is enhanced by the familial Parkinson's disease-linked mutations. *Proc Natl Acad Sci USA*. (2005) 102:2162–7. doi: 10.1073/pnas.0406976102
8. Cuervo AM, Stefanis L, Fredenburg R, Lansbury PT, Sulzer D. Impaired degradation of mutant alpha-synuclein by chaperone-mediated autophagy. *Science*. (2004) 305:1292–5. doi: 10.1126/science.1101738
9. Massey AC, Kaushik S, Sovak G, Kiffin R, Cuervo AM. Consequences of the selective blockage of chaperone-mediated autophagy. *Proc Natl Acad Sci USA*. (2006) 103:5805–10. doi: 10.1073/pnas.0507436103
10. Kaushik S, Cuervo AM. Autophagy as a cell-repair mechanism: activation of chaperone-mediated autophagy during oxidative stress. *Mol Aspects Med*. (2006) 27:444–54. doi: 10.1016/j.mam.2006.08.007
11. Mizuno N, Varkey J, Kegulian NC, Hegde BG, Cheng N, Langen R, et al. Remodeling of lipid vesicles into cylindrical micelles by α-synuclein in an extended α-helical conformation. *J Biol Chem.* (2012) 287:29301–11. doi: 10.1074/jbc.M112.365817
12. Tsigelny IF, Bar-On P, Sharikov Y, Crews L, Hashimoto M, Miller MA, et al. Dynamics of α-synuclein aggregation and inhibition of pore-like oligomer development by β-synuclein. *FEBS J.* (2007) 274:1862–77. doi: 10.1111/j.1742-4658.2007.05733.x
13. McGlinchey RP, Lee JC. Cysteine cathepsins are essential in lysosomal degradation of α-synuclein. *Proc Natl Acad Sci USA*. (2015) 112:9322–7. doi: 10.1073/pnas.1500937112
14. Craab JW, O'Neil J, Miyagi M, West K, Hoff HF. Hydroxynonenal inactivates cathepsin B by forming Michael adducts with active site residues. *Protein Sci*. (2002) 11:831–40. doi: 10.1110/ps.4400102
15. Zeng J, Dunlop RA, Rodgers KJ, Davies MJ. Evidence for inactivation of cysteine proteases by reactive carbonyls via glycation of active site thiols. *Biochem J.* (2006) 398: 197–206. doi: 10.1042/BJ20060019
16. Dehay B, Bové J, Rodríguez-Muela N, Perier C, Recasens A, Boya P, et al. Pathogenic lysosomal depletion in Parkinson's Disease. *J Neurosci*. (2010) 30:12535–44. doi: 10.1523/JNEUROSCI.1920-10.2010
17. Braak H, Del Tredici K, Rüb U, de Vos RA, Jansen Steur EN, Braak E. Staging of brain pathology related to sporadic Parkinson's disease. *Neurobiol Aging*. (2003) 24:197–211. doi: 10.1016/S0197-4580(02)00065-9
18. Terman A, Kurz T, Navratil M, Arriaga E, Brunk U, Mitochondrial turnover and aging of long-lived postmitotic cells: the mitochondrial-lysosomal axis theory of aging. *Antioxid Redox Signal*. (2010) 12:503–35. doi: 10.1089/ars.2009.2598
19. Poehler AM, Xiang W, Spitzer P, May VE, Meixner H, Rockenstein E, et al. Autophagy modulates SNCA/a-synuclein release, thereby generating a hostile microenvironment. *Autophagy.* (2014) 10:2171–92. doi: 10.4161/auto.36436

Conflict of Interest Statement: The author declares that the research was conducted in the absence of any commercial or financial relationships that could be construed as a potential conflict of interest.

frontiers in Neurology

ORIGINAL RESEARCH
published: 22 May 2019
doi: 10.3389/fneur.2019.00503

Tau PET With ^{18}F-THK-5351 Taiwan Patients With Familial Alzheimer's Disease With the APP p.D678H Mutation

Chin-Chang Huang[1,2†], Ing-Tsung Hsiao[3,4†], Chu-Yun Huang[5], Yi-Ching Weng[1], Kuo-Lun Huang[1], Chi-Hung Liu[1], Ting-Yu Chang[1], Hsiu-Chuan Wu[1], Tzu-Chen Yen[3,4] and Kun-Ju Lin[3,4*]*

[1] Department of Neurology, Chang Gung Memorial Hospital, Taoyuan, Taiwan, [2] College of Medicine, Chang Gung University, Taoyuan, Taiwan, [3] Chang Gung Memorial Hospital, Molecular Imaging Center and Nuclear Medicine, Taoyuan, Taiwan, [4] Molecular Imaging and Radiological Sciences, Chang Gung University, Taoyuan, Taiwan, [5] College of Pharmacy, Taipei Medical University, Taipei, Taiwan

OPEN ACCESS

Edited by:
Matthew James Farrer,
University of British Columbia, Canada

Reviewed by:
Anthoula Charalampos Tsolaki,
Aristotle University of Thessaloniki, Greece
Basar Bilgic,
Istanbul University, Turkey

***Correspondence:**
Chin-Chang Huang
cch0537@adm.cgmh.org.tw
Kun-Ju Lin
kunjulin@gmail.com

†These authors have contributed equally to this work

Specialty section:
This article was submitted to Dementia, a section of the journal Frontiers in Neurology

Received: 30 January 2019
Accepted: 26 April 2019
Published: 22 May 2019

Citation:
Huang C-C, Hsiao I-T, Huang C-Y, Weng Y-C, Huang K-L, Liu C-H, Chang T-Y, Wu H-C, Yen T-C and Lin K-J (2019) Tau PET With ^{18}F-THK-5351 Taiwan Patients With Familial Alzheimer's Disease With the APP p.D678H Mutation. Front. Neurol. 10:503. doi: 10.3389/fneur.2019.00503

Background: Brain ^{18}F-AV-45 amyloid positron emission tomography (PET) in Taiwanese patients with familial Alzheimer's disease with the amyloid precursor protein (APP) p.D678H mutation tends to involve occipital and cerebellar cortical areas. However, tau pathology in patients with this specific Taiwan mutation remains unknown. In this study, we aimed to study the Tau PET images in these patients.

Methods: Clinical features, brain magnetic resonance imaging/computed tomography (MRI/CT), and brain ^{18}F-THK-5351 PET were recorded in five patients with the APP p.D678H mutation and correlated with brain ^{18}F-AV-45 PET images. We also compared the tau deposition patterns among five patients with familial mild cognitive impairment (fMCI), six patients with sporadic amnestic mild cognitive impairment (sMCI), nine patients with mild to moderate dementia due to Alzheimer's disease (AD), and 12 healthy controls (HCs). All of the subjects also received brain ^{18}F-AV-45 PET.

Results: The nine patients with sAD and six patients with sMCI had a positive brain AV-45 PET scans, while the 12 HCs had negative brain AV-45 PET scans. All five patients with fMCI received a tau PET scan with the age at onset ranging from 46 to 53 years, in whom increased standard uptake value ratio (SUVR) of ^{18}F-THK-5351 was noted in all seven brain cortical areas compared with the HCs. In addition, the SUVRs of ^{18}F-THK-5351 were increased in the frontal, medial parietal, lateral parietal, lateral temporal, and occipital areas ($P < 0.001$) in the patients with sAD compared with the HCs. The patients with fMCI had a significant higher SUVR of ^{18}F-THK-5351 in the cerebellar cortex compared to the patients with sMCI. The correlations between regional SUVR and Mini-Mental State Examination score and between regional SUVR and clinical dementia rating (sum box) scores within volumes of interest of Braak stage were statistically significant.

Conclusion: Tau deposition was increased in the patients with fMCI compared to the HCs. Increased regional SUVR in the cerebellar cortical area was a characteristic finding in the patients with fMCI. As compared between amyloid and tau PET, the amyloid deposition is diffuse, but tau deposition is limited to the temporal lobe in the patients with fMCI.

Keywords: amyloid, familial Alzheimer's disease, ^{18}F-THK-5351, PET, Taiwan APP p.D678H mutation, brain ^{18}F-AV-45

INTRODUCTION

The novel amyloid precursor protein APP p.D678H mutation (NM 000484.3 APP c.2032G > C) has been reported in two families with autosomal dominant Alzheimer's disease (AD) characterized by an early onset of memory impairment and progress to dementia, and a tendency to develop cerebral amyloid microangiopathy (1–3). The most characteristic findings in brain ^{18}F-AV-45 (florbetapir) positron emission tomography (PET) include high amyloid deposition in the occipital and cerebellar cortical areas (3). In addition, the clinical progression is rapid, and dementia usually develops at 55–60 years of age. In a follow-up brain ^{18}F-AV-45 PET study, an increased regional standard uptake value ratio (SUVR) was found in the brain cortical areas of patients with familial mild cognitive impairment (fMCI), but a slightly decreased regional SUVR was noted in patients with familial AD (4). The mechanisms of the biphasic course in the brain remain unknown. However, a saturation process may be responsible in patients with fMCI, and cortical atrophy and ventricular dilatation may be correlated with the decrease in SUVR in patients with familial AD as that in the world ADNI results (5, 6).

Alzheimer's disease is characterized by extracellular senile plaques composed of amyloid beta and intracellular neurofibrillary tangles consisting of paired helical filaments of hyperphosphorylated tau protein (7). The amyloid protein is considered to be a disease biomarker, while tau protein is considered to be a disease progression biomarker (8). The interaction between amyloid and tau protein remains unclear.

In this study, we aimed to investigate the tau deposition pattern in Taiwanese patients with fMCI with the novel APP p.D678H mutation as well as brain ^{18}F-AV-45 PET to understand the effects of tau and amyloid protein in a specific family. We also compared ^{18}F-THK-5351 PET findings among patients with fMCI, sporadic amnestic mild cognitive impairment (sMCI), sporadic AD (sAD), and healthy controls (HCs).

D678H mutation; VOI, volume of interest.

Abbreviations: AD, Alzheimer's disease; APP, amyloid precursor protein; AV-45 amyloid, Amyvid; CCA, cerebral amyloid ongiopathy; CDR, clinical dementia rating; fMCI, familial mild cognitive impairment; HC, healthy control; MCI, mild cognitive impairment; MMSE, Mini-Mental state examination; MRI/CT, magnetic resonance image/computed tomography; sMCI, sporadic amnestic mild cognitive impairment; sAD, sporadic Alzheimer's disease; SUVR, standard uptake value ratio; PET, positron emission tomography; Tau tracer, 18F-THK-5351; Taiwan mutation, APP p.

MATERIALS AND METHODS

Participants

Ten symptomatic patients with familial AD were recruited from two Taiwanese families with the APP p.D678H mutation (3). Among them, five with MCI received brain ^{18}F-AV-45 PET and ^{18}F-THK-5351 PET scans. The other five patients with familial AD did not participate in this study, including four who had been admitted to a nursing home and could not tolerate the procedure and one who had died due to nasopharyngeal cancer. The medical history, neurological examinations, laboratory tests, and neuroimaging studies of the enrolled patients were reviewed. In addition, 27 patients including six with sMCI, nine with sporadic mild to moderate dementia due to AD (mild in 7, moderate in 2), and 12 HCs were selected for comparison. The 12 HCs were matched for age with the fMCI patients.

The patients with sAD were selected according to the following criteria: (a) a progressive course of memory impairment, (b) neuropsychological tests with the Alzheimer's Disease Assessment Scale-Cognitive subscale (ADAS-Cog), and (c) clinical dementia rating (CDR) score $\geqq$ 0.5 (9). The patients with sMCI were selected based on the following criteria: (a) subjective memory complaints by the patient or an informant, (b) relatively normal performance on other cognitive domains, (c) normal activities of daily living, (d) objective memory impairment on at least one neurocognitive test of memory performance, and (e) no dementia according to DSM-IV criteria (10, 11). The exclusion criteria for this study were: (1) major systemic diseases such as severe heart disease, uremia, hepatic failure, myocardial infarction, poorly controlled diabetes, severe previous head injury, hypoxia, sepsis, and severe infectious diseases, (2) other major neurodegenerative disorders such as frontotemporal dementia, dementia with Lewy bodies, idiopathic Parkinson's disease, progressive supranuclear palsy, cortical basal syndrome, and spinocerebellar degeneration, (3) major cerebral vascular diseases, (4) implantation of metal devices such as a cardiac pacemaker or intravascular devices, (5) major psychiatric disorders including schizophrenia, major depression, drug or alcohol abuse, (6) pregnant women or breast feeding women, and (7) patients in whom MRI was contraindicated.

Methods

Blood samples from all subjects were drawn for apolipoprotein phenotypes and biochemical studies including complete blood count, glutamic-oxaloacetic transaminase, glutamic pyruvic transaminase, blood urea nitrogen, creatinine, triiodothyronine,

free tetraiodothyronine, thyroxine stimulating hormone, vitamin B12, folic acid, cortisol, and venereal disease research laboratory test (12). The HCs underwent the same procedures as the patients with fMCI, sMCI, and sAD. This study was approved by the Institutional Review Board of Chang Gung Memorial Hospital and the Ministry of Health and Welfare in Taiwan. The nature of research was explained to all of the subjects, and all signed informed consent forms. In addition, the next of kin or guardians of the patients with fMCI and sAD also gave written informed consent if the patients could not comprehend the study protocol or could not sign their names.

Clinical Neuropsychological and Cognitive Assessments

All subjects (fMCI, sAD, and sMCI) underwent clinical and neuropsychological examinations. The detailed neuropsychological tests included the Mini-Mental State Examination (MMSE), CDR scale, Wechsler memory scale-revised, visual association memory test, category verbal fluency test, clock-drawing test, and trail-making A test, all of which were administered to obtain objective evidence of cognitive impairment (13).

Brain MRI Procedure

All subjects received an MRI scan with a 3T MR scanner (magneton Trio, a TIM system, Siemens, Erlangen, Germany). The scanning protocol included an axial fluid attenuation inversion recovery (FLAIR) sequence (TR = 9,000 ms, TE = 87 ms, T1 = 2,500 ms, voxel size = $0.9 \times 0.7 \times 4$ mm^3) and whole brain axial three-dimensional (3D) T1-weighted magnetization prepared rapid acquisition gradient echo (MP-RAGE) sequence (TR = 2,000 ms, TE = 2.63 ms, T1-900 ms, flip angle = 9°, voxel size = $1 \times 1 \times 1$ mm^3), which was subsequently reformatted as planes perpendicular to the long axis of the hippocampus in slices 2 mm thick. An additional coronal T2-weighted turbo spin echo sequence (TR = 7,400 ms, TE = 95 ms, voxel size = $0.4 \times 0.4 \times 2$ mm^3) was acquired with identical geometric orientation with the reformed coronal T1-weighted images (12).

Amyloid PET Acquisition

Radiosynthesis and acquisition of ^{18}F-florbetapir PET images were performed as described previously (14). ^{18}F-florbetapir PET scans were performed using a Biograph mCT PET/CT system (Siemens Medical Solutions, Malvern, PA). A 10-min PET scan was acquired 50 min after an injection of 375±18 MBq of ^{18}F-florbetapir. The 3D ordered subsets expectation maximization reconstruction algorithm (four iterations, 24 subjects, Gaussian filter 2 mm, Zoom 3) was applied with CT-based attenuation correction and scatter and random corrections, which resulted in reconstructed images with a matrix size of $400 \times 400 \times 148$ and a voxel size of $0.68 \times 0.68 \times 1.5$ mm (15, 16).

Tau PET Acquisition

Radiosynthesis and preparation of ^{18}F-THK-5351 PET tracers were performed as described previously (17). Tau PET images were acquired 50–60 min after intravenous injections of 378 ± 17 MBq of ^{18}F-THK-5351 on a dedicated PET/CT scanner (Siemens Biograph mCT 16; Siemens Medical Solutions). The same reconstruction protocols were applied as with the amyloid PET images. In addition, all subjects received an MRI scan with a 3T MR scanner (Magneton Trio, a TIM system, Siemens, Erlangen, Germany) to screen for other diseases and obtain structural information.

Image Analysis

PMOD image analysis software (version 3.3; PMOD Technologies Ltd., Zurich, Switzerland) was used for all image processing and analysis. Each PET image was spatially normalized to the Montreal Neurological Institute space using MR-based spatial normalization. Eight volumes of interest (VOIs) were selected including the cerebellum gray, cerebellum white, frontal, medial temporal, lateral temporal, medial parietal, lateral parietal, and occipital areas, based on the anatomic labeling atlas (18). Because the fMCI patients may have had a high SUVR in the cerebellar cortical areas, the reference regions of cerebellum white and pons were used to calculate SUVR images for ^{18}F-florbetapir and ^{18}F-THK-5351, respectively. Regional SUVRs were measured from the mean SUVR of each VOI. For ^{18}F-THK-5351 images, regional SUVRs for VOIs of Braak stage I/II, Braak stage III/IV, and Braak stage V/VI (19) were also computed for analysis.

Statistical Analysis

Data are expressed as means ± SD, or absolute numbers with proportions for descriptive statistics. Regional SUVRs of the ^{18}F-Tau THK-5351 PET images were compared individually region by region using the non-parametric Kruskal-Wallis test with Dunn's multiple comparison *post hoc* analysis for group comparisons between the five patients with fMCI and 12 HCs, between the six patients with sAD and 12 HCs, and between the five patients with fMCI and nine patients with sAD. A p-value of 0.05 was considered to be the threshold for statistical significance in each test.

RESULTS

The demographic data and clinical characteristic of the five patients with fMCI from 2 large Taiwanese familial AD pedigrees are shown in **Table 1** and **Supplement Figure 1**. There were two men and three women aged between 49 and 57 years. The age at onset of memory impairment ranged from 46 to 53 years, and the age at entry to the study ranged from 47 to 54 years. All five patients had memory impairment. The MMSE scores ranged from 23 to 26 (median: 24), and the sum score of CDR ranged from 0.5 to 5.0 (median: 3). The years of education ranged from 9 to 14 years.

Apolipoproteins E3/E3 were recorded in four patients with fMCI and E2/E3 in one. The brain MRI findings were normal in two patients (patients 2 and 4), and cortical atrophy was noted in three patients (patients 1, 3, and 5). Interestingly patient 1 had no microangiopathy initially, but after receiving three courses of passive immunization with a monoclonal antibody (aducanumab), she developed amyloid-related imaging abnormality-hemosiderin deposition (ARIA-H) with 0 to 3

TABLE 1 | Demographic data of the patients with familial MCI and the Taiwan APP p.D678H mutation.

Patient No	Gender/current age (Y)	Age at study (Y)	Onset age (Y)	Education (Y)	Clinical features	APoE	Brain MRI	Current diagnosis
1	F/53	51	50	14	RMI	E3/E3	Multiple cerebral microbleeds*, CA	MCI
2	M/54	52	50	9	RMI	E3/E3	Normal	MCI
3	M/57	54	53	14	RMI	E3/E3	CA	MCI
4	F/49	47	46	12	RMI	E3/E3	Normal	MCI
5	F/54	52	52	14	RMI	E2/E3	Multiple cerebral microbleeds, CA	MCI, CAA

*Y, year; M, male; F, female; MCI, mild cognitive impairment; RMI, recent memory impairment; APoE, apolipoprotein; CA, cortical atrophy; MMSE, Mini-Mental State Examination; CDR, clinical dementia rating; MRI, magnetic resonance imaging; CAA, cerebral amyloid angiopathy, *after 3 courses of passive immunization with aducanumab.*

TABLE 2 | Demographic data of the patients with fMCI, sporadic AD, sporadic MCI, and healthy controls.

	HC ($n = 12$)	sMCI ($n = 6$)	sAD ($n = 9$) mild:7, moderate:2	fMCI ($n = 5$)
Gender	5M/7F	4M/2F	4M/5F	2M/3F
Age(Y)	50–72	70–89	57–79	47–54
Median	56.5	75.5	74	52
Mean ± SD	58.6 ± 6.8	78.5 ± 7.3	69.8 ± 8.5	51.2 ± 2.6
Education(Y)	6–18	6–16	6–16	9–14
Median	12	13	9	12
Mean ± SD	11.8 ± 3.4	12.3 ± 3.4	10.2 ± 3.9	12.2 ± 2.0
MMSE	23–30	21–28	3–21	23–26
Median	28	25.5	16	24
Mean ± SD	28.0 ± 1.9	24.7 ± 3.0	13.3 ± 6.6	24.6 ± 1.3
CDR(Sum)	0	1.0–4.5	2–14	0.5–5.0
Median	0	2.5	5.5	3.0
Mean ± SD	0	2.7 ± 1.4	6.7 ± 3.7	2.6 ± 1.7
APP gene	GG	GG	GG	CG

HC, healthy controls; sMCI, sporadic amnestic mild cognitive impairment due to Alzheimer's disease; sAD, sporadic Alzheimer's disease; fMCI, familial mild cognitive impairment; Y, year; M, male; F, female; MMSE, Mini-Mental State Examination; CDR, clinical dementia rating; APP, amyloid precursor protein; CG, with the D678H APP gene; GG, without the D678H APP gene; PET, positron emission tomography.

microbleeds and subsequently up to 12 microbleeds. After stopping aducanumab treatment, the microbleeds remained stationary. The current diagnosis of the five familial patients was at the stage of MCI and cerebral amyloid angiopathy in one. **Table 2** shows the demographic data of the five patients with fMCI, six with sMCI, nine with sAD (two: moderate, seven: mild), and 12 HCs. All of the fMCI patients had the APP p.D678H mutation, but none of the other groups had this mutation. All of the patients with sMCI, sAD, and fMCI had a positive AV-45 PET scan, while the 12 HCs had a negative AV-45 PET scan. In the patients with fMCI, brain AV-45 PET scans showed prominent amyloid deposition in the frontal, temporal, parietal, and precuneus, and particularly in the occipital cortical areas, while the patients with sAD and sMCI had increased amyloid deposition particularly in the precuneus and frontal areas (**Figure 1**). **Figure 2** shows increased ^{18}F-THK-5351 SUVR uptake in the five patients with fMCI, and in particular the THK-5351 uptake extended to the lateral temporal area. **Figure 3** shows group means of THK-5351 SUVR data after 50–60 min. A trend of a gradual increase in THK-5351 SUVR was observed in the patients with sMCI, followed by those with fMCI and sAD. A significantly high regional THK-5351 SUVR was noted in the patients with fMCI and sAD compared to the HCs. In addition, high cerebellar cortex THK-5351 SUVR was observed in the patients with fMCI compared to the HC or sMCI groups.

Substantial ^{18}F-THK-5351 uptake was noted in the medial temporal area in the HCs. According to Braak stage, the patients with fMCI had a significantly increased SUVR of ^{18}F-THK-5351 than the HCs with Braak stage 1/2, and 5/6 ($p < 0.01$) and with Braak stage 3/4 ($p < 0.05$) (**Figure 4**). In the patients with sMCI, the regional SUVR of ^{18}F-THK-5351 was not significantly increased compared with the HCs. However, in the patients with sAD, the SUVR was significantly increased in those with Braak

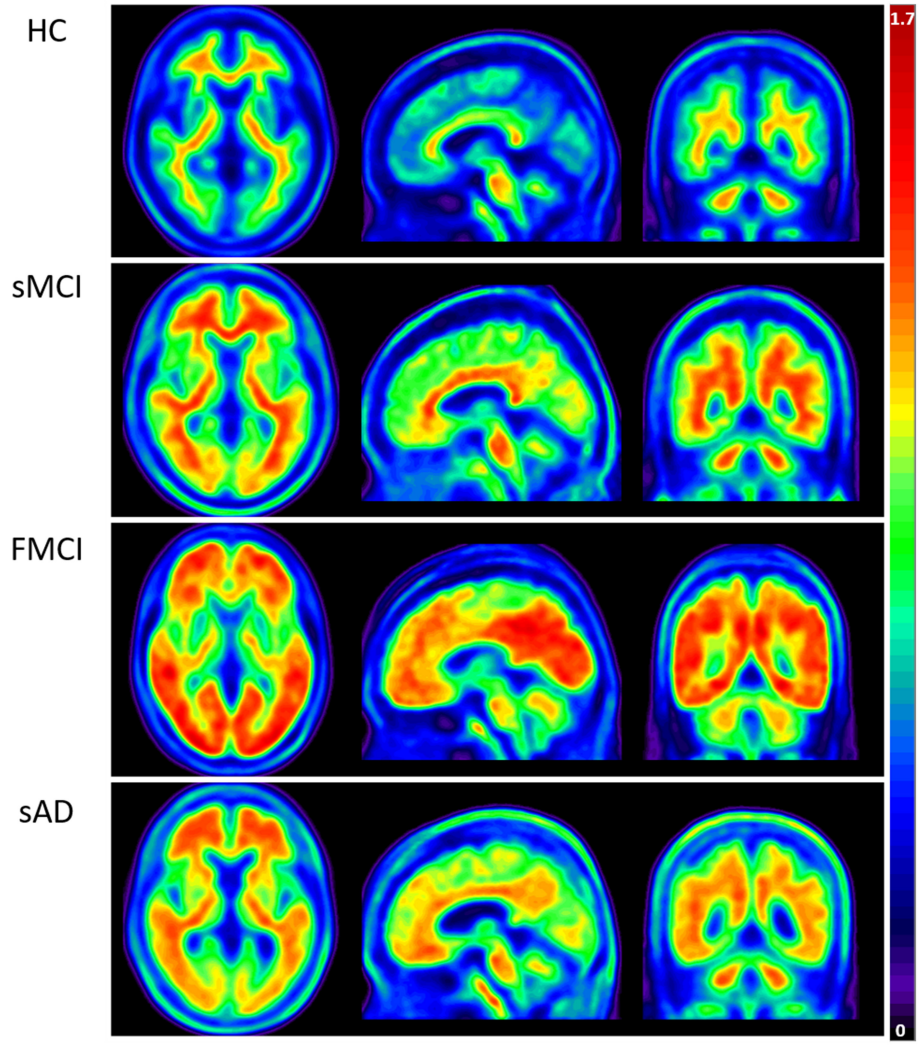

FIGURE 1 | Group means of brain AV-45 PET images of the HCs and patients with sMCI, fMCI, and sAD. The figure shows prominent amyloid deposition in the frontal, temporal, parietal, precuneus, and particularly occipital cortical areas in the patients with fMCI, increased amyloid deposition predominantly in the precuneus and frontal areas in the patients with sAD and sMCI, and no definite uptake in the HCs.

stage 3/4 and 5/6 compared with the HCs ($p < 0.001$). There was no significant increase in ^{18}F-THK-5351 SUVR between the patients with fMCI and sMCI and between those with fMCI and sAD ($p > 0.05$). With regards to regional SUVR of ^{18}F-THK-5351, a significantly increased uptake was noted in the frontal, and lateral temporal areas ($p < 0.05$) and the medial parietal, lateral parietal, medial temporal, occipital, and cerebellar cortical areas ($p < 0.01$) in the patients with fMCI compared to the HCs. In addition, the regional SUVR of ^{18}F-THK-5351 was increased in the frontal, medial parietal, lateral parietal, lateral temporal, and occipital areas ($p < 0.01$) in the patients with sAD compared to the HCs. In cerebellar cortical areas, the SUVR was increased in the patients with fMCI compared to the HCs ($p < 0.01$) and patients with sMCI ($p < 0.05$) (**Figure 5**). There was a statistically significant correlation between regional SUVR and MMSE score in all VOIs of Braak 3/4, 5/6 ($p < 0.0001$) and Braak 1/2 ($p = 0.0096$) (**Figure 6A**). There were statistically significant correlations between CDR sum box scores and regional SUVR in all VOIs of Braak 3/4, Braak 5/6 ($p < 0.0001$), and Braak 1/2 ($p = 0.0022$) (**Figure 6B**).

DISCUSSION

In this study, the patients with fMCI had a significantly increased SUVR of ^{18}F-THK-5351 in the seven cerebral and cerebellar cortical areas ($p < 0.01$) compared with the HCs. In addition, the SUVR of ^{18}F-THK-5351 in the cerebellar cortex was statistically significant compared to the patients with sMCI ($p < 0.05$). Despite a high level of tau deposition in the cerebellar cortex areas in our patients with fMCI, cerebellar symptoms, and

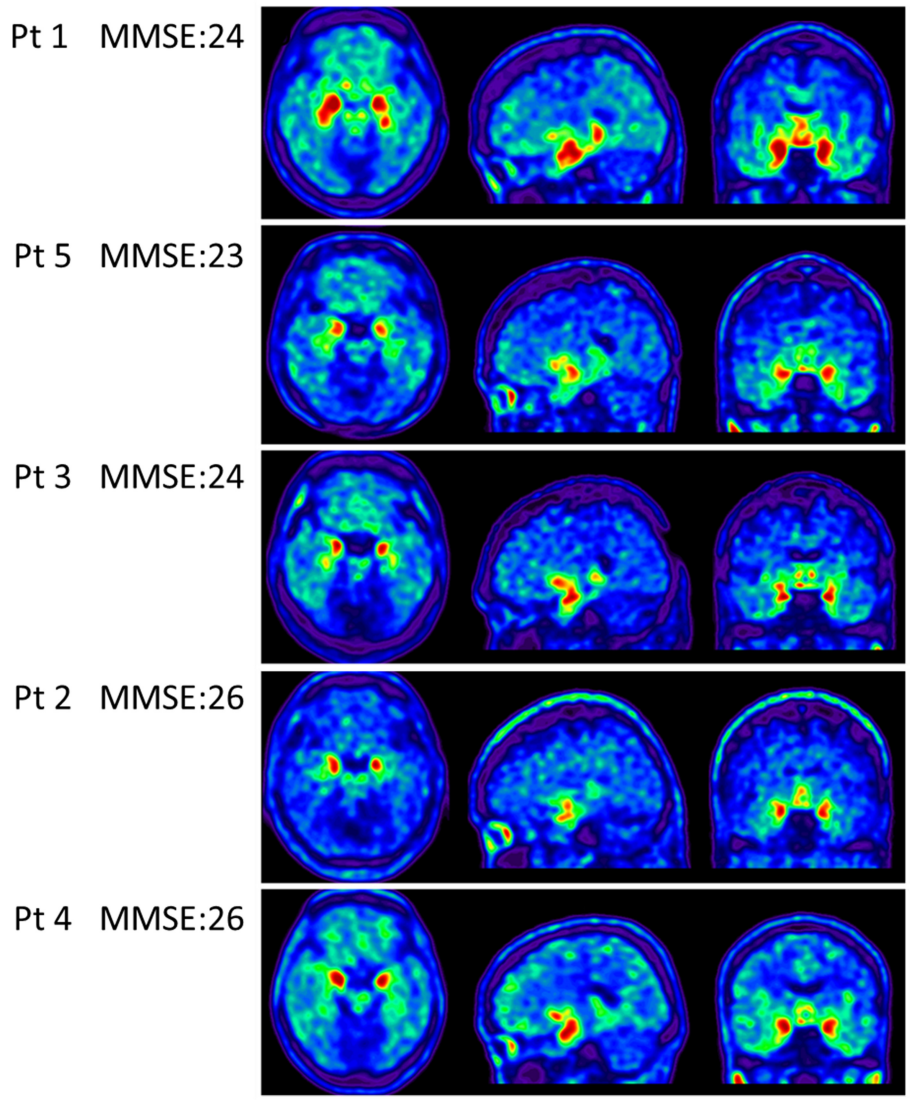

FIGURE 2 | Tau PET scan with THK-5351 in the five patients with fMCI showing an increased SUVR of THK-5351 particularly extending to the lateral temporal area.

signs were not found. Moreover, in the patients with sAD, the regional SUVR of ^{18}F-THK-5351 in most of the cerebral cortical areas including frontal, medial parietal, lateral parietal, lateral temporal, and occipital areas was significantly higher ($p < 0.001$) compared with the HCs.

Furthermore, brain ^{18}F-AV-45 PET showed an increase of amyloid deposition in the frontal, temporal, parietal, and particularly occipital areas in the five patients with fMCI compared with the HCs and patients with sMCI and sAD. These results revealed a higher amyloid burden than those in the patients with sMCI and sAD.

In the clinical course of disease progression, the patients with fMCI had an earlier onset of memory impairment and more rapid progression to dementia than the patients with sMCI (4). In addition, the patients may have had dementia and/or amyloid angiopathy (3). One patient (patient 5) who had multiple microbleeds in brain MRI compatible with cerebral amyloid angiopathy, cannot participate in the anti-amyloid treatment and another (patient 1) had no cerebral microbleed in the initial brain MRI but developed 12 microbleeds (ARIA-H) 3 months after passive immunization with aducanumab. Then she was withdrawn from the study. Although ARIA-H may also be found in other sAD patients who have received aducanumb therapy, these results may suggest a potentially higher risk of microhemorrhages during/after passive immunization in these fMCI patients because they may develop cerebral amyloid angiopathy.

However, tau deposition in these specific Taiwanese patients with the APP p.D678H mutation remains unknown. In this study, we clearly demonstrated tau deposition with THK5351

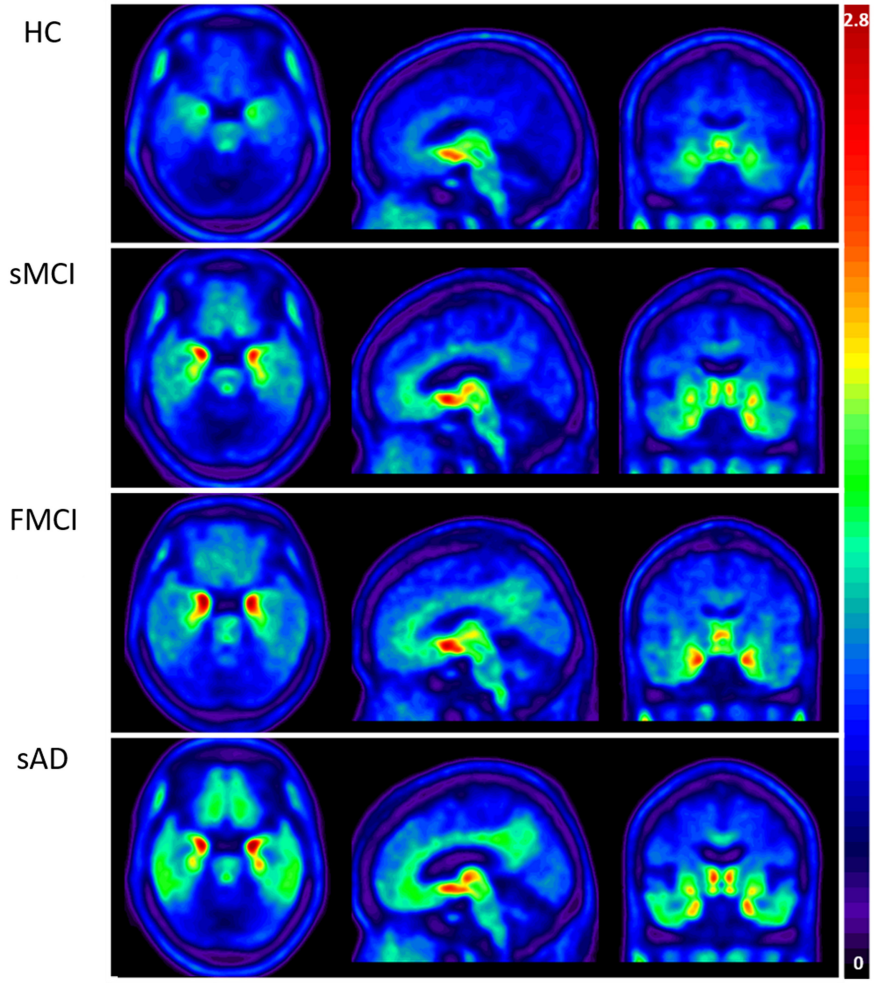

FIGURE 3 | Group mean THK-5351 SUVR images of the HCs and patients with sMCI, fMCI, and sAD showing a trend of gradual uptake increase in the patients with sMCI, followed by those with fMCI and sAD.

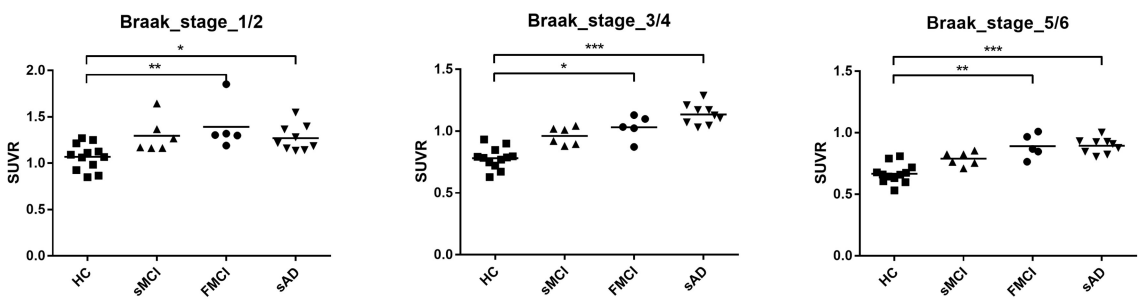

FIGURE 4 | Regional SUVR of THK-5351 in the HCs and patients with sMCI, fMCI, and sAD according to Braak stage 1/2, 3/4, and 5/6. The regional SUVR of the patients with fMCI showed a significant increase compared to the HCs in Braak stage 1/2, and 5/6 ($p < 0.01$) and Braak stage 3/4 ($p < 0.05$). The regional SUVR in the patients with sAD had a significant increase in Braak stages 3/4 and 5/6 compared with the HCs ($p < 0.001$). *$p < 0.05$, **$p < 0.01$, ***$p < 0.001$.

PET scan in the seven cerebral areas, and particularly the cerebellar cortical area compared with the HCs. However, the mechanisms of co-localization of amyloid and tau deposition remain unknown. Tau images may have shown a synergistic effect of burden on the brain in the patients with fMCI compared to the patients with sMCI.

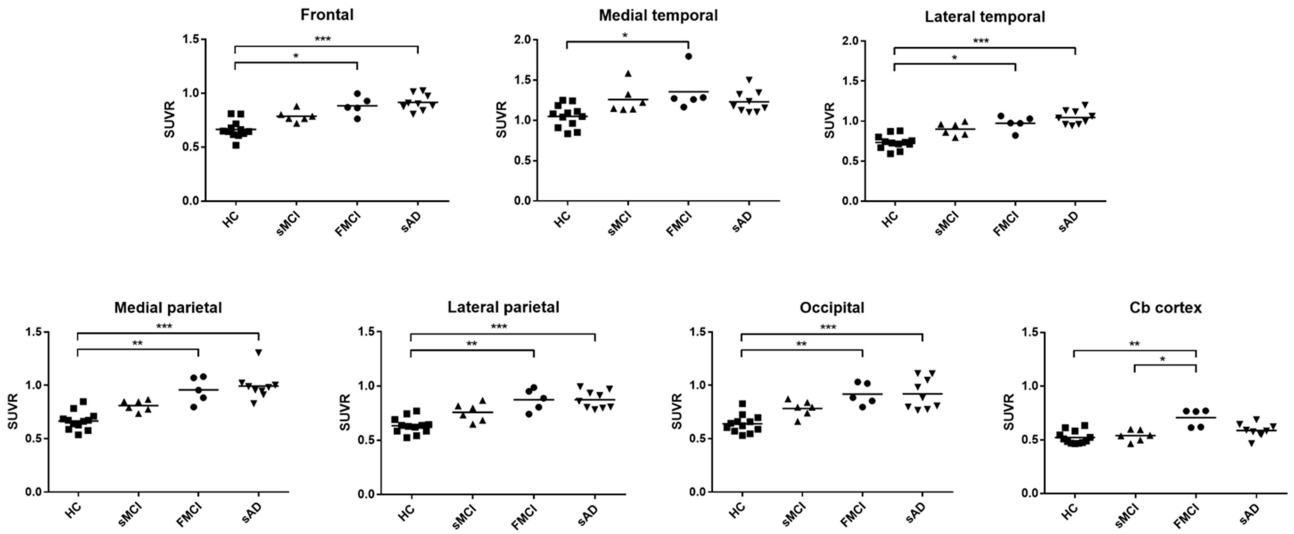

FIGURE 5 | The regional SUVR of THK-5351 imaging in the HCs and patients with sMCI, fMCI and sAD. A significantly increased uptake was noted in the patients with fMCI in the frontal, lateral temporal, medial parietal, lateral parietal, medial temporal, occipital, and cerebellar cortical areas compared with the HCs, while a significantly increased uptake was noted in the frontal, medial parietal, lateral parietal, lateral temporal, and occipital areas in the patients with sAD compared to the HCs. In the cerebellar cortical area, the SUVR was increased in the patients with fMCI compared to those with sMCI. $^{*}p < 0.05$, $^{**}p < 0.01$, $^{***}p < 0.001$.

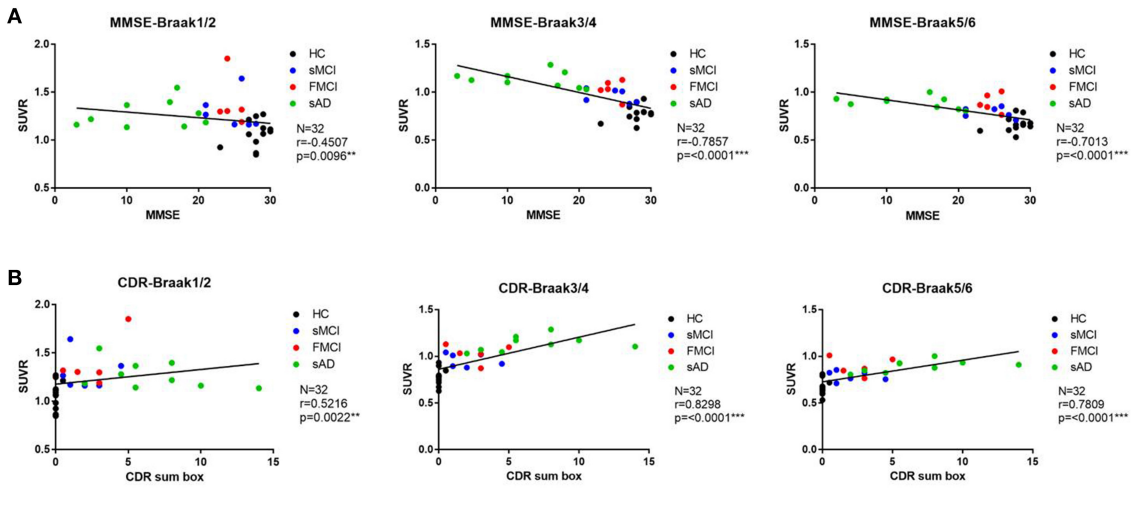

FIGURE 6 | (A) The correlation between regional SUVR and MMSE within VOIs of Braak stages. Statistically significant correlations were noted in all VOIs of Braak 3/4 and 5/6 ($p < 0.0001$) and Braak 1/2 ($p = 0.0096$). **(B)** The correlations between CDR and regional SUVR within VOIs of Braak stages. A statistically significant correlation was noted in all VOIs of Braak 3/4 and Braak 5/6 ($p < 0.0001$) and Braak 1/2 ($p = 0.0022$).

According to the correlation between regional SUVR of ^{18}F-THK-5351 and MMSE, there were statistically significant correlations within VOIs in Braak 1/2 ($p = 0.0096$), Braak 3/4 ($p < 0.0001$), and Braak 5/6 ($p < 0.0001$). In addition the correlations between regional SUVR and CDR sum box scores were also statistically significant in all VOIs of Braak 1/2 ($p < 0.0022$), Braak 3/4 ($p < 0.0001$), and Braak 5/6 ($p < 0.0001$). These results may indicate that ^{18}F-THK-5351 uptake is correlated with disease severity.

In the patients with sMCI, there was a trend of increased SUVR of ^{18}F-THK-5351 PET in all of the cerebral cortex areas, however the differences did not reach statistical significance compared with the HCs, which may be due to a small sample size. In the patients with sAD, the SUVR of ^{18}F-THK-5351 PET was significantly increase in the frontal, medial parietal, lateral parietal, lateral temporal, and occipital areas ($p < 0.001$). This may indicate that ^{18}F-THK-5351 PET can provide important clues for disease progression. In the patients with fMCI, there was statistically significant ^{18}F-THK-5351 SUVR in the cerebellar

cortex compared to the patients with sMCI. This may indicate that tau deposition in the cerebellar cortical area is a characteristic finding in patients with the Taiwan APP p.D678H mutation.

There are several limitations to this study, including that ^{18}F-THK5351 binding may target a non-specific process related to neurodegeneration that is co-localized with tau pathology (20, 21). ^{18}F-THK-5351 may also indicate a non-specific neuronal injury rather than specific tauopathy. The other important findings include off-target regions in the white matter, midbrain, thalamus, and basal ganglia (22). Increased ^{18}F-THK-5351 uptake in the basal ganglia and substantia nigra may also reflect its binding to MAO-B (23, 24). Several different tau tracers such as flortaucipir (25), PBB3 (26), and PMPBB3 (27) have been developed and utilized in clinical studies. The recent study with PMPBB3 have been studied in patients with AD, progressive supranuclear palsy, frontotemporal dementia, and corticobasal degeneration (28). Further investigation with a more specific tau PET tracer such as PMPBB3 for the specific family is indicated. The other limitation is a small sample size of the fMCI patients, and a sMCI and sAD patients with relatively earlier onset and similar education level.

The interaction between amyloid and tau protein remains unclear. However, amyloid β plaques may enhance tau-seeded pathologies by facilitating neuritic tau aggregation (29). In addition, the amyloid β protein may promote the spread of tau through specific components of a neural system, leading to early symptoms of amnesia (30, 31). In this specific family with amyloid APP p.D678H mutation, a widespread of amyloid deposition was noted while a limited tau deposition in the medial and lateral temporal lobe areas is plaucible in patients with fMCI. The group difference of tau deposition between fMCI and sMCI is limited, although a trend is noted. The only difference is noted in the cerebellar cortex area. The real etiologies remained unknown. However, from the amyloid PET study, increased metabolic vulnerability in early onset AD is not related to amyloid burden (32). In our patients with fMCI, although increased SUVR of AV-45 PET in the occipital area, visual symptoms, or signs was not found. In this study the increased tau deposition in the cerebellar cortex area did not make any cerebellar dysfunction in patients with fMCI.

In conclusion, the present data indicate a higher tau burden in patients with fMCI with this specific Taiwan mutation. In addition a higher ^{18}F-THK-5351 SUVR in the cerebellar cortical area was a characteristic finding in the patients with fMCI. ^{18}F-THK-5351 PET may also be a biomarker of disease severity from sMCI to sAD. As compared between amyloid and tau PET, the amyloid deposition is diffuse, and tau deposition is limited to the temporal lobe in the patients with fMCI. Further investigations of the specific family members including asymptomatic heterozygotes and additional tracers are warranted. In addition, if the findings can be supported through cerebrospinal fluid examination and post-mortem neuropathology, we can understand the evolution of the familial dementia.

ETHICS STATEMENT

The study was approved by the ministry of Health and Welfare in Taiwan and the Institutional Review Board of Chang Gung Memorial Hospital.

AUTHOR CONTRIBUTIONS

Y-CW, K-LH, C-HL, T-YC, H-CW, and C-CH: providing information. C-CH, I-TH, and K-JL: conception and design of the study. Y-CW, C-YH, and C-CH: acquisition of data. I-TH, K-JL, C-YH, and C-CH: analysis and/or interpretation of data. I-TH, C-YH, and C-CH: drafting of the manuscript. I-TH, K-JL, and C-CH: reviewing the manuscript critically. T-CY, K-JL, and C-CH: application for the funding. All authors approval of the final version of the paper.

FUNDING

The study was supported by grants from Ministry of Science and Technology (Grant NSC-98-2314-B-182-034-MY2, NSC 98-2314-B-182-056, NSC 100-2314-B-182-003, and NSC-100-2314-B-182-038, MOST 105-2314-B-182-005, 106-2314-B-182A-026-MY3, and 106-2314-B-182-017-MY3) and Chang Gung Memorial Hospital (Grant CMRPG3C0611, CMRPG3C0612, CMRPG3E1001, CMRPD1H0391, and CMRPG3E2191).

SUPPLEMENTARY MATERIAL

The Supplementary Material for this article can be found online at: https://www.frontiersin.org/articles/10.3389/fneur.2019.00503/full#supplementary-material

REFERENCES

1. Lan MY, Liu JS, Wu YS, Peng CH, Chang YY. A novel APP mutation (D678H) in a Taiwanese patient exhibiting dementia and cerebral microvasculopathy. *J Clin Neurosci.* (2013) 21:513–5. doi: 10.1016/j.jocn.2013.03.038
2. Chen WT, Hong CJ, Lin YT, Chang WH, Huang HT, Liao JY, et al. Amyloid-beta (Aβ) D7H mutation increases oligomeric Aβ42 and alters properties of Aβ-Zinc/Copper assemblies. *PLoS ONE*. (2012) 7:e34666. doi: 10.1371/journal.pone.0035807
3. Huang CY, Hsiao IT, Lin KJ, Huang KL, Fung HC, Liu CH, et al. Amyloid PET pattern associated with amyloid angiopathy in Taiwan familial AD with D678H APP mutation. *J Neurol Sci.* (2019) 398:107–16. doi: 10.1016/j.jns.2018.12.039
4. Weng YC, Hsiao IT, Huang CY, Huang KL, Liu CH, Chang TY, et al. Progress of brain amyloid deposition in familial Alzheimer's disease with Taiwan D678H APP mutation. *J Alz Dis.* (2018) 66:775–87. doi: 10.3233/JAD-180824
5. van Berckel BNM, Ossenkoppele R, Tolboom N, Yaqub M, Foster-Dingley JC, Windhorst AD, et al. Longitudinal amyloid imaging using ^{11}C-PiB: methodologic considerations. *J Nucl Med.* (2013) 54:1570–6. doi: 10.2967/jnumed.112.113654
6. Chen K, Roontiva A, Thiyyagura P, Lee W, Liu X, Ayutyanont N, et al. Improved power for characterizing longitudinal amyloid-β PET changes and evaluating amyloid-modifying treatments with

a cerebral white matter reference region. *J Nucl Med.* (2015) 56:560–6. doi: 10.2967/jnumed.114.149732
7. Hardy J, Selkoe DJ. The amyloid hypothesis of Alzheimer's disease: progress and problems on the road to therapeutics. *Science*. (2002) 297:353–6. doi: 10.1126/science.1072994
8. Okamura N, Harada R, Furumoto S, Arai H, Yanai K, Kudo Y. Tau PET imaging in Alzheimer's disease. *Curr Neurol Neurosci Rep*. (2014) 14:500. doi: 10.1007/s11910-014-0500-6
9. Mckhann GM, Knopman DS, Chertkow H, Hyman BT, Jack CR Jr, Kawas CH, et al. The diagnosis of dementia due to Alzheimer's disease: recommendations from the National Institute on aging and the Alzheimer's association workgroup. *Alzheimer Dement.* (2011) 7:263–9. doi: 10.1016/j.jalz.2011.03.005
10. Petersen RC, Doody R, Kurz A, Mohs RC, Morris JC, Rabins PV, et al. Current concepts in mild cognitive impairment. *Arch Neurol.* (2001) 58:1985–92. doi: 10.1001/archneur.58.12.1985
11. American Psychiatric Association. *Diagnostic and Statistical Manual of Mental Disorders, DSM-IV*. Washington, DC: American Psychiatric Association (1994).
12. Huang KL, Lin KJ, Hsiao IT, Kuo HC, Hsu WC, Chuang WL, et al. Regional amyloid deposition in amnestic mild cognitive impairment and Alzheimer's disease evaluated by [18F]AV-45 positron emission tomography in Chinese population. *PLoS ONE.* (2013) 8:e58974. doi: 10.1371/journal.pone.0058974
13. Wang PN, Hong CJ, Lin KN, Liu HC, Chen WT. APOE episilon 4 increase the risk of progression from amnestic mild cognitive impairment to Alzheimer's disease among ethnic Chinese in Taiwan. *J Neurol Neurosurg Psychiatry.* (2011) 82:165–9. doi: 10.1136/jnnp.2010.209122
14. Lin KJ, Hsu WC, Hsiao IT, Wey SP, Jin LW, Skovronsky D, et al. Whole-body biodistribution and brain PET imaging with [18F]AV-45, a novel amyloid imaging agent—a pilot study. *Nucl Med Biol.* (2010) 37:497–508. doi: 10.1016/j.nucmedbio.2010.02.003
15. Yao CH, Lin KJ, Weng CC, Hsiao IT, Ting YS, Yen TC, et al. GMP-compliant automated synthesis of [(18)F]AV-45 (Florbetapir F 18) for imaging beta-amyloid plaques in human brain. *Appl Radiat Isot.* (2010) 68:2293–7. doi: 10.1016/j.apradiso.2010.07.001
16. Wu KY, Liu CY, Chen CS, Chen CH, Hsiao IT, Hsieh CJ, et al. Beta-amyloid deposition and cognitive function in patients with major depressive disorder with different subtypes of mild cognitive impairment: F-florbetapir (AV-45/Amyvid) PET study. *Eur J Nucl Med Mol Imaging.* (2016) 43:1067–76. doi: 10.1007/s00259-015-3291-3
17. Hsiao IT, Lin KJ, Huang KL, Huang CC, Chen HS, Wey SP, et al. Biodistribution and radiation dosimetry for the Tau tracer (18)F-THK-5351 in healthy human subjects. *J Nucl Med.* (2017) 58:1498–503. doi: 10.2967/jnumed.116.189126
18. Tzourio-Mazoyer N, Landeau B, Papathanassiou D, Crivello F, Etard O, Delcroix N, et al. Automated anatomical labeling of activations in SPM using a macroscopic anatomical parcellation of the MNI MRI single-subject brain. *Neuroimage.* (2002) 15:273–89. doi: 10.1006/nimg.2001.0978
19. Ossenkoppele R, Schonhaut DR, Schöll M, Lockhart SN, Ayakta N, Baker SL, et al. Tau PET patterns mirror clinical and neuroanatomical variability in Alzheimer's disease. *Brain.* (2016) 139:1551–67. doi: 10.1093/brain/aww027
20. Harada R, Okamura N, Furumoto S, Furukawa K, Ishiki A, Tomita N, et al. ^{18}F-THK5351: a novel PET radiotracer for imaging neurofibrillary pathology in Alzheimer disease. *J Nucl Med.* (2016) 57:208–14. doi: 10.2967/jnumed.115.164848
21. Harada R, Ishiki A, Kai H, Sato N, Furukawa K, Furumoto S, et al. Correlations of ^{18}F-THK5351 PET with postmortem burden of Tau and astrogliosis in Alzheimer disease. *J Nucl Med.* (2018) 59:671–4. doi: 10.2967/jnumed.117.197426
22. Okamura N, Harada R, Ishiki A, Kikuchi A, Nakamura T, Kudo Y. The development and validation of tau PET tracers: current status and future directions. *Clin Transl Imaging.* (2018) 6:305–16. doi: 10.1007/s40336-018-0290-y
23. Jang YK, Lyoo CH, Park S, Oh SJ, Cho H, Oh M, et al. Head to head comparison of [^{18}F] AV-1451 and [^{18}F] THK5351 for tau imaging in Alzheimer's disease and frontotemporal dementia. *Eur J Nucl Med Mol Imaging.* (2018) 45:432–42. doi: 10.1007/s00259-017-3876-0
24. Ng KP, Pascoal TA, Mathotaarachchi S, Therriault J, Kang MS, Shin M, et al. Monoamine oxidase B inhibitor, selegiline, reduces ^{18}F-THK5351 uptake in the human brain. *Alzheimer's Res Ther.* (2017) 9:25. doi: 10.1186/s13195-017-0253-y
25. Johnson KA, Schultz A, Betensky RA, Becker JA, Sepulcre J, Rentz D, et al. Tau positron emission tomographic imaging in aging and early Alzheimer disease. *Ann Neurol.* (2016) 79:110–9. doi: 10.1002/ana.24546
26. Ono M, Sahara N, Kumata K, Ji B, Ni R, Koga S, et al. Distinct binding of PET ligands PBB3 and AV-1451 to tau fibril strains in neurodegenerative tauopathies. *Brain.* (2017) 140:764–80. doi: 10.1093/brain/aww339
27. Hsiao IT, Huang KL, Chen PY, Lin KJ, Huang CC. Study on tissue-based and histogram-based reference regions for semiquantitation of 18F-APN-1607 Tau PET imaging [Abstract]. In: Johnson KA, editor. *Poster 30, 13th Human Amyloid Imaging.* Miami, FL (2019). p. 112. Available online at: www.worldeventsforum.com/hai
28. Hsu JL, Lin KJ, Hsiao IT, Lian CF, Huang CC, Huang KL, et al. Image features and clinical associations of the novel tau PET tracer 18F-APN-1607 in Alzheimer's disease [Abstract]. In: Johnson KA, editor. *Poster 147, 13th Human Amyloid Imaging.* Miami, FL (2019). p. 398. Available online at: www.worldeventsforum.com/hai
29. Jagust W. Following the pathway to Alzheimer's disease. *Nat Neurosci.* (2018) 21:306–8. doi: 10.1038/s41593-018-0085-5
30. Jacobs HIL, Hedden T, Schultz AP, Sepulcre J, Perea RD, Amariglio RE, et al. Structural tract alterations predict downstream tau accumulation in amyloid-positive older individuals. *Nat Neurosci.* (2018) 21:424–31. doi: 10.1038/s41593-018-0070-z
31. Laure SA, Lemoine L, Chiotis K, Leuzy A, Elemu RV, Nordberg A. Tau PET imaging: present and future directions. *Mol Neurodegener*. (2018) 12:19. doi: 10.1186/s13024-017-0162-3
32. Rabinovici GD, Furst AJ, Alkalay A, Racine CA, O'Neil JP, Janabi M, et al. Increased metabolic vulnerability in early-onset Alzheimer's disease is not related to amyloid burden. *Brain.* (2010) 133:512–28. doi: 10.1093/brain/awp326

Conflict of Interest Statement: The authors declare that the research was conducted in the absence of any commercial or financial relationships that could be construed as a potential conflict of interest.

frontiers in Neurology

MINI REVIEW
published: 28 August 2019
doi: 10.3389/fneur.2019.00935

MEIS1 and Restless Legs Syndrome: A Comprehensive Review

Faezeh Sarayloo[1,2], *Patrick A. Dion*[2,3] *and Guy A. Rouleau*[2,3]*

[1] Department of Human Genetics, McGill University, Montreal, QC, Canada, [2] Montreal Neurological Institute, McGill University, Montreal, QC, Canada, [3] Department of Neurology and Neurosurgery, McGill University, Montreal, QC, Canada

Restless legs syndrome (RLS) is a common sleep-related disorder for which the underlying biological pathways and genetic determinants are not well understood. The genetic factors so far identified explain less than 10% of the disease heritability. The first successful genome-wide association study (GWAS) of RLS was reported in 2007. This study identified multiple RLS associated risk variants including some within the non-coding regions of *MEIS1*. The *MEIS1* GWAS signals are some of the strongest genetic associations reported for any common disease. MEIS1 belongs to the homeobox containing transcriptional regulatory network (HOX). Work in *C. elegans* showed a link between the *MEIS1* ortholog and iron homeostasis, which is in line with the fact that central nervous system (CNS) iron insufficiency is thought to be a cause of RLS. Zebrafish and mice have been used to study the *MEIS1* gene identifying an RLS-associated-SNP dependent enhancer activity from the highly conserved non-coding regions (HCNR) of *MEIS1*. Furthermore, this gene shows a lower expression of mRNA and protein in blood and thalamus of individuals with the *MEIS1* RLS risk haplotype. Simulating this reduced *MEIS1* expression in mouse models resulted in circadian hyperactivity, a phenotype compatible with RLS. While *MEIS1* shows a strong association with RLS, the protein's function that is directly linked to an RLS biological pathway remains to be discovered. The links to iron and the enhancer activity of the HCNRs of *MEIS1* suggest promising links to RLS pathways, however more in-depth studies on this gene's function are required. One important aspect of *MEIS1*'s role in RLS is the fact that it encodes a homeobox containing transcription factor, which is essential during development. Future studies with more focus on the transcriptional regulatory role of MEIS1 may open novel venues for RLS research.

Keywords: restless legs syndrome, *MEIS1*, iron, sleep disorders, neurogenetics

OPEN ACCESS

Edited by:
Yue Huang,
Beijing Tiantan Hospital, China

Reviewed by:
Stefan Clemens,
East Carolina University, United States
Huifang Shang,
Sichuan University, China

***Correspondence:**
Guy A. Rouleau
guy.rouleau@mcgill.ca

Specialty section:
This article was submitted to Neurogenetics, a section of the journal Frontiers in Neurology

Received: *24 May 2019*
Accepted: *12 August 2019*
Published: *28 August 2019*

Citation:
Sarayloo F, Dion PA and Rouleau GA (2019) MEIS1 and Restless Legs Syndrome: A Comprehensive Review. Front. Neurol. 10:935. doi: 10.3389/fneur.2019.00935

INTRODUCTION

Restless legs syndrome is a common neurological disorder. The prevalence of RLS cases based on the minimum diagnostic criteria of the international RLS study group (IRLSSG) was estimated between 3.9 and 14.3% of the adult population. It is more common in women than men and the prevalence increases with age in the European and North American populations (1). RLS is more prevalent in people with iron deficiency or kidney disease (2). Twin studies and a familial aggregation analysis estimated the heritability of RLS between 54.0 and 69.4%,

thus there is a strong genetic element to the disease (3–5). RLS is a complex condition and environmental factors also contribute to its development.

The first attempts to identify RLS genetic risk factors used genome wide linkage (GWL) approaches in large multiplex families, most of which had an autosomal dominant mode of inheritance and one with autosomal recessive inheritance pattern. The GWL identified loci with large genomic regions, but no causative variant was identified by this approach and the results have often not been reproducible (5–12). Considering the complex nature of RLS, the genetic studies on RLS moved forward to association studies in search for common variants with low to moderate effect size.

SIGNIFICANCE OF *MEIS1* IN THE RLS GENETICS STUDIES

RLS is the first common sleep disorder for which genome wide association studies (GWAS) was performed and genetic risk loci identified. In 2007, the first genome-wide association study on RLS using 401 patients with familial RLS and 1,644 control individuals of German and French-Canadian origin identified common variants in three noncoding genomic regions (13). The strongest association signal found is a 32 kb linkage disequilibrium block in the intron 8 of *MEIS1* gene (13). This association has been replicated in several follow up studies in both familial and sporadic RLS cases (odds ratio 1.92, 95% CI 1.85–1.99, p-value = 2.00E−280, from the latest report in 2017) (14–17). Furthermore, common genetic variants with low effect size were identified for RLS in 18 additional loci that each confer a small risk for the disease (17). MEIS1 is a homeobox transcription factor that belongs to the three amino acid loop extension (TALE) family of homeodomain proteins; it is known to have functions in hematopoiesis and vascular patterning (18, 19). This protein forms heterodimeric or heterotrimeric complexes with PBX or HOX proteins for higher DNA binding specificity and affinity (20). It also plays roles in neurodevelopment as well as the development of proximodistal limb axis, with high expression in dopaminergic neurons of substantia nigra and red nucleus (21–24).

Rare coding variants of *MEIS1* were also proposed to contribute to be the cause of RLS. An Arg272-to-His (p.R272H) was found in one of 71 familial probands with RLS. However, a case-control genotyping study of this mutation across a North American cohort failed to validate this variant (25). In another study, an excess of rare null alleles specific to *MEIS1* isoform 1 was observed in RLS cases compared to controls in a burden test on a German population (26). Lastly, in a study conducted by Xiong et al. the thirteen *MEIS1* exons (and their respective splice junctions) were sequenced in 285 familial probands with a confirmed clinical diagnosis and no variants were identified (27). Hence coding variants are at most a very rare cause of RLS. This is not surprising as the gene is involved in many different developmental processes, so functional coding variants would likely have many additional manifestations, in addition to RLS.

REDUCED *MEIS1* EXPRESSION MAY CONTRIBUTE TO THE DEVELOPMENT OF RLS

After the publication of the first GWAS on RLS, a subsequent study by Xiong et al. (27), used human lymphoblastoid cell lines (LCL) as well as two different brain regions (thalamus and pons) from RLS patients for an expression study. A q-RT-PCR followed by western blot analysis showed that the patients who harbor the *MEIS1* risk haplotype (GG/GG, rs12469063–rs2300478) express lower levels of *MEIS1* mRNA and protein in LCL and thalamus (**Figure 1**). The authors argued that lower *MEIS1* expression in a subset of individuals can contribute to the development of RLS symptoms (27).

Given the lower *MEIS1* expression in a subgroup of patients, *in vivo* studies on mouse models with heterozygous *Meis1* knockout were conducted (23, 28). Young male and female mice showed hyperactivity with no effect on anxiety-related behaviors, providing a potential animal model to study RLS (**Figure 1**). Furthermore, considering the age-related manifestation of RLS symptoms in human, effects of *Meis1* haploinsufficiency was also studied in middle aged mice in a study by Salminen et al. (29). *Meis1* haploinsufficiency was associated with a sex dependent increase in the activity more specific to the initial of the rest phase of animal, similar to the circadian rhythm of RLS symptoms observed in human patients. Effects on sensorimotor system in a sex dependent manner were also reported (29).

THE LINKS BETWEEN *MEIS1* AND IRON METABOLISM

Observations made using a *Caenorhabditis elegans* model showed that post developmental inactivation of *Unc-62* (*MEIS1* ortholog) makes it one of the 64 genes that increase the worm's life span. *Unc-62* in the worms has 25% identity with *MEIS1* and almost 80% identity with its homeodomain. Adding iron chelators in the culture media of the worms resulted in changes in the effect of *Unc-62* inactivation on worms' lifespan, suggesting that *Unc-62* is involved in iron metabolism. The link between *Unc-62* and iron was also measured through its impact on the expression of ferritin. It was found that post developmental inactivation of *Unc-62* using RNAi resulted in higher expression of ferritin, a protein that plays a key role in iron metabolism through its ability to store excess iron and to release it into a soluble and nontoxic form (30). Thalamus samples obtained from RLS patients also showed that individuals with the *MEIS1* risk haplotype, who also have a reduced expression of *MEIS1*, show an increased expression of both ferritin (FTN) light and heavy chains. Furthermore, *DMT1* gene expression was higher in these individuals. *DMT1* is a proton-coupled metal transporter that carries iron from the extracellular domain to the cytoplasm (**Figure 1**). This finding also supports a link between *MEIS1* and iron metabolism where DMT1 transports iron into the brain (31). More work remains to be done to clarify the exact role of *MEIS1* in iron metabolism relevant to RLS (32). Recent

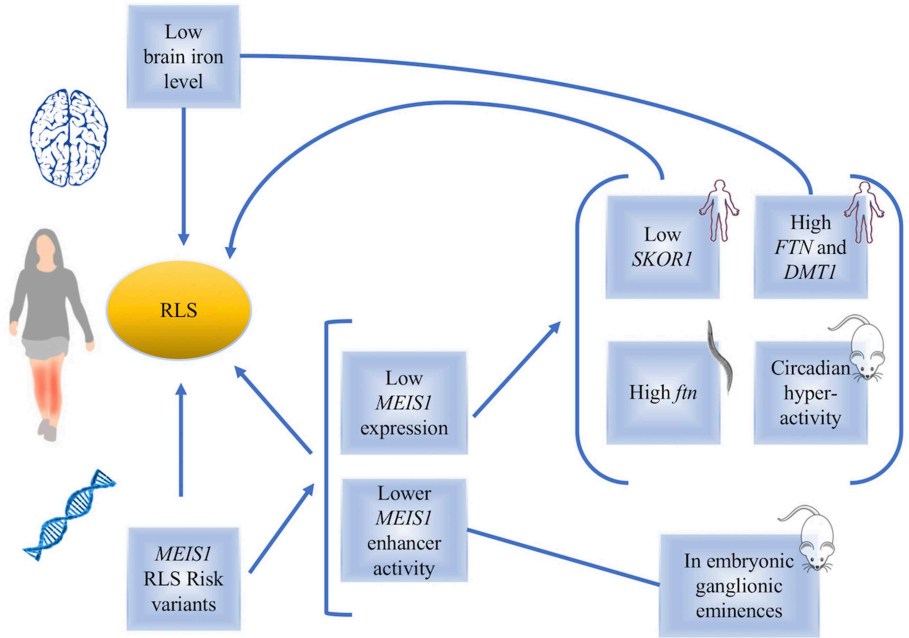

FIGURE 1 | A diagram, summarizing the links between *MEIS1* and restless legs syndrome. Low brain iron level or genetic variations in *MEIS1* have been found in RLS patients. The consequences of low *MEIS1* expression have been identified in human, *C. elegans* and mouse models (indicated in the figure).

studies suggest that DMT1 is expressed in endosomes of brain capillary endothelial cells denoting the blood-brain barrier (BBB) (33). The best well-established neurobiological abnormality in RLS is reduced brain iron, despite a normal peripheral iron level. The fact that some, but not all RLS patients, respond to intravenous (IV) iron provides an opportunity to interrogate the underlying pathways differing between responders versus non-responders. This led some studies to focus their attention toward the iron uptake at the blood-brain barrier (34). A preliminary analysis of *MEIS1* expression showed elevated *MEIS1* levels in the microvasculature isolated from RLS brain tissue by comparison to the tissues of control individuals. Moreover, a cell culture model of the BBB showed that treatment with an iron chelator increased the *MEIS1* expression, while iron loading conversely decreased *MEIS1* expression (unpublished data presented in a review article on the links between iron and RLS by Connor et al.; the small sample size in this report indicates that more investigations remain to be done to further validate this observation) (35, 36). These data suggest a novel role for *MEIS1* in the BBB that warrants further examination. There are also observations revealing peripheral hypoxia to be associated with RLS symptoms (37). Hypoxia pathway is activated in a number of cell types of RLS patients; this activation can result from or be related to cellular iron deficiency (38). Another study used LCLs and showed *MEIS1* down regulation by RNAi techniques resulted in an increase in transferrin-2 receptor and ferroportin and a decrease in hepcidin mRNA expression (39, 40). The authors suggest that *MEIS1* might control cellular iron transfer to mitochondria and cellular export of iron (40). Putting together all these findings, the data suggest that decreased acquisition of iron by the brain cells is an RLS related pathophysiology, for which a possible role for *MEIS1* can be accounted.

MEIS1 HAS AN ALLELE DEPENDENT CIS-REGULATORY FUNCTION IN TELENCEPHALON (A STUDY IN MICE AND ZEBRAFISH)

A cluster of highly conserved non-coding regions (HCNRs) in the *MEIS1* locus suggests the presence of cis-regulatory elements (23). Considering that most variants found by GWAS are located in the regulatory regions, Spieler et al. conducted a study to identify the cis-regulatory role of the common intronic variants in *MEIS1* HCNRs (23). They studied an RLS associated variant (rs12469063), which is in the HCNR 617 of *MEIS1,* in transgenic mice and zebrafish using a reporter assay. They found that in mice, rs12469063 lies within a region of high interspecies conservation with neural enhancer activity and has an allele-specific functional impact. This study found that the risk allele of rs12469063 decreases the enhancer activity of this region in LGE and MGE (lateral and medial ganglionic eminences). The effect of rs12469063 on *MEIS1* enhancer function in the LGE/MGE region suggests that RLS may involve the basal ganglia because these regions give rise to the basal ganglia [also discussed in a review by Salminen et al. (41)]. The enhancer activity of HCNR harboring the RLS associated rs12469063 happens in this mouse model during development, which suggests its predisposition to RLS occurs during embryonic development (**Figure 1**). Affinity

chromatography showed that CREB1 has higher binding affinity to the RLS risk allele compared to the protective allele of rs12469063. A reporter screen in the zebrafish confirms the enhancer activity of HCNR observed in the mice and found two more transcriptionally active enhancers to this region. HCNR 617 harboring rs12469063 is the only RLS-SNP dependent enhancer region (23, 42).

MEIS1 REGULATES *SKOR1*

Expression studies of the RLS associated loci of *BTBD9*, *MAP2K5,* and *SKOR1* (previously called *LBXCOR1*) did not find changes in their levels of expression in lymphoblasts or two brain regions (pons and thalamus) of RLS patients (43). However, RLS patients with the *MEIS1* risk haplotype were observed to have a reduced expression of *SKOR1*, in addition to a reduced expression of *MEIS1* (**Figure 1**) (43). Follow up studies using siRNA targeting *MEIS1,* electromobility shift assays and luciferase reporter assays suggested the expression of *SKOR1* to be under the regulatory control of MEIS1. This transcription factor action of MEIS1 is due to its direct binding on two distinct promoter regions of *SKOR1* (43). Hence the dysregulation of MEIS1 might predispose to RLS both directly and indirectly, possibly throughout its regulatory role on other genes like *SKOR1*. A new SNP reported in this study is 8.7 kb upstream *SKOR1* ATG start site, which acts as a regulatory SNP (rSNP). The risk allele in this locus reduces the binding affinity of MEIS1 to the *SKOR1* promotor and results in reduced expression of *SKOR1* (43). SKOR1 acts as the transcriptional corepressor of LBX1, a homeodomain transcription factor. Skor1 expression in the Mice embryonic CNS is present in a certain subset of post-mitotic neurons generated posterior to the midbrain-hindbrain border. Skor1 is selectively expressed in the dorsal horn interneurons of developing spinal cord in Mice, where Lbx1 is required for proper specification. It is suggested that SKOR1 probably mediates the sensory inputs of RLS, among others. Despite the importance of SKOR1 in RLS genetic, only little is known regarding the actual function of this gene in RLS underlying pathways. The current literature only suggests that MEIS1 dysregulation may causes SKOR1 dysregulation possibly leading to the sensory phenotypes of RLS (44).

MEIS1 AND OTHER SLEEP RELATED DISORDERS LIKE INSOMNIA, PLMS AND RBD

Insomnia is characterized by problems in falling asleep or maintaining asleep. With a heritability estimate of 38 and 59% in men and women, respectively, genetic factors must play a crucial role in insomnia. Recent genetic studies of insomnia using cases from the UK biobank showed that *MEIS1* has the strongest association signal, suggesting *MEIS1* may be a shared genetic risk factor for RLS and insomnia (45–47). Some reports argue that the phenotype overlap could only drive some, and not all of the *MEIS1*'s association with insomnia, thus suggesting that *MEIS1* has a pleiotropic effect on RLS and insomnia (45). However, other reports suggest that the association of *MEIS1* with insomnia only comes from the inclusion of RLS cases (48). Such inconsistencies might be due to the heterogeneous phenotypic definition of insomnia itself which can lead to the inclusion of a substantial number of RLS cases. Furthermore, GWAS on periodic leg movement during sleep (PLMS), which are present in approximately 80% of RLS cases, also shows association with *MEIS1* (49–53). This pleiotropic effect can arise from *MEIS1*'s wide expression pattern during the development (54). So far, no genetic links between RBD (REM sleep behavior disorder) and *MEIS1* have been reported.

CONCLUSION

MEIS1 region is one of the several loci found to be associated with RLS genetic, which overall explain less than 10% of RLS heritability. The many roles for *MEIS1* in development make the study of its role in RLS challenging. MEIS1 establishes motor neuron pool identity and their target-muscle connectivity (55), it also regulates the proximodistal limb axis development (21). This protein is highly expressed in dopaminergic neurons of the substantia nigra and red nucleus, though what it does in these cells remains unknown (22–24). Meanwhile, the biology of RLS is poorly understood, with the most consistent abnormality being altered iron homeostasis with brain iron deficiency (56–59). Data presented in this report suggest that the role of *MEIS1* in RLS involves, among possibly other functions, altered iron homeostasis via altered transcriptional regulatory activity in RLS pathways. More in depth follow up studies on the function of MEIS1 with more focus on its regulatory role as a transcription factor might shed more light on the underlying pathways involved in RLS. To reach this goal, it will be essential to have access to RLS patients brain material carrying different genotypes of the RLS GWAS signals and to detailed clinical data to be used as covariates in the analyses. This combination would increase the likelihood of identifying elements that are critical to the onset and progression of RLS. This clinical data includes patient iron levels, their response to medication, age at onset, familial or sporadic RLS, presence or absence of PLMS, diagnosis by a physician and information about the patients' other health conditions. The next step could involve the use of model organisms to further validate and investigate RLS related mechanisms.

AUTHOR CONTRIBUTIONS

FS contributed to the original concept of the article, did the literature search, wrote the original version of the manuscript and reviewed it as it progressed. PD and GR contributed to the original concept of the manuscript and reviewed the manuscript.

REFERENCES

1. Ohayon MM, O'Hara R, Vitiello MV. Epidemiology of restless legs syndrome: a synthesis of the literature. *Sleep Med Rev.* (2012) 16:283–95. doi: 10.1016/j.smrv.2011.05.002
2. Trenkwalder C, Allen R, Hogl B, Paulus W, Winkelmann J. Restless legs syndrome associated with major diseases: a systematic review and new concept. *Neurology.* (2016) 86:1336–43. doi: 10.1212/WNL.0000000000002542
3. Desai AV, Cherkas LF, Spector TD, Williams AJ. Genetic influences in self-reported symptoms of obstructive sleep apnoea and restless legs: a twin study. *Twin Res.* (2004) 7:589–95. doi: 10.1375/1369052042663841
4. Xiong L, Jang K, Montplaisir J, Levchenko A, Thibodeau P, Gaspar C, et al. Canadian restless legs syndrome twin study. *Neurology.* (2007) 68:1631–3. doi: 10.1212/01.wnl.0000261016.90374.fd
5. Chen S, Ondo WG, Rao S, Li L, Chen Q, Wang Q. Genomewide linkage scan identifies a novel susceptibility locus for restless legs syndrome on chromosome 9p. *Am J Hum Genet.* (2004) 74:876–85. doi: 10.1086/420772
6. Desautels A, Turecki G, Montplaisir J, Sequeira A, Verner A, Rouleau GA. Identification of a major susceptibility locus for restless legs syndrome on chromosome 12q. *Am J Hum Genet.* (2001) 69:1266–70. doi: 10.1086/324649
7. Bonati MT, Ferini-Strambi L, Aridon P, Oldani A, Zucconi M, Casari G. Autosomal dominant restless legs syndrome maps on chromosome 14q. *Brain J Neurol.* (2003) 126(Pt 6):1485–92. doi: 10.1093/Brain/Awg137
8. Levchenko A, Provost S, Montplaisir JY, Xiong L, St-Onge J, Thibodeau P, et al. A novel autosomal dominant restless legs syndrome locus maps to chromosome 20p13. *Neurology.* (2006) 67:900–1. doi: 10.1212/01.wnl.0000233991.20410.b6
9. Pichler I, Marroni F, Volpato CB, Gusella JF, Klein C, Casari G, et al. Linkage analysis identifies a novel locus for restless legs syndrome on chromosome 2q in a South Tyrolean population isolate. *Am J Hum Genet.* (2006) 79:716–23. doi: 10.1086/507875
10. Kemlink D, Plazzi G, Vetrugno R, Provini F, Polo O, Stiasny-Kolster K, et al. Suggestive evidence for linkage for restless legs syndrome on chromosome 19p13. *Neurogenetics.* (2008) 9:75–82. doi: 10.1007/s10048-007-0113-1
11. Levchenko A, Montplaisir JY, Asselin G, Provost S, Girard SL, Xiong L, et al. Autosomal-dominant locus for restless legs syndrome in French-Canadians on chromosome 16p12.1. *Mov Disord Off J Mov Disord Soc.* (2009) 24:40–50. doi: 10.1002/mds.22263
12. Jimenez-Jimenez FJ, Alonso-Navarro H, Garcia-Martin E, Agundez JAG. Genetics of restless legs syndrome: an update. *Sleep Med Rev.* (2018) 39:108–21. doi: 10.1016/j.smrv.2017.08.002
13. Winkelmann J, Schormair B, Lichtner P, Ripke S, Xiong L, Jalilzadeh S, et al. Genome-wide association study of restless legs syndrome identifies common variants in three genomic regions. *Nat Genet.* (2007) 39:1000–6. doi: 10.1038/ng2099
14. Kemlink D, Polo O, Frauscher B, Gschliesser V, Hogl B, Poewe W, et al. Replication of restless legs syndrome loci in three European populations. *J Med Genet.* (2009) 46:315–8. doi: 10.1136/jmg.2008.062992
15. Winkelmann J, Czamara D, Schormair B, Knauf F, Schulte EC, Trenkwalder C, et al. Genome-wide association study identifies novel restless legs syndrome susceptibility loci on 2p14 and 16q12.1. *PLoS Genet.* (2011) 7:e1002171. doi: 10.1371/journal.pgen.1002171
16. Yang Q, Li L, Chen Q, Foldvary-Schaefer N, Ondo WG, Wang QK. Association studies of variants in MEIS1, BTBD9, and MAP2K5/SKOR1 with restless legs syndrome in a US population. *Sleep Med.* (2011) 12:800–4. doi: 10.1016/j.sleep.2011.06.006
17. Schormair B, Zhao C, Bell S, Tilch E, Salminen AV, Putz B, et al. Identification of novel risk loci for restless legs syndrome in genome-wide association studies in individuals of European ancestry: a meta-analysis. *Lancet Neurol.* (2017) 16:898–907. doi: 10.1016/S1474-4422(17)30327-7
18. Azcoitia V, Aracil M, Martinez AC, Torres M. The homeodomain protein Meis1 is essential for definitive hematopoiesis and vascular patterning in the mouse embryo. *Dev Biol.* (2005) 280:307–20. doi: 10.1016/j.ydbio.2005.01.004
19. Hisa T, Spence SE, Rachel RA, Fujita M, Nakamura T, Ward JM, et al. Hematopoietic, angiogenic and eye defects in Meis1 mutant animals. *EMBO J.* (2004) 23:450–9. doi: 10.1038/sj.emboj.7600038
20. Moens CB, Selleri L. Hox cofactors in vertebrate development. *Dev Biol.* (2006) 291:193–206. doi: 10.1016/J.Ydbio.2005.10.032
21. Mercader N, Leonardo E, Azpiazu N, Serrano A, Morata G, Martinez C, et al. Conserved regulation of proximodistal limb axis development by Meis1/Hth. *Nature.* (1999) 402:425–9. doi: 10.1038/46580
22. Barber BA, Liyanage VR, Zachariah RM, Olson CO, Bailey MA, Rastegar M. Dynamic expression of MEIS1 homeoprotein in E14.5 forebrain and differentiated forebrain-derived neural stem cells. *Ann Anat.* (2013) 195:431–40. doi: 10.1016/j.aanat.2013.04.005
23. Spieler D, Kaffe M, Knauf F, Bessa J, Tena JJ, Giesert F, et al. Restless legs syndrome-associated intronic common variant in Meis1 alters enhancer function in the developing telencephalon. *Genome Res.* (2014) 24:592–603. doi: 10.1101/gr.166751.113
24. Mignot E. A step forward for restless legs syndrome. *Nat Genet.* (2007) 39:938–9. doi: 10.1038/ng0807-938
25. Vilarino-Guell C, Chai H, Keeling BH, Young JE, Rajput A, Lynch T, et al. MEIS1 p.R272H in familial restless legs syndrome. *Neurology.* (2009) 73:243–5. doi: 10.1212/WNL.0b013e3181ae7c79
26. Schulte EC, Kousi M, Tan PL, Tilch E, Knauf F, Lichtner P, et al. Targeted resequencing and systematic in vivo functional testing identifies rare variants in MEIS1 as significant contributors to restless legs syndrome. *Am J Hum Genet.* (2014) 95:85–95. doi: 10.1016/j.ajhg.2014.06.005
27. Xiong L, Catoire H, Dion P, Gaspar C, Lafreniere RG, Girard SL, et al. MEIS1 intronic risk haplotype associated with restless legs syndrome affects its mRNA and protein expression levels. *Hum Mol Genet.* (2009) 18:1065–74. doi: 10.1093/hmg/ddn443
28. Meneely S, Dinkins ML, Kassai M, Lyu S, Liu Y, Lin CT, et al. Differential dopamine D1 and D3 receptor modulation and expression in the spinal cord of two mouse models of restless legs syndrome. *Front Behav Neurosci.* (2018) 12:199. doi: 10.3389/fnbeh.2018.00199
29. Salminen AV, Garrett L, Schormair B, Rozman J, Giesert F, Niedermeier KM, et al. Meis1: effects on motor phenotypes and the sensorimotor system in mice. *Dis Model Mech.* (2017) 10:981–91. doi: 10.1242/dmm.030080
30. Harrison PM, Arosio P. The ferritins: molecular properties, iron storage function and cellular regulation. *Biochim Biophys Acta.* (1996) 1275:161–203. doi: 10.1016/0005-2728(96)00022-9
31. Catoire H, Dion PA, Xiong L, Amari M, Gaudet R, Girard SL, et al. Restless legs syndrome-associated MEIS1 risk variant influences iron homeostasis. *Ann Neurol.* (2011) 70:170–5. doi: 10.1002/ana.22435
32. Gunshin H, Mackenzie B, Berger UV, Gunshin Y, Romero MF, Boron WF, et al. Cloning and characterization of a mammalian proton-coupled metal-ion transporter. *Nature.* (1997) 388:482–8. doi: 10.1038/41343
33. Skjorringe T, Burkhart A, Johnsen KB, Moos T. Divalent metal transporter 1 (DMT1) in the brain: implications for a role in iron transport at the blood-brain barrier, and neuronal and glial pathology. *Front Mol Neurosci.* (2015) 8:19. doi: 10.3389/fnmol.2015.00019
34. Wade QW, Chiou B, Connor JR. Iron uptake at the blood-brain barrier is influenced by sex and genotype. *Adv Pharmacol.* (2019) 84:123–45. doi: 10.1016/bs.apha.2019.02.005
35. Connor JR, Patton SM, Oexle K, Allen RP. Iron and restless legs syndrome: treatment, genetics and pathophysiology. *Sleep Med.* (2017) 31:61–70. doi: 10.1016/j.sleep.2016.07.028
36. Gonzalez-Latapi P, Malkani R. Update on restless legs syndrome: from mechanisms to treatment. *Curr Neurol Neurosci Rep.* (2019) 19:54. doi: 10.1007/s11910-019-0965-4
37. Salminen AV, Rimpila V, Polo O. Peripheral hypoxia in restless legs syndrome (Willis-Ekbom disease). *Neurology.* (2014) 82:1856–61. doi: 10.1212/WNL.0000000000000454
38. Patton SM, Ponnuru P, Snyder AM, Podskalny GD, Connor JR. Hypoxia-inducible factor pathway activation in restless legs syndrome patients. *Eur J Neurol.* (2011) 18:1329–35. doi: 10.1111/j.1468-1331.2011.03397.x
39. N Silver RA, CJ Earley. MEIS1 as a potential mediator of the RLS-iron pathology. *Mov Disord.* (2010) 25:S513–4.
40. Guo S, Huang J, Jiang H, Han C, Li J, Xu X, et al. Restless legs syndrome: from pathophysiology to clinical diagnosis and management. *Front Aging Neurosci.* (2017) 9:171. doi: 10.3389/fnagi.2017.00171

41. Salminen AV, Lam DD, Winkelmann J. Role of MEIS1 in restless legs syndrome: from GWAS to functional studies in mice. *Adv Pharmacol.* (2019) 84:175–84. doi: 10.1016/bs.apha.2019.03.003
42. Allen RP, Donelson NC, Jones BC, Li Y, Manconi M, Rye DB, et al. Animal models of RLS phenotypes. *Sleep Med.* (2017) 31:23–8. doi: 10.1016/j.sleep.2016.08.002
43. Catoire H, Sarayloo F, Mourabit Amari K, Apuzzo S, Grant A, Rochefort D, et al. A direct interaction between two restless legs syndrome predisposing genes: MEIS1 and SKOR1. *Sci Rep.* (2018) 8:12173. doi: 10.1038/s41598-018-30665-6
44. Mizuhara E, Nakatani T, Minaki Y, Sakamoto Y, Ono Y. Corl1, a novel neuronal lineage-specific transcriptional corepressor for the homeodomain transcription factor Lbx1. *J Biol. Chem.* (2005) 280:3645–55. doi: 10.1074/jbc.M411652200
45. Hammerschlag AR, Stringer S, de Leeuw CA, Sniekers S, Taskesen E, Watanabe K, et al. Genome-wide association analysis of insomnia complaints identifies risk genes and genetic overlap with psychiatric and metabolic traits. *Nat Genet.* (2017) 49:1584–92. doi: 10.1038/ng.3888
46. Lane JM, Jones SE, Dashti HS, Wood AR, Aragam KG, van Hees VT, et al. Biological and clinical insights from genetics of insomnia symptoms. *Nat Genet.* (2019) 51:387–93. doi: 10.1038/s41588-019-0361-7
47. Lane JM, Liang J, Vlasac I, Anderson SG, Bechtold DA, Bowden J, et al. Genome-wide association analyses of sleep disturbance traits identify new loci and highlight shared genetics with neuropsychiatric and metabolic traits. *Nat Genet.* (2017) 49:274–81. doi: 10.1038/ng.3749
48. El Gewely M, Welman M, Xiong L, Yin S, Catoire H, Rouleau G, et al. Reassessing GWAS findings for the shared genetic basis of insomnia and restless legs syndrome. *Sleep.* (2018) 41. doi: 10.1093/sleep/zsy164
49. Moore Ht, Winkelmann J, Lin L, Finn L, Peppard P, Mignot E. Periodic leg movements during sleep are associated with polymorphisms in BTBD9, TOX3/BC034767, MEIS1, MAP2K5/SKOR1, and PTPRD. *Sleep.* (2014) 37:1535–42. doi: 10.5665/sleep.4006
50. Stefansson H, Rye DB, Hicks A, Petursson H, Ingason A, Thorgeirsson TE, et al. A genetic risk factor for periodic limb movements in sleep. *N Engl J Med.* (2007) 357:639–47. doi: 10.1056/NEJMoa072743
51. Winkelman JW, Blackwell T, Stone K, Ancoli-Israel S, Tranah GJ, Redline S, et al. Genetic associations of periodic limb movements of sleep in the elderly for the MrOS sleep study. *Sleep Med.* (2015) 16:1360–5. doi: 10.1016/j.sleep.2015.07.017
52. Haba-Rubio J, Marti-Soler H, Marques-Vidal P, Tobback N, Andries D, Preisig M, et al. Prevalence and determinants of periodic limb movements in the general population. *Ann Neurol.* (2016) 79:464–74. doi: 10.1002/ana.24593
53. Aurora RN, Kristo DA, Bista SR, Rowley JA, Zak RS, Casey KR, et al. The treatment of restless legs syndrome and periodic limb movement disorder in adults–an update for 2012: practice parameters with an evidence-based systematic review and meta-analyses: an American Academy of Sleep Medicine Clinical Practice Guideline. *Sleep.* (2012) 35:1039–62. doi: 10.5665/sleep.1988
54. Royo JL, Bessa J, Hidalgo C, Fernandez-Minan A, Tena JJ, Roncero Y, et al. Identification and analysis of conserved cis-regulatory regions of the MEIS1 gene. *PLoS ONE.* (2012) 7:e33617. doi: 10.1371/journal.pone.0033617
55. Dasen JS, Tice BC, Brenner-Morton S, Jessell TM. A Hox regulatory network establishes motor neuron pool identity and target-muscle connectivity. *Cell.* (2005) 123:477–91. doi: 10.1016/j.cell.2005.09.009
56. Allen RP, Earley CJ. The role of iron in restless legs syndrome. *Mov Disord Off J Mov Disord Soc.* (2007) 22(Suppl 18):S440–8. doi: 10.1002/mds.21607
57. Ondo W, Romanyshyn J, Vuong KD, Lai D. Long-term treatment of restless legs syndrome with dopamine agonists. *Arch Neurol.* (2004) 61:1393–7. doi: 10.1001/archneur.61.9.1393
58. Godau J, Klose U, Di Santo A, Schweitzer K, Berg D. Multiregional brain iron deficiency in restless legs syndrome. *Mov Disord Off J Mov Disord Soc.* (2008) 23:1184–7. doi: 10.1002/mds.22070
59. Koo BB, Bagai K, Walters AS. Restless legs syndrome: current concepts about disease pathophysiology. *Tremor Other Hyperkinet Mov (N Y).* (2016) 6:401. doi: 10.7916/D83J3D2G

Conflict of Interest Statement: The authors declare that the research was conducted in the absence of any commercial or financial relationships that could be construed as a potential conflict of interest.

frontiers in Neurology

REVIEW
published: 17 December 2019
doi: 10.3389/fneur.2019.01272

VPS35-Based Approach: A Potential Innovative Treatment in Parkinson's Disease

Simona Eleuteri[1]* *and Alberto Albanese*[1,2]

[1] Department of Neurology, Humanitas Research Hospital, Milan, Italy, [2] Department of Neurology, Catholic University, Milan, Italy

Several symptomatic treatments for Parkinson's disease (PD) are currently available. Still, the challenge today is to find a therapy that might reduce degeneration and slow down disease progression. The identification of pathogenic mutations in familial Parkinsonism (fPD) associated to the monogenic forms of PD provided pathophysiological insights and highlighted novel targets for therapeutic intervention. Mutations in the VPS35 gene have been associated with autosomal dominant fPD and a clinical phenotype indistinguishable from idiopathic PD. Although VPS35 mutations are relatively rare causes of PD, their study may help understanding specific cellular and molecular alterations that lead to accumulation α-synuclein in neurons of PD patients. Interacting with such mechanisms may provide innovative therapeutic approaches. We review here the evidence on the physiological role of VPS35 as a key intracellular trafficking protein controlling relevant neuronal functions. We further analyze VPS35 activity on α-synuclein degradation pathways that control the equilibrium between α-synuclein clearance and accumulation. Finally, we highlight the strategies for increasing VPS35 levels as a potential tool to treat PD.

Keywords: endosomal trafficking, retromer complex, therapeutic targets, Parkinson's disease, alpha-synucein, amyloid protein A (AA)

OPEN ACCESS

Edited by:
Giuseppe De Michele, University of Naples Federico II, Italy

Reviewed by:
Darren John Moore, Van Andel Research Institute (VARI), United States
Suzanne Lesage, Institut National de la Santé et de la Recherche Médicale (INSERM), France

***Correspondence:**
Simona Eleuteri
simona.eleuteri@humanitasresearch.it

Specialty section:
This article was submitted to Movement Disorders, a section of the journal Frontiers in Neurology

Received: *12 July 2019*
Accepted: *18 November 2019*
Published: *17 December 2019*

Citation:
Eleuteri S and Albanese A (2019) VPS35-Based Approach: A Potential Innovative Treatment in Parkinson's Disease. Front. Neurol. 10:1272. doi: 10.3389/fneur.2019.01272

INTRODUCTION

Parkinson's disease (PD) is the second most common neurodegenerative disorder affecting 1% of people over 65 and 4.3% of those older than 85 (1).

The clinical hallmark of PD is bradykinesia, in combination with rest tremor and rigidity (1). This phase is preceded by a preclinical stage, when neurodegenerative processes have commenced, but there are no evident symptoms or signs, and by a prodromal phase, when symptoms and signs are present, but are yet insufficient to define disease (2). The motor phenomenology is attributed to the selective loss of dopaminergic neurons (DNs) in the substantia nigra pars compacta (SNpc) resulting in degeneration of the nigrostriatal tract and dopamine deficiency (3).

The neuropathological hallmark of PD is the occurrence of intracellular inclusions, Lewy bodies (LBs) and Lewy neurites, mainly consisting of aggregated α-synuclein (4). A remarkably convincing set of data supports the view that accumulation and aggregation of α-synuclein in neurons may represent a key pathogenic event (5–9). Several approaches aim to reduce the accumulation and propagation of α-synuclein toxic aggregates in the brain (10–12) (**Figure 1**). Ideally, an intervention aimed to reduce α-synuclein should be performed in the preclinical disease phase or—at least—in the prodromal phase, although it may be argued that the early clinical phase may also provide a suitable time window.

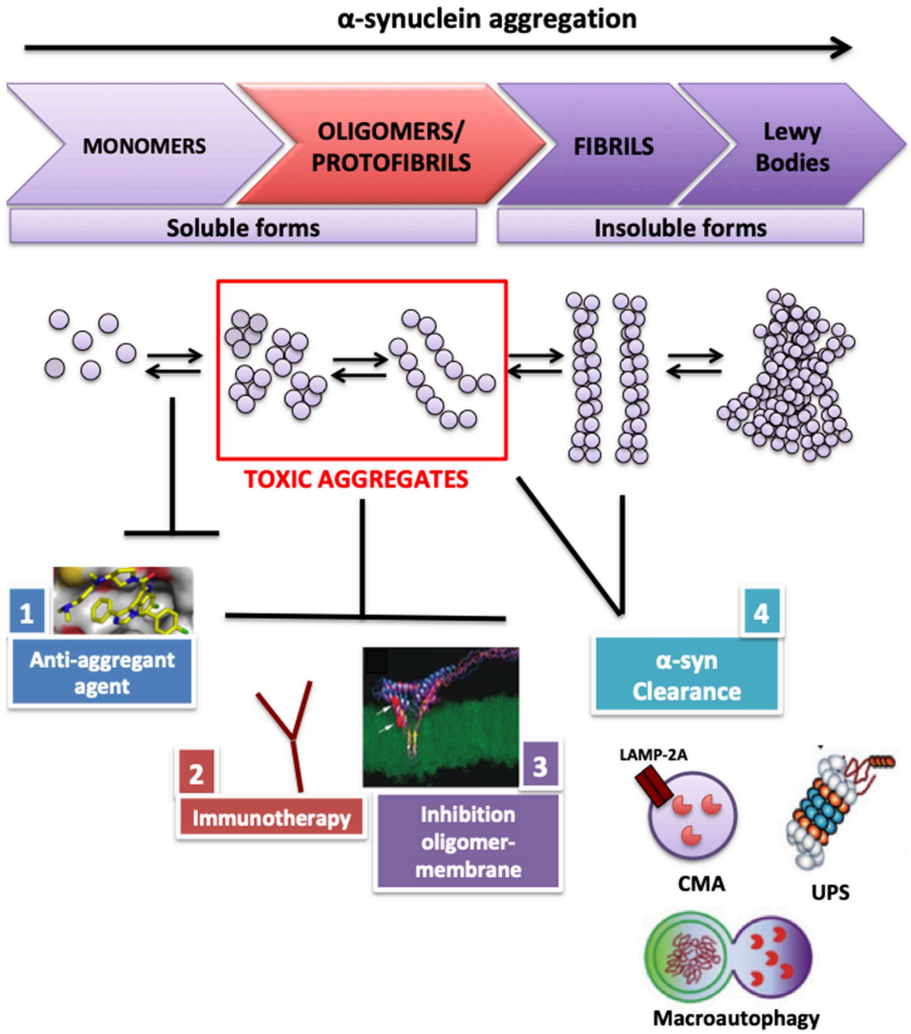

FIGURE 1 | Therapeutic strategies used to reduce α-synuclein toxic aggregates accumulation in neurons. To reduce α-synuclein accumulation in neurons, several therapeutic approaches have been evaluated and tested in murine PD models: (1) antiamyloidogenic agents, such as small molecules or biocomposts to block α-synuclein aggregation and fibrillogenesis; (2) immunotherapy using α-synuclein single-chain antibody able to attenuate neuronal degeneration *in vivo*; (3) peptide design to block the interaction between α-synuclein oligomer and membrane, able to improve deficits in murine PD models; (4) boosting α-synuclein degradation pathways. CMA, chaperone mediated autophagy; UPS, ubiquitin proteosome system; LAMP2A, lysosome-associated membrane protein 2A.

Monogenic PD subtypes represent a powerful tool for understanding the pathogenesis of PD and for developing treatment strategies. Mutations of the VPS35-retromer subunit have been recently shown to cause PD and to play a key role in neurodegenerative processes, as they control balance between degradation and recycling of fundamental proteins for neuronal survival (13). Moreover, this review outlines the genetic and biochemical evidence that pathogenic missense mutation and depletion of VPS35 affect dopamine (DA) neurons function at different levels. More recently, a direct link has been established between VPS35 and α-synuclein in a rodent PD model where VPS35 deficiency causes α-synuclein accumulation (14). This effect of VPS35 could unravel its key role in controlling macroautophagy, chaperone-mediated autophagy (CMA), and lysosomal function, which are the main degradation pathways of α-synuclein (15–17). A growing body of data converges to establish how VPS35 controls the transport and the localization of protein markers involved in α-synuclein degradation pathways, thus linking VPS35 to α-synuclein accumulation (18–21). An increase in VPS35 levels in PD mice rescues α-synuclein accumulation and induces neuroprotection (14), pointing to a possible role of VPS35 as a therapeutic

Abbreviations: AD, Alzheimer's disease; APP, amyloid protein precursor; ATG9A, autophagy-related protein 9A; CI-MPR, cation independent 6 mannose phosphate receptor; CMA, chaperone-mediated autophagy; CTSD, cathepsin D; DN, dopaminergic neurons; DAT, dopamine transporter; EE, Early endosome; LAMP2A, Lysosome-associated membrane protein 2A; PD, Parkinson's disease; SN, substantia nigra; TGN, trans-Golgi Network; WASH, Wiskott–Aldrich syndrome protein; VPS35, vacuolar sorting protein 35.

target for PD. Moreover, VPS35 could represent a diseases-modifying target, and its neuroprotective role could be due to the control on neuronal signaling events (22), synaptic plasticity (23–25), trafficking of protein in dendritic spines (26), membrane dopamine transporter (DAT) recycling in DA neurons (27), and the regulation mitochondrial functions (28).

PATHOGENIC ROLE OF VPS35 IN PD

Two independent studies with exome sequencing identified point mutations in the VPS35 gene causing an autosomal dominant form of PD (PARK17) (29, 30). The p.Asp620Asn (c.1858G>A) mutation has been proven to be pathogenic with a frequency ∼1.3% in familial cases and 0.3% in sporadic PD cases (31, 32). In addition, non-pathogenic VPS35 variants (33) and variant of uncertain significance (34) have been described. The VPS35 gene maps on chromosome 16q11.2 encompasses 29.6 kb and 17 exons (35) (**Figure 2**).

The clinical presentation of PARK17 PD patients bearing pathogenic VPS35 gene mutations is that of a typical clinically definite PD. The mean age at disease onset is 50.3 ± 7.3 years; cognitive and psychiatric features do not predominate, and levodopa response is sustained and not associated to severe dyskinesias (37).

To evaluate the pathogenic the role of VPS35 deletion and the VPS35–D620N mutation, different transgenic mouse models have been developed. Knockout mice with the deletion of the endogenous VPS35 at embryonic stage resulted in early lethality under embryonic day 10 (38). VPS35 heterozygote mice (expressing 50% of protein respect to the wild type) survived to adulthood (38) and did not presented any PD-relevant deficit up to 6 months of age. However, the neuropathological evaluation at late stage (12 months) in VPS35 heterozygote mice revealed DA neuronal loss in SNpc and increase in α-syn levels (16). VPS35$^{DAT-CRE}$ mice demonstrated as the depletion of VPS35 protein in SNpc-DA neurons at 2–3 months of age already showed a reduction in TH$^+$ DA neurons and TH$^+$ fibers in the striatum (28). To evaluate the effect of VPS35–D620N mutation, a viral-mediated gene transfer model in adult rat has been developed, showing that the expression of the mutant in the nigrostriatal pathway was sufficient to induce DA neuronal loss and axonal pathology (39). VPS35–D620N knockin (KI) mice (40) at 3 months of age have shown normal motor functions and no loss of striatal DA neurons (41, 42). However, it has been reported that KI mice showed increased capacity to evoke dopamine release in dorsolateral striatum, consistent with elevated extracellular dopamine (42). The evaluation of the effect of VPS35–D620 KI mice on PD pathology with chronic aging provided evidence that the increase in the endogenous D620N mutant levels has a gain of function or partial-negative dominant mechanism (43). Thus, the endogenous expression of VPS35–D620N is sufficient to recapitulate some features of PD pathology inducing (i) the progressive degeneration of the nigrostriatal pathway, (ii) modest motor deficit with age consistence, and (iii) widespread axonal damage (43). In VPS35–D620N KI mice, α-synuclein accumulation and LB pathology were not detected, but tau-positive pathology, characterized by the abnormal accumulation of early "pretangle," has been described (43). Moreover, VPS35–D620N KI mice or knockdown or knockout of VPS35 mice impacted LRRK2-mediated Rab protein phosphorylation (44) showing that VPS35 could play a major role in controlling LRRKK2 kinase activity and supporting the hypothesis that VPS35–D620N mutation resulted in a gain of function (44).

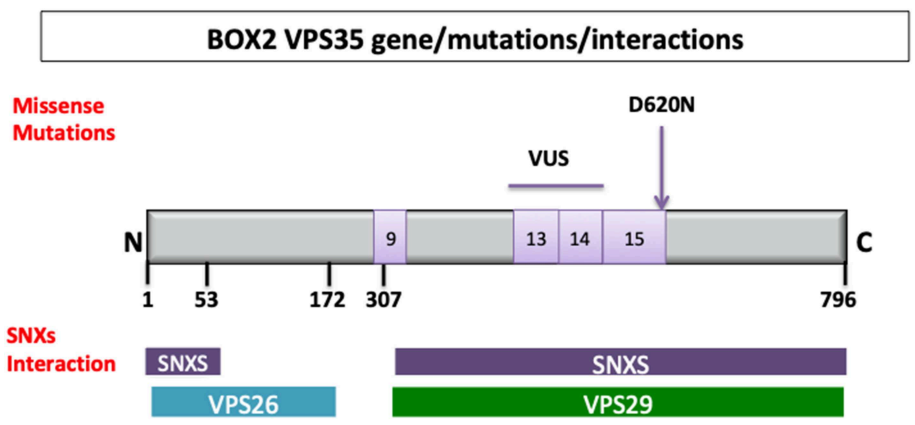

FIGURE 2 | VPS35 gene, protein structure and interactions. Retromer cargo recognition complex is formed by vacuolar sorting protein 26 (VPS26; 38 kDa), vacuolar sorting protein 29 (VPS29; 20 kDa), vacuolar sorting protein 35 (VPS35; 92 kDa); the dimer of sinexin (SNXs). The N-terminal region (in blue) from the amino acid residues 1 to 172 [1–172] and C-terminal region (violet) from 307 to 796 (307–796) are important, respectively, for the interaction with VPS26 and VPS29 (36). The amino acid residues involved in the interaction with the SNXs are at N-terminal region (1–35, 37–54) and C-terminal region (307–796). A structural level VPS35 is a right-handed α-helix solenoid, and it is predicted to have 34 helices, 13 of which are in C-terminal. Different missense mutations have been identified in fPD. VPS35 variant of uncertain significance (VUS) are localized between exon 9 (P316S), exon 13 (R542W), and exon 14 (I560T, H599R, M607V), and the confirmed pathogenic mutation (D620N) is localized on the exon 15 (genes in light violet).

VPS35 SUBUNIT OF THE RETROMER COMPLEX

The VPS35 gene encodes for a subunit of the retromer complex that is composed of 796 amino acids with a molecular weight of 92 kDa (45). The retromer is an evolutionary conserved complex of eukaryotic cells that structurally comprises two subcomplexes: (i) a cargo recognition complex VPS26–VPS29–VPS35 heterotrimer mainly involved in the transport of proteins and (ii) a membrane-targeting dimer of sorting nexin, important for the adhesion of the complex to the endosomal membrane (SNX1, SNX2, SNX5, SNX6, and SNX32) (45) (**Figure 2**). Mammals have two paralogues of VPS26 subunit (VPS26A and VPS26B) that compete for a single binding site on VPS35 (46). Two variants of VPS26A have been identified in a patient with familial PD (46).

The retromer complex represents the master "conductor" of the sorting in the endosomal network; it is localized at the early endosome (EE) and mainly controls the retrograde trafficking of cargo proteins from EE to the trans-Golgi network (TGN) or to the plasma membrane (**Figure 3**). Moreover, the retromer complex mediates vesicular transport from mitochondria to peroxisomes (47). This complex represents the main sorting hub that receives, dissociates, and sorts cargoes of different origin: (i) plasma membrane (recycling of membrane receptors), (ii) biosynthetic pathways (retrieval of trafficking from Golgi), and (iii) lysosomal pathway (cargoes direct to lysosomes) (48) (**Figure 3**). Overall, these activities control the homeostasis of transmembrane proteins at plasma membrane and endolysosomal levels and regulate receptor abundance, signaling receptors, adhesion molecules, and hydrolase receptors.

THE RETROMER COMPLEX CONTROLS SYNAPTIC FUNCTION

It has been recently clarified that the retromer complex plays a key role in neurons, where it can, directly or indirectly, mediate essential neuronal functions through cargo selector accessory proteins (SNX27 and WASH complex). Thus, the retromer influences neuronal signaling events (such as downregulation of receptors activity) (22), synaptic plasticity (23–25), trafficking of protein in dendritic spines (26), and membrane DAT recycling in DA neurons (27). The VPS26-retromer subunit belonging to the β-arrestin family controls the downregulation and recycling

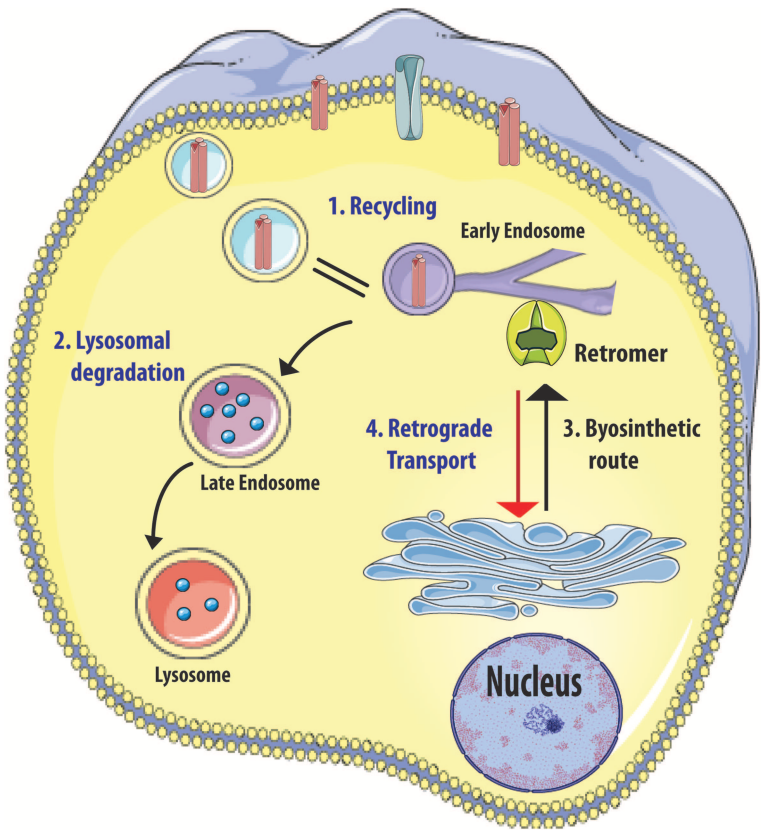

FIGURE 3 | Retromer complex functions. Retromer complex (in green) controls the sorting of cargoes (1) originate from plasma membrane (receptors in red), (2) direct to lysosome for degradation, and (3) trafficking between trans-Golgi Network (TGN) (3, 4). Figure was adapted from Servier Medical Art images (http://smart.servier.com/).

to cell surface of β_2-adrenergic receptor A (22). This is a G-protein-coupled receptor characterized by a cyclical pattern of activation/inactivation through endosomal internalization: the retromer balances the recycling and the degradation of this receptor (49). The retromer could also influence neuronal activity indirectly, controlling function and localization of accessory proteins, such as SNX27 and WASH complex. The SNX27 protein controls recycling of the α-amino-3-hydroxy-5-methyl-4-isoxazolepropionic acid receptor, involved in long-term potentiation, a process linked to learning and memory (23, 25). The D620N VPS35 pathogenic mutation impairs interaction with the WASH complex (15) and may lead to mistrafficking protein cargoes, such as the GluA1 glutamate receptors subunit, the Glut-1 glucose transporter (26, 49, 50) and in α-amino-3-hydroxy-5-methyl-4-isoxazolepropionic acid receptors (51). DAT, which is strictly associated to the activity of DA neurons, undergoes constitutive internalization: its recycling is mediated by the retromer complex (27).

Therefore, retromer disruption via short hairpin RNA-mediated VPS35 knockdown results in DAT depletion from plasma membrane and decrease in DAT recycling (27). In summary, the retromer influences trafficking of signaling receptors and controls rapid signaling events involved in synaptic plasticity and dendritic spine formation that are specifically relevant to DA neuron function (27).

VPS35 INFLUENCES α-SYNUCLEIN ACCUMULATION

Recent studies highlighted the crucial role of the retromer complex in controlling the accumulation of α-synuclein in PD mouse models and in an *in vitro* model of α-synuclein spreading (14). Reduction in VPS35 levels or the expression of mutated VPS35 protein in PD mouse hippocampus displayed defective α-synuclein clearance resulting in widespread accumulation of aggregates (14). These data were confirmed in mouse models showing that VPS35 deficiency or a pathogenic VPS35 mutation leads to accumulation and aggregation of α-synuclein in the SN, accompanied by degeneration of DA neurons, reduction in DA levels, impairment of locomotor behavior, and alteration of lysosomal morphology (16). On the contrary, an excess of wild-type VPS35 expression rescues the accumulation of α-synuclein aggregates and leads to the reduction in neuronal loss and astrogliosis in a PD mouse model overexpressing α-synuclein (14). Using an *in vitro* model of cortical neurons, it has been demonstrated that an increase in wild-type VPS35 levels may counteract the propagation of α-synuclein aggregates from neuron to neuron (14). In keeping with this line of evidence, VPS35 ablation in *Drosophila* results in the accumulation of α-synuclein in lysosomes (17). Furthermore, silencing of endogenous VPS35 in an α-synuclein transgenic fly does not only promote the accumulation of human wild-type α-synuclein but also causes eye degeneration and motor disability (17). These data suggest that endosomal dysfunction caused by VPS35 deficiency impairs the ability of neurons to cope with the accumulation of α-synuclein, thus facilitating the spread of PD pathology.

HOW DOES VPS35 CONTROL α-SYNUCLEIN ACCUMULATION?

The hypothesis that VPS35 could promote α-synuclein clearance is related to the observation of a central role of this retromer protein in controlling interaction and transport of key proteins in α-synuclein degradation pathways.

In normal conditions, the quality control network dealing with α-synuclein accumulation is efficient in promoting its refolding or degradation. In general, to induce α-synuclein degradation, a cell can activate the ubiquitin protein system or alternatively—in the presence of intracytoplasmatic aggregates and LBs—can enhance the endosome-lysosomal degradation system, macroautophagy, or CMA (52) (**Figure 4**). Recent studies highlighted that VPS35 can act at different levels of the α-synuclein degradation pathways (**Figure 5**). Particularly, VPS35 acts indirectly on lysosomal activity by sorting receptors of lysosomal hydrolases, including Sortilin and cation independent 6 mannose phosphate receptor (CI-MPR) (18). VPS35 regulates macroautophagy controlling the localization of WASH complex and the trafficking of ATG9a protein (15). Finally, VPS35 manages CMA by mediating the retrieval and transport of LAMP-2A receptor to lysosomes (16) (**Figure 5**).

VPS35 Controls the Lysosomal Degradation Pathway

α-Synuclein enters through macroautophagy, CMA, and endosomal pathway into lysosome to be degraded by lysosomal hydrolases (53). VPS35 carries several cargoes involved in neurodegenerative disorders and more specifically in the clearance of α-synuclein (48). Two well-studied VPS35 cargoes are Sortilin (20, 21) and CI-MPR (18, 19), and VPS35–D620N mutant showed defects in sorting CI-MPR (54). These two cargoes operate as lysosomal hydrolase receptors, sorting acid hydrolases, such as cathepsins, from TGN to lysosomes. Aspartyl protease (cathepsin D) is the main lysosomal endopeptidase responsible for the degradation of α-synuclein (55). However, cysteine proteases (cathepsin B and L) have been shown to be effective in degraded α-synuclein (53). Direct interaction between α-synuclein and lysosomal proteases was shown in mice and human purified lysosomal extracts (53). CTSD-deficient mice showed accumulation of insoluble α-synuclein aggregates in the brain (55). Accordingly, CTSD-mutant brain from mice, sheep, and human showed selective synucleinopathy-like changes as well as α-synuclein accumulation and formation of ubiquitin-positive inclusions (55). Moreover, haploinsufficiency of CTSD resulted in the reduction in lysosomal functions and also acceleration of the propagation of LB pathology (56). Furthermore, recent studies in *Drosophila* have shown a direct link between VPS35 depletion and defects in CTSD trafficking and maturation (17) (**Figure 5**).

VPS35 Controls Macroautophagy

Macroautophagy has a profound importance in the clearance of intracytoplasmatic aggregate-prone proteins as well as α-synuclein in PD and huntingtin in Huntington's disease (57). The treatment with rapamycin, which stimulates

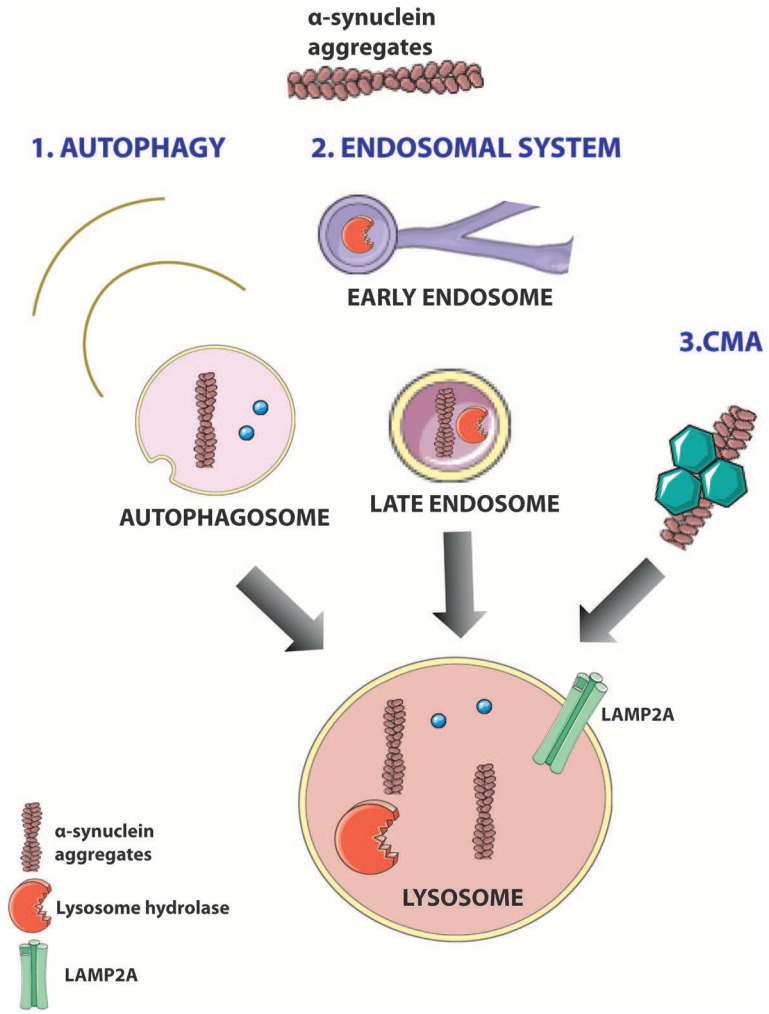

FIGURE 4 | α-Synuclein degradation pathways in cells. Toxic aggregates of α-synuclein can be degraded in the cells through three pathways: macroautophagy (1), endosomal system (2), and chaperone-mediated autophagy (CMA) (3). (1) In the autophagy, key molecules can lead the autophagosome formation and the degradation of aggregates of α-synuclein; (2) lysosomal hydrolases generated in trans-Golgi Network (TGN) are sorted from specific hydrolase sorting receptors [cation-independent 6 mannose phosphate receptor (CI-MPR) and Sortilin], through the endosomal system to the lysosome, and mediate α-synuclein degradation; (3) chaperone-dependent selection of soluble α-synuclein aggregates that are targeted to lysosomes and directly translocated across the lysosomal membrane for degradation. Figure was adapted from Servier Medical Art images (http://smart.servier.com/).

autophagy, enhanced the clearance of aggregate-prone proteins (57). Dysregulation of the autophagy pathway has been observed in the brain of PD patients and in PD mouse models (58), and the overexpression of α-synuclein caused mislocalization of autophagic proteins and impaired macroautophagy (59).

VPS35 controls the endosomal recruitment of WASH complex, a scaffolding protein localized at the EE (15). WASH complex regulates (i) the autophagic process of the autophagosome development (15), (ii) the formation of actin patch on endosomes to promote protein sorting (60), and (iii) endosome-to-cell surface recycling (61). Recently, it has been demonstrated that retromer interacts directly with FAM21–WASH complex controlling its correct localization (15). VPS35–D620N mutant destabilized this interaction, impairing WASH complex recruitment to endosomes (15, 62). The mislocalization of WASH complex induces defects in autophagosome formation, perturbing protein sorting, and specifically altering ATG9A trafficking (15) (**Figure 5**). ATG9A is a multipass transmembrane protein that acts early in the autophagic pathway and controls LC3-positive compartment interaction with autophagosome (15). Moreover, parkin PD mutations could impair the ubiquitination of VPS35, inducing the regulation of retromer-dependent sorting (63). Thus, parkin deficiency leads to the reduction in retromer-associated WASH complex cargo in mouse brains (63).

VPS35 Controls CMA

The clearance of misfolded proteins and aggregates by CMA is essential for the normal cellular functions and its efficiency

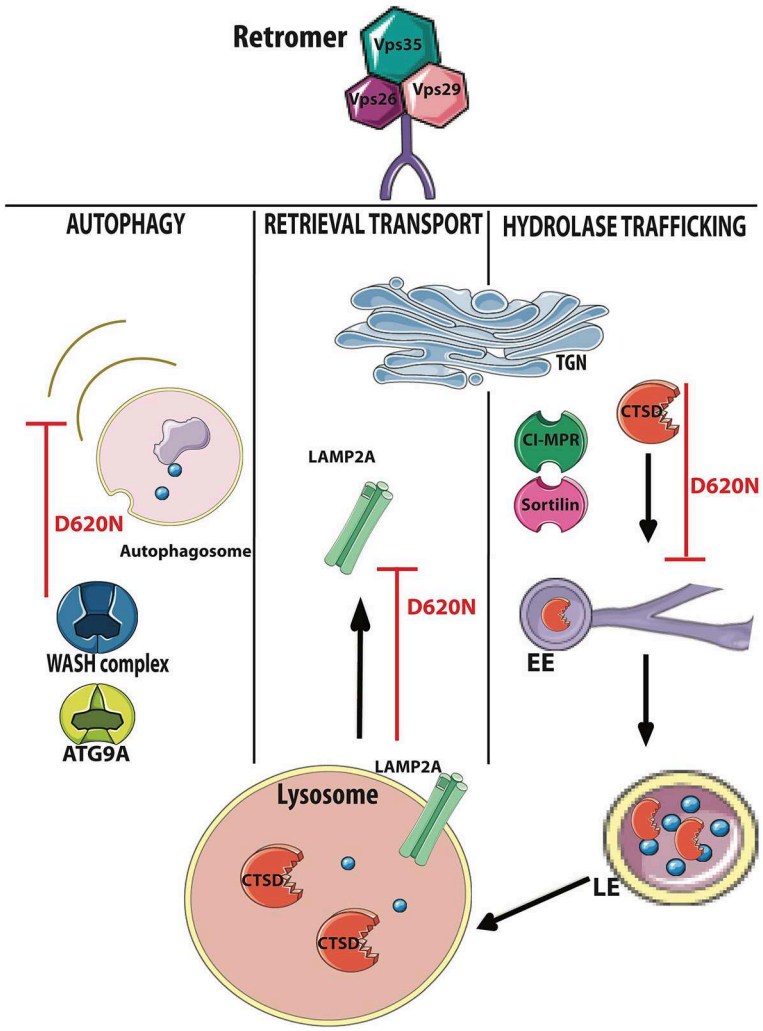

FIGURE 5 | VPS35-retromer subunit controls the main α-synuclein degradation pathways. VPS35 has a relevant role in controlling the degradation of key molecules in the α-synuclein degradation pathways. In the autophagic process, vacuolar sorting protein 35 (VPS35) interacts and controls the trafficking of Wiskott–Aldrich syndrome protein (WASH) complex (blue) and autophagy-related protein 9A (ATG9A; blue) assuring the correct autophagosome formation; in chaperone-mediated autophagy (CMA), VPS35 controls the retrieval trafficking of lysosome-associated membrane protein 2A (LAMP2A) receptor (light green) to the trans-Golgi Network (TGN); VPS35 interacts with CI-MPR (dark green) and Sortilin (pink) leading indirectly to the trafficking of cathepsin D (CTSD, in red) through early endosomes (EE) and late endosomes (LE). VPS35–D620N mutation and VPS35 deficiency lead to dysfunctions in α-synuclein degradation. Figure was adapted from Servier Medical Art images (http://smart.servier.com/).

decline with age. Defects in CMA have been detected in PD patient (64). Therefore, the protein levels of CMA markers (LAMP2A and hsc70) were significantly reduced in SNpc and amygdala of PD patients (64). CMA is controlling the degradation of cytosolic proteins (as well as α-synuclein and LRRK2) carrying the recognition motif (KFERQ) (41). CMA presents multiple steps: (i) the recognition of KFERQ motif by HSPA8/HSC70 which target the substrate to lysosomes, (ii) the binding of the substrate to LAMP2A receptor, (iii) formation of substrate–translocation complex with membrane-bound LAMP2A, (iv) substrate degradation by lysosomal enzymes, and (v) disassembly of translocation complex and degradation of multimeric LAMP2A to be recycled (41). Recent studies have been shown that LAMP2A receptor trafficking from endosome to Golgi is altered in mice with reduced VPS35 levels or VPS35–D620N mutations (**Figure 5**). These mice showed alterations in lysosomal morphology with an increase in LAMP1A, reduction in LAMP2A vesicles, and an a relative increase in α-synuclein accumulation (16) (**Figure 5**).

DISCUSSION AND OUTLOOK

Pathogenic mutations in different PD-related genes with autosomal dominant or autosomal recessive Mendelian inheritance (LRRK2, VPS35, DNAJC13, SYNJ1, TMEM230,

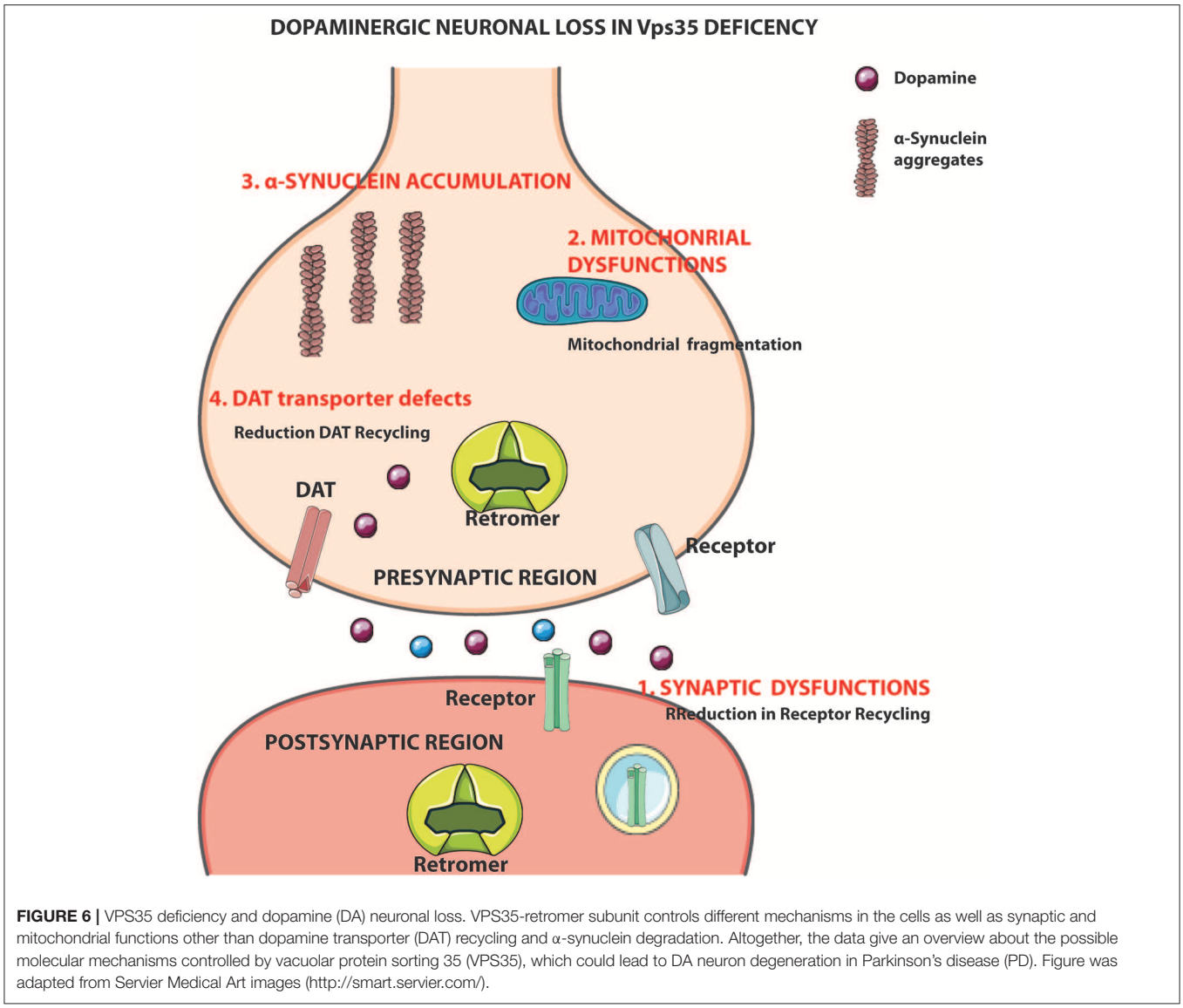

FIGURE 6 | VPS35 deficiency and dopamine (DA) neuronal loss. VPS35-retromer subunit controls different mechanisms in the cells as well as synaptic and mitochondrial functions other than dopamine transporter (DAT) recycling and α-synuclein degradation. Altogether, the data give an overview about the possible molecular mechanisms controlled by vacuolar protein sorting 35 (VPS35), which could lead to DA neuron degeneration in Parkinson's disease (PD). Figure was adapted from Servier Medical Art images (http://smart.servier.com/).

RAB39B) are involved in endosomal trafficking, indicating that DA neurons are specifically susceptible to endosomal dysfunctions (36). Neuropathological and neuroanatomical studies have demonstrated that the impairment of cellular trafficking may preferentially affect SNc DA neurons (36, 65). VPS35 mutations identified in PD lead to retromer dysfunctions (29, 30). Recent studies highlighted the interplay between VPS35 and LRRK2, two endosomal proteins associate to late-onset PD, showing a common pathway for the sorting of proteins through TGN and endolysosomal system (66–68). The loss of VPS35 or LRRK2 in *Drosophila* has been reported to affect synaptic recycling (68). Furthermore, the overexpression of VPS35 or VPS26 retromer subunits ameliorated the pathogenic mutant LRRK2 eye phenotype, protecting from locomotor deficit (67). VPS35–D620N KI mice or knockdown of VPS35 mice impacted LRRK2-mediated Rab protein phosphorylation (44) supporting the hypothesis that VPS35–D620N mutation resulted in a gain of function (44).

Different studies have shown that VPS35 has a key role in controlling α-synuclein accumulation in different PD models (14, 16, 17) even if the development of VPS35–D620N KI mice lack the presence of α-synuclein accumulation (43). Here, we review evidence that the increase in VPS35 levels in neurons represents a potential therapeutic target for the treatment of PD. Boosting VPS35 functions could help DA neurons to degrade α-synuclein toxic aggregates and prevent neuronal loss (**Figure 5**).

Despite the understanding on VPS35 association to PD pathology, very little is known about the molecular mechanisms involved in the control of α-synuclein accumulation and in a possible neuroprotective role of VPS35 from α-synuclein-induced toxicity. The retromer complex is mainly involved in neurodegenerative disorders through the control of synaptic

functions, trafficking, and localization of cargo proteins that are essential for neuronal homeostasis and α-synuclein accumulation vs. clearance. Therefore, VPS35 mutations could cause PD by acting on the α-synuclein degradation pathways (15–17, 69). A more detailed knowledge on the molecular mechanisms by which VPS35 promotes α-synuclein clearance could serve to clarify the role of VPS35-retromer protein in PD and to identify alternative and efficient new potential therapeutic targets downstream to VPS35 action. Besides, validation of new VPS35-based targets could be tested in PD mouse models before being developed in the clinical setting. VPS35 has a wide spectrum of actions within neurons, many of which are potentially relevant for the pathophysiology of PD, particularly synaptic functions (22–24, 26, 48) and control of DAT recycling (27) (**Figure 6**). Moreover, VPS35 controls mitochondrial function: VPS35 deficiency disrupts the mitophagic process, promoting mitochondrial fragmentation and DA neuron loss (28).

However, the role of VPS35 could also be played in a more general level on the control of accumulation/degradation of misfolded proteins, hence representing a potential target for different neurodegenerative disorders, such as PD and AD. Indeed, dysregulation of retromer transport is also strongly implicated in AD (70–73). Alterations of retromer activity in AD mouse models leads to pronounced neurodegeneration (deficit in post-synaptic glutamatergic neurotransmission) and deficiency in development of hippocampal-dependent memory (impairment of long-term potentiation) (36, 65) compatible with the role of retromer complex in controlling synaptic functions (22–24, 26). Moreover, different studies addressing VPS35 loss of function reported an elevation of endogenous Aβ peptide levels, in keeping with a VPS35 role in controlling amyloid protein precursor (APP) sorting and processing (28, 70–73).

New research may seek to develop a VPS35-based therapy. A possible therapeutic strategy to boost VPS35 functions could be a drug promoting the stabilization of retromer complex. Earlier studies identified chemical molecules capable of stabilizing the retromer complex by binding the complex in a bind site between VPS35–VPS29 (74). The stabilization of the retromer complex resulted in the reduction in complex degradation and in the increase in VPS35 and retromer subunit levels in cell lines (74). Starting from this observation, it could be possible to identify a lead compound able to combine the effect on the target with the possibility to cross the blood–brain barrier, to be tested in a clinical trial on PD patients. On the other hand, a second disease-modifying approach to boost VPS35 functions could be the delivery of VPS35 gene in the brain by adeno-associated-2-viral vectors (AAV2). The gene therapy approach will allow the introduction of VPS35 gene in the cells that result in the upregulation of VPS35 expression. Recently, it has been demonstrated that AAV2 treatment represents promising human therapeutic applications, with increasing evidence for safety and efficacy (75). First, AAV2 is the most effective in delivery genes *in vivo* for the presence of the primary adenovirus receptor in human cells that allow easy infection with a high yield of transgene expression. Moreover, currently, there are many clinical trials using AAV2 applications, and doses and routes of administration are already established. Finally, the elucidation of the molecular mechanism used by VPS35 to control neuronal functions, neuroprotection, and α-synuclein clearance could be addressed and may provide a new way to identify new therapeutic strategies in PD and other neurodegenerative disorders where neurotoxic aggregates build up. The other challenges will be to overcome in the translational therapeutic pipeline, including biomarker development, clinical trial strategies, and understanding the potential utility of VPS35 as therapeutic target in different PD backgrounds (sporadic and genetic PD cases).

A clinically related question is when a potentially disease-modifying therapy should be prescribed. Patients who are in the early symptomatic phase are thought to have a significant proportion of viable DA neurons. The diverse functions of VPS35 and its ability to counteract α-synuclein accumulation would justify testing VPS35-based approach from the prodromal until the early symptomatic phase of PD.

AUTHOR CONTRIBUTIONS

SE and AA conceived the study, wrote, and revised the manuscript. SE generated the figures.

FUNDING

This work was supported by Fondazione Umberto Veronesi (grant to SE) and by Fondazione Grigioni (grant to AA).

REFERENCES

1. Postuma RB, Berg D, Stern M, Poewe W, Olanow CW, Oertel W, et al. MDS clinical diagnostic criteria for Parkinson's disease. *Mov Disord.* (2015) 30:1591–601. doi: 10.1002/mds.26424
2. Berg D, Postuma RB, Adler CH, Bloem BR, Chan P, Dubois B, et al. MDS research criteria for prodromal Parkinson's disease. *Mov Disord.* (2015) 30:1600–11. doi: 10.1002/mds.26431
3. Braak H, Braak E. Pathoanatomy of Parkinson's disease. *J Neurol.* (2000) 247:3–10. doi: 10.1007/PL00007758
4. Spillantini MG, Schmidt ML, Lee VM, Trojanowski JQ, Jakes R, Goedert M. α-synuclein in Lewy bodies. *Nature.* (1997) 388:839–40. doi: 10.1038/42166
5. Lashuel HA, Overk CR, Oueslati A, Masliah E. The many faces of α-synuclein : from structure and toxicity to therapeutic target. *Nat Rev Neurosci.* (2013) 14:38–48. doi: 10.1038/nrn3406
6. Krüger R, Kuhn W, Müller T, Woitalla D, Graeber M, Kösel S, et al. Ala30Pro mutation in the gene encoding alpha-synuclein in Parkinson's disease. *Nat Genet.* (1998) 18:106–8. doi: 10.1038/ng0298-106
7. Singleton AB, Farrer M, Johnson J, Singleton A, Hague S, Kachergus J, et al. α-Synuclein locus triplication causes Parkinson's disease. *Science.* (2003) 302:841. doi: 10.1126/science.1090278
8. Chartier-Harlin MC, Kachergus J, Roumier C, Mouroux V, Douay X, Lincoln S, et al. α-Synuclein locus duplication as a cause of familial Parkinson's disease. *Lancet.* (2004) 364:1167–9. doi: 10.1016/S0140-6736(04)17103-1

9. Ibáñez P, Bonnet AM, Débarges B, Lohmann E, Tison F, Pollak P, et al. Causal relation between α-synuclein gene duplication and familial Parkinson's disease. *Lancet.* (2004) 364:1169–71. doi: 10.1016/S0140-6736(04)17104-3
10. Wrasidlo W, Tsigelny IF, Price DL, Dutta G, Rockenstein E, Schwarz TC, et al. A *de novo* compound targeting α-synuclein improves deficits in models of Parkinson's disease. *Brain.* (2016) 139:3217–36. doi: 10.1093/brain/aww238
11. Spencer B, Emadi S, Desplats P, Eleuteri S, Michael S, Kosberg K, et al. ESCRT-mediated uptake and degradation of brain-targeted α-synuclein single chain antibody attenuates neuronal degeneration *in vivo*. *Mol Ther.* (2014) 22:1753–67. doi: 10.1038/mt.2014.129
12. Di Giovanni S, Eleuteri S, Paleologou KE, Yin G, Zweckstetter M, Carrupt PA, et al. Entacapone and tolcapone, two catechol O-methyltransferase inhibitors, block fibril formation of α-synuclein and β-amyloid and protect against amyloid-induced toxicity. *J Biol Chem.* (2010) 285:14941–54. doi: 10.1074/jbc.M109.080390
13. Brodin L, Shupliakov O. Retromer in synaptic function and pathology. *Front Synaptic Neurosci.* (2018) 10:37. doi: 10.3389/fnsyn.2018.00037
14. Dhungel N, Eleuteri S, Li LB, Kramer NJ, Chartron JW, Spencer B, et al. Parkinson's disease genes VPS35 and EIF4G1 interact genetically and converge on α-synuclein. *Neuron.* (2015) 85:76–87. doi: 10.1016/j.neuron.2014.11.027
15. Zavodszky E, Seaman MN, Moreau K, Jimenez-Sanchez M, Breusegem SY, Harbour ME, et al. Mutation in VPS35 associated with Parkinson's disease impairs WASH complex association and inhibits autophagy. *Nat Commun.* (2014) 5:1–16. doi: 10.1038/ncomms4828
16. Tang FL, Erion JR, Tian Y, Liu W, Yin DM, Ye J, et al. VPS35 in dopamine neurons is required for endosome-to-golgi retrieval of Lamp2a, a receptor of chaperone-mediated autophagy that is critical for α-synuclein degradation and prevention of pathogenesis of Parkinson's disease. *J Neurosci.* (2015) 35:10613–28. doi: 10.1523/JNEUROSCI.0042-15.2015
17. Miura E, Hasegawa T, Konno M, Suzuki M, Sugeno N, Fujikake N, et al. VPS35 dysfunction impairs lysosomal degradation of α-synuclein and exacerbates neurotoxicity in a Drosophila model of Parkinson's disease. *Neurobiol Dis.* (2014) 71:1–13. doi: 10.1016/j.nbd.2014.07.014
18. Arighi CN, Hartnell LM, Aguilar RC, Haft CR, Bonifacino JS. Role of the mammalian retromer in sorting of the cation-independent mannose 6-phosphate receptor. *J Cell Biol.* (2004) 165:123–33. doi: 10.1083/jcb.200312055
19. Harbour ME, Breusegem SY, Antrobus R, Freeman C, Reid E, Seaman MN. The cargo-selective retromer complex is a recruiting hub for protein complexes that regulate endosomal tubule dynamics. *J Cell Sci.* (2010) 123:3703–17. doi: 10.1242/jcs.071472
20. Nielsen MS, Madsen P, Christensen EI, Nykjaer A, Gliemann J, Kasper D, et al. The sortilin cytoplasmic tail conveys Golgi-endosome transport and binds the VHS domain of the GGA2 sorting protein. *EMBO J.* (2001) 20:2180–90. doi: 10.1093/emboj/20.9.2180
21. Kim E, Lee Y, Lee HJ, Kim JS, Song BS, Huh JW, et al. Implication of mouse Vps26b-Vps29-Vps35 retromer complex in sortilin trafficking. *Biochem Biophys Res Commun.* (2010) 403:167–71. doi: 10.1016/j.bbrc.2010.10.121
22. Temkin P, Lauffer B, Jäger S, Cimermancic P, Krogan NJ, von Zastrow M. SNX27 mediates retromer tubule entry and endosome-to-plasma membrane trafficking of signalling receptors. *Nat Cell Biol.* (2011) 13:715–23. doi: 10.1038/ncb2252
23. Wang X, Zhao Y, Zhang X, Badie H, Zhou Y, Mu Y, et al. Loss of sorting nexin 27 contributes to excitatory synaptic dysfunction by modulating glutamate receptor recycling in Down's syndrome. *Nat Med.* (2013) 19:473–80. doi: 10.1038/nm.3117
24. Loo LS, Tang N, Al-Haddawi M, Stewart Dawe G, Hong W. A role for sorting nexin 27 in AMPA receptor trafficking. *Nat. Commun.* 5, (2014). doi: 10.1038/ncomms4176
25. Hussain NK, Diering GH, Sole J, Anggono V, Huganir RL. Sorting Nexin 27 regulates basal and activity-dependent trafficking of AMPARs. *Proc Natl Acad Sci USA.* (2014) 111:11840–5. doi: 10.1073/pnas.1412415111
26. Tian Y, Tang FL, Sun X, Wen L, Mei L, Tang BS, et al. VPS35-deficiency results in an impaired AMPA receptor trafficking and decreased dendritic spine maturation. *Mol Brain.* (2015) 8:70. doi: 10.1186/s13041-015-0156-4
27. Wu S, Fagan RR, Uttamapinant C, Lifshitz LM, Fogarty KE, Ting AY, et al. The dopamine transporter recycles via a retromer-dependent postendocytic mechanism: tracking studies using a novel fluorophore-coupling approach. *J Neurosci.* (2017) 37:9438–52. doi: 10.1523/JNEUROSCI.3885-16.2017
28. Tang FL, Liu W, Hu JX, Erion JR, Ye J, Mei L, et al. VPS35 deficiency or mutation causes dopaminergic neuronal loss by impairing mitochondrial fusion and function. *Cell Rep.* (2015) 12:1631–43. doi: 10.1016/j.celrep.2015.08.001
29. Vilariño-Güell C, Wider C, Ross OA, Dachsel JC, Kachergus JM, Lincoln SJ, et al. VPS35 mutations in parkinson disease. *Am J Hum Genet.* (2011) 89:162–7. doi: 10.1016/j.ajhg.2011.06.001
30. Zimprich A, Benet-Pagès A, Struhal W, Graf E, Eck SH, Offman MN, et al. A mutation in VPS35, encoding a subunit of the retromer complex, causes late-onset parkinson disease. *Am J Hum Genet.* (2011) 89:168–75. doi: 10.1016/j.ajhg.2011.06.008
31. Guella I, Soldà G, Cilia R, Pezzoli G, Asselta R, Duga S, et al. The Asp620asn mutation in VPS35 is not a common cause of familial Parkinson's disease. *Mov Disord.* (2012) 27:800–1. doi: 10.1002/mds.24927
32. Kumar KR, Weissbach A, Heldmann M, Kasten M, Tunc S, Sue CM, et al. Frequency of the D620N mutation in VPS35 in Parkinson disease. *Arch Neurol.* (2012) 69:1360–4. doi: 10.1001/archneurol.2011.3367
33. Sharma M, Ioannidis JP, Aasly JO, Annesi G, Brice A, Bertram L, et al. A multi-centre clinico-genetic analysis of the VPS35 gene in Parkinson disease indicates reduced penetrance for disease-associated variants. *J Med Genet.* (2012) 49:721–6. doi: 10.1136/jmedgenet-2012-101155
34. Verstraeten A, Wauters E, Crosiers D, Meeus B, Corsmit E, Elinck E, et al. Contribution of VPS35 genetic variability to LBD in the Flanders-Belgian population. *Neurobiol Aging.* (2012) 33:1844.e11–3. doi: 10.1016/j.neurobiolaging.2012.01.006
35. Deng H, Gao K, Jankovic J. The VPS35 gene and Parkinson's disease. *Mov Disord.* (2013) 28:569–75. doi: 10.1002/mds.25430
36. Hunn BHM, Cragg SJ, Bolam JP, Spillantini MG, Wade-Martins R. Impaired intracellular trafficking defines early Parkinson's disease. *Trends Neurosci.* (2015) 38:178–88. doi: 10.1016/j.tins.2014.12.009
37. Sheerin UM, Charlesworth G, Bras J, Guerreiro R, Bhatia K, Foltynie T, et al. Screening for VPS35 mutations in Parkinson's disease. *Neurobiol Aging.* (2012) 33:838.e1–5. doi: 10.1016/j.neurobiolaging.2011.10.032
38. Wen L, Tang FL, Hong Y, Luo SW, Wang CL, He W, et al. VPS35 haploinsufficiency increases Alzheimer's disease neuropathology. *J Cell Biol.* (2011) 195:765–79. doi: 10.1083/jcb.201105109
39. Tsika E, Glauser L, Moser R, Fiser A, Daniel G, Sheerin UM, et al. Parkinson's disease-linked mutations in VPS35 induce dopaminergic neurodegeneration. *Hum Mol Genet.* (2014) 23:4621–38. doi: 10.1093/hmg/ddu178
40. Ishizu N, Yui D, Hebisawa A, Aizawa H, Cui W, Fujita Y, et al. Impaired striatal dopamine release in homozygous Vps35 D620N knock-in mice. *Hum Mol Genet.* (2016) 25:4507–17. doi: 10.1093/hmg/ddw279
41. Ho PW, Leung CT, Liu H, Pang SY, Lam CS, Xian J, et al. Age-dependent accumulation of oligomeric SNCA/α-synuclein from impaired degradation in mutant LRRK2 knockin mouse model of Parkinson disease: role for therapeutic activation of chaperone-mediated autophagy (CMA). *Autophagy.* (2019) 14:1–24. doi: 10.1080/15548627.2019.1603545
42. Cataldi S, Follett J, Fox JD, Tatarnikov I, Kadgien C, Gustavsson EK, et al. Altered dopamine release and monoamine transporters in Vps35 p.D620N knock-in mice. *NPJ Parkinsons Dis.* (2018) 4:27. doi: 10.1038/s41531-018-0063-3
43. Chen X, Kordich JK, Williams ET, Levine N, Cole-Strauss A, Marshall L, et al. Parkinson's disease-linked D620N VPS35 knockin mice manifest tau neuropathology and dopaminergic neurodegeneration. *Proc Natl Acad Sci USA.* (2019) 116:5765–74. doi: 10.1073/pnas.1814909116
44. Mir R, Tonelli F, Lis P, Macartney T, Polinski NK, Martinez TN, et al. The Parkinson's disease VPS35[D620N] mutation enhances LRRK2-mediated Rab protein phosphorylation in mouse and human. *Biochem J.* (2018) 475:1861–83. doi: 10.1042/BCJ20180248
45. Seaman MNJ. Cargo-selective endosomal sorting for retrieval to the Golgi requires retromer. *J Cell Biol.* (2004) 165:111–22. doi: 10.1083/jcb.200312034
46. Shannon B, Soto-Ortolaza A, Rayaprolu S, Cannon HD, Labbé C, Benitez BA, et al. Genetic variation of the retromer subunits VPS26A/B-VPS29 in Parkinson's disease. *Neurobiol Aging.* (2014) 35:1958.e1–2. doi: 10.1016/j.neurobiolaging.2014.03.004

47. Braschi E, Goyon V, Zunino R, Mohanty A, Xu L, McBride HM. Vps35 mediates vesicle transport between the mitochondria and peroxisomes. *Curr Biol.* (2010) 20:1310–5. doi: 10.1016/j.cub.2010.05.066
48. Wang S, Bellen HJ. The retromer complex in development and disease. *Development*. (2015) 142:2392–6. doi: 10.1242/dev.123737
49. McGarvey JC, Xiao K, Bowman SL, Mamonova T, Zhang Q, Bisello A, et al. Actin-sorting nexin 27 (SNX27)-retromer complex mediates rapid parathyroid hormone receptor recycling. *J Biol Chem*. (2016) 291:10986–1002. doi: 10.1074/jbc.M115.697045
50. Seaman MNJ. Retromer and its role in regulating signaling at endosomes. *Prog Mol Subcell Biol.* (2018) 57:137–49. doi: 10.1007/978-3-319-96704-2_5
51. Munsie LN, Milnerwood AJ, Seibler P, Beccano-Kelly DA, Tatarnikov I, Khinda J, et al. Retromer-dependent neurotransmitter receptor trafficking to synapses is altered by the Parkinson's disease VPS35 mutation p.D620N. *Hum Mol Genet.* (2015) 24:1691–703. doi: 10.1093/hmg/ddu582
52. Ciechanover A, Kwon YT. Degradation of misfolded proteins in neurodegenerative diseases: therapeutic targets and strategies. *Exp Mol Med*. (2015) 47:e147. doi: 10.1038/emm.2014.117
53. McGlinchey RP, Lee JC. Cysteine cathepsins are essential in lysosomal degradation of α-synuclein. *Proc Natl Acad Sci USA*. (2015) 112:9322–7. doi: 10.1073/pnas.1500937112
54. Follett J, Norwood SJ, Hamilton NA, Mohan M, Kovtun O, Tay S, et al. The Vps35 D620N mutation linked to Parkinson's disease disrupts the cargo sorting function of retromer. *Traffic*. (2014) 15:230–44. doi: 10.1111/tra.12136
55. Cullen V, Lindfors M, Ng J, Paetau A, Swinton E, Kolodziej P, et al. Cathepsin D expression level affects alpha-synuclein processing, aggregation, and toxicity *in vivo*. *Mol Brain*. (2009) 2:5. doi: 10.1186/1756-6606-2-5
56. Bae EJ, Yang NY, Lee C, Kim S, Lee HJ, Lee SJ. Haploinsufficiency of cathepsin D leads to lysosomal dysfunction and promotes cell-to-cell transmission of α-synuclein aggregates. *Cell Death Dis.* (2015) 6:e1901. doi: 10.1038/cddis.2015.283
57. Ravikumar B. Aggregate-prone proteins with polyglutamine and polyalanine expansions are degraded by autophagy. *Hum Mol Genet*. (2002) 11:1107–17. doi: 10.1093/hmg/11.9.1107
58. Lynch-Day MA, Mao K, Wang K, Zhao M, Klionsky DJ. The role of autophagy in Parkinson's disease. *Cold Spring Harb Perspect Med.* (2012) 2:a009357. doi: 10.1101/cshperspect.a009357
59. Winslow AR, Chen CW, Corrochano S, Acevedo-Arozena A, Gordon DE, Peden AA, et al. α-Synuclein impairs macroautophagy: Implications for Parkinson's disease. *J Cell Biol.* (2010) 190:1023–37. doi: 10.1083/jcb.201003122
60. Gomez TS, Billadeau DD. A FAM21-containing WASH complex regulates retromer-dependent sorting. *Dev Cell.* (2009) 17:699–711. doi: 10.1016/j.devcel.2009.09.009
61. Piotrowski JT, Gomez TS, Schoon RA, Mangalam AK, Billadeau DD. WASH knockout T cells demonstrate defective receptor trafficking, proliferation, and effector function. *Mol Cell Biol.* (2013) 33:958–73. doi: 10.1128/MCB.01288-12
62. McGough IJ, Steinberg F, Jia D, Barbuti PA, McMillan KJ, Heesom KJ, et al. Erratum: retromer binding to FAM21 and the WASH complex is perturbed by the parkinson disease-linked VPS35(D620N) mutation. *Curr Biol.* (2014) 24:1678. doi: 10.1016/j.cub.2014.07.004
63. Williams ET, Glauser L, Tsika E, Jiang H, Islam S, Moore DJ. Parkin mediates the ubiquitination of VPS35 and modulates retromer-dependent endosomal sorting. *Hum Mol Genet.* (2018) 27:3189–205. doi: 10.1093/hmg/ddy224
64. Alvarez-Erviti L, Rodriguez-Oroz MC, Cooper JM, Caballero C, Ferrer I, Obeso JA, et al. Chaperone-mediated autophagy markers in Parkinson disease brains. *Arch Neurol.* (2010) 67:1464–72. doi: 10.1001/archneurol.2010.198
65. Bolam JP, Pissadaki EK. Living on the edge with too many mouths to feed: why dopamine neurons die. *Mov Disord.* (2012) 27:1478–83. doi: 10.1002/mds.25135
66. MacLeod DA, Rhinn H, Kuwahara T, Zolin A, Di Paolo G, McCabe BD, et al. RAB7L1 interacts with LRRK2 to modify intraneuronal protein sorting and Parkinson's disease risk. *Neuron.* (2013) 77:425–39. doi: 10.1016/j.neuron.2012.11.033
67. Linhart R, Wong SA, Cao J, Tran M, Huynh A, Ardrey C, et al. Vacuolar protein sorting 35 (Vps35) rescues locomotor deficits and shortened lifespan in Drosophila expressing a Parkinson's disease mutant of Leucine-rich repeat kinase 2 (LRRK2). *Mol Neurodegener.* (2014) 9:1–10. doi: 10.1186/1750-1326-9-23
68. Inoshita T, Arano T, Hosaka Y, Meng H, Umezaki Y, Kosugi S, et al. Vps35 in cooperation with LRRK2 regulates synaptic vesicle endocytosis through the endosomal pathway in Drosophila. *Hum Mol Genet.* (2017) 26:2933–48. doi: 10.1093/hmg/ddx179
69. Zavodszky E, Seaman MNJ, Rubinsztein DC. VPS35 Parkinson mutation impairs autophagy via WASH. *Cell Cycle.* (2014) 13:2155–6. doi: 10.4161/cc.29734
70. Muhammad A, Flores I, Zhang H, Yu R, Staniszewski A, Planel E, et al. Retromer deficiency observed in Alzheimer's disease causes hippocampal dysfunction, neurodegeneration, and Aβ accumulation. *Proc Natl Acad Sci USA*. (2008) 105:7327–32. doi: 10.1073/pnas.0802545105
71. Sullivan CP, Jay AG, Stack EC, Pakaluk M, Wadlinger E, Fine RE, et al. Retromer disruption promotes amyloidogenic APP processing. *Neurobiol Dis.* (2011) 43:338–45. doi: 10.1016/j.nbd.2011.04.002
72. Fjorback AW, Seaman M, Gustafsen C, Mehmedbasic A, Gokool S, Wu C, et al. Retromer binds the FANSHY sorting motif in sorLA to regulate amyloid precursor protein sorting and processing. *J Neurosci.* (2012) 32:1467–80. doi: 10.1523/JNEUROSCI.2272-11.2012
73. Wang CL, Tang FL, Peng Y, Shen CY, Mei L, Xiong WC. VPS35 regulates developing mouse hippocampal neuronal morphogenesis by promoting retrograde trafficking of BACE1. *Biol Open.* (2012) 1:1248–57. doi: 10.1242/bio.20122451
74. Mecozzi VJ, Berman DE, Simoes S, Vetanovetz C, Awal MR, Patel VM, et al. Pharmacological chaperones stabilize retromer to limit APP processing. *Nat Chem Biol.* (2014) 10:443–9. doi: 10.1038/nchembio.1508
75. Niethammer M, Tang CC, LeWitt PA, Rezai AR, Leehey MA, Ojemann SG, et al. Long-term follow-up of a randomized AAV2-GAD gene therapy trial for Parkinson's disease. *JCI Insight.* (2017) 2:e90133. doi: 10.1172/jci.insight.90133

Conflict of Interest: The authors declare that the research was conducted in the absence of any commercial or financial relationships that could be construed as a potential conflict of interest.

frontiers in Neurology

BRIEF RESEARCH REPORT
published: 18 December 2019
doi: 10.3389/fneur.2019.01332

Single Molecule Molecular Inversion Probes for High Throughput Germline Screenings in Dystonia

Michaela Pogoda[1†], Franz-Joachim Hilke[1,2†], Ebba Lohmann[3,4,5], Marc Sturm[1], Florian Lenz[1], Jakob Matthes[1], Francesc Muyas[1,6,7], Stephan Ossowski[1,6,7], Alexander Hoischen[8,9], Ulrike Faust[1], Ilnaz Sepahi[1], Nicolas Casadei[1,10], Sven Poths[1], Olaf Riess[1,10], Christopher Schroeder[1] and Kathrin Grundmann[1]*

[1] Institute of Medical Genetics and Applied Genomics, University of Tübingen, Tübingen, Germany, [2] Department of Dermatology, Venereology and Allergology, Charité - Universitätsmedizin Berlin, Berlin, Germany, [3] Behavioral Neurology and Movement Disorders Unit, Department of Neurology, Istanbul Faculty of Medicine, Istanbul University, Istanbul, Turkey, [4] Department of Neurodegenerative Diseases, Hertie Institute for Clinical Brain Research, University of Tübingen, Tübingen, Germany, [5] German Center for Neurodegenerative Diseases, Tübingen, Germany, [6] Bioinformatics and Genomics Program, Centre for Genomic Regulation, The Barcelona Institute of Science and Technology, Barcelona, Spain, [7] Universitat Pompeu Fabra, Barcelona, Spain, [8] Department of Human Genetics, Radboud University Nijmegen Medical Center, Nijmegen, Netherlands, [9] Radboud Institute of Molecular Life Sciences, Radboud University Nijmegen Medical Center, Nijmegen, Netherlands, [10] DFG NGS Competence Center Tübingen, Tübingen, Germany

OPEN ACCESS

Edited by:
Matthew James Farrer,
University of Florida, United States

Reviewed by:
Pedro Chana,
Universidad de Santiago de Chile, Chile
Jong-Min Kim,
Seoul National University Bundang Hospital, South Korea

***Correspondence:**
Christopher Schroeder
christopher.schroeder@med.uni-tuebingen.de

[†] These authors have contributed equally to this work

Specialty section:
This article was submitted to Movement Disorders, a section of the journal Frontiers in Neurology

Received: 05 June 2019
Accepted: 02 December 2019
Published: 18 December 2019

Citation:
Pogoda M, Hilke F-J, Lohmann E, Sturm M, Lenz F, Matthes J, Muyas F, Ossowski S, Hoischen A, Faust U, Sepahi I, Casadei N, Poths S, Riess O, Schroeder C and Grundmann K (2019) Single Molecule Molecular Inversion Probes for High Throughput Germline Screenings in Dystonia. Front. Neurol. 10:1332. doi: 10.3389/fneur.2019.01332

Background: This study's aim was to investigate a large cohort of dystonia patients for pathogenic and rare variants in the *ATM* gene, making use of a new, cost-efficient enrichment technology for NGS-based screening.

Methods: Single molecule Molecular Inversion Probes (smMIPs) were used for targeted enrichment and sequencing of all protein coding exons and exon-intron boundaries of the *ATM* gene in 373 dystonia patients and six positive controls with known *ATM* variants. Additionally, a rare-variant association study was performed.

Results: One patient (0.3%) was compound heterozygous and 21 others were carriers of variants of unknown significance (VUS) in the *ATM* gene. Although mutations in sporadic dystonia patients are not common, exclusion of pathogenic variants is crucial to recognize a potential tumor predisposition syndrome. SmMIPs produced similar results as routinely used NGS-based approaches.

Conclusion: Our results underline the importance of implementing *ATM* in the routine genetic testing of dystonia patients and confirm the reliability of smMIPs and their usability for germline screenings in rare neurodegenerative conditions.

Keywords: dystonia, *ATM*, NGS, ataxia-telangiectasia, MIPs

INTRODUCTION

Ataxia-telangiectasia (A-T) is a rare autosomal recessively inherited disease usually characterized by ataxia, neuro-motor impairment, ocular or cutaneous telangiectasia, high risk of malignancies and immunodeficiency (1–3). A-T patients are often extraordinarily sensitive to ionizing radiation, contraindicating radiation therapy for them as a standard therapy in case of cancer (4, 5). The disease is caused by mutations of the Ataxia telangiectasia mutated (*ATM*) gene located on chromosome 11q22-23 (6). *ATM* encodes the 350 kDa ATM protein, a nuclear

serine/threonine-protein kinase which is crucial in the cellular response to DNA damage such as double-strand breaks (7, 8). Classic A-T is caused by biallelic truncating *ATM* mutations which lead to a total loss of ATM protein, resulting in an impaired cell cycle (9). Since variants in *ATM* are known to confer cancer risk in heterozygous carriers (10), and at the same time cause increased sensitivity of the patients to toxic effects of ionizing radiation (4, 5), identifying *ATM* mutation carriers can be highly relevant for adequate treatment and regular cancer control examinations.

Furthermore, recent reports describe non-classic forms of A-T or "variant A-T" (11, 12). In these cases, some residual ATM kinase function is maintained and the phenotype is highly variable, including incomplete or atypical phenotypes, e.g., ataxia plus extrapyramidal symptoms or choreoathetosis lacking the classical hallmarks, often masking the correct diagnosis (11, 13). Some of these *ATM* mutations manifest as pure generalized or focal dystonia (14).

However, the frequency of *ATM* mutations in different cohorts of dystonia patients is not well-described. Therefore, we tested a cohort of 373 dystonia patients for *ATM* alterations.

We applied single molecule Molecular Inversion Probes (smMIPs) for targeted enrichment and sequencing of all protein coding exons and exon-intron boundaries of *ATM*. SmMIPs represent a cost-efficient and fast high-throughput technique to identify sequence variation in genes containing many exons (15). SmMIPs are oligonucleotide probes possessing two sequences complementary to defined genomic target regions (16–21). These complementary sequences are located at the 3′-end and at the 5′-end of the probe and hybridize to the single-stranded sample DNA upstream and downstream of the chosen target region of variable length. The gap between the complementary sequences is filled with the copy of the DNA target region by a polymerase, circularizing the probe in an additional ligation reaction.

The circular smMIP-target molecule can then be amplified in a PCR reaction and is, after a single library purification step, ready for sequencing. One main advantage of smMIPs is that probes can be designed in a modular way, tiling all relevant regions as closely as necessary, covering both DNA strands if desired (22). This is especially relevant for the avoidance of artifactual DNA sample damage, since artifacts usually only occur randomly in one strand (17, 23). Another asset of smMIPs is the usage of a unique single molecule (sm) molecular identifier (UMI = unique molecular identifier), a sequence of (in our case) 8 random bases in the probe that is individual for $4^8 \approx 65{,}500$ molecules. Since every smMIP molecule with an individual UMI-tag can only hybridize to one genomic DNA fragment, the UMI sequence can be used to retrace all originally different DNA molecules and to correct for PCR duplicates in the bioinformatical analysis. Thus, an accurate representation of the diversity of DNA molecules in the sample allows the sensitive detection of variants, even at low frequencies (17, 23, 24). Therefore, it is also most suitable for especially cost-efficient, reliable germline mutation screenings in large cohorts. An asset of the technology is that smMIPs can be designed in a customized way (22) and can be used for massively parallel resequencing of many thousands of target regions (25). In addition, most of the chemistry is independent of a specific supplier.

METHODS

Informed consent was obtained from all patients. All samples were taken in accordance with the local Ethical Committee (# 847/2017BO). Genomic DNA was isolated from blood of 373 dystonia patients of Caucasian origin, who had been examined by specialists in movement disorders according to the current clinical criteria (26). Inclusion criteria were as follows: various degrees of dystonia as defined by published clinical criteria and a clinical course compatible with primary dystonia without features indicating secondary dystonia.

Probe Design and Pooling

The whole smMIPs protocol was only slightly modified according to established protocols (beside the protocol, a detailed scheme of the methodology and workflow can be found in 15, 17, 21).

We designed smMIPs to screen the patients' DNA using the open source tool MIPGen (22). The design resulted in 190 smMIPs spanning all 62 protein coding exons of the *ATM* gene [transcript ENST00000278616, Ensemble (27)], covering both the sense and anti-sense strand of the DNA. Probes were synthesized by IDT (Integrated DNA Technologies; Coralville, USA). Upon arrival, all smMIPs were pooled in an equimolar manner. Six random samples were processed and sequenced to assess probe performance. Using the read depth of all individual probes, the pool was rebalanced twice, in order to improve uniformity of coverage of the target regions (17, 28) (see Supplementary Material for further information).

Targeted Enrichment and Amplification

One hundred nanogram isolated DNA were used as input for the targeted capture of genomic regions of interest, and incubated for 21 h with smMIPs, using a ratio of 1:800 (DNA molecules:smMIPs), adding a polymerase and ligase for gap-filling and circularization. Subsequently, a 1-h exonuclease digestion was performed to remove any linear DNA. Thus, only circular smMIPs were amplified in a PCR using a high-fidelity polymerase. A small amount of each PCR product was categorized semi-quantitatively on an agarose gel, and the remaining PCR products were pooled accordingly to obtain equimolar representation of all samples. The pools were cleaned up for Illumina sequencing in one step using XP Ampure beads and the DNA concentration and fragment size was measured using a Qubit 2.0 device and an Agilent TapeStation 2200 to calculate the molarity of each pool. Samples were sequenced on a HiSeq2500 platform with 2×125 cycles (paired-end) and a target of 500 clusters per smMIP per sample.

Sequencing Analyses and Statistics

Sequencing data were analyzed using an adapted in-house pipeline (available on https://github.com/imgag/megSAP, version 0.1-663-ged5a95d). Briefly, all sequences were identified by the UMI to allow later grouping and correction for PCR duplicates. Reads were aligned and mapped using paired-end

TABLE 1 | Rare variants in the *ATM* gene among the 373 dystonia patients detected with smMIPs.

Patient	Genomic variant	Protein change	CADD	Classification
Dys1	c.115A>G	p. (Thr39Ala)	14.38	VUS
Dys2	c.670A>G	p. (Lys224Glu)	23.5	VUS
Dys3	c.670A>G	p. (Lys224Glu)	23.5	VUS
Dys4	c.1066-6T>G	–	–	VUS
	c.7618G>A	p. (Val2540Ile)	20.6	VUS
Dys5	c.1066-6T>G	–	–	VUS
Dys6	c.1066-6T>G	–	–	VUS
Dys7	c.2386A>T	p. (Asn796Tyr)	7.75	VUS
Dys8	c.3802G>A	p. (Val1268Met)	26.9	VUS
Dys9	c.4060C>A	p. (Pro1354Thr)	14.83	VUS
Dys10	c.4297T>G	p. (Tyr1433Asp)	27.3	VUS
Dys11	c.4388T>G	p. (Phe1463Cys)	28.7	VUS
Dys12	c.4424A>G	p. (Tyr1475Cys)	18.12	VUS
Dys13	c.5005+7_5005+8delTA	–	–	VUS
Dys14	c.5693G>A	p. (Arg1898Gln)	18.17	VUS
Dys15	c.5890A>G	p. (Lys1964Glu)	17.81	VUS
Dys16	c.6860G>C	p. (Gly2287Ala)	10.23	VUS
Dys17	c.6983C>T	p. (Pro2328Leu)	22.4	VUS
Dys18	c.7276C>T	p. (Leu2426Phe)	29.3	VUS
Dys19	c.7475T>G	p. (Leu2492Arg)	28.3	VUS
Dys20	c.7796C>T	p. (Thr2599Ile)	11.78	VUS
Dys21	c.8147T>C	p. (Val2716Ala)	26.2	5
	c.8578_8580delTCT	p. (Ser2860del)	–	VUS*
Dys22	c.8314G>A	p. (Gly2772Arg)	31	VUS

*CADD-scores (Combined Annotation-Dependent Depletion) (35, 36) are not available for intronic variants and deletions. *Evidence in literature for pathogenicity (14), but missing functional analyses.*

reads (29), PCR duplicates were used to correct random PCR or sequencing errors labeling their base-quality to 0 to avoid calling falls-positive variants. BAM-files were generated, and variants called using the tool FreeBayes, version 1.1.0 (30). Variants were annotated and saved in GSvar-format.

For rare-variant association, a case-control study was performed (31). As a control cohort, vcf-files of the 1000 genomes project (32) were downloaded for 404 patients with European descent (populations Italian, Spanish, British, and Utah with European ancestry; Finnish not included). In order to obtain a representative and unbiased control cohort, we chose a public database for control data. Only target regions that were covered in both groups, case and control, were analyzed. All variants were subsequently filtered by the following criteria.

For filtering the variants, allele frequencies in the 1000 genomes database and in the ExAC database were necessitated to be below 1% and all variants needed to be reported <50 times in our in-house database. Synonymous and intronic variants (cut-off ± 8 bp) were excluded as well as variants that had been classified as benign or likely benign in our diagnostic in-house database. All variants were classified according to slightly modified guidelines (33, 34).

Statistical analyses were performed using JMP software version 13.0.0 (SAS Institute, Cary, NC). For rare-variant association, a Fisher's exact test was performed ($\alpha = 0.05$).

The raw data supporting the conclusions of this manuscript will be made available by the authors, without undue reservation, to any qualified researcher. The data (vcf-files) of the control cohort were obtained from the 1000 genomes project (32) and are publicly available.

RESULTS

The median target region read depth for all samples ($n = 373$) was 218×, ranging from 34× for one sample to 840× in the sample with the highest coverage. The 20×-coverage of all target regions was 98.0%. Note that these figures only comprise condensed reads (no PCR duplicates) which were shown to be sufficient for allele frequencies typical in germline analyses (17).

Among 373 dystonia patients, we found 21 different variants in 22 of the dystonia patients (**Table 1**). Of these, 20 were of uncertain clinical significance (VUS) (33). Ten of them had high *in silico* prediction of pathogenicity [Combined Annotation-Dependent Depletion, CADD-Score > 20, (35, 36)]. One variant was classified as pathogenic (p. (Val2716Ala), class 5). There was no significant difference from the control group from the 1000 genomes project ($p > 0.05$ for both VUS or predicted pathogenic variants).

Among the dystonia patients, one patient was found with two variants in the *ATM* gene: one was pathogenic and one a VUS with evidence for pathogenicity (p. (Val2617Ala), p. (Ser2860del)). Clinical examination had produced highly elevated AFP levels, familial aggregation of malignancies and

a deterioration of the dystonic symptoms that were largely insensitive to treatment. This patient was recently published (14). In contrast, we found no biallelic pathogenic or likely pathogenic variants in the 1000 genomes control cohort.

All pathogenic variants reported for the **six** positive controls were also detected using smMIPs. The comparison of all variants showed no discrepancy between smMIPs and the diagnostic results.

DISCUSSION

Dystonia

Although we found no statistical association of *ATM* variants between dystonia patients and a control group, we found one patient with a pathogenic variant (p. (Val2617Ala)) and a VUS with evidence for pathogenicity (p. (Ser2860del)) among 373 dystonia patients. In accordance with other published data on the patient (14), our study confirms the efficiency of smMIPs as a diagnostic screening tool (15) and moreover the importance of identifying *ATM* as rare underlying cause in dystonia (37, 38). The genetic causes of dystonia, a rare disease, are very heterogeneous (39), and many genes have been identified in recent times. Among these genetic causes, *ATM* sequence variations are a crucial factor for patients regarding cancer susceptibility (10), disease progression and radiation toxicity (3, 4, 40, 41). Thus, we stress the importance of including *ATM* to the general screening for causes of dystonia.

smMIPs

Due to the usage of UMIs, smMIPs increase the confidence in variants without the necessity of a high coverage, because PCR duplicates can be used to correct for artifacts (17, 23). We successfully established smMIPs in a screening for *ATM* germline variants in dystonia patients. All pathogenic variants that had been detected with different diagnostic NGS approaches in six control patients (and one dystonia patient) were confirmed, validating smMIPs as a sensitive, competitive methodology. They provide a straight-forward wet lab protocol, with customizable chemistry, flexible probe design, sensitive variant detection, and cost-efficient sample processing, especially for high-throughput genetic testing (15, 21, 28, 42). Thus, they constitute a convenient tool for panel-based genetic testing.

CONCLUSION

Since *ATM* mutations confer a higher risk of developing cancer and radiation toxicity, it is crucial to detect *ATM*-variants as the underlying cause in any dystonic patient. In our study, we found smMIPs to be as sensitive as other NGS-based approaches while being highly cost-efficient and flexible.

DATA AVAILABILITY STATEMENT

The raw data supporting the conclusions of this article will be made available by the authors, without undue reservation, to any qualified researcher. The data (vcf-files) of the control cohort were obtained from the 1000 genomes project and are publicly accessible here: http://www.internationalgenome.org/data#download.

ETHICS STATEMENT

All experimental protocols in this study were reviewed and approved by the Ethics Committee of the Eberhard Karls University of Tübingen and of the Medical Faculty of the University Hospital Tübingen. All patients gave written informed consent in accordance with the Declaration of Helsinki. The patients/participants provided their written informed consent to participate in this study.

AUTHOR CONTRIBUTIONS

The research project was conceptualized by OR, CS, F-JH, EL, and KG. Sample acquisition was accomplished by EL, KG, and UF. Methodology was implemented and supported by AH, F-JH, MP, NC, and SP. The computational analyses were developed and/or conducted by CS, MS, FL, SO, FM, and JM. Variant classification and (statistical) analyses were conducted by MP, IS, and SO. All authors revised and approved the final manuscript.

FUNDING

The study was funded by the Exzellenzinitiative Zukunftskonzept Universität Tübingen, project ID D.27.13047.

ACKNOWLEDGMENTS

Illumina sequencing was performed by the DFG NGS Competence Center Tübingen (NCCT, Tübingen, Germany). We would also like to acknowledge all patients and their families who contributed to this study, as well as the clinicians and the technical staff. We acknowledge support by the Deutsche Forschungsgemeinschaft and the Open Access Publishing Fund of the University of Tübingen. This manuscript has been part of an unpublished Master Thesis (43).

REFERENCES

1. Boder E, Sedgwick RP. Ataxia-telangiectasia. *Pediatrics.* (1958) 21:526–54.
2. Gatti RA, Painter RB. *Ataxia-telangiectasia.* Luxembourg: Springer Science & Business Media (2013).
3. Gilad S, Chessa L, Khosravi R, Russell P, Galanty Y, Piane M, et al. Genotype-phenotype relationships in ataxia-telangiectasia and variants. *Am J Hum Genet.* (1998) 62:551–61. doi: 10.1086/301755
4. Abadir R, Hakami N. Ataxia telangiectasia with cancer. An indication for reduced radiotherapy and chemotherapy doses.

Brit J Radiol. (1983) 56:343–5. doi: 10.1259/0007-1285-56-665-343
5. Gatti RA. Ataxia-telangiectasia. *Dermatol Clin.* (1995) 13:1–6. doi: 10.1016/S0733-8635(18)30100-1
6. Savitsky K, Bar-Shira A, Gilad S, Rotman G, Ziv Y, Vanagaite L, et al. A single ataxia telangiectasia gene with a product similar to PI-3 kinase. *Science.* (1995) 268:1749–53. doi: 10.1126/science.7792600
7. Gutiérrez-Enríquez S, Fernet M, Dörk T, Bremer M, Lauge A, Stoppa-Lyonnet D, et al. Functional consequences of ATM sequence variants for chromosomal radiosensitivity. *Genes Chromosomes Cancer.* (2004) 40:109–19. doi: 10.1002/gcc.20025
8. Savitsky K, Sfez S, Tagle DA, Ziv Y, Sartiel A, Collins FS, et al. The complete sequence of the coding region of the ATM gene reveals similarity to cell cycle regulators in different species. *Hum Mol Genet.* (1995) 4:2025–32. doi: 10.1093/hmg/4.11.2025
9. McKinnon PJ. ATM and the molecular pathogenesis of ataxia telangiectasia. *Annu Rev Pathol.* (2012) 7:303–21. doi: 10.1146/annurev-pathol-011811-132509
10. Renwick A, Thompson D, Seal S, Kelly P, Chagtai T, Ahmed M, et al. ATM mutations that cause ataxia-telangiectasia are breast cancer susceptibility alleles. *Nat Genet.* (2006) 38:873–5. doi: 10.1038/ng1837
11. Lohmann E, Krüger S, Hauser A-K, Hanagasi H, Guven G, Erginel-Unaltuna N, et al. Clinical variability in ataxia–telangiectasia. *J Neurol.* (2015) 262:1724–7. doi: 10.1007/s00415-015-7762-z
12. Méneret A, Ahmar-Beaugendre Y, Rieunier G, Mahlaoui N, Gaymard B, Apartis E, et al. The pleiotropic movement disorders phenotype of adult ataxia-telangiectasia. *Neurology.* (2014) 83:1087–95. doi: 10.1212/WNL.0000000000000794
13. McConville CM, Stankovic T, Byrd PJ, McGuire GM, Yao Q-Y, Lennox GG, et al. Mutations associated with variant phenotypes in ataxia-telangiectasia. *Am J Hum Genet.* (1996) 59:320.
14. Kuhm C, Gallenmüller C, Dörk T, Menzel M, Biskup S, Klopstock T. Novel ATM mutation in a German patient presenting as generalized dystonia without classical signs of ataxia-telangiectasia. *J Neurol.* (2015) 262:768–70. doi: 10.1007/s00415-015-7636-4
15. Neveling K, Mensenkamp AR, Derks R, Kwint M, Ouchene H, Steehouwer M, et al. BRCA testing by single-molecule molecular inversion probes. *Clin Chem.* (2017) 63:503–12. doi: 10.1373/clinchem.2016.263897
16. Nilsson M, Malmgren H, Samiotaki M, Kwiatkowski M, Chowdhary BP, Landegren U. Padlock probes: circularizing oligonucleotides for localized DNA detection. *Science.* (1994) 265:2085–8. doi: 10.1126/science.7522346
17. Eijkelenboom A, Kamping EJ, Kastner-van Raaij AW, Hendriks-Cornelissen SJ, Neveling K, Kuiper RP, et al. Reliable next-generation sequencing of formalin-fixed, paraffin-embedded tissue using single molecule tags. *J Mol Diagn.* (2016) 18:851–63. doi: 10.1016/j.jmoldx.2016.06.010
18. Cantsilieris S, Stessman HA, Shendure J, Eichler EE. Targeted capture and high-throughput sequencing using molecular inversion probes (MIPs). *Genotyping.* (2017) 1492:95–106. doi: 10.1007/978-1-4939-6442-0_6
19. Hardenbol P, Banér J, Jain M, Nilsson M, Namsaraev EA, Karlin-Neumann GA, et al. Multiplexed genotyping with sequence-tagged molecular inversion probes. *Nat Biotechnol.* (2003) 21:673. doi: 10.1038/nbt821
20. Umbarger MA, Kennedy CJ, Saunders P, Breton B, Chennagiri N, Emhoff J, et al. Next-generation carrier screening. *Genet Med.* (2014) 16:132. doi: 10.1038/gim.2013.83
21. O'Roak BJ, Vives L, Fu W, Egertson JD, Stanaway IB, Phelps IG, et al. Multiplex targeted sequencing identifies recurrently mutated genes in autism spectrum disorders. *Science.* (2012) 338:1619–22. doi: 10.1126/science.1227764
22. Boyle EA, O'Roak BJ, Martin BK, Kumar A, Shendure J. MIPgen: optimized modeling and design of molecular inversion probes for targeted resequencing. *Bioinformatics.* (2014) 30:2670–2. doi: 10.1093/bioinformatics/btu353
23. Hiatt JB, Pritchard CC, Salipante SJ, O'Roak BJ, Shendure J. Single molecule molecular inversion probes for targeted, high-accuracy detection of low-frequency variation. *Genome Res.* (2013) 23:843–54. doi: 10.1101/gr.147686.112
24. Shen P, Wang W, Krishnakumar S, Palm C, Chi A-K, Enns GM, et al. High-quality DNA sequence capture of 524 disease candidate genes. *Proc Natl Acad Sci USA.* (2011) 108:6549–54. doi: 10.1073/pnas.1018981108
25. Turner EH, Lee C, Ng SB, Nickerson DA, Shendure J. Massively parallel exon capture and library-free resequencing across 16 genomes. *Nat Methods.* (2009) 6:315. doi: 10.1038/nmeth.f.248
26. Fahn S, Eldridge R. Definition of dystonia and classification of the dystonic states. *Adv Neurol.* (1976) 14:1–5.
27. Aken BL, Ayling S, Barrell D, Clarke L, Curwen V, Fairley S, et al. The Ensembl gene annotation system. *Database.* (2016) 2016:baw093. doi: 10.1093/database/baw093
28. Porreca GJ, Zhang K, Li JB, Xie B, Austin D, Vassallo SL, et al. Multiplex amplification of large sets of human exons. *Nat Methods.* (2007) 4:931. doi: 10.1038/nmeth1110
29. Li H, Durbin R. Fast and accurate short read alignment with Burrows–Wheeler transform. *Bioinformatics.* (2009) 25:1754–60. doi: 10.1093/bioinformatics/btp324
30. Garrison E, Marth G. Haplotype-based variant detection from short-read sequencing. *arXiv preprint.* (2012) arXiv *arXiv:1207.3907*.
31. Lee S, Abecasis GR, Boehnke M, Lin X. Rare-variant association analysis: study designs and statistical tests. *Am J Hum Genet.* (2014) 95:5–23. doi: 10.1016/j.ajhg.2014.06.009
32. Genomes Project Consortium. A global reference for human genetic variation. *Nature.* (2015) 526:68–74. doi: 10.1038/nature15393
33. Plon SE, Eccles DM, Easton D, Foulkes WD, Genuardi M, Greenblatt MS, et al. Sequence variant classification and reporting: recommendations for improving the interpretation of cancer susceptibility genetic test results. *Hum Mutat.* (2008) 29:1282–91. doi: 10.1002/humu.20880
34. Spurdle AB, Healey S, Devereau A, Hogervorst FB, Monteiro AN, Nathanson KL, et al. ENIGMA—Evidence-based network for the interpretation of germline mutant alleles: an international initiative to evaluate risk and clinical significance associated with sequence variation in BRCA1 and BRCA2 genes. *Hum Mutat.* (2012) 33:2–7. doi: 10.1002/humu.21628
35. Kircher M, Witten DM, Jain P, O'roak BJ, Cooper GM, Shendure J. A general framework for estimating the relative pathogenicity of human genetic variants. *Nat Genet.* (2014) 46:310–5. doi: 10.1038/ng.2892
36. Velde KJ, Kuiper J, Thompson BA, Plazzer JP, Valkenhoef G, Haan M, et al. Evaluation of CADD scores in curated mismatch repair gene variants yields a model for clinical validation and prioritization. *Hum Mutat.* (2015) 36:712–9. doi: 10.1002/humu.22798
37. Bodensteiner JB, Goldblum RM, Goldman AS. Progressive dystonia masking ataxia in ataxia-telangiectasia. *Arch Neurol.* (1980) 37:464–5. doi: 10.1001/archneur.1980.00500560094020
38. Thompson S, Iyer A, Byrd P, Taylor M, Spinty S. Dopa-Responsive dystonia and chorea as a presenting feature in ataxia-telangiectasia. *Mov Disord Clin Pract.* (2014) 1:249–51. doi: 10.1002/mdc3.12048
39. Lohmann K, Klein C. Genetics of dystonia: what's known? What's new? What's next? *Mov Disord.* (2013) 28:899–905. doi: 10.1002/mds.25536
40. Barlow C, Eckhaus MA, Schäffer AA, Wynshaw-Boris A. Atm haploinsufficiency results in increased sensitivity to sublethal doses of ionizing radiation in mice. *Nat Genet.* (1999) 21:359. doi: 10.1038/7684

41. Verhagen MM, Last JI, Hogervorst FB, Smeets DF, Roeleveld N, Verheijen F, et al. Presence of ATM protein and residual kinase activity correlates with the phenotype in ataxia-telangiectasia: a genotype–phenotype study. *Hum Mutat.* (2012) 33:561–71. doi: 10.1002/humu.22016
42. Niedzicka M, Fijarczyk A, Dudek K, Stuglik M, Babik W. Molecular Inversion Probes for targeted resequencing in non-model organisms. *Sci Rep.* (2016) 6:24051. doi: 10.1038/srep24051
43. Pogoda M. *Establishing single molecule molecular inversion probes: screening a large cohort of dystonia patients for rare genomic variants in ATM* (Master Thesis). University of Tuebingen, Tübingen, Germany (2018).

Conflict of Interest: The authors declare that the research was conducted in the absence of any commercial or financial relationships that could be construed as a potential conflict of interest.

frontiers in Neurology

REVIEW
published: 14 January 2020
doi: 10.3389/fneur.2019.01373

Can the Cognitive Phenotype in Neurofibromatosis Type 1 (NF1) Be Explained by Neuroimaging? A Review

Eloïse Baudou[1,2], Federico Nemmi[2], Maëlle Biotteau[2], Stéphanie Maziero[2,3], Patrice Peran[2] and Yves Chaix[1,2]*

[1] Children's Hospital, Purpan University Hospital, Toulouse, France, [2] ToNIC, Toulouse NeuroImaging Center, University of Toulouse, Inserm, UPS, Toulouse, France, [3] Octogone-Lordat, University of Toulouse, Toulouse, France

Neurofibromatosis type 1 (NF1) is one of the most frequent monogenetic disorders. It can be associated with cognitive dysfunctions in several domains such as executive functioning, language, visual perception, motor skills, social skills, memory and/or attention. Neuroimaging is becoming more and more important for a clearer understanding of the neural basis of these deficits. In recent years, several studies have used different imaging techniques to examine structural, morphological and functional alterations in NF1 disease. They have shown that NF1 patients have specific brain characteristics such as Unidentified Bright Objects (UBOs), macrocephaly, a higher volume of subcortical structures, microstructure integrity alterations, or connectivity alterations. In this review, which focuses on the studies published after the last 2 reviews of this topic (in 2010 and 2011), we report on recent structural, morphological and functional neuroimaging studies in NF1 subjects, with special focus on those that examine the neural basis of the NF1 cognitive phenotype. Although UBOs are one of the most obvious and visible elements in brain imaging, correlation studies have failed to establish a robust and reproducible link between major cognitive deficits in NF1 and their presence, number or localization. In the same vein, the results among structural studies are not consistent. Functional magnetic resonance imaging (fMRI) studies appear to be more sensitive, especially for understanding the executive function deficit that seems to be associated with a dysfunction in the right inferior frontal areas and the middle frontal areas. Similarly, fMRI studies have found that visuospatial deficits could be associated with a dysfunction in the visual cortex and especially in the magnocellular pathway involved in the processing of low spatial frequency and high temporal frequency. Connectivity studies have shown a reduction in anterior-posterior "long-range" connectivity and a deficit in deactivation in default mode network (DMN) during cognitive tasks. In conclusion, despite the contribution of new imaging techniques and despite relative advancement, the cognitive phenotype of NF1 patients is not totally understood.

Keywords: NF1, cognitive phenotype, cerebral substrate, brain imagery, fMRI

OPEN ACCESS

Edited by:
Matthew James Farrer, University of Florida, United States

Reviewed by:
Andrea Domenico Praticò, University of Catania, Italy
Maria Augusta Montenegro, Campinas State University, Brazil

****Correspondence:***
Eloïse Baudou
baudou.e@chu-toulouse.fr

Specialty section:
This article was submitted to Pediatric Neurology, a section of the journal Frontiers in Neurology

Received: *10 June 2019*
Accepted: *11 December 2019*
Published: *14 January 2020*

Citation:
Baudou E, Nemmi F, Biotteau M, Maziero S, Peran P and Chaix Y (2020) Can the Cognitive Phenotype in Neurofibromatosis Type 1 (NF1) Be Explained by Neuroimaging? A Review. Front. Neurol. 10:1373. doi: 10.3389/fneur.2019.01373

INTRODUCTION

In recent years, the cognitive and behavioral phenotypes of Neurofibromatosis 1 (NF1) have been well described in affected children. Despite some heterogeneity, which is not yet clearly understood in the absence of established genotype-phenotype correlation, the main cognitive characteristics that have been highlighted are:

- On average, an intelligence quotient (IQ) score lower by 1 standard deviation (SD) compared to the general population (1) with intellectual deficit for about 6% of the NF1 patients.
- Visuospatial impairment, highlighted in particular with the Benton Judgment of Line orientation test (JLO) (1).
- Language disabilities in about 50% of the cases, especially in phonological processes (2).
- Attention deficit according to the diagnostic criteria for Attention Deficit and Hyperactivity Disorder (ADHD) in 30 to 40% of the cases (3, 4), and in general, executive function deficits (5).
- Social cognition deficit, sometimes with the Autism Spectrum Disorder (ASD) criteria (6).
- Motor coordination disorder (7).

Therefore, different cognitive domains are affected, which suggests that different brain networks are involved in the physiopathology of NF1.

However, NF1 patients present specific neuroimaging features. Among them, Unidentified Bright Objects (UBOs) are the best known and are suggested as diagnostic criteria by some authors (8). However, the presence of UBOs does not explain the cognitive and behavioral phenotype in NF1 disease (9, 10). A recent study using multimodal neuroimaging including structural, diffusion and resting state functional magnetic resonance imaging (fMRI) (11) showed that NF1 patients and healthy controls can be differentiated using neuroimaging that combines the measurement of gray matter volume, fractional anisotropy and mean diffusivity. This suggests a complex physiopathology involving gray and white matter abnormalities.

The links between behavioral and cognitive phenotypes and the cerebral substratum are poorly understood. However, the number of brain imaging studies has considerably increased since the reviews of literature by Payne et al. (9) and Hachon et al. (10).

Based on the evidences established in the two previous reviews, we pursued an examination of the literature since 2010 concerning brain imaging in NF1 disease. The aim of this literature review is to find out whether in 2019, nearly 10 years after the last reviews, there is a clearer understanding of the link between cognitive and behavioral patterns and NF1 cerebral physiopathology in children with NF1.

Abbreviations: ACC, anterior cingulate cortex; AD, axial diffusion; ADC, apparent diffusion coefficient; ADHD, Attention Deficit and Hyperactivity Disorder; ASD, Autism Spectrum Disorder; ATR, anterior thalamic radiation; BRIEF, Behavioral Rating Inventory of Executive Function; CBCL, Child Behavior Check List; CC, corpus callosum; DLPFC, dorsolateral prefrontal cortex; DEX, Dysexecutive Questionnaire; DMN, default mode network; DTI, diffusion tensor imaging; FA, fractional anisotropy; FDG, fluorodeoxyglucose; FEF, frontal eye fields; FLAIR, Fluid-Attenuated Inversion Recovery; fMRI, functional magnetic resonance imaging; GABA, gamma-aminobutyric acid; GM, gray matter; IQ, intelligence quotient; JLO, Judgment of Line Orientation; MD, mean diffusivity; MRI, magnetic resonance imaging; MRS, magnetic resonance spectroscopy; NAA, N-acetyl-aspartate; NF1, Neurofibromatosis type 1; PET, positron emission tomography; RD, radial diffusion; ROI, region of interest; SRS, Social Responsiveness Scale; UBOs, unidentified bright objects; WM, white matter.

REVIEW

Structural Level

Summary of the Findings Before 2010

On average, NF1 patients have a larger brain volume than the general population, with macrocephalia in 50% of the cases. This difference in brain volume is predominant in white matter (WM), and less significant in gray matter (GM) (12). Up until now, results from brain imaging studies have been unable to clearly indicate any correlation between total brain volume, WM volume or GM volume and the neuropsychological profile. For example, the majority of studies report an NF1-related increase in corpus callosum (CC) volume (13, 14), sometimes with a positive correlation with learning disability (13) and sometimes a negative correlation with ADHD (14) (**Table 1**).

Billingsley et al. highlighted focal architectural abnormalities in NF1 (15, 16). They showed a link between language disability/low academic achievement (reading and/or mathematics) and reduced asymmetry of the left/right planum temporale (**Table 1**). They also found a positive interaction between an atypically structured right inferior frontal gyrus and language level (**Table 1**). These studies suggest an atypical lateralization of linguistic functions in NF1 subjects.

Post-2010 Studies: From the Macrostructural to the Microstructural Level

In an NF1 group, Huijbregts et al. (17) found a larger WM volume associated with a larger volume of all subcortical structures (hippocampus, thalami, striatum, amygdala, accumbens nucleus) and a lower GM density in frontal and parietal regions (**Table 1**). Positive correlations were found between cognitive abilities and social skills, and the volume of subcortical structures:

- Right amygdala volume correlated with executive functions assessed with the Behavioral Rating Inventory of Executive Function (BRIEF) and autistic behavior assessed with the Social Responsiveness Scale (SRS).
- Left putamen volume correlated with executive functions assessed with the Dysexecutive Questionnaire (DEX) and social problems assessed with the Child Behavior Check List (CBCL).

Violante et al. (20) also found that subcortical structures (thalami, right caudate, middle CC) had larger volumes in a group of 14 NF1 children aged 8 to 16 years compared to 14 controls. In this study, the authors confirmed a larger whole brain volume (+10%) with a greater difference between WM (+20%) and GM (+8%) compared to controls. They analyzed the volume variation in more detail according to the function of the region and found a greater difference in bilateral frontal and temporal regions and in the left parietal region for lobar WM volumes. They observed less distinctive gyrification in NF1 subjects, without any difference in

TABLE 1 | Correlation between Structural MRI analysis and Neuropsychological findings: main characteristics of the neuroimaging studies included.

References	Participants	Mean age (SD); range	Neuroimaging acquisition	Neuroimaging results	Neuropsychological correlations
Moore et al. (13)	52 NF1 19 controls	9,8 (3,6); r: 3-16,9 10,9 (2,7); r: 7-16	MRI T1	Higher volume of GM	Learning disability
				Larger CC size	Academic achievement and visual-spatial and motor-skills
Kayl et al. (14)	36 NF1 18 controls	10,6 (2,8); r: 6-16 11,0 (2,7); r: 6-16	MRI T1	Larger total CC area	Less attention problems
Billingsley et al. (15)	24 NF1 24 controls	10,8; r: 7,4-15,8 11,5; r: 7-16,6	MRI T1	Less leftward asymmetry	Poorer reading and math achievement
Billinsley et al. (16)	38 NF1 38 controls	10,8; r: 7,4-15,8 11,5; r: 7-16,6	MRI T1	Right IFG: typical pattern	Worse for all language measurements (phonologic fluency, verbal knowledge, reading, spelling and verbal memory)
				Heschl's gyrus: doubling in left hemisphere	Poorer performance on verbal memory, fine motor speed and coordination measurements
				Heschl's gyrus: doubling in right hemisphere	Better performance on math, verbal memory and fine motor speed
Huijbregts et al. (17)	15 NF1 18 controls	12,9 (2,6) 13,8 (3,6)	MRI T1	Larger left putamen volume and larger total WM volume	More social problems and poorer executive functioning
				Larger right amygdala volume	Poorer executive functioning and autistic mannerisms
Aydin et al. (18)	37 NF1 31 controls	12,9 (2,6) 9,83 (3,76)	MRI DWI: ADC	Genu CC: higher ADC values	Poorer arithmetic, digit span and coding scores
			MRI DWI: FA	Genu CC: higher FA values	Poorer coding scores
Koini et al. (19)	16 NF1 32 controls	12,45 (2,75); r: 9,3-18,6 12,43 (2,99); r: 9,2-19,0	MRI DWI: FA MD AD RD	Altered whole brain microstructure (MD and AD) and ATR; but not CB and SLF	Poorer executive functioning: inhibitory control. No correlation with verbal and performance abilities

AD, axial diffusion; ADC, apparent diffusion coefficient; ATR, anterior thalamic radiation; CB, cingulate bundle; CC, corpus callosum; DWI, diffusion weighted images; FA, fractional anisotropy; GM, gray matter; IFG, inferior frontal gyrus; MD, mean diffusivity; MRI, magnetic resonance imaging; NF1, neurofibromatosis type 1; r, range; RD, radial diffusion; SD, standard deviation; SLF, superior longitudinal fasciculus; WM, white matter.

cortical volume, cortical surface or cortical thickness. In human phylogenic evolution, an increase in brain volume is associated with an increase in cortical gyrification (21). However, in NF1 patients, gyrification is not proportional to brain volume.

Aydin et al. (18) found a higher CC volume in NF1 children (**Table 1**). This study focused on micro- and macrostructural measurements of the CC (midsagittal CC area measurements, fractional anisotropy (FA), and absolute diffusion coefficient (ADC) values of the genu and splenium of the CC). Negative correlations were shown between the ADC values of the genu of the CC and the arithmetic and digit span scores and between the FA values in the genu and coding scores in children with NF-1.

Karlsgodt et al. (22) compared 14 young adults with NF1 and 12 healthy controls using Diffusion Tensor Imaging (DTI) analyses. These authors confirmed an increase in WM volume in NF1 patients and showed an alteration in WM integrity in the anterior thalamic radiation (ATR). This study specifically showed a decrease in FA and an increase in ADC and radial diffusivity (RD) and, to a lesser extent, in axial diffusivity (AD) in the ATR. This pattern suggests an increase in diffusivity due to reduced myelination and reduced axonal organization. More recently, Koini et al. (19) showed a correlation between a decrease in executive functions (inhibitory control evaluated by a sustained attention test) and modifications in microstructure parameters (a decrease in FA and an increase in mean diffusivity, RD and AD) in the ATR (**Table 1**). It is noteworthy that there was no link between these alterations and the presence of thalamic UBOs.

Summary

In comparison to the general population, NF1 subjects present an increase in brain volume that is more pronounced in WM than in GM. However, cortical gyrification is proportionally less compared to healthy subjects. Similarly, the volume of the CC, the thalamus and the striatum is larger in the NF1 population. At the microstructural level, a decrease in FA and an increase in mean diffusivity seem to be systematic, possibly due to an alteration in myelination. Finally, a link can be established between abnormalities in the ATR and the executive dysfunction observed in NF1 subjects. Characteristics of the main neuroimaging studies that show a link between structural features and cognitive functions are indicated in **Table 1**.

UBOs

Summary of Findings Before 2010

UBOs are an anatomical feature of the brain of NF1 children and adults. However, they are not considered to be a criterion in the diagnosis of NF1. UBOs are hyperintensities on T2-weighted or Fluid-Attenuated Inversion Recovery (FLAIR) MRI sequences, without mass effect, and without contrast enhancement. We will interchangeably use the term UBOs and T2-hyperintensities in the following paragraphs. UBOs are found in approximately 70% of NF1 subjects (23), but only between 0.8 and 2.2% in the general population, depending on the study. UBOs can be discrete or diffuse. They are principally located in basal ganglia, thalami, cerebellum and brainstem. In less than 20% of the cases UBOs are supratentorial and hemispheric. They tend to regress with age, at least for those located in the basal ganglia and the brainstem (24). There are different hypotheses concerning their nature: e.g., low grade tumor, hamartoma, heterotopias or a modification in the water content of myelin with dysplastic glial cells. Some authors used MRI to try to clarify the microstructural nature of UBOs. Using DTI, they showed an increase in ADC (25, 26) and a decrease in FA (27). The only anatomo-pathological study of UBOs was conducted by Dipaolo et al. (28). Their histological analysis showed that UBOs result from a vacuolar and spongiotic alteration in WM caused by intramyelinic edema. However, a limitation of their study is the heterogeneity of the NF1 population investigated, since one subject was born prematurely and another received chemotherapy for fibrosarcoma.

The most important question concerning UBOs is their possible involvement in cognitive impairment and their impact on learning, especially in NF1 children. The literature does not provide a definitive answer, even though some studies have highlighted the importance of the location of UBOs in cognition rather than their numbers, with a possible link between thalamic location and cognitive impairment (IQ, attention span) (29). Feldman et al. (30) showed a link between a decrease in T2-hyperintensities in basal ganglia (thalami) and IQ point gain (**Table 2**).

Post 2010 Studies

Morphologic neuroimaging and the relationship with cognitive phenotype

In a large cohort, Sabol et al. (8) confirmed the presence of UBOs in 73.5% of 162 NF1 children aged 2 to 18 years, vs. 4.3% of 163 healthy controls. This provides excellent specificity for the diagnosis of NF1 when UBOs are present (specificity: 98%, sensitivity: 81% before 7 years of age). This study confirmed that the basal ganglia were the most frequent location of T2-hyperintensities and that they decrease with age. Payne et al. (31) highlighted this decrease in T2-hyperintensities through a longitudinal study in which the authors presented cognitive (IQ) and structural neuroimaging data (UBOs) (**Table 2**). They showed a decrease of 35% in T2-hyperintensities over an 18-year period, with differences in progression depending on the type of lesion (discrete lesions decreased and diffuse lesions remained unaltered) and the location (deep lesions in the basal ganglia, cerebellum, and brainstem decreased while hemispheric lesions remained unaltered). A decrease in UBOs was associated with an increase in IQ only on the third assessment, while IQ remained stable in subjects without T2-hyperintensities.

Piscitelli et al. (32) showed a relationship between cerebellum T2-hyperintensities and the neurocognitive profile. Subjects with cerebellar UBOs (31 out of 49 NF1 children in the study) presented worse scores on verbal IQ, full-scale IQ and visuospatial tests (reasoning and memory) than subjects without cerebellar hyperintensities (18 out of 49 NF1 children in the study). However, Roy et al. (33) showed no relationship between executive functions, evaluated with a test or a questionnaire, and the presence, number or location of T2-hyperintensities (**Table 2**).

Diffusion imaging for a better understanding of UBOs

MRI, especially DTI sequences, has been used in several studies to further the understanding of the microstructure of UBOs. Ferraz-Filho et al. (34) showed a decrease in FA values in the bilateral cerebellum and thalami in NF1 patients, regardless

TABLE 2 | Correlation between the MRI analysis of UBOs and neuropsychological findings: main characteristics of the neuroimaging studies included.

References	Participants	Mean age (SD); range	Neuroimaging acquisition	Neuroimaging results	Neuropsychological correlations
Moore et al. (29)	84 NF1	12,04; r: 8-16	MRI T2	Thalamic T2H location	IQ, memory, motor, distractibility and attention
Feldman et al. (30)	67 NF1 20 controls	16,3 (8,7); r: 6-37 16,6 (8,6); r: 6-39	MRI T2	Decreased T2H (basal ganglia, thalamus) on 3-year follow up	Improved IQ (+8 points)
Payne et al. (31)	18 NF1 5 controls	12,4 (2,5); r: 8-16,8 12,0 (2,3); r: 8,9-15,2	MRI T2	Decreased T2H on 18-year follow up	Improved IQ
Piscitelli et al. (32)	49 NF1	10,2 (2,9); r: 6-16,9	MRI T2	Cerebellar T2H location	Lower scores for subtest information and vocabulary on the WISC-III, arithmetic and vocabulary, total IQ, fluid reasoning IQ
Roy et al. (33)	36 NF1	9,62 (1,74); r: 7-12,92	MRI T2	Number, size, location T2H	No correlation with executive functions and IQ

IQ, intellectual quotient; MRI, magnetic resonance imaging; NF1, neurofibromatosis type 1; r, range; SD, standard deviation; T2H, T2 hyperintensity; UBOs, unidentified bright objects; WISC-III, Wechsler Intelligence Scale for Children III.

of the occurrence of UBOs in the thalami. This suggests that microstructural abnormalities can be present even if there are no hyperintensities in the brain. In a second study (35) with 27 NF1 subjects on whom 2 MRI examinations were performed between 1 and 5 years, the authors confirmed a decrease in T2-hyperintensities with a non-linear pattern of progression after the first decade of life. During the first decade of life, hyperintensities can remain stable or increase in number. The author found a reduction in the mean FA in UBOs regions and in regions where UBOs have disappeared (i.e., thalami, cerebellum and basal ganglia).

To better understand the microstructural modifications in UBOs sites, Billiet et al. (36) combined DTI analysis with other MRI-based techniques such as multi-exponential T2 relaxation, diffusion kurtosis imaging or neurite orientation dispersion and density imaging. They compared these parameters in 17 NF1 subjects, within UBOs sites and in contralateral normal-appearing WM. The authors found a lower FA, greater mean diffusivity (MD), RD and AD, and a longer T2 time for intracellular and extracellular water in UBOs in comparison to contralateral normal appearing WM. The authors considered that these results might have been related to intramyelinic edema. Ertan et al. (37) analyzed DTI parameters (FA, MD, AD and RD) in regions of interest in 14 NF1 subjects and 14 healthy controls, comparing UBOs sites and normal appearing sites. The decrease in FA was found in GM and WM UBOs, but mostly in WM. Previous studies suggested that a combined decrease in FA and increase in AD and RD could be explained by a combination of myelin damage and axonal disturbance. Tractography showed WM fiber integrity in 15 UBOs out of 18.

Multimodal approach

Barbier et al. (38) compared spectroscopic imaging in a multivoxel approach in basal ganglia and thalami in 25 NF1 children aged 8 to 15 years divided into two groups, one without UBOs (UBOs − group: 10 subjects) and one with UBOs (UBOs + group: 15 subjects). These authors found lower N-acetyl-aspartate (NAA)/creatinine, NAA/Choline and NAA/myoInositol ratios and a higher MyoInositol/Choline ratio in the right lateral thalamus in the UBOs + group, compared with the UBOs − group. These results could suggest a thalamic dysfunction that affects the thalamo-cortico-frontal loops related to neural and/or astroglial abnormalities. In a multimodal approach that combines spectroscopy MRI and DTI, Nicita et al. (39) analyzed spectroscopy imaging and 2 DTI parameters (ADC and FA) for 4 regions of interest (the caudate nucleus, the globus pallidus, the putamen and the thalamus) in 14 NF1 subjects aged 8 to 31 years and 8 healthy controls. The authors found (1) lower NAA, NAA/choline and NAA/creatinine ratios regardless of the subject's age (under or above 18 years of age) and the presence or absence of UBOs when the NF1 subjects were compared with the controls; (2) and a higher ADC without FA changes in UBOs subjects and subjects under 18 years of age. The presence of metabolic and microstructural abnormalities was an indication of axonal damages associated with an increase in myelin turnover in areas of intramyelinic edema, especially in young subjects. Interestingly, the subjects in this study manifested no developmental delay or cognitive deficits. These results somewhat contradict those of Rodrigues et al. (40), who found a preservation of NAA values but an increase in MyoInositol/Creatinine and Choline/Creatinine ratios in the basal ganglia with the use of a larger sample (42 NF1 subjects aged 4 to 24 years and 25 healthy controls) regardless of the UBOs status (presence or absence). Lastly, Violante et al. (41) used magnetic resonance spectroscopy (MRS) and [11C]-flumazenil PET, to compare 14 NF1 adults and 13 matched controls. These authors found a lower gamma-aminobutyric acid (GABA) concentration in the visual cortex and the frontal eye fields (FEF) (11.5 and 22% respectively), and a reduction in the binding of $GABA_A$ receptors in the left parieto-occipital cortex, midbrain and thalami, which were not explained by a lower GM volume. Only a correlation between GABA concentration and $GABA_A$ receptor density was found.

Summary

UBOs are present in almost ¾ of the NF1 children, with the basal ganglia being the most frequent anatomical location. UBOs decrease in number after the first decade and this decrease is associated by cognitive improvement. This decrease affects discrete lesions (vs. diffuse) and deep lesions (vs. hemispheric). The microstructural studies found lower FA and higher MD, RD, AD, and mean T2 time, which supports the notion of a myelin edema. These microstructural abnormalities persist after UBOs regression, which indicates that structural abnormalities exist with or without macroscopic lesions (UBOs). Studies using MRS confirm these results but are contradictory with regards to the axonal damage associated with myelin damage. Characteristics of main neuroimaging studies showing a link between UBOs and cognitive functions are indicated in the **Table 2**.

Functional Level

Summary of the Findings Before 2010

Few studies used functional brain imaging to investigate NF1 physiopathology before 2010. Studies with Positron Emission Tomography (PET) scans that utilized [18F] fluorodeoxyglucose (FDG) usually included a small number of subjects (<30). They suggested thalamic hypometabolism in 9 NF1 children [Kaplan et al. (42)] and 29 NF1 adults [Buchert et al. (43)] compared to matching healthy controls.

Four studies published before 2010 used functional MRI (fMRI). In 2003, Billingsley's team (16) compared brain activation during a phonologic and an orthographic task in NF1 children and healthy controls (**Table 3**). They showed greater activation in the right hemisphere during the phonologic task in the NF1 children. They also reported greater involvement of posterior regions (middle temporal and occipital regions) than frontal regions during the orthographic tasks in the same group. The authors interpreted these results as compatible with a "disconnection" between anterior and posterior brain regions in the NF1 population, related to the WM damage that exists in this disease. In 2004, Billingsley et al. (44), the same 2 groups were compared during a letter and number identification task presented under 3 different conditions: baseline condition, mirror condition (targets were inverted) and rotation condition

(targets were rotated at varying degrees). The authors found higher brain activity in posterior regions (middle temporal, parietal and occipital cortices) than in anterior regions (frontal cortices) in the NF1 subjects compared to the controls during visual-spatial analysis. They suggested that the functional abnormalities observed in this study could be related to structural abnormalities that were previously reported by the same team in these regions. Lastly, Clements-Stephens et al. (45) (**Table 3**) showed an inefficient right hemisphere network and more significant involvement of the left hemisphere in an NF1 group during a JLO task. The authors also found decreased activation in the primary visual cortex of the NF1 sample in comparison to the healthy controls. Shilyansky et al. (46) (**Table 3**) found lower activation in NF1 subjects within several cortical and subcortical regions of the right hemisphere dorsolateral prefrontal cortex, FEF and striatum during a visuospatial working memory task.

Post-2010 Studies

PET

To our knowledge, since 2010 only one PET study by Apostolova et al. (54) using PET FDG in a large population (compared with previous studies) of 50 adult NF1 patients and 50 controls showed a single 11.2 ml cluster of reduced FDG uptake in the thalamus of NF1 patients compared with the control.

fMRI

Several research lines related to fMRI studies have been developed.

The relationship between cerebral dysfunction and cognitive deficit. Some studies have tried to link cerebral dysfunction and deficient cognitive processes in NF1. For example, North's team tried to correlate executive deficit, one of the characteristic deficits in NF1, and brain dysfunction. Pride et al. (47) (**Table 3**), using a Go/No-Go task to explore response inhibition, showed reduced activation compared to controls in the pre-motor and pre-supplementary motor area, the right anterior cingulate cortex, the right inferior frontal gyrus, the inferior occipital gyrus and the left fusiform gyrus. The literature identifies a relationship between impulsivity and sustained attention deficit, and hypoactivation of the right inferior frontal gyrus, known to be involved in the inhibition response (55). In a second study, Pride et al. (48) (**Table 3**) used an region of interest (ROI) approach focused on the attentional networks to identify hypoactivation in the exogenous attention system or bottom-up or ventral attention system during an auditory attention task. This network included the bilateral temporoparietal junctions and the anterior cingulate cortex. Moreover, the authors showed a correlation between brain activation level in the right inferior frontal gyrus and attention scores during the task.

Functional connectivity. Due to the known abnormalities in the macro and micro structures of white matter, several groups have investigated the possible abnormalities in functional connectivity of the brain of NF1 subjects. In adults, Ibrahim et al. (49) (**Table 3**) showed reduced recruitment of the left dorsolateral prefrontal cortex (DLPFC) and parietal cortex during a visuospatial working memory task, which confirms previous results by Shilyansky et al. (46). The authors also found differences in the task-related functional connectivity between NF1 subjects and control subjects: during a visuospatial working memory task they observed greater connectivity between bilateral parietal regions and the visual cortex and lower connectivity between the posterior cingulate cortex and the left temporal region in NF1 subjects compared to controls. These connectivity differences suggest an inactivation deficit of the default mode network (DMN) in NF1 subjects, an inactivation that usually occurs during cognitive tasks. This confirms the results of a previous study in children conducted by Loitfelder et al. (50) (**Table 3**). In this study, functional imaging data were collected during resting state fMRI (rs-fMRI) and cognitive and social skills were evaluated with parent questionnaires (BRIEF, DEX, SRS, Social Skills Rating system: SSRS, CBCL). Among the more significant results, the authors showed an increase in connectivity between the left ventral anterior cingulate cortex and the frontal cortex, between the left amygdala and the posterior cingulate cortex/precuneus, and between the left orbito-frontal cortex and the homolateral pallidum in NF1 children compared to controls. Using rs-fMRI, Tomson et al. (56) found a reduction in postero-anterior "long distance" connectivity in NF1 subjects compared to controls along with a less organized DMN and visual network.

ADHD is frequent in the NF1 population and Jonas et al. (53) consequently explored the hypothesis of a deficit in reward processing since this has been shown in ADHD patients without NF1 (**Table 3**). Neuroimaging revealed reduced neuronal activity in the regions involved in the reward circuitry (anterior cingulate, paracingulate, supramarginal, and angular gyri) and a different blood oxygenation level dependent (BOLD) signal development across ages between NF1 subjects and controls, especially in frontal regions, with a decrease in neural activity related to an increase in age in the controls and an increase in neural activity related to an increase in age in the patients with NF1.

Multimodal approach. Violante et al. (51) focused on the analysis of visuoperceptual deficit in NF1 (**Table 3**). To this end, the authors used fMRI with a block design, including a rest period and a different visual stimulus presentation that stimulated either magnocellular or parvocellular pathways: M stimuli (25 cycles per degree, 18 Hz, low contrast: 18%) and P stimuli (2 cycles per degree, 2 Hz, high contrast: 100%). They used an ROI approach that focused on the occipital lobe: areas V1, V2, and V3. The main results were: a functional deficit for low-level stimuli, magno- or parvocellular, in children as well as adults; greater hypoactivation in the extrastriate cortex (V2 and V3) of the dorsal pathway, and abnormal activation during low-level M stimuli (suggesting an interference by deficient deactivation) in the DMN (medial prefrontal cortex, anterior cingulate cortex (ACC), the posterior parietal cortex and parietal cortex) related to ADHD frequency in this population. To pursue the physiopathological analysis of the visual cortex in NF1 patients, the same team conducted a study that combined fMRI, spectroscopy (GABA/Creatinine and Glutamate/Creatinine ratios in the occipital cortex) and genetic analysis (57). Eighteen NF1 children and 26 controls aged 7 to 19 years performed a simple fMRI visual task in which they had to press a button whenever a target disappeared.

TABLE 3 | Correlation between fMRI analysis and neuropsychological findings, main characteristics of the neuroimaging studies included.

References	Participants	Mean age (SD); range	Neuroimaging acquisition	Neuroimaging results in NF1 group	Neuropsychological correlations in NF1 group
Billingsley et al. (16)	15 NF1 15 controls	14,4 (4,0) 15,3 (3,7)	fMRI: visual orthographic task	Higher activation in posterior regions than in frontal regions (left inferior frontal, left DLPFC, premotor cortices)	Poorer performance in visual orthographic task
			fMRI: auditory rhyme task	Higher activation in right hemisphere (right STG)	Poorer performance in auditory rhyme task
Billingsley et al. (44)	15 NF1 15 controls	14,4 (4,0) 15,3 (3,7)	fMRI: mental rotation task	Greater activity in the middle temporal, parietal, and lateral occipital cortices than in anterior cortical regions	Visuospatial deficit
Clements-Stephens et al. (45)	13 NF1 13 controls	9,80 (1,83) 9,78 (2,56); r: 7-15	fMRI: blocked paradigm (visual discrimination task)	Left hemisphere volume of activation greater than right across the frontal lobe and in posterior regions	Lower scores on Benton's JLO
Shilyansky et al. (46)	14 NF1 12 controls	24 (4,93) 22,58 (4,56)	fMRI: visuospatial working memory task	Hypoactivation of DLPFC, FEF, parietal cortex	Impairment in working memory maintenance task
Pride et al. (47)	25 NF1 18 controls	10,5 (7,3) 10,6 (2,9); r: 7-16	fMRI: Go/No-Go	Hypoactivation of pre-SMA, IFG, IOG and the fusiform gyrus/posterior cerebellum	Lower inhibition
Pride et al. (48)	19 NF1 18 controls	11,0 (2,8) 10,5 (2,5); r: 7-16	fMRI: auditory oddball processing	Hypoactivation in the ACC	Selective attention and attentional control
Ibrahim et al. (49)	23 NF1 25 controls	32,69 (9,03) 33,08 (8,89); r: 18-47	fMRI: spatial capacity working memory task	Hypoactivation of right IPS and left DLPFC (working memory circuitry). Greater connectivity between bilateral parietal regions and visual cortices, especially in left hemisphere, and lower connectivity between left temporal regions and PCC	Lower score in working memory task
Loitfelder et al. (50)	14 NF1 30 controls	12,49 (2,65) 12,30 (2,94)	fMRI: resting state	Positive coupling between left vACC and the frontal pole and the left amygdala and the right OFC	Worse executive, social and behavioral performance (no IQ correlation)
Violante et al. (51)	15 NF1 children and 13 NF1 adults 24 control children and 15 control adults	11,7 (2,9); r: 7-17 and 33,1 (4,9); r: 25-42 12,0 (2,3); r: 7-16 and 32,7 (5,6); r: 26-44	fMRI: blocked paradigm (low level visual stimulation)	Hypoactivation of low-level visual cortex. Failure to deactivate DMN during low level visual stimulation	Visuospatial deficit
Ribeiro et al. (52)	16 NF1 16 controls	14,1 (2,7); r: 10,2-19,7 13,8 (2,7); r: 10,4-19,5	fMRI: Go/No-Go task + EEG data + MRS (Ratios GABA/Cr and Glutamate/Cr)	Lower ratio GABA/Cr in the medial frontal reduced in frontal cortices	Inhibitory control: greater number of errors commission and faster reaction times in go trials indicating an impulsive response style
Jonas et al. (53)	29 NF1 22 controls	11,93 (2,64); r: 8-16 12,73 (3,49); r: 8-19	fMRI: Cake Gambling Task	Decreased neural activity in multiple regions including PCC and frontal pole	Risky decision making: non significant tendency to make fewer risky decisions across all reward categories

ACC, anterior cingulate cortex; Cr, creatinine; DLPFC, dorsolateral prefrontal cortex; DMN, default mode network; EEG, electroencephalogram; FEF, frontal eye field; fMRI, functional magnetic resonance imaging; GABA, gamma-aminobutyric acid; IFG, inferior frontal gyrus; IQ, intellectual quotient; IOG, inferior occipital gyrus; IPS, intraparietal sulcus; JLO, judgement line orientation; MRS, magnetic resonance spectroscopy; NF1, neurofibromatosis type 1; PCC, posterior cingulate cortex; pre-SMA, pre-supplementary motor area; r, range; SD, standard deviation; STG, superior temporal gyrus, OFC, orbitofrontal cortex, vACC, ventral anterior cingulate cortex.

Through the results, the authors were able to show a reduction in the GABA/Creatinine ratio in NF1 subjects compared to the controls but no difference in the Glutamate/Creatinine ratio, which suggests an alteration in the balance between excitatory and inhibitory mechanisms with altered inhibition in the NF1 occipital cortex. The authors also found a correlation between mutation type and GABA level suggesting a role of neurofibromin in GABAergic neurotransmission. Lastly, they showed a negative correlation between GABA/Creatinine and BOLD level with no difference between the NF1 subjects and

the controls. The same team [**Table 3**; Ribeiro et al. (52)], using combined high-density electroencephalography, MRS and fMRI with a Go/No Go task, examined the neural mechanisms of impulsive behavior in NF1. During the Go/No Go task in visual modality, NF1 subjects made more errors of omission and had a faster reaction time, which confirms the impulsive phenotype. This behavior was correlated with a decrease in GABA/Creatinine ratio found in the medial frontal cortex (including the pre-motor area, the supplementary motor area and the ACC). However, the decrease in this same ratio in the occipital regions was not correlated with the behavioral data. Regarding evoked potentials, an early component corresponding to early visual processing and a later component in the frontal regions matched the inhibitory response that was altered in NF1 subjects. However, in this study, there was no link between genetic findings and altered GABAergic neurotransmission in frontal regions.

Evaluation of the therapeutic care of NF1 patients. In conclusion with regards to functional neuroimaging, two research teams used fMRI as a means to evaluate NF1 patient therapy. The first research, conducted by Charbernaud et al. (58), did not include a control group, which limits the interpretation of the results. In this phase 1, open label trial including 7 children aged 10 to 15 years treated with lovastatin for 12 weeks, an MRI was performed 1 day prior to the start of treatment and on the last day of treatment. The authors compared functional activity in rs-fMRI on the first neuroimaging and functional activity in the resting block between periods of visual stimuli on the second MRI, which they considered as a "pseudo rs-fMRI." The main result was an increase in anterior-posterior long-range connectivity and a decrease in short-range connectivity as observed in normal development. A second preliminary study, conducted by Yoncheva et al. (59) in 16 NF1 children aged 8 to 15 years with a deficit in working memory, evaluated the impact of cognitive training (Cogmed Training) in 25 sessions for 6 and 10 weeks. An rs-fMRI was performed before and after training. Four rs-fMRI indices previously used in typically developing children were analyzed: the amplitude of low frequency fluctuations (ALFF) and the fractional amplitude of low frequency fluctuations (fALFF) that characterize intrinsic neural activity, regional homogeneity (ReHo) that characterizes local synchronization and voxel mirrored homotopic connectivity (VMHC) that reflects interhemispheric synchronization. After training a reduction in fALFF in the cerebellum (left cerebellum I to IV and right cerebellum V) and in the thalamus (right and left), the authors observed a reduction in ReHo in the right middle frontal gyrus and an increase in ReHO in the left

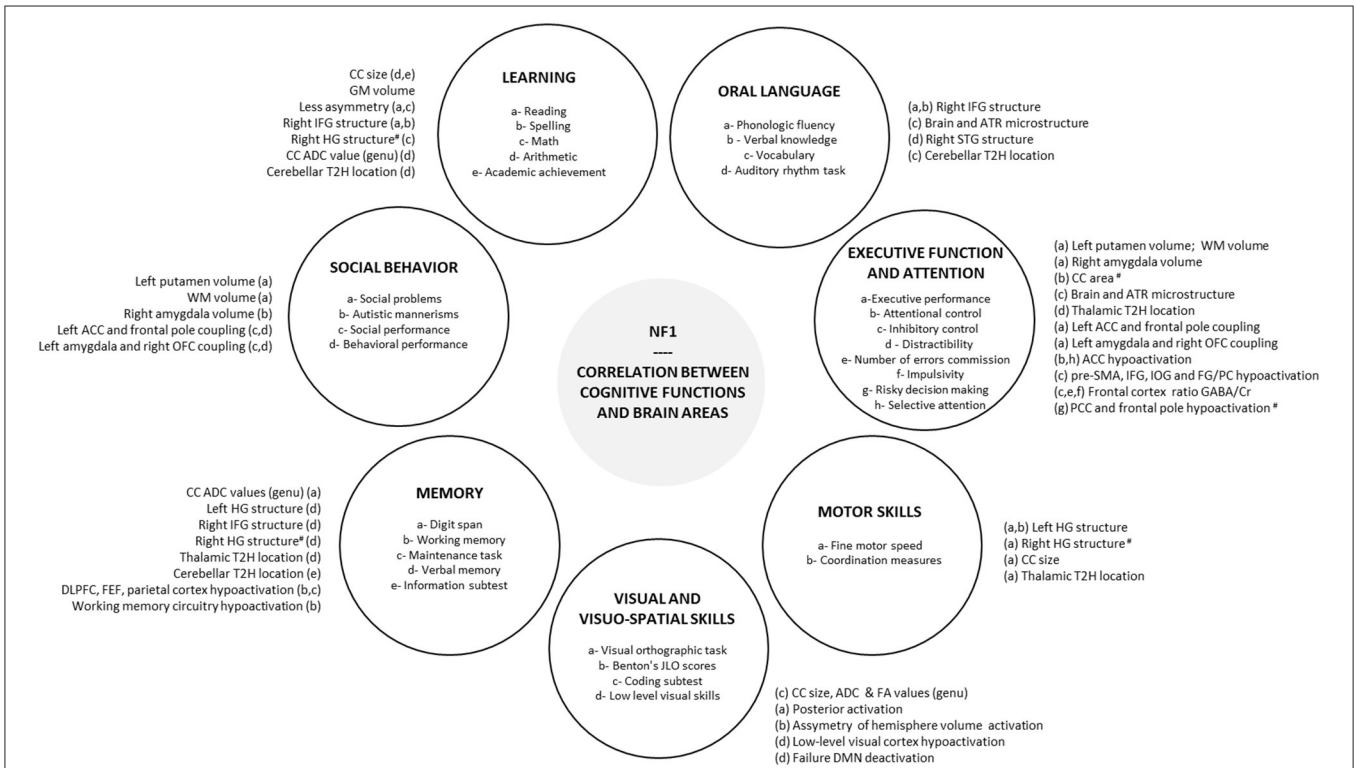

FIGURE 1 | Correlation between cognitive functions and brain areas. Correlations reported in the literature between brain areas and each cognitive and behavioral functions impacted in NF1 are summarized in peripheral circles. #, negative correlation; ACC, anterior cingulate cortex; ADC, apparent diffusion coefficient; ATR, anterior thalamic radiation; CC, corpus callosum; Cr, creatinine; DLPFC, dorsolateral prefrontal cortex; DMN, default mode network; EF, executive function; FA, fractional anisotropy; FEF, frontal eye field; FG, fusiform gyrus; GABA, gamma-aminobutyric acid; HG, Heschl's gyrus; IFG, inferior frontal gyrus; IOG, inferior occipital gyrus; JLO, judgement line orientation; NF1, neurofibromatosis type 1; OFC, orbitofrontal cortex; PC, posterior cerebellum; PCC, posterior cingulate cortex; pre-SMA, pre-supplementary motor area; SLF, superior longitudinal fasciculus; STG, superior temporal gyrus; T2H, T2 hyperintensity, WM, white matter.

fusiform gyrus. This was a preliminary study that showed the possibility to record neural activity changes after training, but this did not enable us to distinguish a developmental effect vs. a specific effect of training because of the absence of a control group.

Summary

Functional neuroimaging studies have primarily explored two main characteristics of the NF1 cognitive phenotype: executive function deficit and visuospatial deficit.

The deficit in executive functions is characterized by deficient inhibitory control and a deficit in exogenous attention depending on the external stimuli. It appears to be associated with a dysfunction in the right inferior frontal areas and the middle frontal areas (pre-motor area, supplementary motor area and ACC). A GABAergic deficit has also been shown for these regions.

Concerning the visuospatial deficit, studies have suggested a dysfunction in the visual cortex (V2-V3) and especially in the magnocellular pathway involved in the processing of low spatial frequency and high temporal frequency. This dysfunction could be associated with a disruption in excitatory-inhibitory balance, which involves neurofibromin, with a decrease in inhibitory GABA in the occipital cortex in NF1.

Studies that specifically address the issue of connectivity show an altered neural connectivity in NF1 subjects compared to controls with a reduction in anterior-posterior "long-range" connectivity and a deficit in deactivation in DMN during cognitive tasks.

Abnormalities observed in brain activity can serve as a basis to evaluate the efficacy of new therapeutics that could be used in NF1 subjects over the next few years. Preliminary studies suggest the possibility to use this technique as a biomarker in future treatment trials.

Characteristics of the main neuroimaging studies showing a link between functional features and cognitive functions are indicated in the **Table 3**.

CONCLUSION

Although the link between the specific cognitive and behavioral features of NF1 and cerebral characteristics is not totally clear at present, comprehension of the neural basis has improved thanks to emerging neuroimaging methods. Executive dysfunction in NF1 children seems to be associated with a dysfunction in the right inferior frontal areas and the middle frontal areas and an alteration in microstructural integrity (DTI) in ATR. Visuospatial deficit appears to be correlated with a dysfunction in the visual cortex (V2-V3) and especially in the magnocellular pathway involved in the processing of low spatial frequency and high temporal frequency. Moreover, connectivity studies show an altered neural connectivity with a reduction in anterior-posterior "long-range" connectivity and a deficit in deactivation in DMN during cognitive tasks. Therefore, functional MRI has become a widely used technique over the past years and might be helpful in the understanding of the cerebral basis of NF1 cognitive phenotype. However, at present there are inconsistencies in the findings of several studies with regard to morphological and macrostructural neuroimaging brain features (UBOs, megalencephaly, higher volume of sub-cortical structures) in NF1. Therefore, it is difficult to find a conclusive link between these features and neurocognitive phenotype (**Figure 1**).

Recently, a study by our group using a multimodal approach involving measures of gray matter volume, fractional anisotropy, and mean diffusivity highlighted a NF1 brain signature (11). Considering that studies using a monomodal approach have failed to explain the cognitive phenotype in NF1, in the future, the development of multimodal approaches could help to clarify the relationships with NF1 phenotype and evaluate the efficacy of specific therapeutics. Moreover, the cognitive phenotype of NF1 subjects is extremely variable from one individual to another. This heterogeneity is probably multifactorial resulting from genetic and environmental factors in such a way that an approach exclusively based on neuroimaging cannot entirely explain the cognitive phenotype. The study of the impact of various factors that influence the cognitive phenotype (genetic, environmental, etc.) remains an indispensable complement to the neuroimaging approach in NF1.

AUTHOR CONTRIBUTIONS

YC wrote the first draft of the manuscript. EB translated and completed a part of the manuscript, and drew up the tables. FN made critical amendments and gave essential feedback for the manuscript. MB developed and formatted the figure and helped to improve tables. SM gave essential feedback for the manuscript. PP made critical amendments especially for the figure. All authors read and approved the final manuscript.

ACKNOWLEDGMENTS

We would like to thank SARL TTP-AMPLUS for his careful checking of the English language and the reviewers for their constructive comments.

REFERENCES

1. Hyman SL, Shores A, North KN. The nature and frequency of cognitive deficits in children with neurofibromatosis type 1. *Neurology.* (2005) 65:1037–44. doi: 10.1212/01.wnl.0000179303.72345.ce
2. Chaix Y, Lauwers-Cancès V, Faure-Marie N, Gentil C, Lelong S, Schweitzer E, et al. Deficit in phonological processes: a characteristic of the neuropsychological profile of children with NF1. *Child Neuropsychol.* (2018) 24:558–74. doi: 10.1080/09297049.2017.1313970
3. Payne JM, Hyman SL, Shores EA, North KN. Assessment of executive function and attention on children with neurofibromatosis type 1: relationships between cognitive measures and real-world behavior. *Child Neuropsychol.* (2011) 17:313–29. doi: 10.1080/09297049.2010.542746

4. Payne JM, Arnold S, Pride NA. Does attention-deficit-hyperactivity disorder exacerbate execution dysfunction in children with neurofibromatosis type 1? *Dev Med Child Neurol*. (2012) 54:898–904. doi: 10.1111/j.1469-8749.2012.04357.x
5. Beaussart ML, Barbarot S, Mauger C, Roy A. Systematic review and meta-analysis of executive functions in preschool and school-age children with neurofibromatosis Type 1. *Int Neuropsychol Soc*. (2018) 24:977–94. doi: 10.1017/S1355617718000383
6. Plasschaert E, Descheemaeker MJ, Van Eylen L. Prevalence of Autism spectrum disorder in children with neurofibromatosis type 1. *Am J Med Genet B Neuropsychiatr Genet*. (2015) 168B:72–80. doi: 10.1002/ajmg.b.32280
7. Rietman AB, Oostenbrink R, Bongers S, Gaukema E, Van Abeelen S, Hendriksen JG, et al. Motor problems in children with neurofibromatosis type 1. *J Neurodev Disord*. (2017) 9:19. doi: 10.1186/s11689-017-9198-5
8. Sabol Z, Resić B, Gjergja Juraski R, Sabol F, Kovač ŠiŽgorić M, Oršolić K, et al. Clinical sensitivity and specificity of multiple T2-hyperintensities on brain magnetic resonance imaging in diagnosis of neurofibromatosis type 1 in children: diagnostic accuracy study. *Croat Med J*. (2011) 52:488–96. doi: 10.3325/cmj.2011.52.488
9. Payne JM, Moharir MD, Webster R, North KN. Brain structure and function in neurofibromatosis type 1: current concepts and future directions. *J Neurol Neurosurg Psychiatry*. (2010) 81:304–9. doi: 10.1136/jnnp.2009.179630
10. Hachon C, Iannuzzi S, Chaix Y. Behavioural and cognitive phenotypes in children with neurofibromatosis type 1 (NF1): the link with the neurobiological level. *Brain Dev*. (2011) 33:52–61. doi: 10.1016/j.braindev.2009.12.008
11. Nemmi F, Cignetti F, Assaiante C, Maziero S, Audic F, Péran P, et al. Discriminating between neurofibromatosis-1 and typically developing children by means of multimodal MRI and multivariate analyses. *Hum Brain Mapp*. (2019) 40:3508–21. doi: 10.1002/hbm.24612
12. Steen RG, Taylor JS, Langston JW, Glass JO, Brewer VR, Reddick WE, et al. Prospective evaluation of the brain in asymptomatic children with neurofibromatosis type 1: relation- ship of macrocephaly to T1 relaxation changes and structural brain abnormalities. *Am J Neuroradiol*. (2001) 22:810–7.
13. Moore BD, Slopis JM, Jackson EF, De Winter AE, Leeds NE. Brain volume in children with neurofibromatosis type 1: relation to neuropsychological status. *Neurology*. (2000) 54:914–20. doi: 10.1212/WNL.54.4.914
14. Kayl AE, Moore BD, Slopis JM, Jackson EF, Leeds NE. Quantitative morphology of the corpus callosum in children with neurofibromatosis and attention-deficit hyperactivity disorder. *J Child Neurol*. (2000) 15:90–6. doi: 10.1177/088307380001500206
15. Billingsley RL, Schrimsher GW, Jackson EF, Slopis JM, Moore III BD. Significance of planum temporale and planum parietale morphologic features in neurofibromatosis 1. *Arch Neurol*. (2002) 59:616–22. doi: 10.1001/archneur.59.4.616
16. Billingsley RL, Jackson EF, Slopis JM, Swank PR, Mahankali S, Moore BD. Functional magnetic resonance imaging of phonologic processing in neurofibromatosis 1. *J Child Neurol*. (2003) 18:732–40. doi: 10.1177/08830738030180110701
17. Huijbregts SC, Loitfelder M, Rombouts SA, Swaab H, Verbist BM, Arkink EB, et al. Cerebral volumetric abnormalities in neurofibromatosis type 1: associations with parent ratings of social and attention problems, executive dysfunction, and autistic mannerisms. *J Neurodev Disord*. (2015) 7:32. doi: 10.1186/s11689-015-9128-3
18. Aydin S, Kurtcan S, Alkan A, Guler S, Filiz M, Yilmaz TF, et al. Relationship between the corpus callosum and neurocognitive disabilities I children with NF-1: diffusion tensor imaging features. *Clin Imaging*. (2016) 40:1092–5. doi: 10.1016/j.clinimag.2016.06.013
19. Koini M, Rombouts SARB, Veer IM, Van Buchem MA, Huijbregts SCJ. White matter microstructure of patients with neurofibromatosis type 1 and its relation to inhibitory control. *Brain Imaging Behav*. (2017) 11:1731–40. doi: 10.1007/s11682-016-9641-3
20. Violante IR, Ribeiro MJ, Silva ED, Castelo-Branco M. Gyrification, cortical and subcortical morphometry in neurofibromatosis type 1: an uneven profile of developmental abnormalities. *J Neurodev Disord*. (2013) 5:3. doi: 10.1186/1866-1955-5-3
21. Zilles K, Armstrong E, Schleicher A, Kretschmann HJ. The human pattern of gyrification in the cerebral cortex. *Anat Embryol*. (1988) 179:173–9. doi: 10.1007/BF00304699
22. Karlsgodt KH, Rosser T, Lutkenhoff ES, Cannon TD, Silva A, Bearden CE. Alterations in white matter microstructure in neurofibromatosis-1. *PLoS ONE*. (2012) 7:e47854. doi: 10.1371/journal.pone.0047854
23. Lopes Ferraz Filho JR, Munis MP, Soares Souza A, Sanches RA, Goloni-Bertollo EM, Pavarino-Bertelli EC. Unidentified bright objects on brain MRI in children as a diagnostic criterion for neurofibromatosis type 1. *Pediatr Radiol*. (2008) 38:305–10. doi: 10.1007/s00247-007-0712-x
24. Gill DS, Hyman SL, Steinberg A, North KN. Age-related findings on MRI in neurofibromatosis type 1. *Pediatr Radiol*. (2006) 36:1048–56. doi: 10.1007/s00247-006-0267-2
25. Tognini G, Ferrozzi F, Garlaschi G, Piazza P, Patti A, Virdis R, et al. Brain apparent diffusion coefficient evaluation in pediatric patients with neurofibromatosis type 1. *J Comput Assist Tomogr*. (2005) 29:298–304. doi: 10.1097/01.rct.0000162406.71300.b7
26. van Engelen SJ, Krab LC, Moll HA, de Goede-Bolder A, Pluijm SM, Catsman-Berrevoets CE, et al. Quantitative differentiation between healthy and disordered brain matter in patients with neurofibromatosis type I using diffusion tensor imaging. *Am J Neuroradiol*. (2008) 29:816–22. doi: 10.3174/ajnr.A0921
27. Zamboni SL, Loenneker T, Boltshauser E, Martin E, Il'yasov KA. Contribution of diffusion tensor MR imaging in detecting cerebral microstructural changes in adults with neurofibromatosis type 1. *AJNR*. (2007) 28:773–6.
28. DiPaolo DP, Zimmerman RA, Rorke LB, Zackai EH, Bilaniuk LT, Yachnis AT. Neurofibromatosis type 1: pathologic substrate of high signal intensity foci in the brain. *Radiology*. (1995) 195:721–4. doi: 10.1148/radiology.195.3.7754001
29. Moore BD, Slopis JM, Schomer D, Jackson EF, Levy BM. Neuropsychological significance of areas of high signal intensity on brain MRIs of children with neurofibromatosis. *Neurology*. (1996) 46:1660–8. doi: 10.1212/WNL.46.6.1660
30. Feldmann R, Schuierer G, Wessel A, Neveling N, Weglage J. Development of MRI T2 hyperintensities and cognitive functioning in patients with neurofibromatosis type 1. *Acta Paediatr*. (2010) 99:1657–60. doi: 10.1111/j.1651-2227.2010.01923.x
31. Payne JM, Pickering T, Porter M, Oates EC, Walia N, Prelog K, et al. Longitudinal assessment of cognition and T2-hyperintensities in NF1: an 18-year study. *Am J Med Genet A*. (2014) 164A:661–5. doi: 10.1002/ajmg.a.36338
32. Piscitelli O, Digilio MC, Capolino R, Longo D, Di Ciommo V. Neurofibromatosis type 1 and cerebellar T2-hyperintensities: the relationship to cognitive functioning. *Dev Med Child Neurol*. (2012) 54:49–51. doi: 10.1111/j.1469-8749.2011.04139.x
33. Roy A, Barbarot S, Charbonnier V, Gayet-Delacroix M, Stalder JF, Roulin JL, et al. Examining the frontal subcortical brain vulnerability hypothesis in children with neurofibromatosis type 1: Are T2-weighted hyperintensities related to executive dysfunction? *Neuropsychology*. (2015) 29:473–84. doi: 10.1037/neu0000151
34. Ferraz-Filho JR, da Rocha AJ, Muniz MP, Souza AS, Goloni-Bertollo EM, Pavarino-Bertelli EC. Diffusion tensor MR imaging in neurofibromatosis type 1: expanding the knowledge of microstructural brain abnormalities. *Pediatr Radiol*. (2012) 42:449–54. doi: 10.1007/s00247-011-2274-1
35. Ferraz-Filho JR, José da Rocha A, Muniz MP, Souza AS, Goloni-Bertollo EM, Pavarino-Bertelli EC. Unidentified bright objects in neurofibromatosis type 1: conventional MRI in the follow-up and corrélation of microstructural lesions on diffusion tensor images. *Eur J Paediatr Neuro J*. (2012) 16:42–7. doi: 10.1016/j.ejpn.2011.10.002
36. Billiet T, Mädler B, D'Arco F, Peeters R, Deprez S, Plasschaert E, et al. Characterizing the microstructural basis of ≪ unidentified Bright objects ≫ in neurofibromatosis type 1: A combined *in vivo* multicomponent T2 relaxation and multi-shell diffusion MRI analysis. *Neuroimage Clin*. (2014) 4:649–58. doi: 10.1016/j.nicl.2014.04.005
37. Ertan G, Zan E, Yousem DM, Ceritoglu C, Tekes A, Poretti A, et al. Diffusion tensor imaging of neurofibromatosis bright objects in children with neurofibromatosis type 1. *Neuroradiol J*. (2014) 27:616–26. doi: 10.15274/NRJ-2014-10055
38. Barbier C, Chabernaud C, Barantin L, Bertrand P, Sembely C, Sirinelli D, et al. Proton MR spectroscopic imaging of basal ganglia and

thalamus in neurofibromatosis type 1: correlation with T2 hyperintensities. *Neuroradiology*. (2011) 53:141–8. doi: 10.1007/s00234-010-0776-4
39. Nicita F, Di Biasi C, Sollaku S, Cecchini S, Salpietro V, Pittalis A, et al. Evaluation of the basal ganglia in neurofibromatosis type 1. *Childs Nerv Syst*. (2014) 30:319–25. doi: 10.1007/s00381-013-2236-z
40. Rodrigues AC Jr, Ferraz-Filho JR, Torres US, da Rocha AJ, Muniz MP, Souza AS, et al. Is magnetic resonance spectroscopy capable of detecting metabolic abnormalities in neurofibromatosis type 1 that are not revealed in brain parenchyma of normal appearance? *Pediatr Neurol*. (2015) 52:314–9. doi: 10.1016/j.pediatrneurol.2014.11.014
41. Violante IR, Patricio M, Bernardino I, Rebola J, Abrunhosa AJ, Ferreira N, et al. GABA deficiency in NF1: a multimodal [11C]-flumazenil and spectroscopy study. *Neurology*. (2016) 87:897–904. doi: 10.1212/WNL.0000000000003044
42. Kaplan AM, Chen K, Lawson MA, Wodrich DL, Bonstelle CT, Reiman EM. Positron emission tomography in children with neurofibromatosis type 1. *J Child Neurol*. (1997) 12:499–506. doi: 10.1177/088307389701200807
43. Buchert R, von Borczyskowski D, Wilke F, Gronowsky M, Friedrich RE, Brenner W, et al. Reduced thalamic 18-F flurodeoxyglucose retention in adults with neurofibromatosis type 1. *Nucl Med Commun*. (2008) 29:17–26. doi: 10.1097/MNM.0b013e3282f1bbf5
44. Billingsley RL, Jackson EF, Slopis JM, Swank PR, Mahankali S, Moore BD. Functional MRI of visual-spatial processing in neurofibromatosis, type 1. *Neuropsychologia*. (2004) 42:395–404. doi: 10.1016/j.neuropsychologia.2003.07.008
45. Clements-Stephens AM, Rimrodt SL, Gaur P, Cutting LE. Visuospatial processing in children with neurofibromatosis type 1. *Neuropsychologia*. (2008) 46:690–7. doi: 10.1016/j.neuropsychologia.2007.09.013
46. Shilyansky C, Karlsgodt KH, Cummings DM, Sidiropoulou K, Hardt M, James AS, et al. Neurofibromin regulates corticostriatal inhibitory networks during working Memory performance. *Proc Natl Acad Sci USA*. (2010) 107:13141–6. doi: 10.1073/pnas.1004829107
47. Pride NA, Korgaonkar MS, North KN, Barton B, Payne JM. The neural basis of deficient response inhibition in children with neurofibromatosis type 1 : evidence from a functional MRI study. *Cortex*. (2017) 93:1–11. doi: 10.1016/j.cortex.2017.04.022
48. Pride NA, Korgaonkar MS, North KN, Payne JM. Impaired engagement of the ventral attention system in neurofibromatosis type 1. *Brain Imaging Behav*. (2018) 12:499–508. doi: 10.1007/s11682-017-9717-8
49. Ibrahim AFA, Montojo CA, Haut KM, Karlsgodt KH, Hansen L, Congdon E, et al. Spatial working Memory in neurofibromatosis 1: altered neural activity and functional connectivity. *Neuroimage Clin*. (2017) 15:801–11. doi: 10.1016/j.nicl.2017.06.032
50. Loitfelder M, Huijbregts SC, Veer IM, Swaab HS, Van Buchem MA, Schmidt R, et al. Functional connectivity changes and executive and social problems in neurofibromatosis type I. *Brain Connect*. (2015) 5:312–20. doi: 10.1089/brain.2014.0334
51. Violante IR, Ribeiro MJ, Cunha G, Bernardino I, Duarte JV, Ramos F, et al. Abnormal brain activation in neurofibromatosis type 1: a link between visual processing and the default mode network. *PLoS ONE*. (2012) 7:e38785. doi: 10.1371/journal.pone.0038785
52. Ribeiro MJ, Violante IR, Bernardino I, Edden RA, Castelo-Branco M. Abnormal relationship between GABA, neurophysiology and impulsive behavior in neurofibromatosis type 1. *Cortex*. (2015) 64:194–208. doi: 10.1016/j.cortex.2014.10.019
53. Jonas RK, Roh E, Montojo CA, Pacheco LA, Rosser T, Silva AJ, et al. Risky decision making in neurofibromatosis type 1: an exploratory study. *Biol Psychiatry Cogn Neurosci Neuroimaging*. (2017) 2:170–9. doi: 10.1016/j.bpsc.2016.12.003
54. Apostolova I, Derlin T, Salamon J, Amthauer H, Granström S, Brenner W, et al. Cerebral glucose metabolism in adults with neurofibromatosis type 1. *Brain Res*. (2015) 1625:97–101. doi: 10.1016/j.brainres.2015.08.025
55. Sakai H, Uchiyama Y, Shin D, Hayashi MJ, Sadato N. Neural activity changes associated with impulsive responding in the sustained attention to response task. *PLoS ONE*. (2011) 8:e67391. doi: 10.1371/journal.pone.0067391
56. Tomson SN, Schreiner MJ, Narayan M, Rosser T, Enrique N, Silva AJ, et al. Resting state functional MRI reveals abnormal network connectivity in neurofibromatosis 1. *Hum Brain Mapp*. (2015) 36:4566–81. doi: 10.1002/hbm.22937
57. Violante IR, Ribeiro MJ, Edden RA, Guimarães P, Bernardino I, Rebola J, et al. GABA deficit in the visual cortex of patients with neurofibromatosis type 1 : genotype-phenotype correlations and functional impact. *Brain*. (2013) 136:918–25. doi: 10.1093/brain/aws368
58. Chabernaud C, Mennes M, Kardel PG, Gaillard WD, Kalbfleisch ML, Vanmeter JW, et al. Lovastatin regulates brain spontaneous low-frequency brain activity in Neurofibromatosis type 1. *Neurosci Lett*. (2010) 515:28–33. doi: 10.1016/j.neulet.2012.03.009
59. Yoncheva YN, Hardy KK, Lurie DJ, Somandepalli K, Yang L, Vezina G, et al. Computerized cognitive training for children with neurofibromatosis type 1: A pilot resting-state fMRI study. *Neuroimaging*. (2017) 266:53–8. doi: 10.1016/j.pscychresns.2017.06.003

Conflict of Interest: The authors declare that the research was conducted in the absence of any commercial or financial relationships that could be construed as a potential conflict of interest.

frontiers in Neurology

CASE REPORT
published: 15 January 2020
doi: 10.3389/fneur.2019.01331

A Novel Homozygous Variant in the Fork-Head-Associated Domain of Polynucleotide Kinase Phosphatase in a Patient Affected by Late-Onset Ataxia With Oculomotor Apraxia Type 4

*Rosa Campopiano[1], Rosangela Ferese[1], Fabio Buttari[1], Cinzia Femiano[1], Diego Centonze[1,2], Francesco Fornai[1,3], Francesca Biagioni[1], Maria Antonietta Chiaravalloti[1], Mauro Magnani[4], Emiliano Giardina[5,6], Anna Ruzzo[4] and Stefano Gambardella[1,4]**

[1] IRCCS Neuromed, Pozzilli, Italy, [2] Dipartimento di Medicina dei Sistemi, Università di Roma Tor Vergata, Rome, Italy, [3] Department of Translational Research and New Technologies in Medicine and Surgery, University of Pisa, Pisa, Italy, [4] Department of Biomolecular Sciences, University of Urbino "Carlo Bo", Urbino, Italy, [5] Department of Biomedicine and Prevention, University of Rome "Tor Vergata", Rome, Italy, [6] Molecular Genetics Laboratory UILDM, Santa Lucia Foundation, Rome, Italy

OPEN ACCESS

Edited by:
Matthew James Farrer, University of Florida, United States

Reviewed by:
Mario Reynaldo Cornejo-Olivas, National Institute of Neurological Sciences, Peru
Luca Marsili, University of Cincinnati, United States

***Correspondence:**
Stefano Gambardella
stefano.gambardella@neuromed.it

Specialty section:
This article was submitted to Neurogenetics, a section of the journal Frontiers in Neurology

Received: 07 June 2019
Accepted: 02 December 2019
Published: 15 January 2020

Citation:
Campopiano R, Ferese R, Buttari F, Femiano C, Centonze D, Fornai F, Biagioni F, Chiaravalloti MA, Magnani M, Giardina E, Ruzzo A and Gambardella S (2020) A Novel Homozygous Variant in the Fork-Head-Associated Domain of Polynucleotide Kinase Phosphatase in a Patient Affected by Late-Onset Ataxia With Oculomotor Apraxia Type 4. Front. Neurol. 10:1331. doi: 10.3389/fneur.2019.01331

Ataxia with oculomotor apraxia (AOA) is a clinical syndrome featuring a group of genetic diseases including at least four separate autosomal-recessive cerebellar ataxias. All these disorders are due to altered genes involved in DNA repair. AOA type 4 (AOA4) is caused by mutations in DNA repair factor polynucleotide kinase phosphatase (*PNKP*), which encodes for a DNA processing enzyme also involved in other syndromes featured by microcephaly or neurodegeneration. To date, only a few AOA4 patients have been reported worldwide. All these patients are homozygous or compound heterozygous carriers for mutations in the kinase domain of *PNKP*. In this report, we describe a 56 years old patient affected by AOA4 characterized by ataxia, polyneuropathy, oculomotor apraxia, and cognitive impairment with the absence of dystonia. The disease is characterized by a very late onset (50 years) when compared with other AOA4 patients described so far (median age of onset at 4 years). In this proband, Clinical Exome Analysis through Next Generation Sequencing (NGS) consisting of 4,800 genes, identified the *PNKP* homozygous mutation p.Gln50Glu. This variant, classified as a likely pathogenic variant according to American College of Medical Genetics (ACMG) guidelines, does not involve the kinase domain but falls in the fork-head-associated (FHA) domain. So far, mutations in such a domain were reported to associate only with a pure seizure syndrome without the classic AOA4 features. Therefore, this is the first report of patients carrying a mutation of the FHA domain within the *PNKP* gene which expresses the clinical phenotype known as the AOA4 syndrome and the lack of any seizure activity. Further studies are required to investigate specifically the significance of various mutations within the FHA domain, and it would be worth to correlate these variants with the age of onset of the AOA4 syndrome.

Keywords: ataxia with oculomotor apraxia, *PNKP* gene, clinical exome, late onset, neurogenetics

INTRODUCTION

Mutations in the DNA repair factor polynucleotide kinase phosphatase (*PNK*P) have been linked to multiple distinct human inherited syndromes. These include (i) microcephaly with seizures (MCSZ, MIM 613402, also known as early infantile epileptic encephalopathy-10), which is characterized by microcephaly, early-onset, intractable seizures, and developmental delay (1), (ii) progressive cerebellar atrophy and polyneuropathy (2), and (iii) ataxia with oculomotor apraxia type 4 (AOA4) (3, 4).

Ataxia with oculomotor apraxia (AOA), is a group of at least four autosomal-recessive cerebellar ataxia syndromes. They are related to genes which provide instructions for making proteins that are involved in repairing damaged DNA: (i) *APTX* (aprataxin), responsible for AOA1 (MIM 208920), a progressive syndrome associated with hypoalbuminemia and elevated levels of cholesterol (5–7); (ii) *SETX* (senataxin), responsible for AOA2 or *SCAR1* (MIM 606002), a progressive ataxia occurring later than AOA1, characterized by increased alpha-fetoprotein levels (8, 9), (iii) *PIK3R5* (phosphoinositide-3-kinase, regulatory subunit 5), responsible for AOA3 (MIM 615217), with clinical features similar to AOA2; (iv) *PNKP* (polynucleotide kinase 3′-phosphatase) responsible for AOA4 (MIM 616267) characterized by ataxia, oculomotor apraxia, peripheral neuropathy, and dystonia (3).

These syndromes impact cerebellar function and result in a profound loss of motor control characterized by cerebellar degeneration, apraxia, and oculomotor apraxia (abnormal saccadic eye movement). Very often these symptoms occur in the presence of dystonia and peripheral neuropathy (5, 10).

AOA4 is characterized by prominent dystonia which spontaneously attenuates during the course of the disease. Muscle wasting in the hands and feet and neuropathy are also common and lead to tetraplegia and short atrophic hands and feet. Usually, cognitive function is not affected, although some people may present intellectual disability. AOA diseases are characterized by an early onset which occurs in the first decade; strikingly, AOA4 is characterized by the earliest disease onset among AOAs which occurs at about 4 years of age (11).

PNKP is a DNA processing enzyme in which the C-terminal catalytic domain contains a fused bimodal phosphatase and kinase domain, with a fork-head-associated (FHA) domain at its N-terminus (12).

The FHA domain of *PNKP* is important for interaction with either the XRCC1 or XRCC4 scaffold proteins, which are required for assembling single-strand break repair (SSBR) or dominant pathway for DNA double-strand break repair (DSBR) (NHEJ, non-homologous end-joining) components respectively (13–15). In fact, *PNK*P is important for both the SSBR/Base excision repair (BER) and NHEJ pathways (12).

To date, only a few patients with mutations in *PNKP* have been reported worldwide. Substantial variation exists among affected individuals with *PNKP* mutations, as individuals diagnosed with MCSZ show no neurodegeneration, while individuals with AOA4 show pronounced neurodegeneration.

Among AO4 patients, the different phenotypes associated with mutations in *PNK*P do not seem to relate to either the type or the location of the mutation (3). So far, all *PNKP* mutations related to AOA4 have been described in the kinase domain.

In this report, we describe a patient affected by AOA4 related to a homozygous mutation in *PNKP*, with very late onset at 50 years. Despite the occurrence of AOA4 phenotype, this variant falls within the FHA domain, which was never reported before in AOA4 patients.

MATERIALS AND METHODS

Genetic Testing

The pedigree of the proband's family is shown in **Figure 1A**. After genetic counseling, written informed consent was obtained, and clinical exome sequencing (4,800 human genes) was performed including 100 genes related to Ataxia and or Spastic Paraplegia (Clinical Exome Solution, SOPHiA genetics) on MiSeq platform (Illumina) (16).

SOPHiA DDM (SOPHiA genetics) was used for annotation and characterization of variants. Sequence analysis identified the homozygous mutation NM_007254.3:c.[148C>G]; NP_009185.2: p. (Gln50Glu) (rs756746191:C>G).

In the FHA domain *PNKP* (OMIM #605610), resulting in the replacement of glutamine with glutamic acid in the protein at position 50. The variant was confirmed by Sanger sequencing (ABI 3130xl Genetic Analyzer, Applied Biosystem) (**Figure 1B**). No mutations in other ataxia-related genes were identified. The variant has been submitted to Clinical Variant (ClinVar Accession Number SUB6349616).

The frequency of the variant is not known either in the ExAC database (http://evs.gs.washington.edu/EVS) or in the 1,000 Genomes database (http://browser.1000genomes.org). The prediction analysis *in silico* reveals a damaging effect in three out of four tools used [Mutation taster (http://www.mutationtaster.org), SIFT (http://sift.jcvi.org), and Polyphen-2 (http://genetics.bwh.harvard.edu/pph2)]. The PROVEAN (http://provean.jcvi.org/index.php) tool alone predicts it as neutral. The analysis using the PhyloP (http://compgen.bscb.cornell.edu/phast/) and GERP (http://mendel.stanford.edu/sidowlab/downloads/gerp/index.html) tools gave respectively a positive score (1) and an neutral rate (NR) equal to 5.4 indicating that both the wild type nucleotide and the amino acid are conserved in mammals.

The presence of p.Gln50Glu was evaluated in II:2 (54 years old brother) and II:3 (49 years old sister), who are asymptomatic heterozygous carriers (**Figure 1A**).

According to ACMG guidelines, which consider data on familial segregation, bioinformatic analysis, and allele frequencies, p. (Gln50Glu) has been classified as a likely pathogenic variant.

RESULTS

A 56-year-old Italian male (II:1) was referred to the Neurology Unit of the Scientific Institute for Research and Healthcare Neuromed in Pozzilli (IS) Italy, with a 6 years history of distal weakness and tactile hypoesthesia of the legs and arms, cramps, urinary urgency, dysarthria, and mild dysphagia. He was born at term by unrelated parents that died late in life. His comorbidity

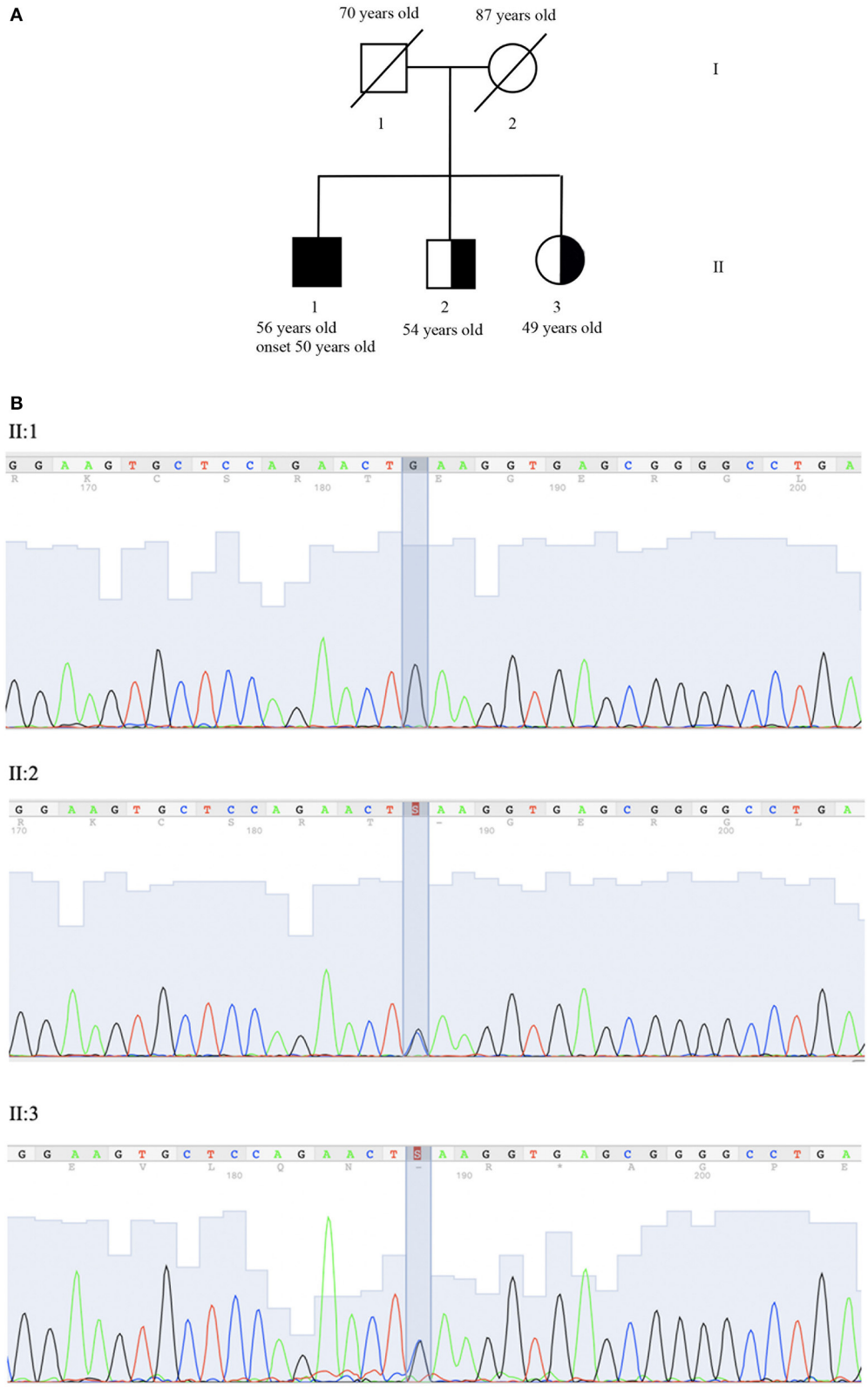

FIGURE 1 | Genetic evaluation. **(A)** Pedigree: II:1 corresponds to proband, II:2 and II:3 to the asymptomatic carrier brother and sister. **(B)** Co-segregation analysis of NM_007254.3:c.[148C>G]; NP_009185.2: p. (Gln50Glu) (rs756746191:C>G) (Clin Var Accession Number SUB6349616) in exon 2 of gene *PNKP* (OMIM #605610). Sequence analysis is shown for proband (II:1) who is homozygous for variant and brother (II:2) and his sister (II:3) who is heterozygous carrier of the same variant.

consists of allergic bronchial asthma which was routinely treated with beta$_2$-agonists and corticosteroids (**Figure 1A**).

On neurological examination, he had cerebellar dysarthria, gait ataxia (the patient was able to walk without support but with moderate gait instability), mild bilateral dysmetria, oculomotor apraxia, distal weakness of the arms and legs, distal hypoesthesia, absent tendon reflexes. The International Cooperative Ataxia Rating Scale (ICARS) total score was 40/100. Electroneuromyography (ENMG) indicated the presence of a sensory-motor axonal polyneuropathy. Motor evoked potentials (MEPs) were characterized by increased central motor conduction time. Somatosensory evoked potentials (SEP) were not measurable due to a lack of reproducibility of peripheral responses. Brain Magnetic Resonance Imaging (MRI) at the age of 55 showed marked subtentorial atrophy without spinal cord alteration. In detail, Axial T1-weighted showed

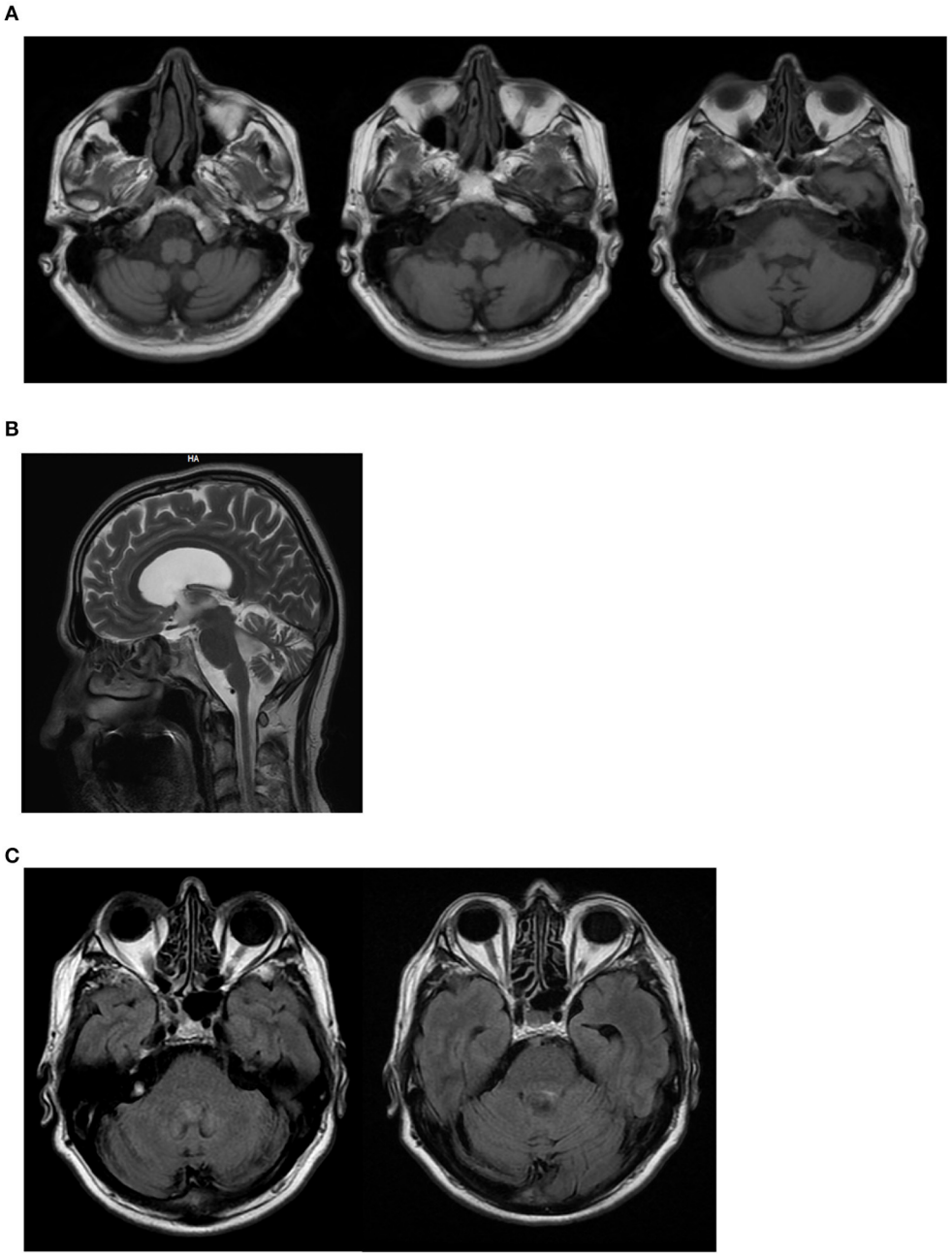

FIGURE 2 | II:1 Brain MRI. **(A)** Axial T1-weighted shows cerebellar and brainstem atrophy; **(B)** Sagittal MRI scan shows global cerebellar atrophy; **(C)** Axial FLAIR MRI sequences shows no dentate nucleus hyperintensity.

cerebellar and brainstem atrophy, Sagittal MRI scan showed global cerebellar atrophy, and Axial FLAIR MRI sequences showed no dentate nucleus hyperintensity (**Figure 2**). The neuropsychological assessment showed impairment of short-term memory, attention and constructive apraxia. Nothing relevant was found on body Computer Tomography (CT) scan. There were no alterations in the liquor analyzed after lumbar puncture. A second neurological examination performed after 6 months showed no significant deterioration, suggesting a slow progression of the disease.

Blood tests showed mild hyper-CKemia (624 UI/l), hypercholesterolemia (263 mg/dl), hight alfa-fetoprotein (10.85 ng/ml), and low albumin level (3.4 g/dl). BMI index was 24.22. LDL increased level (173 mg/dl, nv < 130) confirmed data by Scheiss et al. (4), who reported increased LDL and IgE levels in AOA4 patients. The immunoglobulin dosage was not performed. High-density lipoprotein (HDL), triglycerides, thyroid hormones, vitamins, autoimmune screen, anti-ganglioside, and anti-neuronal antibodies were normal.

DISCUSSION

A variety of human neurologic diseases are caused by inherited defects in DNA repair, underscoring the critical requirement for genome stability in this tissue (17). An example is provided by the defective enzymatic activity of the genes responsible for ataxia with AOA, a subgroup involving cerebellar ataxia, axonal neuropathy, oculomotor apraxia, and extrapyramidal features. Genes responsible for this condition provide instructions for making proteins that are involved in repairing damaged DNA. DNA damage that is not repaired makes the cell unstable and can lead to cell death, producing a severe effect in the cerebellum, as witnessed by the occurrence of ataxia with oculomotor apraxia (18).

Recently described in a Portuguese family (19), AOA4 is a complex, progressive movement disorder characterized by phenotypic heterogeneity like other AOAs. In most patients, the first symptom is dystonia, which spontaneously attenuates during the course of the disease. Other features include cerebellar ataxia, oculomotor apraxia, and polyneuropathy. Cognitive impairment is rare, while a few patients at later stages of the disease present abnormal values of alfa-fetoprotein, albumin, and cholesterol.

In this report, we describe the later onset of AOA4 in a patient that did not experience dystonia but a classic cerebellar syndrome with gait ataxia, mild dysmetria, oculomotor apraxia, and cerebellar dysarthria and dysphagia. Sensorial-motor axonal polyneuropathy was also present. Cerebellar ataxia was compatible with cerebellar atrophy detected at brain MRI (20) (**Figure 2**). Dysphagia could be explained by the involvement of the nucleus ambiguous in the brainstem atrophy detected at MRI. However, considering the concomitance of cerebellar dysarthria, the presence of dysphagia is likely to be due to the cerebellar involvement. Similarly, brainstem atrophy could be further investigated concerning the potential involvement of pre-cerebellar nuclei. Mild hyper-CKemia, although non-specific, is likely to be due to the motor component of polyneuropathy.

The AO4 patient here described is unique considering his age of onset at 50. In fact, age of onset of AO4 patients ranges from 1 to 9 years (with a mean of 4.3). So far, only a German woman was described with a delayed onset although she was much younger (23-year-old), compared with the present case report. Additionally, this 23 year old diagnosed patient possessed an AOA phenotype which was combined with a cerebellar pilocytic astrocytoma (21).

The present paper reports a patient who is a carrier of the homozygous mutation NM_007254.3:c.[148C>G]; NP_009185.2: p. (Gln50Glu) (rs756746191:C>G) in the FHA domain PNKP. To date, multiple distinct human syndromes have been linked to mutations in *PNKP*, leading to microcephaly or neurodegeneration (17). *PNKP* is a multifunctional DNA repair enzyme important for both the SSBR/BER and NHEJ pathways (12), and this dual functionality potentially explains the presence of both microcephaly and neurodegeneration in patients with certain inherited *PNKP* mutations (22).

In support of this, it's well-known that different domains of the protein are linked to different diseases. The kinase domain of *PNKP* is associated with neurodegeneration associated with AOA4, as witnessed by the variants p.G375W, p.T408del, p.R439fs, p.T442fs, p.Thr424fs*49, and p.Tyr515* (21). Mutations responsible for MCSZ are mainly located in the phosphatase domain (p.L176F and p.E326) but spread along the whole gene. In detail, an MCSZ patient carries the compound heterozygote genotype p.G292R/p.A55S, falling respectively in the phosphatase and FHA domains; while another MCSZ patient is homozygous for p.T424GfsX48 in the kinase domain (a variant which was also reported in a compound heterozygous AOA4 patient) (2, 23).

Remarkably, so far variants in the FHA domain have never been associated with AOA4 and even with neurodegeneration or microcephaly, as they have been solely reported in individuals who manifest only seizures (p.P20S, p.A55S) (11).

The genetic analysis performed in this paper has limitations. In fact, although the sequencing analysis has been carried out on 4,800 human genes including 100 genes related to Ataxia and Spastic paraplegia, these can't rule out the involvement of other genes related to clinical phenotype. Probably, a more extensive approach like whole exome or whole genome sequencing would guarantee more informative data. Moreover, segregation analysis is not fully informative. In fact, the age of the brother and the sister of the proband, both asymptomatic heterozygous carriers, can't rule out the appearance of clinical symptoms in the next years.

The present paper describes the first variant in the FHA domain leading to neurodegeneration and appearing with an AOA4 phenotype. Further studies are required to establish the role of mutations in different PNKP domains with a special emphasis of site-specificity within the FHA domain, and to identify and understand the role of modifier genes (24). This is required to explain the molecular mechanisms leading to the onset of AOA4 phenotype and to understand whether a late disease onset is a typical feature of AOA4 when this is produced by FHA domain specific mutations.

AUTHOR CONTRIBUTIONS

SG and RF interpretation of data and drafting of manuscript. FF and DC acquisition of data, analysis and interpretation of data, and critical revision. RC, RF, FBi, and MC acquisition of data, analysis and interpretation of data. FBu and CF neurological history and interpretation of clinical data. MM, EG, and AR analysis and interpretation of data and critical revision. SG study conception and design, analysis and interpretation of data, and drafting of manuscript.

FUNDING

This work was supported by the Italian Ministry of Health (Current Research 2019-2023: Identification of New Variants and/or New Genes Responsible for Ataxia and Spastic Paraplegia).

ACKNOWLEDGMENTS

We thank the patients and their family for participating in the study.

REFERENCES

1. Shen J, Gilmore EC, Marshall CA, Haddadin M, Reynolds JJ, Eyaid W, et al. Mutations in *PNKP* cause microcephaly, seizures and defects in DNA repair. *Nat Genet*. (2010) 42:245–9. doi: 10.1038/ng.526
2. Poulton C, Oegema R, Heijsman D, Hoogeboom J, Schot R, Stroink H, et al. Progressive cerebellar atrophy and polyneuropathy: expanding the spectrum of *PNKP* mutations. *Neurogenetics*. (2013) 14:43–51. doi: 10.1007/s10048-012-0351-8
3. Bras J, Alonso I, Barbot C, Costa MM, Darwent L, Orme T, et al. Mutations in *PNKP* cause recessive ataxia with oculomotor apraxia type 4. *Am J Hum Genet*. (2015) 96:474–9. doi: 10.1016/j.ajhg.2015.01.005
4. Schiess N, Zee DS, Siddiqui KA, Szolics M, El-Hattab AW. Novel PNKP mutation in siblings with ataxia-oculomotor apraxia type 4. *J. Neurogenet*. (2017) 31:23–5. doi: 10.1080/01677063.2017.1322079
5. Barbot C, Coutinho P, Chorão R, Ferreira C, Barros J, Fineza I, et al. Recessive ataxia with ocular apraxia: review of 22 Portuguese patients. *Arch Neurol*. (2001) 58:201–5. doi: 10.1001/archneur.58.2.201
6. Moreira MC, Barbot C, Tachi N, Kozuka N, Mendonça P, Barros J, et al. Homozygosity mapping of Portuguese and Japanese forms of ataxia-oculomotor apraxia to 9p13, and evidence for genetic heterogeneity. *Am J Hum Genet*. (2001) 68:501–8. doi: 10.1086/318191
7. Moreira MC, Barbot C, Tachi N, Kozuka N, Uchida E, Gibson T, et al. The gene mutated in ataxia-ocular apraxia 1 encodes the new HIT/Zn-finger protein aprataxin. *Nat Genet*. (2001) 29:189–93. doi: 10.1038/ng1001-189
8. Le Ber I, Bouslam N, Rivaud-Péchoux S, Guimarães J, Benomar A, Chamayou C, et al. Frequency and phenotypic spectrum of ataxia with oculomotor apraxia 2: a clinical and genetic study in 18 patients. *Brain*. (2004) 127:759–67. doi: 10.1093/brain/awh080
9. Moreira MC, Klur S, Watanabe M, Németh AH, Le Ber I, Moniz JC, et al. Senataxin, the ortholog of a yeast RNA helicase, is mutant in ataxia-ocular apraxia 2. *Nat Genet*. (2004) 36:225–7. doi: 10.1038/ng1303
10. Anheim M, Tranchant C, Koenig M. The autosomal recessive cerebellar ataxias. *N Engl J Med*. (2012) 366:636–46. doi: 10.1056/NEJMra1006610
11. Paucar M, Malmgren H, Taylor M, Reynolds JJ, Svenningsson P, Press R, et al. Expanding the ataxia with oculomotor apraxia type 4 phenotype. *Neurol. Genet*. (2016) 2:e49. doi: 10.1212/NXG.0000000000000049
12. Weinfeld M, Mani RS, Abdou I, Aceytuno RD, Glover JN. Tidying up loose ends: the role of polynucleotide kinase/phosphatase in DNA strand break repair. *Trends Biochem Sci*. (2011) 36:262–71. doi: 10.1016/j.tibs.2011.01.006
13. Ali AA, Jukes RM, Pearl LH, Oliver AW. Specific recognition of a multiply phosphorylated motif in the DNA repair scaffold XRCC1 by the FHA domain of human PNK. *Nucleic Acids Res*. (2009) 37:1701–12. doi: 10.1093/nar/gkn1086
14. Bernstein NK, Williams RS, Rakovszky ML, Cui D, Green R, Karimi-Busheri F, et al. The molecular architecture of the mammalian DNA repair enzyme, polynucleotide kinase. *Mol Cell*. (2005) 17:657–70. doi: 10.1016/j.molcel.2005.02.012
15. Loizou JI, El-Khamisy SF, Zlatanou A, Moore DJ, Chan DW, Qin J, et al. The protein kinase CK2 facilitates repair of chromosomal DNA single-strand breaks. *Cell*. (2004) 117:17–28. doi: 10.1016/S0092-8674(04)00206-5
16. Richards S,Aziz N, Bale S, Bick D, Das S, Gastier-Foster J, et al. ACMG Laboratory Quality Assurance Committee. Standards and guidelines for the interpretation of sequence variants: a joint consensus recommendation of the American College of Medical Genetics and Genomics and the Association for Molecular Pathology. *Genet Med*. (2015) 17:405–24. doi: 10.1038/gim.2015.30
17. Dumitrache LC, McKinnon PJ. Polynucleotide kinase-phosphatase (PNKP) mutations and neurologic disease. *Mech Ageing Dev*. (2017) (Pt A):121–9. doi: 10.1016/j.mad.2016.04.009
18. Gueven N, Becherel OJ, Howe O, Chen P, Haince JF, Ouellet ME, et al. A novel form of ataxia oculomotor apraxia characterized by oxidative stress and apoptosis resistance. *Cell Death Differ*. (2007) 14:1149–61. doi: 10.1038/sj.cdd.4402116
19. Rudenskaya GE, Marakhonov AV, Shchagina OA, Lozier ER, Dadali EL, Akimova IA, et al. Ataxia with oculomotor apraxia type 4 with PNKP common "Portuguese" and novel mutations in two Belarusian families. *J Pediatr Genet*. (2019) 8:58–62. doi: 10.1055//s-0039-1684008
20. Ronsin S, Hannoun S, Thobois S, Petiot P, Vighetto A, Cotton F, et al. A new MRI marker of ataxia with oculomotor apraxia. *Eur J Radiol*. (2019) 110:187–92. doi: 10.1016/j.ejrad.2018.11.035
21. Scholz C, Golas MM, Weber RG, Hartmann C, Lehmann U, Sahm F, et al. Rare compound heterozygous variants in PNKP identified by whole exome sequencing in a German patient with ataxia-oculomotor apraxia 4 and pilocytic astrocytoma. *Clin Genet*. (2018) 94:185–6. doi: 10.1111/cge.13216.
22. Hoch NC, Hanzlikova H, Rulten SL, Tétreault M, Komulainen E, Ju L, et al. XRCC1 mutation is associated with PARP1 hyperactivation and cerebellar ataxia. *Nature*. (2017) 541:87–91. doi: 10.1038/nature20790
23. Nakashima M, Takano K, Osaka H, Aida N, Tsurusaki Y, Miyake N, et al. Causative novel PNKP mutations and concomitant PCDH15 mutations in a patient with microcephaly with early-onset seizures and developmental delay syndrome and hearing loss. *J Hum Genet*. (2014) 59:471–4. doi: 10.1038/jhg.2014.51

24. Leuzzi V, D'Agnano D, Menotta M, Caputi C, Chessa L, Magnani M. Ataxia-telangiectasia: a new remitting form with a peculiar transcriptome signature. *Neurol. Genet*. (2018) 4:e228. doi: 10.1212/NXG.0000000000000228

Conflict of Interest: The authors declare that the research was conducted in the absence of any commercial or financial relationships that could be construed as a potential conflict of interest.

frontiers in Pediatrics

CASE REPORT
published: 24 January 2020
doi: 10.3389/fped.2019.00543

Outcomes of Bone Marrow Mononuclear Cell Transplantation for Neurological Sequelae Due to Intracranial Hemorrhage Incidence in the Neonatal Period: Report of Four Cases

Nguyen Thanh Liem[1], Truong Linh Huyen[1], Le Thu Huong[2], Ngo Van Doan[2], Bui Viet Anh[1], Nguyen Thi Phuong Anh[2] and Dang Thanh Tung[2]*

[1] Cellular Manufacturing Department, Vinmec Research Institute of Stem Cell and Gene Technology, Hanoi, Vietnam, [2] Vinmec Times City General Hospital, Hanoi, Vietnam

OPEN ACCESS

Edited by:
Matthew James Farrer, University of Florida, United States

Reviewed by:
Wang-Tso Lee, National Taiwan University Hospital, Taiwan
Juan Dario Ortigoza-Escobar, Pediatric Research Hospital Sant Joan de Déu, Spain

***Correspondence:**
Nguyen Thanh Liem
v.liemnt@vinmec.com

Specialty section:
This article was submitted to Pediatric Neurology, a section of the journal Frontiers in Pediatrics

Received: *13 June 2019*
Accepted: *12 December 2019*
Published: *24 January 2020*

Citation:
Liem NT, Huyen TL, Huong LT, Doan NV, Anh BV, Anh NTP and Tung DT (2020) Outcomes of Bone Marrow Mononuclear Cell Transplantation for Neurological Sequelae Due to Intracranial Hemorrhage Incidence in the Neonatal Period: Report of Four Cases. Front. Pediatr. 7:543. doi: 10.3389/fped.2019.00543

Aim: The aim of this study was to present primary outcomes of autologous bone marrow mononuclear cell (BMMNC) transplantation to improve neurological sequelae in four children with intracranial hemorrhage (ICH) incidence during the neonatal period.

Methods: GMFM88 and modified Ashworth score were used to assess motor function and muscle spasticity before BMMNC transplantation and after transplantation. Brain MRI was performed to evaluate brain morphology before and after BMMNC transplantation. Bone marrow were harvested from anterior iliac crest puncture and BMMNCs were isolated using Ficoll gradient centrifugation. The microbiological testing, cell counting, and hematopoietic stem cell (hHSC CD34+ cell) analysis were performed, following which BMMNCs were infused intrathecally.

Results: Improvement in motor function was observed in all patients after transplantation. In addition, muscle spasticity was reduced in all four patients.

Conclusion: Autologous BMMNC transplantation may improve motor function and reduce muscle spasticity in children with ICH incidence during the neonatal period.

Keywords: intracranial hemorrhage, neurological sequelae, bone marrow mononuclear cells, autologous, neonate

INTRODUCTION

Intracranial hemorrhage (ICH), including extra-ventricular hemorrhage and intra-ventricular hemorrhage, is a severe condition in neonates, especially in preterm babies with high morbidity and mortality. It severely affects the central nervous system because the neonatal period is a critical window for brain development (1, 2).

Intra-ventricular hemorrhage is the common type of ICH in premature newborns. The incidence of intra-ventricular hemorrhage among infants born between 24 and 31 complete weeks in China in 2013–2014 was 15.4% (3), whereas the rate of severe intra-ventricular hemorrhage among infants born between 22 and 31 weeks of gestation at hospitals in California, United States, between 2005 and 2015 was 7.7% (4). Different mechanisms are cited to explain the etiology

of intra-ventricular hemorrhage in premature babies, including fragility of the germinal matrix vasculature, disturbance in the cerebral blood flow, and coagulation disorders. Many factors such as a low gestational age and birth weight, intrauterine infection, vaginal delivery, low Apgar score, severe respiratory distress syndrome, pneumothorax, hypoxia, hypercapnia, seizures, patent ductus arteriosus, and thrombocytopenia are thought to be risk factors associated with intra-ventricular hemorrhage (5–7).

ICH occurred not only in preterm infants but also in full-term babies related to brain trauma, vascular malformation, vitamin K deficiency, and many other conditions (1, 8–13).

ICH in neonates results in severe neurodevelopmental adverse effects. Bolisetty et al. showed that infants born at 23 to 28 weeks' gestation with grade III–IV intra-ventricular hemorrhage had high rates of developmental delay (17.5%), cerebral palsy (30%), deafness (8.6%), and blindness (2.2%) (2). According to Pierrat et al., the overall rate of cerebral palsy in infants born at 24–26, 27–31, and 32–34 weeks of gestation was 6.9, 4.3, and 1%, respectively (14).

Traditional treatments of neurological sequelae after ICH in newborns have limited effect. Recently, stem cell transplantation is being applied in the management of neurological impairment in children, resulting in promising outcomes (15–21). In 2018, Ahn et al. published the first report using stem cell transplantation for severe intra-ventricular hemorrhage to reduce neurological complications (22). However, to our knowledge there have been no publications using stem cell transplantation in the management of neurological sequelae after ICH incidence in the neonatal period.

The aim of this report is to present outcomes of bone marrow mononuclear cell (BMMNC) transplantation in four children with neurological sequelae due to ICH incidence during the neonatal period.

PATIENTS AND METHODS

Patient's Enrollment

The study was approved by the Hospital ethical committee and performed at Vinmec International Hospital in Hanoi, Vietnam. The parents were carefully educated about anticipated benefits and potential side effects of the procedures and provided written informed consent according to the Good Clinical Practice and the Helsinki Declaration. The general data collected before the transplantation consisted of age, gender, past medical history, clinical findings on admission, and brain MRI manifestations.

Prior to the treatment, the patients were thoroughly examined by an experienced physiotherapist using Gross Motor Function Classification System (GMFCS), Gross Motor Function Measure-88 (GMFM-88) scores, and modified Ashworth scale, and by an experienced psychologist using Denver II scale (23–25).

Four children with neurological sequelae due to ICH incidence in the neonatal period were enrolled in this study. Written informed consent was obtained from the minor(s)' legal guardian/next of kin for the publication of any potentially identifiable images or data included in this article.

BMMNC Procedure

Bone Marrow Aspiration

Bone marrow was harvested through anterior iliac crest puncture under general anesthesia in the operating theater. The volume collected depended on the patients' body weight as follows: 8 ml/kg for patients under 10 kg [80 ml + (body weight in kg – 10) × 7 ml] for patients above 10 kg (18).

BMMNC Isolation, Characterization, and Preparation for Transplantation

BMMNCs were isolated by gradient centrifugation using Ficoll-Paque (GE Healthcare, Sweden) in a clean room following ISO 14644 standard at Vinmec Research Institute of Stem Cell and Gene Technology. The cell suspension was washed with phosphate-buffered saline (PBS) solution and re-suspended in autologous plasma up to a total of 10 ml for injection. The sterility of the product was confirmed by microbiological evaluation by BacT/Alert® 3D microbial detection System (Biomerieux, USA). The total blood components before and after the Ficoll-Paque separation was evaluated by Beckman Coulter LH780 hematocytometer. The hematopoietic stem cell content (hHSC CD34+) was assessed according to the International Society of Hematotherapy and Graft Engineering guideline (ISHAGE guideline) using Stem-Kit™ Reagent, Beckman Coulter in Navios flow cytometer. Before injection, cell products were examined for endotoxin levels by using the Endosafe-PTS kit (Charles River).

BMMNC Infusion

BMMNCs were infused intrathecally between the 4th and 5th lumbar vertebrae over the course of 30 min using an electrical pump, through an 18-gauge spinal needle.

Follow-Up Assessment

The GMFM-88 was applied to evaluate improvement of motor function, modified Ashworth scale was used to assess muscle spasticity, and child development was measured by Denver II testing (24–26).

Case Presentation

Case 1

A 2,900-g boy was born at 40 weeks' gestation by C-section on 29th October 2014 due to prolonged labor. Asphyxia occurred right after birth, and ICH was detected at 1 day postpartum. Respirator support with a ventilator plus medical treatment was required for 3 weeks. Motor skill milestones were delayed and cerebral palsy was diagnosed at 5 months of age. Since then, the patient underwent 2 h of physiotherapy per day.

Examination on 10th December, 2015 when he was 14 months old, confirmed cerebral palsy at severe level (GMFCS level V) with mental retardation, tetraplegia, poor motor function skills, muscle spasticity, retracted Achilles tendons, and dysphagia. He could sit down with arm propping but could not crawl or stand (**Figure 1**—*A permission from his mother was obtained to let his image be published*). His vision was impaired, in which he could only distinguish between dark and light at very short distance. Brain MRI showed diffuse cortical and sub-cortical lesions on both sides (temporal lobe, parietal lobe, occipital lobe, and one

FIGURE 1 | The improvement of motor functions and muscle tone in Case 1 before and after stem cell transplantation.

TABLE 1 | Details in BMNMCs transplantations.

Patient	Transplantation	Date	Age (months)	Total MNCs	Total hHSC (CD34+)
1	1st	11/12/2015	14	147×10^6	18.55×10^6
	2nd	11/03/2016	17	105×10^6	13.25×10^6
	3rd	26/10/2016	24	553×10^6	67.40×10^6
	4th	18/01/2018	39	630×10^6	57.75×10^6
2	1st	02/08/2016	47	588×10^6	48.05×10^6
	2nd	14/02/2017	53	866×10^6	40.30×10^6
	3rd	28/08/2017	59	672×10^6	35.49×10^6
3	1st	06/12/2017	15	300×10^6	37.20×10^6
4	1st	19/05/2017	68	590×10^6	40.55×10^6
	2nd	27/11/2017	74	490×10^6	19.95×10^6

BMMNCs, Bone marrow mononuclear cells; MNCs, Mononuclear cells; hHSC, human Hematopoietic Stem Cell.

part of frontal lobe) with diffuse brain atrophy, dilation of third ventricle, and bilateral ventricles.

The patient underwent four BMMNC transplantations at the age of 14, 17, 24, and 39 months with cellular information as presented in **Table 1**. No adverse effects were observed. After discharge, physiotherapy was given 2 h per day for 12 days at the rehabilitation department and then continued at home.

Progress After Transplantations

Improvements of motor functions and muscle tonus were observed after transplantations (**Table 2**). The patient was observed to be capable of sitting and crawling at 3 months after the first transplantation, standing by holding furniture at 10 months after the first transplantation, and walking with support by holding parents' hand since 25 months after first transplantation (**Figure 1**). Muscle spasticity was reduced from 2 to 1 on the modified Ashworth scale. Dysphagia disappeared since 10 months after the first transplantation.

His vision was well improved from recognizing the light from mobile phone or other tools at 10 months after transplantation to identifying and finding objects of his desire at 25 months after first transplantation.

Brain MRI taken on 15th January 2018, when he was 39 months old, showed that dilatation of ventricles was reduced in comparison with pre-transplantation brain MRI.

Case 2

A boy was born on 10th September 2012 at 32 weeks' gestation by emergency C-section due to Oligohydramnios and Chorioamnionitis with a birth weight of 1,800 g. He suffered from perinatal asphyxia and ICH was diagnosed at 1 day after birth. He required respiration support with ventilator for 10 days and then oxy mask for 2 weeks. Ventriculoperitoneal shunt was inserted at 2 months of age due to hydrocephalus. His motor skills were delayed and cerebral palsy were confirmed at 9 months of age. Since then, he underwent 3 h of physiotherapy per day.

Examination on 1st August 2016, at 47 months old, showed cerebral palsy at severe level (GMFCS level V) with mental retardation, tetraplegia, poor gross motor function skills and poor fine motor skill, poor head control, muscle spasticity, stiffness bent arms, wrist deformities, retracted Achilles tendons, and dysphagia. He could roll, but could not sit up.

Seizures occurred 1–2 times per week requiring antiepilepsy medicament (Depakine) with a dose of 200 mg two times per day.

Brain MRI demonstrated diffuse cortical and sub-cortical lesions on the left sides (temporal lobe, parietal lobe, occipital lobe and frontal lobe) with diffuse brain atrophy dilated bilateral ventricles (**Figure 2**).

The patient underwent three BMMNC transplantations at the age of 47, 53, and 59 months without any adverse effects. The details of each cell transplantation are shown in **Table 1**. After discharge, physiotherapy was given 2 h per day at the rehabilitation department for 12 days and then continued at home.

TABLE 2 | Improvement of motor function, muscle spasticity, and Denver II after transplantation.

	Patient 1		Patient 2		Patient 3		Patient 4	
	Before	**After**	**Before**	**After**	**Before**	**After**	**Before**	**After**
Modified Ashworth	2	1	4	2	2	1	4	2
GMFCS	5	2	5	3	2	1	4	3
GMFM-88								
Lying, rolling	28	51	24	51	49	51	40	47
Sitting	18	60	7	49	53	60	42	58
Crawling and Kneeling	0	39	0	8	33	42	10	37
Standing	0	12	0	10 (12 with KAFO)	2	39	6	12
Walking, running and jumping	0	18	0	8 (23 with KAFO)	0	60	6	12
Denver II (months)								
Personal—social	3	12	7	8	11	22	24	30
Fine motor—adaptive	3.5	9	–	–	–	–	–	–
Right hand	–	–	3	4	5	12	6	6
Left hand	–	–	6	7	11	23	30	42
Reception language	5	15	8	12	14	23	50	52
Expressive language	3	9	5	6	14	23	50	52
Gross motor	5	12	7	10	10	24	12	13

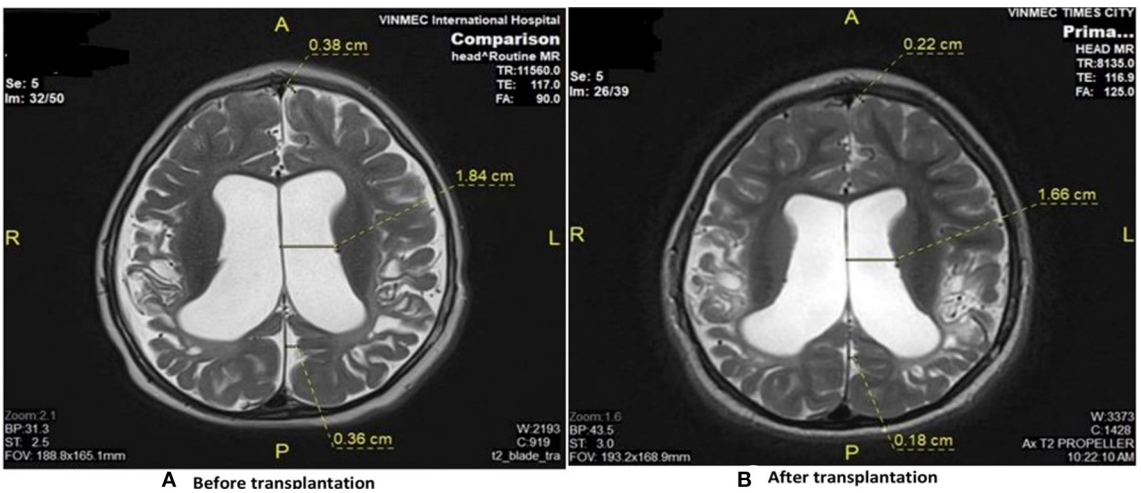

FIGURE 2 | Brain MRI results revealed the improvement before and after stem cell transplantation. **(A)** Diffuse cortical and subcortical lesions with diffuse brain atrophy and dilated ventricles before transplantation. **(B)** Diffuse brain atrophy, and dilation of ventricles reduced after transplantation.

Progress After Transplantations

Improvement of the gross motor function and fine motor skills were observed at 6 months after the first transplantation. He could sit up with support on the wall or stand with holding furniture.

These motor functions continuously improved significantly, as he could stand without support, walk with support by parents holding hands or wheels pulpit frame at 22 months after the first transplantation. The improvement in motor function measured by GMFM-88 before and after three transplantations is shown in **Table 2**.

Muscle spasticity was reduced. At 22 months after the first transplantation, the modified Ashworth score reduced from level 4 to 2 (**Table 2**). Stiffness bent arms, wrist deformities, and retracted Achilles tendons were improved.

Dysphagia subsided at 6 months after the first transplantation and disappeared thereafter so he could eat solid food.

Depakine was reduced from 200 mg per day to 150 mg per day since 12 months after the first transplantation and then was stopped since 22 months without seizure.

Brain MRI taken on 11th June 2018 when he was 69 months old showed diffuse brain atrophy of supratentorial region and slightly decreased dilated third ventricle and bilateral ventricle and subarachnoid space compared to MRI study date 2nd June 2016 (**Figure 2**).

Case 3

A 3,300-g boy was born on 27th September 2016, at 42 weeks' gestation by emergency C-section because of prolonged labor. At 33 days old, he suddenly suffered from cyanosis and then coma. ICH was diagnosed and an operation was performed to remove a hematoma. Since 6 months old, hydrotherapy was applied 3 days per week, 30 min per day.

Examination on 4th December 2017 (15 months old) showed cerebral palsy at level II of GMFCS with right side hemiplegia, poor fine motor function at right hand, muscle spasticity, right stiffness bent arm, hand and wrist deformities, and jumping knee gait. He could stand with holding furniture but could not step.

Brain MRI revealed diffuse cortical and sub-cortical lesions on the left sides (temporal lobe, parietal lobe, occipital lobe, and frontal lobe). Periventricular leukomalacia adjacent to the right lateral ventricular, dilatation of the left lateral ventricular, diffuse corpus callosum atrophy.

The patient underwent a BMMNC transplantation at the age of 15 months with the cell dose of 300×10^6 MNCs and 37.2×10^6 hHSCs (CD34+). No adverse effects were observed. He continued to receive the same regimen of physiotherapy.

Progress After Transplantation

Significant improvement of motor functions and muscle spasticity were observed at 7 months after the first transplantation. The patient could walk, jump, and climb stairs without support. Right stiffness bent arm was improved; no more hand and wrist deformities or jumping knee gait. The improvement in motor function and Denver II score was presented in **Table 2**. There were no significant changes on brain MRI taken on 26th July 2018 compared to brain MRI before the transplantation.

Case 4

A boy was born on 16th September 2011, at 40 weeks' gestation by emergency C-section due to placenta previa with a birth weight of 2,900 g. At 28 days after birth, he suffered from severe vomiting, cyanosis, and then coma, requiring respiration support with ventilator. ICH was diagnosed and managed medically without operation for 20 days.

Examination on 18th May 2017 (68 months old) confirmed cerebral palsy at level IV of GMFCS with mental retardation, tetraplegia, poor fine motor function, muscle spasticity, stiff knee gait, jumping knee gait, retracted Achilles tendons, stiffness bent arms, and hand and wrist deformities. He could sit without support but could not crawl, and could not stand either.

Brain MRI revealed diffuse cortical and sub-cortical lesions on the left sides (temporal lobe, parietal lobe, occipital lobe, and frontal lobe) and the right frontal lobe, dilated left lateral ventricular, and diffuse corpus callosum atrophy.

The patient underwent two BMMNC transplantations at the age of 68 and 74 months, respectively, without any adverse effects, and received the same physiotherapy regimen. The details for each cell transplantation are presented in **Table 1**.

Motor function in four patients with intracranial hemorrhage in the neonatal period before and after bone marrow mononuclear cell transplantation was displayed in **Supplementary Videos 1–4**, respectively.

Progress After Transplantations

His gross motor function improved, enabling him to take steps by holding onto furniture and walking with support by parents holding hand at 6 months after first transplantation. At 14 months after the first transplantation, he could stand without support, and walked with hand holding. Retracted Achilles tendons, stiffness bent arms, stiffness knee gait, and jumping knee gait were improved at 14 months after the first transplantation. The muscle spasticity was reduced from 4 to 2 on the modified Ashworth scale. The improvement in motor function and Denver II score is shown in **Table 2**.

Brain MRI taken 14 months after the first transplantation when he was 82 months old did not show any significant changes compared to pre-transplantation brain MRI.

DISCUSSION

ICH causes immediate and delayed injury to the brain. Mass effect of hematoma, increased intracranial pressure, decreased cerebral perfusion pressure, released inflammatory cytokines, and free radicals result in ischemia and hypoxia of the brain parenchyma, white matter injury, and periventricular leukomalacia (27). These effects cause many severe neurological sequelae such as cerebral palsy, seizures, cognitive deficits, hydrocephalus, and death (2, 14).

Physical therapy is a standard treatment. However, Harries et al. showed that only 22% of children with severe cerebral palsy could improve after physical therapy (28). The contribution of physical therapy is to reduce the adverse effects of disuse, inexperience, and secondary complications (29).

To improve neurological sequelae after intra-ventricular hemorrhage, many research efforts using stem cells have been carried out in animals (30–32). Ahn et al. performed intra-ventricular transplantation of umbilical cord blood-derived mesenchymal stem cells (MSCs) for induced intra-ventricular hemorrhage in Newborn Sprague–Dawley rats. They noticed that stem cells can significantly attenuate the post hemorrhagic hydrocephalus and brain injury after intra-ventricular hemorrhage (30). Wang et al. carried out an experimental study to assess the effectiveness of bone marrow MSC transplantation for rats with induced intracranial hematoma. The results suggested that intravenous BM-MSC infusion exerts therapeutic effects on ICH in spontaneously hypertensive rats (32).

In rodents with experimental ICH, Suda et al. also found that autologous BMMNC transplantation can improve long-term structural and functional outcomes (31).

Bone marrow contains a population of pluripotent cells that can differentiate into a variety of cell lineages, including neural cells, and MSCs could secrete neurotrophic factors, anti-inflammatory cytokines, and angiogenic factors to assist in nerve repair and regeneration, thereby facilitating neural stem cell growth and differentiation (33). Whole bone marrow-derived mononuclear cells (BMMCs), which are a mixture of undifferentiated cells including both HSCs and MSCs, could potentially produce a better and synergic effect as compared to each cell line alone. Furthermore, autologous BMMCs can be

readily isolated from bone marrow and have no risk of rejection and no ethical restrictions.

Based on results of experimental studies, the role of stem cell in management of ICH in humans is being investigated. Sobrino et al. found that the higher level of circulating HSCs at admission and at 7 ± 1 days after ICH was associated with the better functional outcome at 3 months (34). England et al. used G-CSF to mobilize HSCs into the circulation and found that HSCs could promote functional recovery from not only ischemic stroke but also ICH (35).

Zhu et al. compared outcomes of surgery combined with autologous bone marrow stromal cell transplantation vs. surgery alone for treatment of intra-cerebral hemorrhage. The findings of this trial showed that surgery combined with autologous bone marrow stromal cell transplantation is safe, providing short-term therapeutic benefits for ICH (36).

Four patients in our report had ICH during the neonatal period. In two patients, ICH occurred on the first day after birth related to premature birth and asphyxia. In two other patients, ICH happened at later stages (28 and 33 days after birth) that may be related to vitamin K deficiency.

Four patients underwent BMMNCs transplantations without occurrence of any adverse side effects, indicating this treatment to be safe. Improvement of different aspects including muscle spasticity and motor function after BMMNC transplantations were observed in all four patients.

Before BMMNC transplantation, neither patient could walk but they were able to walk after transplantation. GMFCS decreased three levels in patients 1 and 2, and one level in patients 3 and 4. It suggests that BMMNC transplantation affords patients requiring less support as they become more independent due to significant improvement of gross motor function.

The total GMFM-88 score and the scores of all component domains increased after the intervention in all four patients. The improvement was observed not only in motor function but also in the fine motor skill in all patients. Personal–social, fine motor–adaptive, and language skills were improved after transplantations.

All patients had muscle spasticity before BMMNC transplantation (two patients at level 4 and two patients at level 2). However, muscle spasticity decreased remarkably after transplantation in all of them. That reduction could contribute to the improvement of motor functions.

Two patients suffered from dysphagia before transplantation, which ceased after BMMNC transplantation. Dysphagia could be caused by spasticity of muscles that coordinate swallowing activities. Disappearance of dysphagia could be related to reduction of muscle spasticity after BMMNC transplantation.

One patient had associated epilepsy, which ceased after transplantation. This result has not been mentioned in any previous reports. This suggests that stem cell transplantation may have beneficial effects to associated epilepsy in patients with neurological sequelae after ICH.

One patient of our cohort had visual impairment, which was improved after stem cell transplantation. Li et al. also reported one patient who had visual impairment associated with cerebral palsy whose impaired vision improved after stem cell transplantation (37). The question whether stem cell transplantation can repair impaired vision in patients with neurologic sequelae after ICH requires additional research in the future to further verify this outcome.

In this study, important clinical improvements have been observed in all patients. However, significant changes of brain MRI were observed only in one case whose dilatation of ventricles was reduced after the transplantation. It suggests that stem cells may improve brain function but may not result in significant changes in brain morphology. That is why a more sensitive tool like PET CT or PET MRI should be used to assess functional changes of the brain after stem cell transplantation in future studies.

CONCLUSION

In conclusion, our results showed that BMMNC transplantation may improve neurological sequelae due to ICH incidence during the neonatal period. However, studies with larger patient numbers should be carried out to achieve a more accurate conclusion.

DATA AVAILABILITY STATEMENT

All datasets generated for this study are included in the article/**Supplementary Material**.

AUTHOR CONTRIBUTIONS

NL: conception and design, data analysis and interpretation, manuscript writing, and final approval of manuscript. TH: collection and assembly of data, data analysis and interpretation, and manuscript writing. LH: provision of study material or patients, collection, assembly of data, and manuscript writing. ND, BA, NA, and DT: provision of study material or patients, collection, assembly of data, data analysis and interpretation.

ACKNOWLEDGMENTS

We are grateful to Dr. Michael Heke, Stanford University, for manuscript revising.

SUPPLEMENTARY MATERIAL

The Supplementary Material for this article can be found online at: https://www.frontiersin.org/articles/10.3389/fped.2019.00543/full#supplementary-material

Supplementary Video 1 | Motor function in case 1 with intracranial hemorrhage in the neonatal period before and after bone marrow mononuclear cell transplantation.

Supplementary Video 2 | Motor function in case 2 with intracranial hemorrhage in the neonatal period before and after bone marrow mononuclear cell transplantation.

Supplementary Video 3 | Motor function in case 3 with intracranial hemorrhage in the neonatal period before and after bone marrow mononuclear cell transplantation.

Supplementary Video 4 | Motor function in case 4 with intracranial hemorrhage in the neonatal period before and after bone marrow mononuclear cell transplantation.

REFERENCES

1. Tan AP, Svrckova P, Cowan F, Chong WK, Mankad K. Intracranial hemorrhage in neonates: a review of etiologies, patterns and predicted clinical outcomes. *Eur J Paediatr Neurol.* (2018) 22:690–717. doi: 10.1016/j.ejpn.2018.04.008
2. Bolisetty S, Dhawan A, Abdel-Latif M, Bajuk B, Stack J, Lui K, et al. Intraventricular hemorrhage and neurodevelopmental outcomes in extreme preterm infants. *Pediatrics.* (2014) 133:55–62. doi: 10.1542/peds.2013-0372
3. Kong X, Xu F, Wu R, Wu H, Ju R, Zhao X, et al. Neonatal mortality and morbidity among infants between 24 to 31 complete weeks: a multicenter survey in China from 2013 to 2014. *BMC Pediatr.* (2016) 16:174. doi: 10.1186/s12887-016-0716-5
4. Handley SC, Passarella M, Lee HC, Lorch SA. Incidence trends and risk factor variation in severe intraventricular hemorrhage across a population based cohort. *J Pediatr.* (2018) 200:24–9.e3. doi: 10.1016/j.jpeds.2018.04.020
5. Babnik J, Stucin-Gantar I, Kornhauser-Cerar L, Sinkovec J, Wraber B, Derganc M. Intrauterine inflammation and the onset of peri-intraventricular hemorrhage in premature infants. *Biol Neonate.* (2006) 90:113–21. doi: 10.1159/000092070
6. Osborn DA, Evans N, Kluckow M. Hemodynamic and antecedent risk factors of early and late periventricular/intraventricular hemorrhage in premature infants. *Pediatrics.* (2003) 112(1 Pt 1):33–9. doi: 10.1542/peds.112.1.33
7. Vural M, Yilmaz I, Ilikkan B, Erginoz E, Perk Y. Intraventricular hemorrhage in preterm newborns: risk factors and results from a University Hospital in Istanbul, 8 years after. *Pediatr Int.* (2007) 49:341–4. doi: 10.1111/j.1442-200X.2007.02381.x
8. Chen TY, Wang HK, Yeh ML, Wei SH, Lu K. Subdural hemorrhage as a first symptom in an infant with a choledochal cyst: case report. *J Neurosurg Pediatr.* (2012) 9:414–6. doi: 10.3171/2011.12.PEDS11279
9. Danielsson N, Hoa DP, Thang NV, Vos T, Loughnan PM. Intracranial haemorrhage due to late onset vitamin K deficiency bleeding in Hanoi province, Vietnam. *Arch Dis Child Fetal Neonatal Ed.* (2004) 89:F546–50. doi: 10.1136/adc.2003.047837
10. Elalfy MS, Elagouza IA, Ibrahim FA, AbdElmessieh SK, Gadallah M. Intracranial haemorrhage is linked to late onset vitamin K deficiency in infants aged 2–24 weeks. *Acta Paediatr.* (2014) 103:e273–6. doi: 10.1111/apa.12598
11. Goto T, Kakita H, Takasu M, Takeshita S, Ueda H, Muto D, et al. A rare case of fetal extensive intracranial hemorrhage and whole-cerebral hypoplasia due to latent maternal vitamin K deficiency. *J Neonatal Perinatal Med.* (2018) 11:191–4. doi: 10.3233/NPM-181745
12. Hong HS, Lee JY. Intracranial hemorrhage in term neonates. *Childs Nerv Syst.* (2018) 34:1135–43. doi: 10.1007/s00381-018-3788-8
13. Unal E, Ozsoylu S, Bayram A, Ozdemir MA, Yilmaz E, Canpolat M, et al. Intracranial hemorrhage in infants as a serious, and preventable consequence of late form of vitamin K deficiency: a selfie picture of Turkey, strategies for tomorrow. *Childs Nerv Syst.* (2014) 30:1375–82. doi: 10.1007/s00381-014-2419-2
14. Pierrat V, Marchand-Martin L, Arnaud C, Kaminski M, Resche-Rigon M, Lebeaux C, et al. Neurodevelopmental outcome at 2 years for preterm children born at 22 to 34 weeks' gestation in France in 2011: EPIPAGE-2 cohort study. *BMJ.* (2017) 358:j3448. doi: 10.1136/bmj.j3448
15. Chen G, Wang Y, Xu Z, Fang F, Xu R, Wang Y, et al. Neural stem cell-like cells derived from autologous bone mesenchymal stem cells for the treatment of patients with cerebral palsy. *J Transl Med.* (2013) 11:21. doi: 10.1186/1479-5876-11-21
16. Mancias-Guerra C, Marroquin-Escamilla AR, Gonzalez-Llano O, Villarreal-Martinez L, Jaime-Perez JC, Garcia-Rodriguez F, et al. Safety and tolerability of intrathecal delivery of autologous bone marrow nucleated cells in children with cerebral palsy: an open-label phase I trial. *Cytotherapy.* (2014) 16:810–20. doi: 10.1016/j.jcyt.2014.01.008
17. Min K, Song J, Kang JY, Ko J, Ryu JS, Kang MS, et al. Umbilical cord blood therapy potentiated with erythropoietin for children with cerebral palsy: a double-blind, randomized, placebo-controlled trial. *Stem Cells.* (2013) 31:581–91. doi: 10.1002/stem.1304
18. Nguyen TL, Nguyen HP, Nguyen TK. The effects of bone marrow mononuclear cell transplantation on the quality of life of children with cerebral palsy. *Health Qual Life Outcomes.* (2018) 16:164. doi: 10.1186/s12955-018-0992-x
19. Sharma A, Sane H, Gokulchandran N, Kulkarni P, Gandhi S, Sundaram J, et al. A clinical study of autologous bone marrow mononuclear cells for cerebral palsy patients: a new frontier. *Stem Cells Int.* (2015) 2015:905874. doi: 10.1155/2015/905874
20. Wang X, Hu H, Hua R, Yang J, Zheng P, Niu X, et al. Effect of umbilical cord mesenchymal stromal cells on motor functions of identical twins with cerebral palsy: pilot study on the correlation of efficacy and hereditary factors. *Cytotherapy.* (2015) 17:224–31. doi: 10.1016/j.jcyt.2014.09.010
21. Nguyen LT, Nguyen AT, Vu CD, Ngo DV, Bui AV. Outcomes of autologous bone marrow mononuclear cells for cerebral palsy: an open label uncontrolled clinical trial. *BMC Pediatr.* (2017) 17:104. doi: 10.1186/s12887-017-0859-z
22. Ahn SY, Chang YS, Sung SI, Park WS. Mesenchymal stem cells for severe intraventricular hemorrhage in preterm infants: phase I dose-escalation clinical trial. *Stem Cells Transl Med.* (2018) 7:847–56. doi: 10.1002/sctm.17-0219
23. Bohannon RSM. *Modified Ashworth Scale Instructions.* (1987). Available online at: www.rehabmeasures.org.
24. CanChild. *Gross Motor Function Classification System - Expanded & Revised (GMFCS - E&R).* CanChild (2017). Available online at: https://canchild.ca/en/resources/42-gross-motor-function-classification-system-expanded-revised-gmfcs-e-r (accessed December 27, 2017).
25. Frankenburg WK, Dodds J, Archer P, Shapiro H, Bresnick B. The Denver II: a major revision and restandardization of the Denver Developmental Screening Test. *Pediatrics.* (1992) 89:91–7.
26. Sralab. *Modified Ashworth Scale Instructions.* (2016). Available online at: https://www.sralab.org/sites/default/files/2017-06/Modified%20Ashworth%20Scale%20Instructions.pdf
27. Whitelaw A. Intraventricular haemorrhage and posthaemorrhagic hydrocephalus: pathogenesis, prevention and future interventions. *Semin Neonatol.* (2001) 6:135–46. doi: 10.1053/siny.2001.0047
28. Harries N, Kassirer M, Amichai T, Lahat E. Changes over years in gross motor function of 3-8 year old children with cerebral palsy: using the Gross Motor Function Measure (GMFM-88). *Isr Med Assoc J.* (2004) 6:408–11.
29. Molnar GE. Rehabilitation in cerebral palsy. *West J Med.* (1991) 154:569–72.
30. Ahn SY, Chang YS, Sung DK, Sung SI, Yoo HS, Lee JH, et al. Mesenchymal stem cells prevent hydrocephalus after severe intraventricular hemorrhage. *Stroke.* (2013) 44:497–504. doi: 10.1161/STROKEAHA.112.679092
31. Suda S, Yang B, Schaar K, Xi X, Pido J, Parsha K, et al. Autologous bone marrow mononuclear cells exert broad effects on short- and long-term biological and functional outcomes in rodents with intracerebral hemorrhage. *Stem Cells Dev.* (2015) 24:2756–66. doi: 10.1089/scd.2015.0107
32. Wang C, Fei Y, Xu C, Zhao Y, Pan Y. Bone marrow mesenchymal stem cells ameliorate neurological deficits and blood-brain barrier dysfunction after intracerebral hemorrhage in spontaneously hypertensive rats. *Int J Clin Exp Pathol.* (2015) 8:4715–24.
33. An YH, Wan H, Zhang ZS, Wang HY, Gao ZX, Sun MZ, et al. Effect of rat Schwann cell secretion on proliferation and differentiation of human neural stem cells. *Biomed Environ Sci.* (2003) 16:90–4.
34. Sobrino T, Arias S, Perez-Mato M, Agulla J, Brea D, Rodriguez-Yanez M, et al. Cd34+ progenitor cells likely are involved in the good functional recovery after intracerebral hemorrhage in humans. *J Neurosci Res.* (2011) 89:979–85. doi: 10.1002/jnr.22627
35. England TJ, Abaei M, Auer DP, Lowe J, Jones DR, Sare G, et al. Granulocyte-colony stimulating factor for mobilizing bone marrow stem cells in subacute

stroke: the stem cell trial of recovery enhancement after stroke 2 randomized controlled trial. *Stroke.* (2012) 43:405–11. doi: 10.1161/STROKEAHA.111.636449

36. Zhu J, Xiao Y, Li Z, Han F, Xiao T, Zhang Z, et al. Efficacy of surgery combined with autologous bone marrow stromal cell transplantation for treatment of intracerebral hemorrhage. *Stem Cells Int.* (2015) 2015:318269. doi: 10.1155/2015/318269
37. Li M, Yu A, Zhang F, Dai G, Cheng H, Wang X, et al. Treatment of one case of cerebral palsy combined with posterior visual pathway injury using autologous bone marrow mesenchymal stem cells. *J Transl Med.* (2012) 10:100. doi: 10.1186/1479-5876-10-100

Conflict of Interest: The authors declare that the research was conducted in the absence of any commercial or financial relationships that could be construed as a potential conflict of interest.

frontiers in Neurology

SYSTEMATIC REVIEW
published: 18 February 2020
doi: 10.3389/fneur.2019.01369

A Scoping Review of Inborn Errors of Metabolism Causing Progressive Intellectual and Neurologic Deterioration (PIND)

Hilde A. G. Warmerdam[1†], Elise A. Termeulen-Ferreira[1†], Laura A. Tseng[1], Jessica Y. Lee[2], Agnies M. van Eeghen[1,3], Carlos R. Ferreira[4] and Clara D. M. van Karnebeek[1,5]*

[1] Department of Pediatrics, Emma Children's Hospital, Amsterdam Gastroenterology and Metabolism, Amsterdam University Medical Centres, University of Amsterdam, Amsterdam, Netherlands, [2] Centre for Molecular Medicine and Therapeutics, BC Children's Hospital Research Institute, University of British Columbia, Vancouver, BC, Canada, [3] 's Heeren Loo Care Group, Amsterdam, Netherlands, [4] National Human Genome Research Institute, National Institutes of Health, Bethesda, MD, United States, [5] Department of Pediatrics, Radboud Centre for Mitochondrial Medicine, Radboud University Medical Centre, Nijmegen, Netherlands

OPEN ACCESS

Edited by:
Matthew James Farrer, University of Florida, United States

Reviewed by:
Johnathan Cooper-Knock, University of Sheffield, United Kingdom
Filippo M. Santorelli, Fondazione Stella Maris (IRCCS), Italy

****Correspondence:***
Clara D. M. van Karnebeek
clara.vankarnebeek@radboudumc.nl

[†]These authors share first authorship

Specialty section:
This article was submitted to Neurogenetics, a section of the journal Frontiers in Neurology

Received: *07 July 2019*
Accepted: *11 December 2019*
Published: *18 February 2020*

Citation:
Warmerdam HAG, Termeulen-Ferreira EA, Tseng LA, Lee JY, van Eeghen AM, Ferreira CR and van Karnebeek CDM (2020) A Scoping Review of Inborn Errors of Metabolism Causing Progressive Intellectual and Neurologic Deterioration (PIND). Front. Neurol. 10:1369. doi: 10.3389/fneur.2019.01369

Background: Progressive intellectual and neurological deterioration (PIND) is a rare but severe childhood disorder characterized by loss of intellectual or developmental abilities, and requires quick diagnosis to ensure timely treatment to prevent possible irreversible neurological damage. Inborn errors of metabolism (IEMs) constitute a group of more than 1,000 monogenic conditions in which the impairment of a biochemical pathway is intrinsic to the pathophysiology of the disease, resulting in either accumulation of toxic metabolites and/or shortage of energy and building blocks for the cells. Many IEMs are amenable to treatment with the potential to improve outcomes. With this literature review we aim to create an overview of IEMs presenting with PIND in children, to aid clinicians in accelerating the diagnostic process.

Methods: We performed a PubMed search on IEMs presenting with PIND in individuals aged 0–18 years. We applied stringent selection criteria and subsequently derived information on encoding genes, pathways, clinical and biochemical signs and diagnostic tests from IEMbase (www.iembase.org) and other sources.

Results: The PubMed search resulted in a total of 2,152 articles and a review of references added another 19 articles. After applying our selection criteria, a total of 85 IEMs presenting with PIND remained, of which 57 IEMs were reported in multiple unrelated cases and 28 in single families. For 44 IEMs (52%) diagnosis can be achieved through generally accessible metabolic blood and urine screening tests; the remainder requires enzymatic and/or genetic testing. Treatment targeting the underlying pathophysiology is available for 35 IEMs (41%). All treatment strategies are reported to achieve stabilization of deterioration, and a subset improved seizure control and/or neurodevelopment.

Conclusions: We present the first comprehensive overview of IEMs presenting with PIND, and provide a structured approach to diagnosis and overview of treatability. Clearly IEMs constitute the largest group of genetic PIND conditions and have the advantage of

detectable biomarkers as well as amenability to treatment. Thus, the clinician should keep IEMs at the forefront of the diagnostic workup of a child with PIND. With the ongoing discovery of new IEMs, expanded phenotypes, and novel treatment strategies, continuous updates to this work will be required.

Keywords: PIND, inherited metabolic diseases, neurodegeneration, dementia, loss of skills, genetic, treatment, diagnosis

INTRODUCTION

Progressive intellectual and neurological deterioration (PIND) in children is defined as "progressive deterioration for more than 3 months with loss of already attained intellectual or developmental abilities and development of abnormal neurological signs" (1–6). Initial psychomotor development might be delayed, but this is not required. PIND is a rare, yet alarming phenomenon. It will urge every pediatrician to find a diagnosis and quickly start treatment in order to halt or even reverse the intellectual decline in the patient. Additionally, this will provide an opportunity for accurate prognostication and genetic counseling for the family.

However, evaluation is extremely challenging given the immense heterogeneity of underlying disorders, varying from genetic causes such as intellectual disability syndromes (e.g., Rett disease, MIM#312750), neurodegenerative repeat expansion diseases, chromosome breakage diseases as well as inborn errors of metabolism, to environmental causes such as infectious encephalitis, traumatic brain injury, anoxic brain injury, or immune mediated conditions such as anti-MNDA receptor encephalitis (8, 9). Inborn errors of metabolism (IEMs) constitute a well-known cause of PIND and intellectual developmental disabilities in general; examples include neuronal ceroid lipofuscinosis (NCL), Niemann-Pick disease type C (NPC), and different types of mucopolysaccharidosis (MPS) (8–10). Nonetheless, a complete overview of IEMs causing PIND remains unavailable in the current literature, and this group of single gene disorders is not commonly screened for with biochemical urine/blood tests, despite increasing opportunities to causally treat and improve prognosis. Treatment strategies include diet, vitamin supplements, medications, and hematopoietic stem cell transplantation (HSCT) to enzyme replacement or gene therapy.

Here we aim to present an up-to-date literature review of all known IEMs reported with a clinical presentation of PIND. With the information provided about phenotypic features, diagnostic tests and therapeutic modalities, we hope to aid the clinician in the efficient identification and management of IEMs in children presenting with PIND.

METHODS

Search Strategy and Defining PIND and IEMs

We searched PubMed with terms encompassing and describing our definitions of PIND and IEMs to ensure the search yielded articles meeting our search query, i.e., IEMs presenting with PIND in children (**Table 1**).

Inborn metabolic diseases were re-defined in 2015 by Morava et al. as "a disruption of a metabolic pathway irrespective of whether it is associated with abnormalities in biochemical laboratory tests" (7). Recently Ferreira et al. proposed a new nosology using this re-definition of IEMs, the inclusion criteria of which are shown in **Table 2** (8). These criteria were subsequently used to define IEMs in this review.

Table 3 shows the definition of PIND as used for this review and is based on the definition of UK (1–4), Canadian (5) and Australian (6) research groups exploring which disorders present with symptoms consistent with PIND (1–6). Our definition of PIND includes progressive deterioration with loss of already attained intellectual and developmental abilities and development of neurological signs including epilepsy. Deterioration through loss of intellectual or developmental

TABLE 1 | Terms used for search strategy in Pubmed.

Neurocognitive regression	Progressive intellectual and neurologic deterioration, PIND, neurologic/neurocognitive/psychomo tor/mental/cognitive/ developmental/intellectual regression/deterioration/decline, developmental arrest, dementia, loss of skill(s), loss of milestone(s), neurobehavioral signs and symptoms, loss of (intellectual) abilities, disintegrative/neurodegenerative disease/disorder.
Inborn errors of metabolism	Inborn/inherited errors of metabolism, inborn/inherited/genetic metabolic/neurometabolic/ metabolic brain disorder/disease, IEMs
Age group (birth-18 years)	Newborn, infant, child, pediatric, adolescent.

TABLE 2 | Criteria inborn errors of metabolism by Ferreira et al. (8).

- Disruption of a metabolic pathway is considered necessary and sufficient for inclusion
- Regardless of laboratory abnormalities in standard biochemical tests
- Regardless of association with clinical manifestations of disease (unless defect is universal to all humans)
- Severity alone is not considered sufficient for separation into different entries when a single gene product is involved
- A different pathomechanism is considered necessary for separation into different entries when a single gene product is involved, regardless of the mode of inheritance
- The involvement of different gene products is considered sufficient for separation into different entries, even if the phenotype is similar
- The error must have been reported in more than a single family, and the involvement of the gene product must haven well characterized on an enzymatic or molecular level

TABLE 3 | Definition PIND.

Children aged 0–18 years at onset of symptoms who fulfill the following criteria:
• Progressive deterioration during 3 months
• Loss of already attained intellectual or developmental abilities
• Development of neurological signs including epilepsy
• No (static) loss of skill due to:
- Encephalitis
- Head injury
- Near drowning

abilities may be present in children with previously normal or delayed development. No distinction is made in this review.

Expert Opinion

If the literature was inconclusive, individual experts were consulted for their input on specific (groups) of IEMs and requested to provide an evidence- or expert-based opinion on the presence or absence of PIND as a presenting feature. If literature of sufficient quality meeting our criteria was available, then the IEM was included in this list.

Literature Search and Selection

We searched PubMed for all articles published between 1953 and October 2018 with the aim of establishing which inborn errors of metabolism cause neurocognitive regression in children aged 0–18 years.

A flow diagram representing the different phases of the selection process is shown in **Figure 1**. Selection of articles according to inclusion and exclusion criteria was performed with the use of Rayyan (https://rayyan.qcri.org), a web and mobile app for systematic reviews (9). Exclusion criteria were as followed: (1) not meeting definitions of IEM and/or PIND; (2) IEM not manifesting with PIND; (3) IEM presenting with completely reversible intellectual and neurologic deterioration, e.g., during (febrile) disease; (4) IEM presenting with neurologic or movement disorders without intellectual deterioration; (5) IEM presenting solely with developmental delay; (6) age of proband(s) over 18 years; (7) animal studies; (8) no (English or Dutch) full text available.

We compared our list of selected IEMs with those of PIND research groups and added IEMs of the latter if these met our selection criteria. Also, we consulted experts for their opinion.

Articles publishing on IEMs causing symptoms meeting the definition of PIND were further pursued. When meeting all criteria, the IEMs were categorized in nine groups using the proposed nosology by Ferreira et al.: A. Disorders of nitrogen-containing compounds; B. Disorders of vitamins, cofactors, metals and minerals; C. Disorders of carbohydrates; D. Mitochondrial disorders of energy metabolism; E. Disorders of lipids; F. Disorders of tetrapyrroles; G. Storage disorders; H. Disorders of peroxisomes and oxalate; and I. Congenital disorders of glycosylation (8).

Disease Information

If the literature search yielded multiple articles for a specific disorder (e.g., neuronal ceroid lipofuscinosis and Leigh syndrome), databases such as GeneReviews, OMIM, OMMBID and IEMbase were consulted for more concise summaries or reviews.

IEMbase (www.iembase.org), an online IEM knowledgebase, was searched for information on each IEM such as encoding genes, pathways, clinical symptoms, biochemical signs, and diagnostic tests. Other databases such as Online Mendelian Inheritance in Man (OMIM)[1], GeneReviews (11) and the Online Metabolic and Molecular Bases of Inherited Disease (OMMBID) (12) were consulted if additional information was required.

Diagnostic Strategies

To facilitate a practical guide for biochemical and genetic diagnosis, we assessed which tests are necessary to diagnose each of the conditions. Accordingly, we grouped the diseases into IEMs diagnosed via "metabolic screening tests" vs. IEMs diagnosed via "enzymatic and/or genetic testing". As screening tests we defined biochemical tests in blood and urine for IEMs with reliable biomarkers, generally available in biochemical laboratories in most developed countries.

Therapeutic Modalities

Information about treatment was extracted from two articles on treatable intellectual disabilities, i.e., IEMs causing global developmental delay (DD)/intellectual disability (ID) which are amenable to causal treatment (13, 14) (this information is available via an online digital tool, www.treatable-id.org) (15). A treatable IEM is defined as the availability of a particular therapeutic modality capable of preventing or improving the DD/ID phenotype, or halting/slowing neurocognitive decline with acceptable adverse effects, i.e., positively influencing the "outcome measures". Therapeutic modalities include dietary restriction/supplementation, cofactor or vitamin supplementation, substrate inhibition (small molecule), substrate reduction, enzyme replacement, bone marrow and hematopoietic stem cell transplant and gene therapy. Outcome measure/effect are defined as primary = IQ, developmental testing score/performance, survival; secondary = epilepsy, behavior, psychiatric, neurological deficit (e.g., movement disorder), neuro-imaging, or systemic symptoms influencing developmental/cognitive performance (e.g., ichthyosis, liver disease). The level of evidence, i.e., the quality of the evidence describing the beneficial effect of each therapeutic modality, was ranked 1–5 according to the Center of Evidence Based Medicine (www.cebm.net).

RESULTS

Literature Yield

Our Pubmed search yielded 2,152 articles. After applying inclusion and exclusion criteria we identified a total of 79 IEMs

[1]OMIM® and Online Mendelian Inheritance in Man® are registered trademarks of the Johns Hopkins University. www.omim.org.

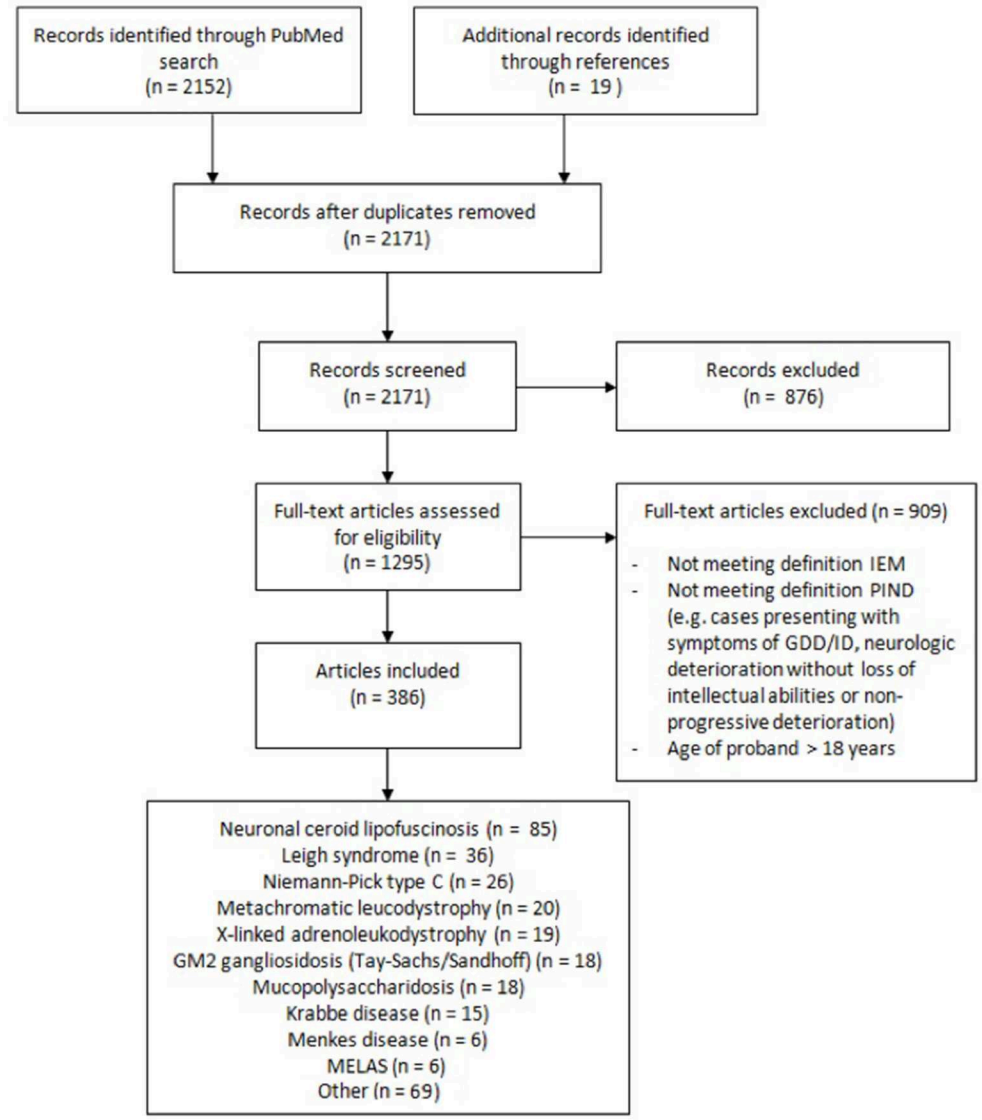

FIGURE 1 | Flow diagram showing the different phases of the literature selection process.

presenting with PIND. Of these 79 IEMs, 55 (70%) presented with PIND in multiple cases and in multiple families, while the remaining 24 IEMs presented with PIND in single cases or single families (**Supplemental Table S1**).

We added four IEMs to **Supplemental Table S1** that did not emerge from our literature search but rather were reported in articles by PIND research groups, and agreed upon by our expert colleagues as IEMs to present with PIND. Based on expert opinion, we included two more IEMs, mitochondrial DNA polymerase-gamma catalytic subunit (POLG) deficiency, and folate receptor-alfa deficiency, resulting in a total of 85 IEMs presenting with PIND.

Taking the total of 85 IEMs presenting with PIND, storage disorders (n = 34/85, 40%) represented the largest category. The other IEMs were classified as follows: nitrogen-containing compounds (n = 15); disorders of vitamins, cofactors, metals and minerals (n = 15); disorders of carbohydrates (n = 1); mitochondrial disorders of energy metabolism (n = 14); disorders of lipids (n = 2); disorders of tetrapyrroles (n = 1); disorders of peroxisomes and oxalate (n = 2); and congenital disorders of glycosylation (n = 1).

Neurologic and systemic symptoms registered in IEMBase are shown in **Supplemental Table S1** Besides PIND, these disorders present with a variety of neurologic symptoms, most commonly: seizures (or epilepsy, convulsions, 67 IEMs, 79%), global developmental delay/intellectual disability (GDD/ID, 33 IEMs, 39%), and ataxia (54 IEMs, 63%), but hypotonia, nystagmus, MRI abnormalities, loss of vision and loss of hearing may also be present. Non-neurologic symptoms vary widely from vomiting, retinopathy and hepatosplenomegaly to psychiatric and behavioral disorders.

TABLE 4 | Diagnostic tests.

METABOLIC BLOOD AND URINE TESTS			
Urine Tests			
Urine organic acids ($n = 11$)	3-Hydroxyisobutyryl-CoA deacylase deficiency	Canavan disease	Costeff syndrome
	Glutaric aciduria type 1	HSD10 deficiency	L-2-hydroxyglutaric aciduria (&PAA)
	MEGDEL syndrome	Methylmalonic aciduria and homocystinuria, cblC type (&PAA&PTH)	
	Beta-alanine alpha-ketoglutarate transaminase deficiency	Methylglutaconic aciduria type I	Methylcobalamin deficiency, cblE type
Urine glycosaminoglycans ($n = 11$)	GM1 gangliosidosis (&ET)	GM2 gangliosidosis, AB variant (&ET)	Mucolipidosis type 1 (&ET)
	Mucopolysaccharidosis type 1	Mucopolysaccharidosis type 2	Mucopolysaccharidosis type 3A
	Mucopolysaccharidosis type 3B	Mucopolysaccharidosis type 3C	Mucopolysaccharidosis type 3D
	Mucopolysaccharidosis type 7	Multiple sulfatase deficiency	
Urine creatine metabolites ($n = 1$)	Guanidinoacetate methyltransferase (GAMT) deficiency		
Urine oligosaccharides ($n = 9$)	Aspartylglucosaminuria	Fucosidosis	GM1 gangliosidosis
	GM2 gangliosidosis, AB variant	Alpha-Mannosidosis	Pompe disease
	Salla disease	Sandhoff disease	Tay-Sachs disease
Urine purines and pyrimidines ($n = 2$)	CAD deficiency	Suphite oxidase deficiency	
Blood Tests			
Plasma amino-acids ($n = 9$)	Adenylosuccinate lyase deficiency	Arginase 1 deficiency	
	Carbamoylphosphate synthetase I deficiency	Hyperornithinemia-hyperammonemia-homocitrullinemia syndrome	
	L-2-hydroxyglutaric aciduria (&UOA)	Maple syrup urine disease (MSUD)	
	Methylenetetrahydrofolate reductase deficiency (PTH)	Methylmalonic aciduria and homocystinuria, cblC type (&UOA&PTH)	
	Nonketotic hyperglycinemia (&CAA)		
Plasma total homocysteine ($n = 2$)	Methylenetetrahydrofolate reductase deficiency (&PAA)	Methylmalonic aciduria and homocystinuria, cblC type (&UOA&PAA)	
Serum copper and ceruloplasmin ($n = 2$)	Menkes disease	Wilson disease	
GENETIC AND ENZYMATIC TESTS			
Genetic testing ($n = 30$)	Aicardi-Goutieres syndrome	Beta-propeller protein-associated neurodegeneration	Combined Oxidative Phosphorylation Defect 6
	COQ2 deficiency	Crigler-Najjar syndrome	IBA57 deficiency
	Leber Hereditary Optic Neuropathy	Leigh syndrome	Leukoencephalopathy associated with APOA1BP gene mutations
	MELAS	MitCHAP-60 disease	Mitochondrial DNA polymerase-gamma catalytic subunit deficiency
	Mucolipidosis type 4	Neurodegeneration with brain iron accumulation	Neuronal ceroid lipofuscinosis type 3
	Neuronal ceroid lipofuscinosis type 5	Neuronal ceroid lipofuscinosis type 6	Neuronal ceroid lipofuscinosis type 7
	Neuronal ceroid lipofuscinosis type 8	Neuronal ceroid lipofuscinosis type 10	Neuronal ceroid lipofuscinosis type 12
	Neuronal ceroid lipofuscinosis type 14	OPA1 disease	Pantothenate kinase-associated neurodegeneration
	Thiamine transporter 2 deficiency	TWINKLE mitochondrial DNA helicase deficiency	Vanishing White Matter/Childhood Ataxia with Central Nervous System Hypomyelination/eIF2Brelated diseases
Enzymatic testing ($n = 14$)	Zellweger spectrum disorders - Peroxin 1 deficiency	Zellweger spectrum disorders - Peroxin 3 deficiency	Zellweger spectrum disorders - Peroxin 6 deficiency
	Farber disease	Gaucher disease	GM1 gangliosidosis (&UGAG)
	GM2 gangliosidosis, AB variant (&UGAG)	Krabbe disease	Metachromatic leucodystrophy
	Mucolipidosis type 1 (&UGAG)	Neuronal ceroid lipofuscinosis type 1	Neuronal ceroid lipofuscinosis type 2
	Niemann-Pick type A	Pompe disease	
(OTHER) SPECIFIC TESTS			
Plasma VLCFA	X-linked adrenoleukodystrophy	CSF MTHF (n=2)	Folate receptor-alfa deficiency
Plasma folate	Hereditary folate malabsorption (&CMTHF)		Hereditary folate malabsorption (&PF)
Plasma transferrins isoelectric focusing	Congenital disorder of glycosylation, type 1a	CSF amino acids	Nonketotic hyperglycinemia (&PAA)
Plasma sterol analysis	Cerebrotendinous xanthomatosis	CSF-plasma glucose ratio	Glucose transporter deficiency
Plasma oxysterols ($n = 2$)	Niemann-Pick disease type C1 Niemann-Pick disease type C2	Urine sulfocyetine	Molybdenum cofactor deficiency

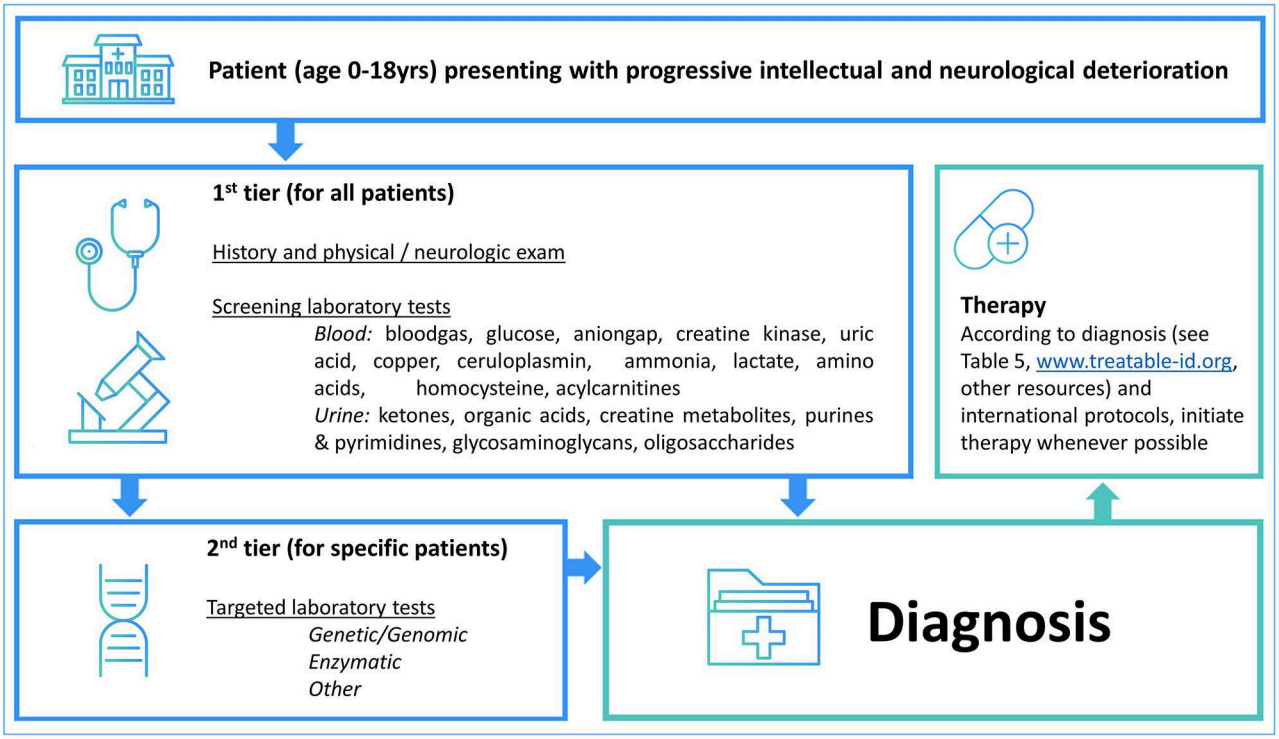

FIGURE 2 | Two-tiered diagnostic biochemical and genetic algorithm. The potential yield of the 1st tier laboratory tests is 52% ($n = 44$ IEMs) while the remaining 41 IEMs are identified via the 2nd tier tests. Exome/genome sequencing can be initiated according to the local availability and clinical practice as well as specialists' insights.

The case of Leigh syndrome (MIM#256000), one of the IEMs associated with PIND, deserves special mention. Leigh syndrome is a progressive neurodegenerative disorder with developmental regression, usually between ages 3 and 12 months, due to mitochondrial oxidative phosphorylation defects. Typical MRI abnormalities include symmetrical lesions in the basal ganglia or brainstem. This syndrome is not associated with mutations in a single gene, but is caused by many different gene defects; currently there are 178 genes associated with Leigh syndrome in the Leigh Map (available at vmh.uni.lu/#leighmap) (16).

Diagnostic Strategies

Table 4 summarizes the diagnostic methods required for identification of IEMs presenting with PIND. A total of 44 IEMs can be identified through metabolic screening tests in blood and urine, 14 IEMs require enzymatic analysis, while for the remaining 30 IEMs, reliable biomarkers are lacking and genetic testing is obligatory. This information is summarized in **Figure 2**, i.e., a two-tiered diagnostic algorithm comprising biochemical and genetic testing. Exome/genome sequencing should be initiated according to the insight of the clinician. Finally, 7 IEMs associated with PIND are included in newborn screening (NBS) panels in various countries (**Supplemental Table S1**).

Therapeutic Modalities

Table 5 provides an overview of all IEMs presenting with PIND for which causal treatment is available, totaling 35 IEMs (41%).

The main effect of therapy is stabilization of clinical deterioration, as this effect is reported for every registered therapeutic modality. Other reported effects include improvement of seizure control ($n = 9$); behavior ($n = 2$); and neurological and/or systemic manifestations ($n = 19$).

The level of evidence for these therapies varies; for the majority the level of evidence is 4 (case series) to 5 (single case report/expert opinion) ($n = 24$, 69%). For 4 therapeutic strategies (11%), the level of evidence is 1 including: HSCT in MPS I, miglustat treatment in Niemann-Pick type C1 and C2, enzyme replacement therapy in neuronal ceroid lipofuscinosis type 2, and HSCT in X-linked adrenoleukodystrophy.

DISCUSSION

Here we present, for the first time, a comprehensive list of IEMs presenting with PIND, based on a PubMed search of relevant literature. The total number ($n = 85$) is higher than previously estimated, although prevalence remains unknown in the PIND and general population. Several groups have analyzed and published data on the etiology and epidemiology of PIND while researching childhood dementia, progressive deterioration, or prevalence of variant Creutzfeld-Jacob disease in children. An

TABLE 5 | Therapeutic modalities for IEMs causing PIND.

IEM name	Therapeutic modality (-ies)	Level of evidence	Treatment effect	References
α-mannosidosis	HSCT	4/5	Stabilizes clinical deterioration	Treatable ID
Aspartylglucosaminuria	HSCT	4/5	Stabilizes clinical deterioration	Treatable ID
Arginase 1 deficiency	Dietary protein restriction, arginine supplement, sodium benzoate, phenylbutyrate	2b	Prevents metabolic decompensation; stabilizes clinical deterioration; improves behavior, seizure control, neurological and systemic manifestations	Treatable ID
Biotinidase deficiency	Biotin supplements	2c	Improves psychomotor development/IQ, neurological and systemic manifestations	Treatable ID
CAD deficiency	Uridine supplements	4	Seizure control, stabilizes clinical deterioration, improves psychomotor development/IQ	Koch et al. (31)
Carbamoylphosphate synthetase I deficiency*	Dietary protein restriction, arginine supplement, sodium benzoate, phenylbutyrate	2b	Prevents metabolic decompensation; stabilizes clinical deterioration; improves behavior, seizure control, neurological and systemic manifestations	Treatable ID
Cerebral folate receptor-α deficiency	Folinic Acid	4	Stabilizes clinical deterioration; improves psychomotor development/IQ; seizure control and neurological manifestations	Treatable ID
Cerebrotendinous xanthomatosis	Chenodeoxycholic Acid, HMG Reductase Inhibitor	4	Stabilizes clinical deterioration, improves behavior, neurological and systemic manifestations	Treatable ID
COQ2 deficiency	CoQ supplements	4	Improves neurological manfestation and seizure control	Treatable ID
Gaucher disease (type III)	HSCT	4/5	Stabilizes clinical deterioration, improves systemic manifestations	Treatable ID
Glucose transporter deficiency	Ketogenic or analog diets	2b	Improves seizure control, improves neurological manifestations, improves psychomotor development/IQ	Daci et al. (32)
Guanidinoacetate methyltransferase (GAMT) deficiency	Arginine restriction, Creatine and Ornithine supplements	4	Stabilizes clinical deterioration; improves behavior, seizure control and neurological manifestations	Treatable ID
HSD10 deficiency	Avoid fasting, Sick day management, Isoleucine restricted diet	5	Prevents metabolic decompensation	Treatable ID
Hyperornithinemia-hyperammonemiahomocitrullinemia syndrome	Dietary protein restriction, Ornithine supplement, sodium benzoate, phenylacetate	4	Prevents metabolic decompensation; stabilizes clinical deterioration; improves behavior, seizure control, neurological and systemic manifestations	Treatable ID
Krabbe disease	HSCT	2a	Stabilizes clinical deterioration	Escolar et al. (33)
l.o. Glutaric aciduria type 1	Lysine Restriction, Carnitine supplements	2c	Prevents metabolic decompensation; stabilizes clinical deterioration; improves neurological and systemic manifestations	Treatable ID
l.o. Metachromatic leucodystrophy	HSCT	4/5	Stabilizes clinical deterioration	Treatable ID
Maple syrup urine disease (variant)	Amino acids, Avoid fasting	4	Stabilizes clinical deterioration; prevents metabolic decompensation; improves behavior	Treatable ID
Menkes disease occipital horn syndrome	Copper Histidine	4	Stabilizes clinical deterioration	Treatable ID
Methylcobalamin deficiency, cblE type	Hydroxy-/Methylcobalamin, Betaine	4	Prevents metabolic decompensation, stabilizes clinical deterioration; improves systemic manifestations	Treatable ID
Methylenetetrahydrofolate reductase deficiency	Betaine supplements, +/– Folate, Carnitine, Methionine supplements	4	Prevents metabolic decompensation; stabilizes clinical deterioration; improves systemic manifestations	Treatable ID
Methylglutaconic aciduria type I	Carnitine supplements, Avoid fasting, Sick day management	5	Prevents metabolic decompensation	Treatable ID
Methylmalonic aciduria and homocystinuria, cblC type	Hydroxocobalamin	4	Prevents metabolic decompensation; stabilizes clinical deterioration; improves systemic manifestations	Treatable ID

(Continued)

TABLE 5 | Continued

IEM name	Therapeutic modality (-ies)	Level of evidence	Treatment effect	References
Mitochondrial Myopathy, Encephalopathy, Lactic Acidosis and Stroke-like episodes (MELAS)	Arginine supplements	4/5	Prevents metabolic decompensation, stabilizes clinical deterioration, improves seizure control & neurological manifestations	Treatable ID
Molybdenum cofactor deficiency	Cyclic pyranopterin monophosphate (cPMP) supplements	2b	Stabilizes clinical deterioration; improves neurological manifestations	Schwahn et al. (34)
Mucopolysaccharidosis type 1 (MPS I)	HSCT	1c	Stabilizes clinical deterioration; improves systemic manifestations	Treatable ID
Mucopolysaccharidosis type 2 (MPS II)	HSCT	4/5	Stabilizes clinical deterioration; improves systemic manifestations	Treatable ID
Mucopolysaccharidosis type 3A (MPS IIIA)	HSCT	4/5	Stabilizes clinical deterioration	Treatable ID
Mucopolysaccharidosis type 3B (MPS IIIB)	HSCT	4/5	Stabilizes clinical deterioration	Treatable ID
Mucopolysaccharidosis type 3C (MPS IIIC)	HSCT	4/5	Stabilizes clinical deterioration	Treatable ID
Mucopolysaccharidosis type 3D (MPS IIID)	HSCT	4/5	Stabilizes clinical deterioration	Treatable ID
Mucopolysaccharidosis type 7 (MPS VII)	HSCT	4/5	Stabilizes clinical deterioration	Treatable ID
Neuronal ceroid lipofuscinosis type 2	Enzyme replacement therapy	1c	Stabilizes clinical deterioration	Geraets et al. (35)
Niemann-Pick disease type C1	Miglustat	1b	Stabilizes clinical deterioration; improves neurological manifestations	Treatable ID
Niemann-Pick disease type C2	Miglustat	1b	Stabilizes clinical deterioration; improves neurological manifestations	Treatable ID

Legend: l.o., Late onset.

HSCT, Haematologic stem cell transplantation.

Levels of evidence (source www.cebm.net): 1a. Systematic review of randomized controlled trials (RCTs), 1b. Individual RCT, 1c. All or none. 2a. Systematic review of cohort studies, 2b. Individual cohort study, 2c. "Outcomes" research, 3. Systematic review of case-control studies, 4.Individual case-control study or case-series/report, 4/5. Single case report, 5. Expert opinion without critical appraisal.

overview of the reported presence of inborn errors of metabolism in children with PIND is shown in **Table 6**. These studies show varying causes of PIND and report that 62.5–75.0% of all PIND cases are caused by IEMs. In the surveillance reports from the large cohort of the UK PIND research group, IEMs represent 82.3–88.2% of the most common diagnoses (1, 4). These numbers indicate that IEMs represent a significant proportion of the diagnoses reported in children presenting with PIND.

Interestingly, most of these IEMs represent storage disorders, but other categories are represented as well. In summary, more than half, 59% of the well-documented IEMs (34/57) were categorized in the group "storage disorders" mainly due to different types of MPS (type I, II, IIIA, IIIB, IIIC, IIID, VII) and NCL (type 1, 2, 3, 5, 6, 7, 8, 10, 12, 14) which represent 17 of the 34 included storage disorders (50%).

It is known that IEMs may present with stable DD/ID. Metabolic evaluation is advised in children with DD/ID and yields a diagnosis in 0.2–4.6% of tested children (17). In 2012, 81 IEMs presenting with intellectual disability were listed in the review of Karnebeek et al. (22). By 2018, this number had increased to more than 110 (14, 18, 19). Since 52% of the IEMs presenting with PIND ($n = 44$) can be detected through standard metabolic blood and urine tests and a growing number of IEMs are amenable to treatment. Leading to stabilization or reversal of deterioration, early diagnosis of IEMs is advantageous. In addition, the correct diagnosis of IEMs will aid in accurate care of the child, through management of symptoms or co-morbidities and genetic counseling including assessment of prognosis to the family. Diagnosis of IEMs is becoming more accessible through exome and genome sequencing. Its place in the diagnostic work-up varies according to local availability and clinical practice as well as the patient's phenotype; the yield of exomes in metabolic and neurogenetic phenotypes varies form 16–68% (20, 21). Metabolic testing has the advantage of a fast turn-around time, relative affordability and specificity and can validate exome findings or point toward the affected pathway.

Treatment such as vitamin supplementation or dietary management may lead to halt of progression or reversal of symptoms caused by IEMs. An example is hydroxocobalamin in cobalamin C deficiency (MIM#277400), where supplementation of hydroxocobalamin stabilizes clinical deterioration, prevents metabolic decompensation, and improves systemic manifestations. Biotinidase deficiency (MIM#253260) is another example of an IEM causing intellectual disability where treatment through biotin supplementation improves psychomotor

TABLE 6 | Overview of articles reporting the identified etiology of PIND, overall and specifically the IEMs.

	PIND cases	Etiology known	IEMs (% of PIND cases)
Nunn et al. (6)*	80	63	50 (62.5%)
Keene et al. (5)	60	52	45 (75.0%)
Verity et al. (3)	548	362	141**
Devereux et al. (1)	598	577	135***
Verity et al. (2)	1259	1114	660****
Verity et al. (4)	2050	1925	675*****

Excluded children with Rett disorder; 134 cases during study duration.
**Only ten most common diagnoses reported. IEMs represent 82.9% of the ten most common diagnoses.*
***Only five most common diagnoses reported. IEMs represent 82.3% of the five most common diagnoses.*
****Only thirty most common diagnoses reported. IEMs represent 83.2% of the thirty most common diagnoses.*
*****Only ten most common diagnoses reported. IEMs represent 88.2% of the ten most common diagnoses.*

development, neurological and systemic manifestations. Dietary restrictions range from dietary phenylalanine restrictions in patients with phenylketonuria (MIM#261600), protein restriction in patients with isovaleric acidemia (MIM#243500), citrullinemia (MIM#215700) and argininemia (MIM#207800), to a ketogenic diet as treatment for patients with GLUT1 deficiency syndrome (MIM#606777) and PDH complex deficiency (MIM#312170) (15). New therapeutic modalities for IEMs that may present with PIND are continuously under development, and treatments targeting the pathophysiology of IEMs are showing promising results. Cerliponase alfa (Brineura^{TM}), a recombinant human tripeptidyl peptidase-1 (TPP1) is an example of a recently developed treatment for neuronal ceroid lipofuscinosis type 2 (NCL2, MIM# 204500). NCL2 presents with progressive intellectual and neurological deterioration in children due to tripeptidyl peptidase-1 (TPP1) deficiency which causes accumulation of ceroid lipopigments in cells. Infusion of cerliponase alfa into the cerebrospinal fluid has shown to significantly slow the rate of deterioration of motor and language function in children with NCL2 (22, 23). Another emerging therapeutic modality is hematopoietic stem cell gene therapy (HSCGT). HSCGT which is currently under development for IEMS such as metachromatic leukodystrophy (MIM#250100) (24), X-linked adrenoleukodystrophy (MIM#300100) (25), Canavan disease (MIM#271900) (26, 27), mucopolysaccharidosis (MPS type I, II, IIIA, IIIB, VI) (28, 29) and neuronal ceroid lipofuscinosis (NCL type 1, 2, 3, 5, 6, 10, and 11) (30). The possibility of treating IEMs and thereby halting or reversing symptoms enhances the demand of an expeditious diagnostic process to ensure timely treatment in children presenting with symptoms caused by IEMs.

LIMITATIONS

Progressive intellectual and neurological deterioration is a definition used by PIND research groups and in this review, but this definition is not used consistently throughout the medical literature. We tried to include all potential terms for PIND, and discussed this with experts specialized in metabolic diseases and an intellectual disability physician. However, it remains possible that some articles describe PIND with terms that were not included in the search. Therefore, this article should be perceived as a scope of the latest articles of PIND and not a full review.

Several of the included case reports described symptoms insufficiently, for example not mentioning frequency of seizures, leading to difficulties matching these symptoms with our definition of PIND. This contributed to the extensive list of IEMs with PIND in single cases or families, for example with IEMs like MERRF, Wilson's disease, thiamine 2 transporter deficiency, and vanishing white matter leucodystrophy.

An additional limitation of this review is the occurrence of seizures and metabolic strokes in IEMs. Neurocognitive regression or loss of skills appearing after seizures or metabolic strokes may be due to brain damage rather than a primary consequence of the IEMs. Since, in turn, seizures or metabolic strokes are caused by the underlying IEMs, these disorders were not excluded. When epilepsy or metabolic decompensation is recorded in IEMbase, the data is displayed in **Supplemental Table S1**. An example is the inclusion of MELAS, in which metabolic strokes are a characteristic feature, and thus PIND may be due to progressive brain damage caused by these strokes (10).

We are aware of the aforementioned limitations and acknowledge the risk of bias due to the low level of evidence in this review. Additional research on these rare IEMs and consultation of metabolic disease experts should decrease this risk.

CONCLUSIONS

In summary, we present the first comprehensive overview of IEMs presenting with PIND, and provide a structured approach to diagnosis and treatment. Clearly IEMs constitute the largest group of genetic PIND conditions and have the advantage of detectable biomarkers as well as amenability to treatment. Thus, the clinician should keep IEMs at the forefront of the diagnostic workup of a child with PIND. With the ongoing discovery of new IEMs, expanded phenotypes, and novel treatment strategies, continuous updates to this work will be required. We invite colleagues from around the world to provide input on this topic which will enable us to practice precision medicine, optimizing clinical care and outcomes for these individuals and their families.

DATA AVAILABILITY STATEMENT

Publicly available datasets were analyzed in this study. This data can be found here: https://www.ncbi.nlm.nih.gov/pubmed/; http://www.iembase.org/; http://treatable-id.org/.

AUTHOR CONTRIBUTIONS

HW, ET-F, and LT performed the literature review, selected articles and extracted data, prepared the 1st draft of manuscript and tables (all under subversion). JL extracted data on each IEM from diverse research sources and contributed to the tables and manuscript. AE contributed to the systematic search, supervision of co-authors and editing of the manuscript. CF and CK designed the study, supervised the work of the co-authors and drafted the manuscript and made edits. All authors critically read, revised, and approved the current manuscript.

FUNDING

This work was supported by Foundation Metakids provides a salary award to CK.

ACKNOWLEDGMENTS

We are grateful to our patients and families who teach and inspire us. We thank Prof. Dr. F. Wijburg and Dr. A. Bosch (Amsterdam UMC, NL) for their valuable input and expert opinion on IEMs and PIND, and acknowledge our colleagues who maintain the IEMbase and Treatable ID tools, which are important information sources for the current manuscript.

SUPPLEMENTARY MATERIAL

The Supplementary Material for this article can be found online at: https://www.frontiersin.org/articles/10.3389/fneur.2019.01369/full#supplementary-material

REFERENCES

1. Devereux G, Stellitano L, Verity CM, Nicoll A, Will RG, Rogers P. Variations in neurodegenerative disease across the UK : and neurological deterioration (PIND). *Arch Dis Child*. (2004) 89:8–13.
2. Verity CM, Winstone AM, Stellitano L, Will R, Nicoll A. The epidemiology of progressive intellectual and neurological deterioration in childhood. *Arch Dis Child*. (2010) 95:361–4. doi: 10.1136/adc.2009.173419
3. Verity CM, Nicoll A, Will RG, Devereux G, Stellitano L. Variant Creutzfeldt-Jakob disease in UK children: a national surveillance study. *Lancet*. (2000) 356:1224–7. doi: 10.1016/S0140-6736(00)02785-9
4. Verity C, Winstone AM, Will R, Powell A, Baxter P, de Sousa C, et al. Surveillance for variant CJD: should more children with neurodegenerative diseases have autopsies? *Arch Dis Child*. (2019) 104:360–5. doi: 10.1136/archdischild-2018-315458
5. Keene DL, Sutcliffe T, Harman P, Grenier D. Surveillance for progressive intellectual and neurological deterioration in the Canadian paediatric population. *Can J Neurol Sci*. (2004) 31:220–4. doi: 10.1017/S0317167100053865
6. Nunn K, Williams K. The Australian childhood dementia study. *Eur Child Adolesc Psychiatr*. (2002) 70:63–70. doi: 10.1007/s007870200012
7. Morava E, Rahman S, Peters V, Baumgartner MR, Patterson M, Zschocke J. Quo vadis: the re-definition of "inborn metabolic diseases." *J Inherit Metab Dis*. (2015) 38:1003–6. doi: 10.1007/s10545-015-9893-x
8. Ferreira CR, van Karnebeek CDM, Vockley J, Blau N. A proposed nosology of inborn errors of metabolism. *Genet Med*. (2018) 21:102–6. doi: 10.1038/s41436-018-0022-8
9. Ouzzani M, Hammady H, Fedorowicz Z, Elmagarmid A. Rayyan — a web and mobile app for systematic reviews. *Syst Rev*. (2016) 5:210. doi: 10.1186/s1364.-016-0384-4
10. OMIM® and Online Mendelian Inheritance in Man® are registered trademarks of the Johns Hopkins University. Available online at: www.omim.org
11. Adam MP, Ardinger HH, Pagon RA, Wallace SE, editors. *GeneReviews®*. Seattle, WA: University of Washington S (1993–2018). Available online at: https://www.ncbi.nlm.nih.gov/books/NBK1116.GeneReviews (accessed October 17, 2018).
12. Valle D, Beaudet AL, Vogelstein B, Kinzler KW, Antonarakis SE, Ballabio A, et al. editors. *OMMBID Copyright © McGraw-Hill Education*. Available online at: https://ommbid.mhmedical.com/ (accessed October 17, 2018).
13. Van Karnebeek CDM, Shevell M, Zschocke J, Moeschler JB, Stockler S. The metabolic evaluation of the child with an intellectual developmental disorder: diagnostic algorithm for identification of treatable causes and new digital resource. *Mol Genet Metab*. (2014) 111:428–38. doi: 10.1016/j.ymgme.2014.01.011
14. Van Karnebeek CDM, Stockler S. Treatable inborn errors of metabolism causing intellectual disability: a systematic literature review. *Mol Genet Metab*. (2012) 105:368–81. doi: 10.1016/j.ymgme.2011.11.191
15. Sirrs S, Lehman A, Stockler S, van Karnebeek C. Treatable inborn errors of metabolism causing neurological symptoms in adults. *Mol Genet Metab*. (2013) 110:431–8. doi: 10.1016/j.ymgme.2013.10.002
16. Rahman J, Noronha A, Thiele I, Rahman S. Leigh map: a novel diagnostic resource for mitochondrial disease. *Neuromuscul Disord*. (2017) 27:S19. doi: 10.1016/S0960-8966(17)30274-2
17. Michelson DJ, Shevell MI, Sherr EH, Moeschler JB, Gropman AL, Ashwal S. Evidence report: genetic and metabolic testing on children with global developmental delay: report of the quality standards Subcommittee of the American Academy of Neurology and the Practice Committee of the Child Neurology Society. *Neurology*. (2011) 77:1629–35. doi: 10.1212/WNL.0b013e3182345896
18. Flore LA, Milunsky JM. Updates in the genetic evaluation of the child with global developmental delay or intellectual disability. *Semin Pediatr Neurol*. (2012) 19:173–80. doi: 10.1016/j.spen.2012.09.004
19. Breuning M, de Coo IFM, van den Elzen APM, van Karnebeek CDM, Klaassens M, Kleefstra T, et al. Nederlandse Vereniging voor Kindergeneeskunde—various authors. Richtlijn voor de initiële etiologische diagnostiek bij kinderen met een ontwikkelingsachterstand/verstandelijke beperking. (2017):1–87.
20. Al-Shamsi A, Hertecant JL, Souid AK, Al-Jasmi FA. Whole exome sequencing diagnosis of inborn errors of metabolism and other disorders in United Arab Emirates. *Orphanet J Rare Dis*. (2016) 312:1870–9. doi: 10.1186/s13023-016-0474-3
21. Shakiba M, Keramatipour M. Effect of whole exome sequencing in diagnosis of inborn errors of metabolism and neurogenetic disorders. *Iran J Child Neurol*. (2018) 12:7–15.
22. Schulz A, Ajayi T, Specchio N, de Los Reyes E, Gissen P, Ballon G, et al. Study of intraventricular cerliponase alfa for CLN2 disease. *N Engl J Med*. (2018) 378:1898–907. doi: 10.1056/NEJMoa1712649
23. Markham A. Cerliponase alfa: first global approval. *Drugs*. (2017) 77:1247–9. doi: 10.1007/s40265-017-0771-8
24. Sessa M, Lorioli L, Fumagalli F, Acquati S, Redaelli D, Baldoli C, et al. Lentiviral haemopoietic stem-cell gene therapy in early-onset metachromatic leukodystrophy: an ad-hoc analysis of a non-randomised, open-label, phase 1/2 trial. *Lancet*. (2016) 388: 476–87. doi: 10.1016/S0140-6736(16)30374-9
25. Eichler F, Duncan C, Musolino PL, Orchard PJ, De Oliveira, SThrasher AJ, et al. Hematopoietic stem-cell gene therapy for cerebral adrenoleukodystrophy. *N Engl J Med*. (2017) 377:1630–8. doi: 10.1056/NEJMoa1700554
26. Janson C, McPhee S, Bilaniuk L, Haselgrove J, Testaiuti M, Freese A, et al. Gene therapy of Canavan disease: AAV-2 vector for neurosurgical delivery

of aspartoacylase gene (ASPA) to the human brain. *Hum Gene Ther*. (2002) 13:1391–412. doi: 10.1089/104303402760128612
27. Leone P, Shera D, McPhee SW, Francis JS, Kolodny EH, Bilaniuk LT, et al. Long-term follow-up after gene therapy for canavan disease. *Sci Transl Med*. (2012) 4:165ra163. doi: 10.1126/scitranslmed.3003454
28. Tardieu M, Zérah M, Gougeon ML, Ausseil J, de Bournonville S, Husson B, et al. Intracerebral gene therapy in children with mucopolysaccharidosis type IIIB syndrome: an uncontrolled phase 1/2 clinical trial. *Lancet Neurol*. (2017) 16:712–20. doi: 10.1016/S1474-4422(17)30169-2
29. Fraldi A, Serafini M, Sorrentino NC, Gentner B, Aiuti A, Bernardo ME. Gene therapy for mucopolysaccharidoses: *in vivo* and *ex vivo* approaches. *Ital J Pediatr*. (2018) 44(Suppl. 2):130. doi: 10.1186/s13052-018-0565-y
30. Donsante A, Boulis NM. Progress in gene and cell therapies for the neuronal ceroid lipofuscinoses. *Expert Opin Biol Ther*. (2018) 18:755–64. doi: 10.1080/14712598.2018.1492544
31. Koch J, Mayr JA, Alhaddad B, Rauscher C, Bierau J, Kovacs-Nagy R, et al. CAD mutations and uridine-responsive epileptic encephalopathy. *Brain*. (2017) 140:279–86. doi: 10.1055/s-0037-1602868
32. Daci A, Bozalija A, Jashari F, Krasniqi S. Individualizing treatment approaches for epileptic patients with glucose transporter type1 (GLUT-1) deficiency. *Int J Mol Sci*. (2018) 19:E122. doi: 10.3390/ijms 19010122
33. Escolar ML, West T, Dalavecchia A, Poe MD, LaPoint K. Clinical management of Krabbe disease. *J Neuroschience Res*. (2016) 94:1118–25. doi: 10.1002/jnr.23891
34. Schwahn BC, van Spronsen FJ, Belaidi AA, Bowhay S, Christodoulou J, Derks TG. Efficacy and safety of cyclic pyranopterin monophosphate substitution in severe molybdenum cofactor deficiency type A: a prospective cohort study. *Lancet2*. (2015) 386:1955–63. doi: 10.1016/S0140-6736(15)00124-5
35. Geraets RD, Koh SY, Hastings ML, Kielian T, Pearce DA, Weimer JM. Moving towards effective therapeutic strategies for Neuronal Ceroid Lipofuscinosis. *Orphanet J Rare Dis*. (2016) 11:40. doi: 10.1186/s13023-016-0414-2

Conflict of Interest: The authors declare that the research was conducted in the absence of any commercial or financial relationships that could be construed as a potential conflict of interest.

frontiers in Neurology

ERRATUM
published: 28 July 2020
doi: 10.3389/fneur.2020.00884

Erratum: A Scoping Review of Inborn Errors of Metabolism Causing Progressive Intellectual and Neurologic Deterioration (PIND)

*Frontiers Production Office**

Frontiers Media SA, Lausanne, Switzerland

OPEN ACCESS

Approved by:
Frontiers Editorial Office, Frontiers Media SA, Switzerland

***Correspondence:**
Frontiers Production Office
production.office@frontiersin.org

Specialty section:
This article was submitted to Neurogenetics, a section of the journal Frontiers in Neurology

Received: *08 July 2020*
Accepted: *10 July 2020*
Published: *28 July 2020*

Citation:
Frontiers Production Office (2020) Erratum: A Scoping Review of Inborn Errors of Metabolism Causing Progressive Intellectual and Neurologic Deterioration (PIND). Front. Neurol. 11:884. doi: 10.3389/fneur.2020.00884

Keywords: PIND, inherited metabolic diseases, neurodegeneration, dementia, loss of skills, genetic, treatment, diagnosis

An Erratum on

A Scoping Review of Inborn Errors of Metabolism Causing Progressive Intellectual and Neurologic Deterioration (PIND)
by Warmerdam, H. A. G., Termeulen-Ferreira, E. A., Tseng, L. A., Lee, J. Y., van Eeghen, A. M., Ferreira, C. R., et al. (2020). Front. Neurol. 10:1369. doi: 10.3389/fneur.2019.01369

Due to a production error, the incorrect **Supplementary Material** was published online. The publisher apologizes for this mistake.

The original article has been updated.

Advantages of publishing in Frontiers

OPEN ACCESS
Articles are free to read for greatest visibility and readership

FAST PUBLICATION
Around 90 days from submission to decision

HIGH QUALITY PEER-REVIEW
Rigorous, collaborative, and constructive peer-review

TRANSPARENT PEER-REVIEW
Editors and reviewers acknowledged by name on published articles

Frontiers
Avenue du Tribunal-Fédéral 34
1005 Lausanne | Switzerland

Visit us: www.frontiersin.org
Contact us: info@frontiersin.org | +41 21 510 17 00

REPRODUCIBILITY OF RESEARCH
Support open data and methods to enhance research reproducibility

DIGITAL PUBLISHING
Articles designed for optimal readership across devices

FOLLOW US
@frontiersin

IMPACT METRICS
Advanced article metrics track visibility across digital media

EXTENSIVE PROMOTION
Marketing and promotion of impactful research

LOOP RESEARCH NETWORK
Our network increases your article's readership